ALMA MATER STUDIORUM
UNIVERSITÀ DI BOLOGNA

DOTTORATO DI RICERCA IN

BENI CULTURALI E AMBIENTALI

Ciclo 36

Settore Concorsuale: 04/A3 - GEOLOGIA APPLICATA, GEOGRAFIA FISICA E GEOMORFOLOGIA

Settore Scientifico Disciplinare: GEO/05 - GEOLOGIA APPLICATA

ASSESSMENT OF THE EFFECTS OF WATER SALINITY ON GREENHOUSE GAS FLUXES AND CARBON BALANCE IN COASTAL WETLANDS

Presentata da: Emilia Chiapponi

Coordinatore Dottorato

Donatella Restani

Supervisore

Sonia Silvestri

Co-supervisore

Beatrice Maria Sole Giambastiani

Esame finale anno 2024

ACKNOWLEDGEMENTS

Completing this dissertation was a challenging yet transformative experience that brought joy and personal growth, also thanks to the support of a dedicated team of supervisors, colleagues, and family, all of whom played a crucial role in making this achievement possible.

I would like to express my deepest gratitude to my supervisors, Prof. Sonia Silvestri and Prof. Beatrice Giambastiani, for their support, guidance, and expertise throughout my doctoral journey.

I am truly grateful for the time, dedication, and patience they have invested in me, pushing me to try achieve the best and to think critically. Their mentorship has showed me how to work with passion and to stand tall for one's-own ideas. It has been an immense luck to work with such an example of scientists and strong women.

I would like to extend my sincere gratitude to Prof. Antonella Buccianti and Prof. Curtis J. Richardson for their meticulous and insightful revisions, which significantly enhanced the overall quality of this thesis.

I also want to thank all the great scientists and staff who enriched this journey in one way or another. Prof. Dinelli, who has seen me grew from the very beginning as a student, Prof. Antonellini, Prof. Costantini and Prof. Buscaroli, for sharing their invaluable knowledge; to Dr. Greggio ,Dr. Zannoni, Dr. Campo and Dr. Toller for their kindness and all the help. To all my PhD colleagues, Qiqi, Regine, Veronica, Cristina, Riccardo, and Carlotta thanks for sharing the good and the bad of this adventure. To Mauro, without whom the majority of the data for this work would not have been collected, thank you for all the assistance provided during the sampling sessions.

To my family and friends, thanks for always having my back on this long path. Finally, to my loving husband Jack, "Thanks for all the fishes". This journey would not have been the same without your support and love. Here's to many more years of making each other proud!

ABSTRACT

This thesis is submitted in partial fulfilment of the requirements for obtaining a Doctor of Philosophy (Ph.D.) degree. This Ph.D. project started in November 2020 and was carried out till January 2023.

Part I of this study gives an overlook on coastal wetlands and their integral role for climate change mitigation, as reservoirs for organic carbon in soils.

Part II of this study investigates the impact of salinity on greenhouse gas emissions, particularly methane (CH_4), in four wetlands along the northeast Adriatic coast. Over a year, comprehensive measurements, including soil properties, CH_4 and carbon dioxide (CO_2) fluxes, and water parameters, revealed a significant reduction in CH_4 emissions at water heights exceeding 50 cm. Notably, temperature and irradiance strongly influenced CH_4 emissions, with distinctions observed between freshwater and brackish systems.

Part III delves into the relationship between microbial communities, biogeochemical processes, and potential climate-related feedbacks in temperate coastal wetlands. Addressing the dual role of these ecosystems as carbon sinks and CH_4 sources, the study characterizes microbial communities using advanced sequencing techniques. Focused on three temperate wetlands along a salinity gradient, results highlight the prevalence of sulfur-reducing bacteria in salinized sites, impacting CH_4 and CO_2 emissions. This section underscores the need for a better understanding of wetland ecosystems, salinity effects, and climate-related feedbacks to inform conservation and climate change mitigation strategies.

In Part IV, the study aims at reviewing hydrological processes and carbon dynamics in temperate wetlands. Analyzing data extracted from 50 wetlands, this section examines the interplay between environmental variables such as temperature, salinity, and water level, and their significant impact on CH_4 budgets and carbon balances. The water column height, emerges as a critical factor influencing wetland biogeochemistry. Seasonal dynamics, including alternating inundation and drought periods, affect redox conditions, impacting CH_4 generation by methanogenic bacteria. This chapter highlights some limitation of the sampling techniques used in this research.

Part V resumes the finals remarks of this study. The multidisciplinary approach of this work seeks to enhance carbon storage strategies, combat climate change, and better understand the role of temperate coastal wetlands in climate change mitigation.

Summary

List of acronyms

- AVS: Acid Volatile Sulfides
- C: Carbon
- CAV: Cavedone
- CER: Cerba
- CH_4: Methane
- CO_2: Carbon Dioxide
- GHGs: Green House Gases
- H_2S: Hydrogen Sulfide
- KDE: Kernel Density Estimates
- LOI: Loss on Ignition
- NCS: natural climate solutions
- O_2: molecular oxygen
- PA: Punte Alberete
- PCA: Principal Component Analysis
- PDF: Probability Density Function
- PIR: Pirottolo
- SCI: Site of Community Importance
- SLR: Sea Level Rise
- SO_4^{2-}: Sulfate
- SOB: Sulfate oxidizing bacteria
- SPA: Special Protected Area
- SRB: Sulfate reducing bacteria
- SVP: San Vitale Pinewood
- TEAs: alternative terminal acceptors
- TOC: Total Organic Carbon
- XRF: X-ray fluorescence spectrometry

Part I - Introduction

1.1 Climate Change and coastal wetlands

Global climate systems have seen remarkable change since the 1950s, driving significant research into climate change and greenhouse gas (GHG) emissions (Lynas et al., 2021; Salimi et al., 2021).

Climate change refers to long-term changes in Earth's temperature and weather patterns. The Earth's surface has seen warmer climate over the past three decades in a row. According to United Nation Intergovernmental Panel on Climate Change (IPCC, 2023), in 2011-2020 global surface temperature was 1.09°C higher than in 1850-1906, with greater increases over land (1.59 °C) than over water (0.88°C). The global surface temperature in the first two decades of the twenty-first century (2001-2020) was 0.99 °C higher than in the previous two decades (1850-1900). Since 1970, global surface temperature has risen faster than during any other 50-year period in the last 2000 years (IPCC, 2023).

Methane (CH_4) is a powerful climate warmer: it is commonly regarded to as the second most significant greenhouse gas (GHG) after carbon dioxide (CO_2), accounting for around 20% of direct radiative forcing since 1750 (Forster et al., 2023). CH_4, despite its short lifetime, is a potent GHG, being around 80 times more potent than CO_2 in the first two decades after production (Saunois et al., 2016a). Along with contributing to global air pollution, methane is also a precursor of tropospheric ozone (O_3) (Jackson et al., 2020). To achieve net zero GHG emissions, significant cuts in CO_2, CH_4, and other GHG emissions are necessary. Net negative CO_2 emissions are also implied (IPCC, 2023).

Conservation of high-carbon ecosystems (e.g., peatlands, wetlands, rangelands, mangroves, and forests) delivers immediate benefits, while outcome of restoration of high carbon ecosystem could take decades to deliver measurable results (IPCC, 2023). NCS have low to moderate costs, may be quickly implemented using existing technology, and include co-benefits related to better ecological conditions for high-carbon ecosystems (Holmquist et al., 2023).

At least 6.5% of the Earth's land surface is covered by inland wetlands, and around 8% (12.8 million km^2) is covered by both inland and coastal wetlands combined (Finlayson et al., 1999). Wetlands store more than 20% of global organic ecosystem carbon (all live and dead organic matter from terrestrial, freshwater, and marine systems combined) (Saunois et al., 2016a; Bar-On et al., 2018). Furthermore, wetland carbon sequestration rates can be orders of magnitude higher than rates in terrestrial and marine environments (Mcleod et al., 2011).

Coastal wetlands are potential NCS (Temmink et al., 2022), for the collection and storage of carbon from the atmosphere through photosynthesis and sediment trapping, resulting in high sequestration rates (Mcleod et al., 2011). Moreover, these ecosystems provide adaptation to climate changes, stabilizing the coastline and protecting the inland from floods, storm surges, and sea level rise (SLR) (Barbier, 2019).

1.2 Coastal wetlands

Because of their large geographic spread and considerable variations in hydrology, wetlands in general can be challenging to characterize. The major features defining a wetland along with Mitsch and Gosselink (2015) and Reddy and DeLaune (2008) include: i) the presence of water, either at the surface or within the root zone; ii) the presence of hydric or hydromorphic soils, peculiar soils with saturated

conditions exhibiting temporary or permanent anaerobiosis and iii) wetland ecosystems sustain vegetation such as hydrophytes well adapted to persistent flooded condition, and lack on the other hand, of flooding-intolerant biota (Fig.1.1). The Ramsar Convention classifies as wetlands a wide range of habitats, including marshes, peatlands, floodplains, rivers, lakes, and coastal areas like salt marshes, mangroves, and seagrass beds (Ramsar Convention Secretariat, 2013). Coral reefs and other marine areas that are no deeper than six meters at low tide are also considered wetlands, as are man-made wetlands like waste-water treatment ponds and reservoirs (Ramsar Convention Secretariat, 2013).

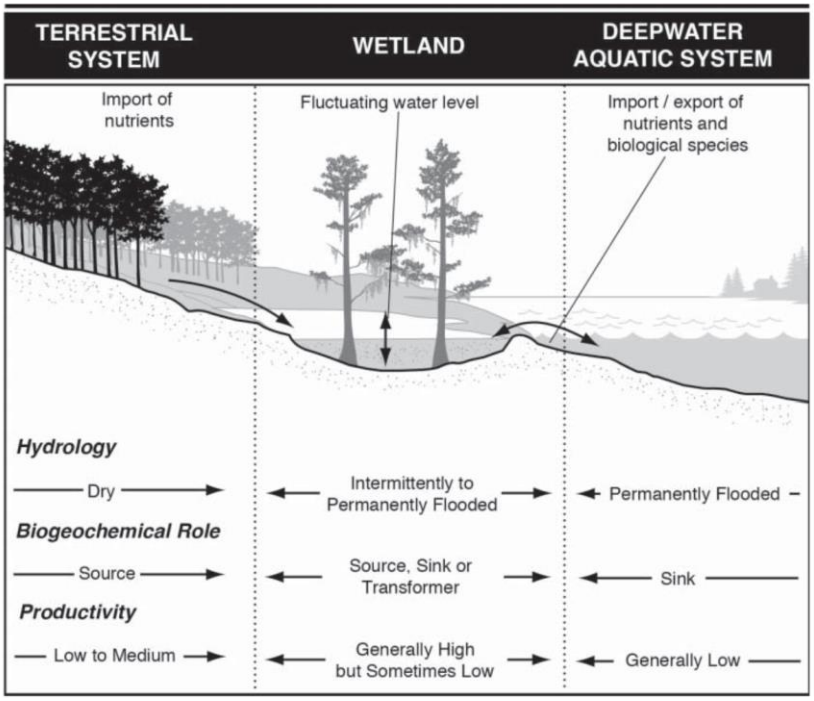

Fig. 1.1 Wetlands are frequently found isolated basins with minimal outflow and no nearby deepwater system, or between constantly flooded deepwater aquatic systems as rivers, lakes, estuaries, or oceans (Mitsch and Gosselink, 2015).

Wetlands in the Mediterranean region comprise of salt marshes and lagoons, freshwater lakes, karstic cave systems, temporary ponds, artificial wetlands including rice paddies, salinas, reservoirs, and fish ponds, as well as tiny, dispersed peatlands (Balbo et al., 2017). The Mediterranean region is characterized by summer droughts and a wide range of arid and semiarid conditions. The climate characteristics cause them to be highly seasonal in their water supply outside of the summer, and they also go through an extended vegetation period, which sets them apart from the traditional limnological paradigm (ONU, 2016). Given their dependency on climate, Mediterranean wetlands are highly threatened by climate change. Increase in both drought frequency and average temperature is expected to affect wetland characteristics and functioning, disrupting their biogeochemical cycles (Mariotti et al., 2008; Erwin, 2009a). Furthermore, sea-level rise is one of the more certain consequences of global warming, possibly leading to the inundation of low-lying coastal wetland ecosystems (Reddy and DeLaune, 2008). The combined impacts of localized human pressures, sea level rise, warming, and extreme climate events have resulted in the loss of about 50% of coastal wetlands during the past 100 years (IPCC, 2023).

1.3 Carbon cycle in wetlands

Wetlands are highly dynamic ecosystems rich in organic matter (OM), with changing sulfate concentration due to freshwater-saltwater exchange, which makes them hotspots for microbial metabolism, biogeochemical cycling, and CH_4 production (Bridgham et al., 2013; Hamdan and Wickland, 2016). At a global scale, wetland emissions account for ≈30% of the global CH_4 budget, emitting on median 164 Tg yr^{-1}, therefore wetlands are the single biggest natural source of CH_4 (Bridgham et al., 2013) (Fig.1.2). A high degree of uncertainty (≈50%) exists due to a scarcity of data on these systems. CH_4 emissions from coastal and estuarine environments are only a small portion of the total emissions from wetlands, with 13 Tg CH_4 yr^{-1} and 7 Tg CH_4 yr^{-1} emitted respectively (Borges et al. 2016).

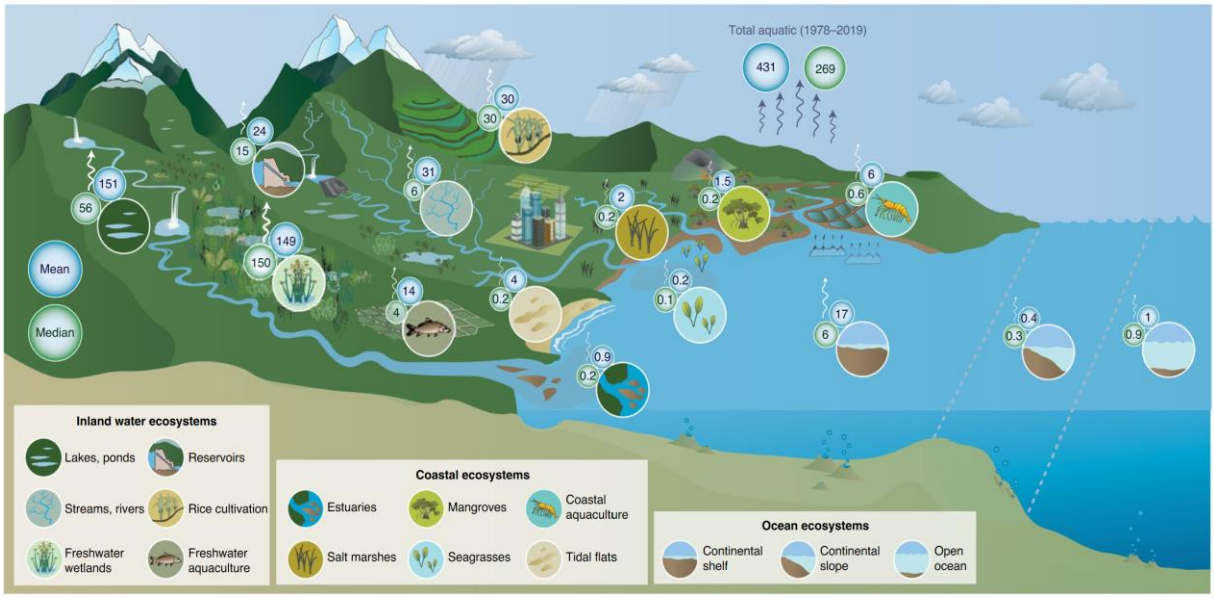

Fig. 1.2 – Global methane emissions from different sources. Mean emissions are reported in the blue circle, and median in green circle, expressed in Tg CH_4 yr^{-1}. (from Rosentreter et al., 2021)

The major processes of carbon transformation under aerobic and anaerobic conditions comprehend photosynthesis, respiration, fermentation, methanogenesis, and methane oxidation (anaerobic and aerobic) (Fig. 1.3) (Mitsch and Gosselink, 2015). Two of the major anaerobic processes are fermentation and methanogenesis. However, C sequestration rates in coastal wetlands, and net GHG emissions vary on spatiotemporal scales, depending on seasonal patterns and environmental settings (Hu et al., 2020). When organic matter is the last electron acceptor in anaerobic respiration by microbes, fermentation takes place, producing a variety of low-molecular-weight acids, alcohols, and CO_2 (Fig. 3, blue boxes) (Mitsch and Gosselink, 2015). Fermentation can be carried out in wetland soils by either facultative or obligate anaerobes (Kotsyurbenko et al., 2019).

The supply of electron acceptors typically limits the breakdown of organic materials, as opposed to the availability of carbon as in highland environments (Reddy and DeLaune, 2008). The concentration and kind of electron acceptors present in soils influence the various kinds of microbial communities engaged in organic matter decomposition, and the rate of the process (Reddy and DeLaune, 2008). Wetlands soils differ from upland soils in their biogeochemistry, which is distinguished by the presence of molecular oxygen (O_2) in a confined zone (Reddy and DeLaune, 2008). For bacteria, O_2 is the first sought electron acceptor to involve in organic matter decomposition. Specialized soil microorganisms

are able to transition to alternative terminal acceptors (TAEs) instead of O_2 when the supply of oxygen is reduced, facilitating the biological oxidation of organic substrates (Reddy and DeLaune, 2008). Several complex factors influence the availability of TEAs and, hence, the significance of competitive inhibition of CH_4 generation (Bridgham et al., 2013).

O_2 is followed by nitrate > manganese oxides > iron oxides > sulfate > carbon dioxide (Tab. 1.1, Fig. 1.3 – red boxes) (Reddy and DeLaune, 2008). The rate of consumption of these electron acceptors in soil systems is determined by their concentration, the presence of easily biodegradable organic molecules, and the microbial population engaged in the processes (Reddy and DeLaune, 2008).

Wetland's hydrology and hydroperiod have an impact on O_2 supply and availability. Under permanent flooded conditions, O_2 availability is restricted to the water-soil interface and to the rhizosphere, due to roots-mediated transport (Reddy and DeLaune, 2008). Nitrate, is the next favored TEAs after O_2, but its contribution in the process of organic matter degradation is low, due to minimal concentration in soil pore water or in the water column (Reddy and DeLaune, 2008). Fe and Mn oxides in mineral wetland soils have a high capability for organic matter decomposition, especially in those soils experiencing regular alternation of wet and dry period (Reddy and DeLaune, 2008). In brackish and salt water wetlands, tidal exchange provides a continual supply of SO_4^{2-} (Fig. 1.3, yellow box), which inhibits methanogenesis and dominates anaerobic decomposition, resulting in CO_2 fluxes (Bridgham et al., 2013). There is ample proof in the literature that methanogenesis is the major process regulating organic matter decomposition in freshwater wetlands, while sulfate reduction is prominent in saltwater wetlands (Poffenbarger et al., 2011a; Bridgham et al., 2013; La et al., 2022). Anyway, sulfate reduction can also occur in freshwater systems, despite limited sulfate availability, because of the rapid sulfur cycle in these systems (Vile et al., 2003). Methanogenesis occurs when certain bacteria (methanogens) use CO_2 or a low molecular weight fatty acid (LMWF) as an electron acceptor for the production of gaseous methane CH_4 (Fig. 1.3, light blue boxes) (Mitsch and Gosselink, 2015). Because there are often more carbon resources available in freshwater wetlands with lower concentrations of electron acceptors, methanogenesis is the predominant activity (Torres-Alvarado et al., 2005). It is generally accepted that in freshwater ecosystems, H_2 and acetate are the only fermentation products used by methanogens (Fig.1.3) (Bridgham et al., 2013). H_2 is oxidized to CH_4 during hydrogenotrophic methanogenesis, while acetate is split during acetoclastic methanogenesis to form CO_2 and CH_4.

Obligate methanotrophic bacteria are responsible for CH_4 oxidation (Fig. 1.3, orange boxes). They convert methane gas sequentially into methanol (CH_3OH), formaldehyde (HCHO), and CO_2 (Mitsch and Gosselink, 2015). Wetlands with an oxic layered horizon over a lower anoxic zone are characterized by the predominance of methanogens in the anoxic zone and methanotrophs in the oxygenated zone that perform methane oxidation, thus modulating the CH_4 fluxes (Mitsch and Gosselink, 2015). Freshwater and saltwater wetlands both produce significant amounts of methane emissions, which are the net product of methanogenesis and methane oxidation (Mitsch and Gosselink, 2015).

Gases released from wetlands enter the atmosphere through the vascular system of emergent plants or emerge from the sediment or soil surface through the water column by diffusive flux or diffusion (Mitsch and Gosselink, 2015; Kotsyurbenko et al., 2019). They then bubble to the surface in a process known as ebullitive flux or ebullition (Mitsch and Gosselink, 2015).

Tab. 1.1 - Sequence of the terminal electron acceptors involved in the organic matter decomposition (Reddy and DeLaune, 2008).

SEQUENCE OF REDUCTION	SYSTEM	OXIDIZED FORM	PROPERTIES	REDUCED FORM	PROPERTIES
1	Oxygen	0_2	Soluble	H_2O	
2	Nitrogen	NO_3	Very soluble	NH4	Soluble
		NO_2	Not adsorbed on soil	NH4	Adsorbed on exchange complex
		N_2O	Soluble	N_2O	Soluble
				N2	Slightly soluble
2	Manganese	$Mn0_2$	Insoluble pH dependent	Mn2+	Slightly soluble pH dependant
3	Iron	Fe_2O_3	Insoluble	Fe^2+	Slightly soluble
		$Fe(OH)_3$	pH dependent		pH dependant
4	Sulfur	$S0^{2-}_4$	Relatively soluble	S^{2-}	Slightly soluble
			pH dependent	HS^-	Precipitates with metallic cations
				H_2S	Precipitates with metallic cations
5	Carbon dioxide	$CO_2(g)$	Soluble	CH_4	Slightly soluble
		CO_3^{2-}	pH dependent		
		HCO_3	pH dependent		
5	Hydrogen	H_2O		H_2	
6	Phosphate	$P0^{3-}_4$	Soluble	PH_3	Slightly soluble
		$HP(X^-$	pH dependent		
		H_2P0	pH dependent		

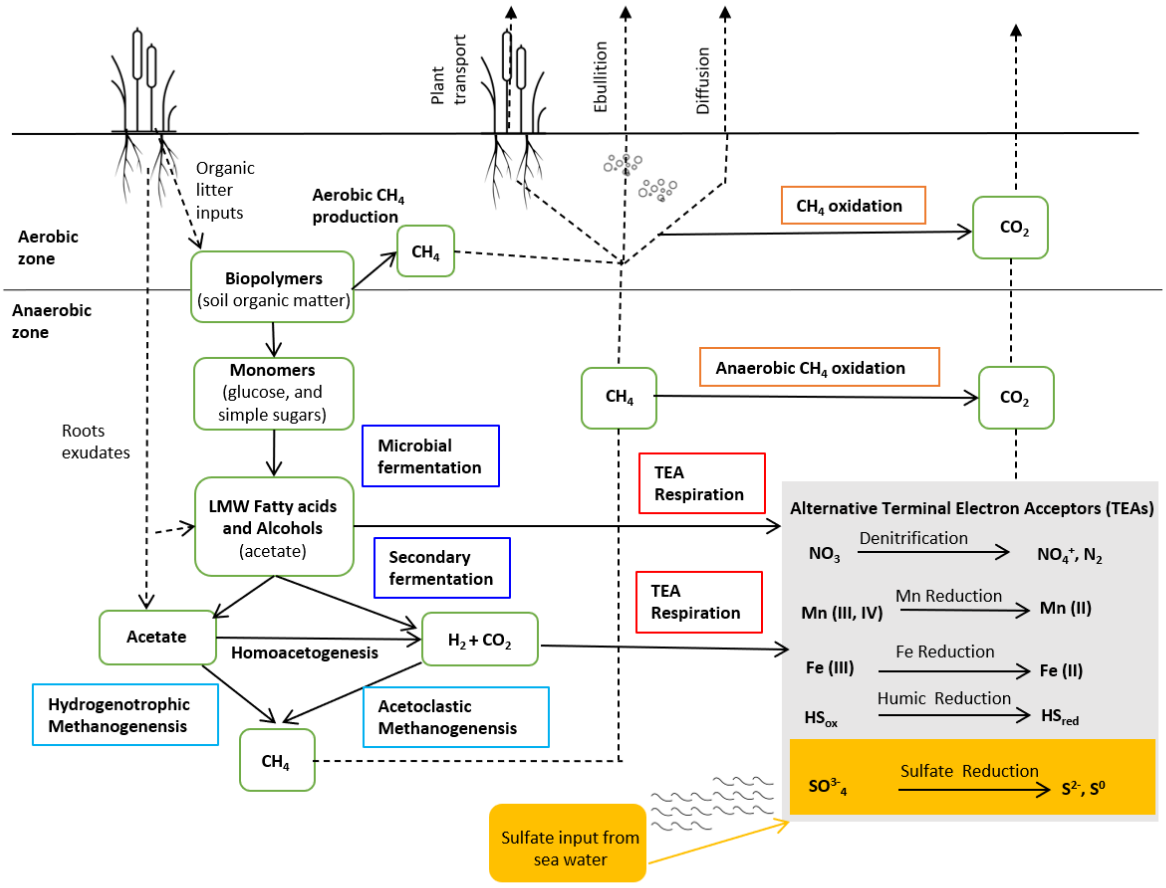

Fig.1.3 – CH4 cycle in wetlands. Carbon pools are depicted in white and green boxes, with solid arrows indicating the gradual mineralization of these carbon pools by the recognized microbial activities or groups. Carbon inputs from the plant community are shown by dotted lines. The dotted lines reflect the flow of these processes' gaseous end products (CH_4 and CO_2) into the atmosphere. In the bottom right is shown the influence of sea water in the yellow box. Different colors boxes highlight different key processes of CH_4 cycle: fermentation in blue, methanogenesis in light blue, TEA alternative respiration in red, and CH_4 oxidation in orange. (adapted from Bridgham et al., 2013)

1.4 Major controls in coastal wetlands

Carbon storage in wetlands is defined by the net result of organic matter production and organic matter loss and is regulated by wetlands biogeochemistry (Mitsch and Gosselink, 2015; Stagg et al., 2018).

When taking into consideration the effect of an ultimate driver, such as factor related to climate change (e.g. SLR, rising temperature, drought, etc.), intrinsic and extrinsic drivers will have direct and indirect effects on the carbon cycling (Stagg et al., 2018). Intrinsic drivers depend on the organic matter composition itself, while extrinsic factors are characteristics of the environment, like the soil bacteria community composition, and abiotic factor such as temperature, hydrological patterns and salinity (Melillo et al., 1984; Weston et al., 2006; Stagg et al., 2018). These drivers exercise a control on the production and consumption rates of organic matters, and transport patterns (Kristensen et al., 2022), resulting in GHG fluxes patterns varying on spatiotemporal scales (Fig. 1.4) (Hu et al., 2020).

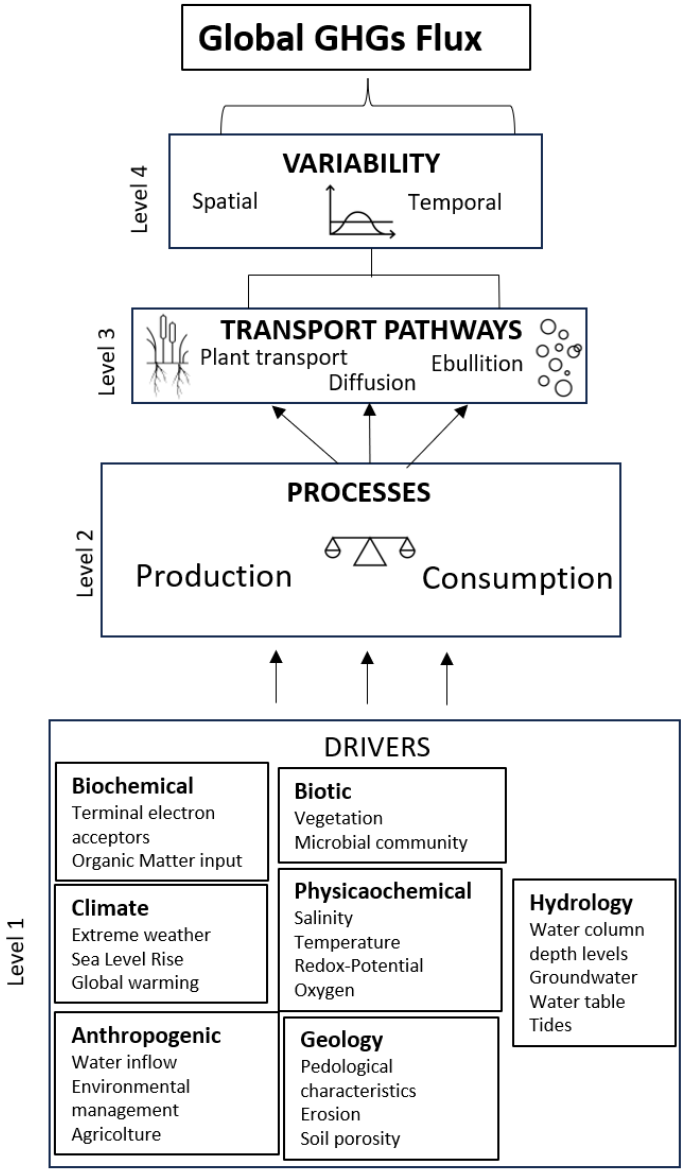

Fig. 1.4 – Ecosystem drivers that can directly or indirectly influence GHGs emissions in coastal wetlands. At level 1 are listed the drivers that influence the balance between GHG production and consumption (level 2), that control the different exchange process at the soil-water interfaces (level 3). Finally, temporal and geographical differences influence net GHGs flow (level 4).

1.4.1 Temperature

Temperature is one of the main regulators playing a role in biogeochemical processes in wetlands, by influencing the growth, activity, and survival of organisms (Mitsch and Gosselink, 2015). Microbial activity and organic matter decomposition shows accelerated rates with increasing temperature (Reddy and DeLaune, 2008). Temperature sensitivity of methanogenesis also depends on the availability of election acceptors, redox potential condition and availability of substrates (Reddy and DeLaune, 2008). The development of methanogenetic bacteria is directly correlated with temperature rise, which explains why tropical wetlands release more CH_4, and mid-latitude wetlands release more CH_4 during the warmer season than in winter (Torres-Alvarado et al., 2005). Also seasonal variation can be observed in biogeochemical processes controlling organic matter decomposition (Reddy and DeLaune, 2008). The temperature response to biogeochemical processes can be quantitatively described and

expressed with the Q_{10} function, which takes into account decompositions rates at different temperature (Reddy and DeLaune, 2008).

1.4.2 Salinity

Methanogenesis is the major mechanism controlling organic matter decomposition in freshwater wetlands, while sulfate reduction predominates in saltwater marshes, according to many studies (Bartlett et al., 1987; Reddy and DeLaune, 2008; Poffenbarger et al., 2011a; An et al., 2023). It was shown that there is a negative link between sulfate content and CH_4 emission in brackish wetlands, which are known for their continuous supply of sulfates (Poffenbarger et al., 2011a) . Reduction process is preferred over methanogenesis because SRB competes with MB more effectively for the available substrates, namely acetate and hydrogen, than methanogens does (Fig. 1.3) (Torres-Alvarado et al., 2005; Reddy and DeLaune, 2008).

Both inorganic (pyrite, iron and hydrogen sulfide, monosulfides, sulfate, and elemental sulfur) and organic (animal and microbial plant tissue) forms of sulfur are found in wetlands, but organic sulfur is the most abundant in wetland soils (Reddy and DeLaune, 2008). Organic sulfur in wetlands is derived from soil organic matter, periphyton, and detrital matter from plants (Peterson et al., 1986). Inorganic sulfur compounds, such as sulfate and elemental sulfur, serve as electron acceptors for obligate anaerobes (Reddy and DeLaune, 2008). Sulfate reduction releases more energy than methanogenesis; hence, no detectable methane is produced until all sulfate is reduced (Reddy and DeLaune, 2008) (Fig. 1.5).

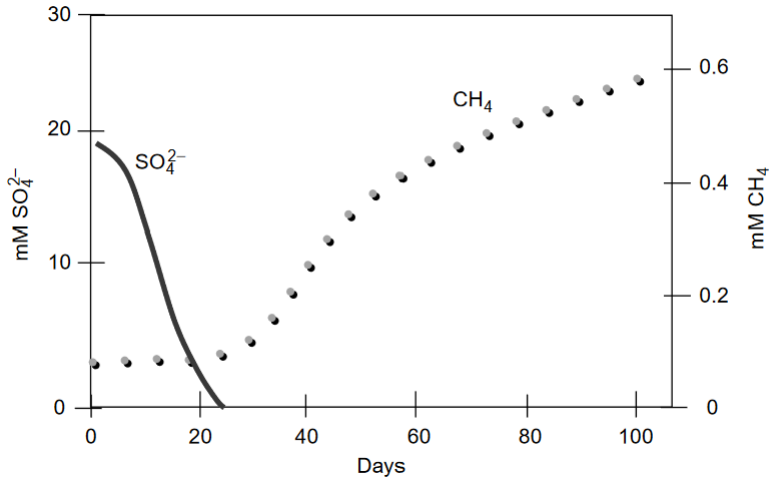

Fig. 1.5 – Relationship between sulfate reduction and methane production (Reddy and DeLaune, 2008)

1.4.3 Hydrology

Wetlands hydrology is determined by three factors: hydrodynamics (water direction and speed), hydroperiod (depth, duration, and frequency of flooding or soil saturation), and water supply (surface or groundwater) (Reddy and DeLaune, 2008). However, some types of wetlands, including coastal ones, do not highly depend just on precipitation, receiving water from tides. Similarly, also riparian or riverine wetlands, receive water from rivers and streams. Hydrology is a major factor on methanogenesis, being the process favored in wetland soils that are anoxic and flooded (Bartlett et al., 1987; Reddy and

DeLaune, 2008; Bhullar et al., 2013). The conventional link between emissions and the water table relies on the assumption that an oxic zone of net consumption (above the water table) and an anoxic zone of net production (below the water table) are separate entities (Bridgham et al., 2013). On the other hand, relatively aerated wetland soils can act as a sink where aerobic methanotrophs consume CH_4 , oxidizing it (Bartlett et al., 1987; Reddy and DeLaune, 2008). CH_4 oxidation can occurs only with the presence of O_2, therefore the process if particularly relevant in the oxic-anoxic boundary or within the plant root rhizosphere, where oxygen is transported from the plant to its root (Reddy and DeLaune, 2008).

1.5 Study site

1.5.1 Territory

This thesis has taken place in four different types of wetlands falling inside the territory of the San Vitale Pinewood (SVP). The site comprises the northernmost and largest remaining of the ancient Ravenna pine forest and is rich in wet lowlands derived from the ancient dune cordons (RER, 2018). The SVP is in the North-East Adriatic coast of Emilia Romagna, in the Ravenna province, and its extension covers approximately 1133 hectares, for length of around 11 km along the coastline (Fig. 1.6).
The SVP is delimited to the north border by the Destra Reno Canal, and to the south by the Canala drain and the Staggi Canal and by the Piallassa Baiona to the east. To the west the boundary is defined by the reclamation canals, while the southern area is delimited by the water pump installed in Via Cerba, and by the II Bacino water pump to the north. The entire San Vitale Pinewood is included in the Po Delta Park and is designated as a “Pre-Parco” Zone. It is also subject to the hydrogeological forestry constraint R.D. 3267/23 and is a SCI= SPA area (IT4070003 – “Pineta di San Vitale e Bassa del Pirottolo”) in accordance with EEC DIR 79/409 and EEC DIR 92/43.
This study includes also the nearby wetland of Punte Alberete (PA), which consists of the last remaining portions of the Lamone River extension reservoir covering about 190 hectares. PA also falls within the perimeter of the Delta Park as Zone A and is therefore classified as Ramsar Zone, and is likewise classified as a SCI= SPA area (IT4070001 - "Punte Alberete, Valle Mandriole").
The area is also characterized by the presence of the Pialassa Baiona, a brackish lagoon that is mostly connected to the sea and thus subject to the natural tidal cycle; it is distinguished by a complex network of canals linking semi-submerged sections with a depth of less than one meter.

Inside this territory, for the purpose of the study, four wetlands have been identified as study sites:

- **Cerba**: this site is located inside the SVP, and is a freshwater backdunal lowland, characterized by the presence of floating vegetation and cattail (*Typha* spp.) with sandy and calcareous soils on consolidated beach-ridge deposits;
- **Punte Alberete**: freshwater flooded hygrophilous forest with flooded lowlands. The area is characterized by fine-textured soils, calcareous and moderately alkaline;
- **Bassa del Pirottolo**: is a natural swamp with brackish water. The vegetation is characterized by the presence of a reed bed. Soils are sandy and calcareous;
- **Buca del Cavedone**: a rush grove swamp with brackish to slightly saline waters and sandy calcareous soils.

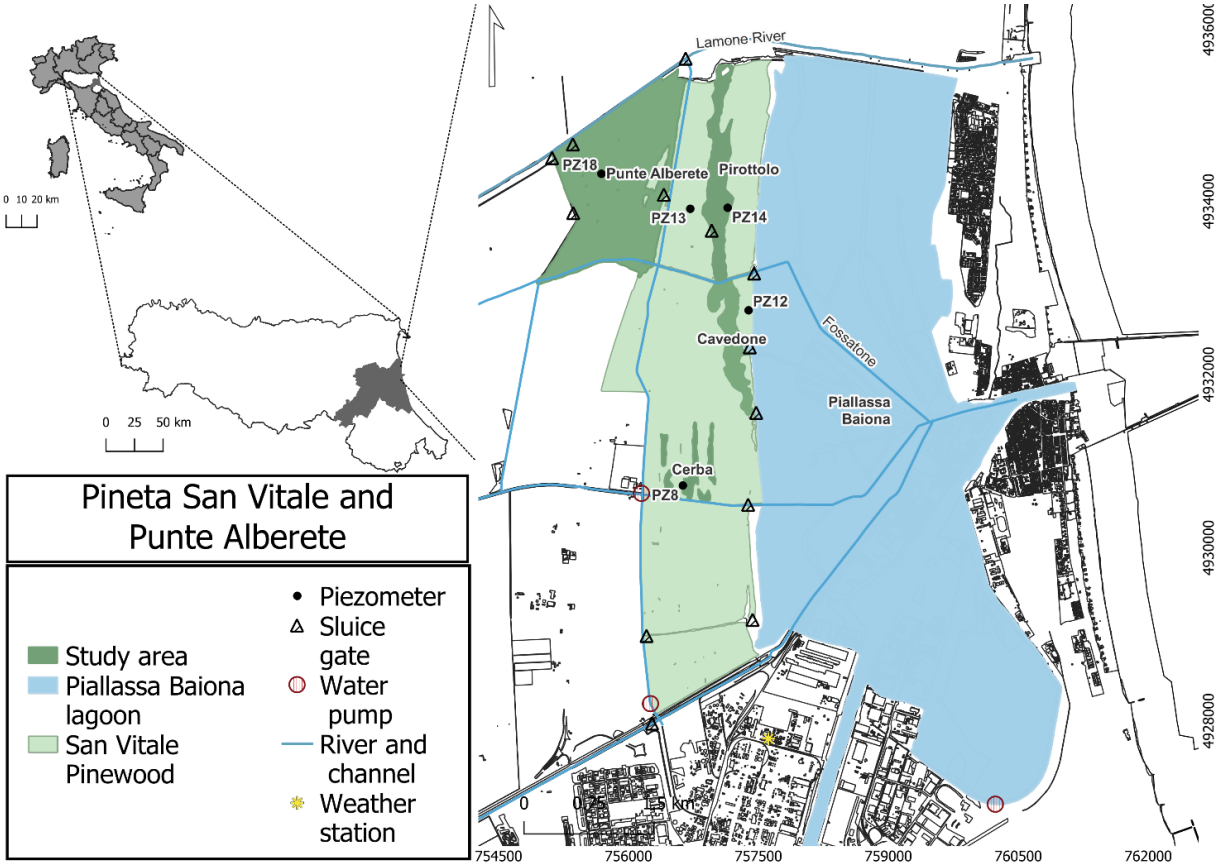

Fig. 1.6 – Location of the studied area. Data from Geoportal - Emilia Romagna Region (https://geoportale.regione.emilia-romagna.it/, last access Jan 2024. Elaborated in QGIS 3.26.0, EPSG: 32632)

1.5.2 Vegetation

The SVP and Punte Alberete are both part of the Natura 2000 framework, and represent an important biodiversity hotspot for the region, both from a floristic and faunistic point of view.

In SVP 80% of the area is covered by habitats of communitarian interest. The area is characterized by the presence of a dune forest, with *Pinus pinea* and *Pinus pinaster* alternated by transitional corridors characterized by a mixed xerophilous oak forest with *Quercus ilex* and a hygrophilous forest dominated by *Populus alba*, and *Fraxinus oxycarpa*. In this site mediterranean flooded grasslands are present with *Juncetalia maritimi*, fixed dunes with herbaceous vegetation, natural eutrophic lakes with aquatic vegetation as *Magnopotamion* or *Hydrocharition*, temporary Mediterranean ponds, and Mediterranean grasslands with herbaceous plants (Fig. 1.7).

Bassa del Pirottolo is a pond with undefined banks, permanently flooded with considerable seasonal differences in water height. It's characterized by the presence of marsh vegetation adapted to different levels of floodings, with flooded grasslands and meadows, reed beds, hygrophilous groves, and shrublands.

Punte Alberete is a hygrophilous forest with *Fraxinus oxycarpa, Ulmus minor, Populus alba, Salix alba*. This site is characterized by the presence of several microenvironments, hosting open ponds in the most depressed areas, with plant formations in relation to their depth and seasonal water level fluctuations. On the pond borders calcareous marshes with *Cladium mariscus* and species of *Caricion davallianae* can be found, also with *Magnopotamion* or *Hydrocharitio*n vegetation.

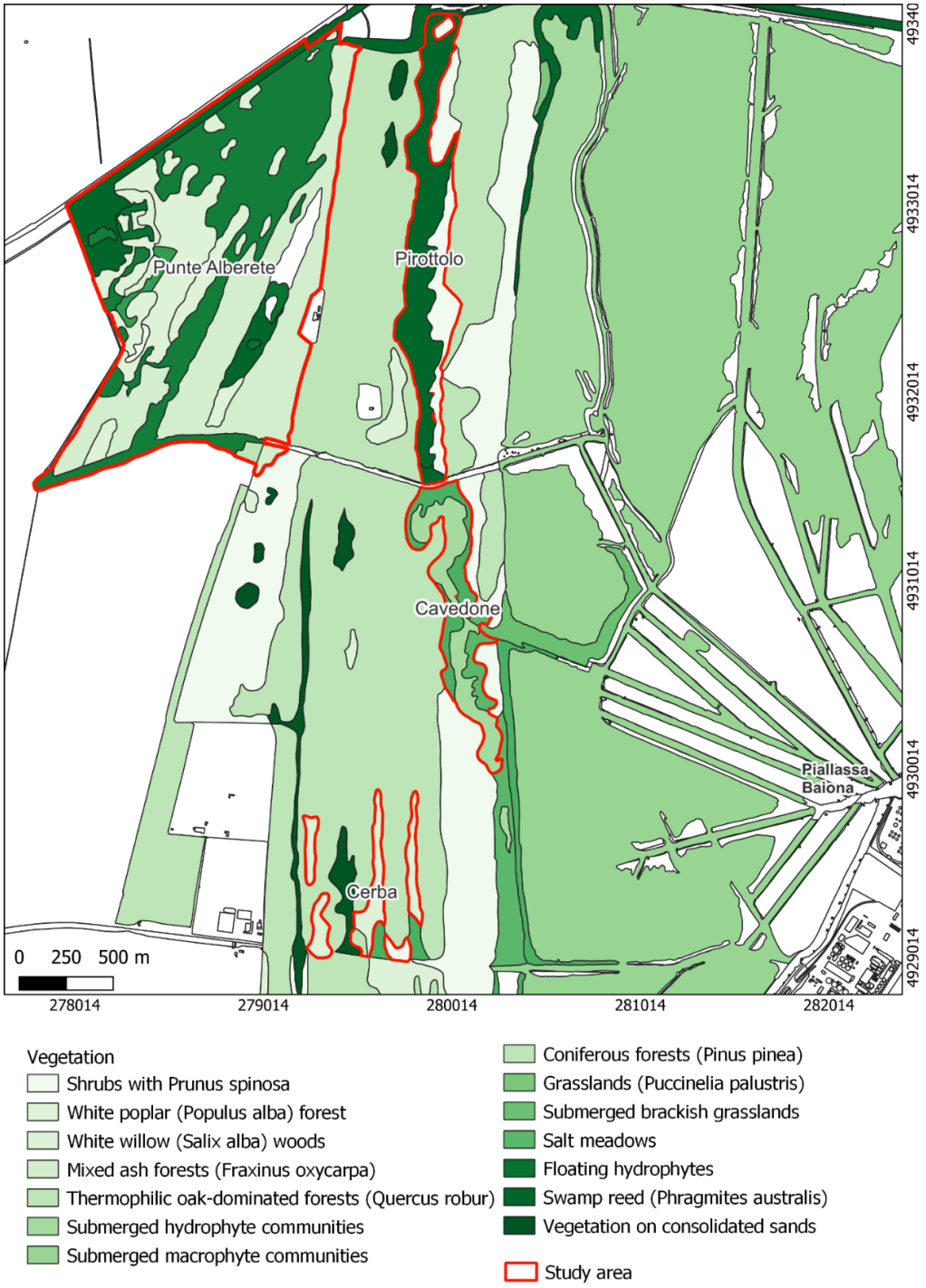

Fig. 1.7 – Vegetation map of the studied area, data from Geoportal - Emilia Romagna Region (https://geoportale.regione.emilia-romagna.it/, last access Jan 2024. Elaborated in QGIS 3.26.0, EPSG: 32632)

1.5.3 Soil

The area is characterized by the prevalent presence of alluvial deposits of interfluvial type and marsh deposits. The territory is generally between 0.40 m and 2.23 m a.s.l., with a mean value of 0.78 m a.m.s.l. The area consists of the coastal floodplain soils, with average slope of 0.01-0.1%. These soils origin from organic materials, marine sediments, or river deposits. They have a great degree of textural variety, ranging from coarse to fine, and contain peaty layers and carbonates.

Referring to the “Carta dei suoli della Regione Emilia-Romagna, scala 1:50.000” (RER, 2022), the soils in this area fall into delineation n. 118 and are classified as A1: soils in the coastal plain and delta front, with low profile differentiation (Holocene), shallow hydromorphic, and predominantly coarse texture. PSV soils can be further divided in three types of soils listed below (Fig. 1.8 and 1.9):

- Pirottolo soils: occurring at shallow locations with an outcropping or semi-outcropping water table depending on seasonality. The pH is sub-alkaline near the surface and becomes more alkaline as depth increases. The organic matter concentration is high near the surface and steadily decreases along the depth. They are defined as *Calcaric Gleyic Arenosols* along the WRB classification (IUSS, 2022) and *Typic Psammaquents*, mixed, mesic along with the Soil Taxonomy (SSS, 2022);
- Cerba soils: found in transitional areas between lowlands and tops of dune belts. They are mostly sandy soils and affected by the presence of the water table, especially during the rainy season. The pH is neutral near the top horizons and gradually becomes alkaline as one descends. Organic matter is present in traces at the top horizons. They are defined as *Calcaric Arenosols (Gleyic)* along the WRB classification (IUSS, 2022)and *Aquic Ustipsamments*, mixed, mesic along with the Soil Taxonomy (SSS, 2022);
- San Vitale soils: are found on the dune belt summits. They are sandy in texture and represent well drained soils. The pH is sub-acidic near the top and gradually goes from neutral to sub-alkaline as one descends along the depth. Organic matter is present in relatively high concentrations. They are defined as *Calcaric Arenosols* or *Arid Calcaric Arenosols* along the WRB classification (IUSS, 2022) and *Typic Ustipsamments*, *mixed, calcareus, mesic* along with the Soil Taxonomy (SSS, 2022)

In the last 2000 years, there has been advancement and retreat of the coastline, which corresponds to advancement and emersion phenomena (during which sandy cords have been created by wave motion and littoral transport) and submergence, in which the environment has been transformed first into freshwater marsh and then into brackish-water lagoon with clay deposition. The four study areas are therefore established on palaeodunes with a subparallel trend to the coast, developed as a result of coastal progradation caused by sedimentary inputs from the Reno, Lamone, Montone, Ronco, and Savio rivers. The morphology of pine forests still reflects the alternation between humps, called "staggi," and interdunal lowland, where water stagnates consistently, influencing the distribution of the local vegetation and soils development.

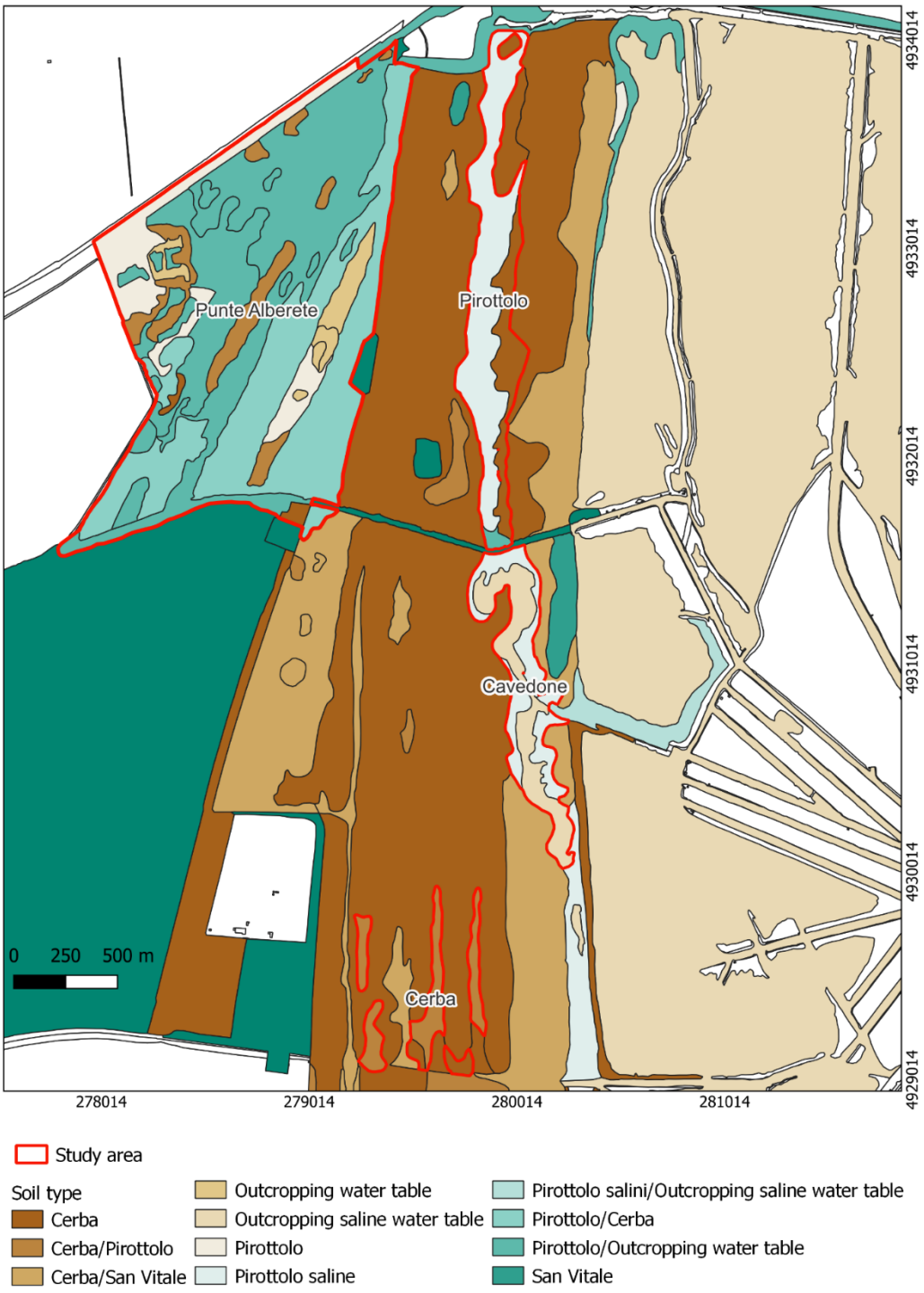

Fig. 1.8 – Soil map of the study area. Data extracted from Geoportal - Emilia Romagna Region (https://geoportale.regione.emilia-romagna.it/, last access Jan 2024. Elaborated in QGIS 3.26.0, EPSG: 32632)

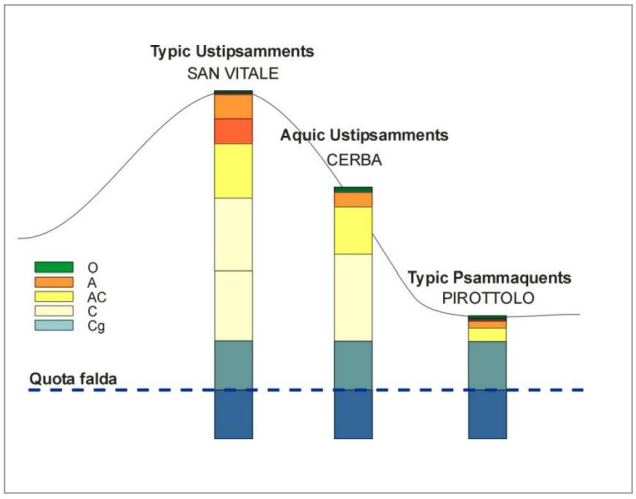

Fig. 1.9 - Morphosequence of soil types present in the San Vitale Pine Forest, as indicated by the Emilia-Romagna Region (from Zannoni, 2008)

1.5.4 Hydrogeology

The shallow aquifer of the study area are characterized by coastal plain deposits typical of the eastern portion of the Emilia-Romagna plain along a north-south oriented coastal band (RER - Regione Emilia Romagna, 2018). The aquifer has a maximum thickness of 25-30 m and overlie multi-layered alluvial aquifers. Due to being generally sandy, it has strong permeability that is decreased locally by the presence of silty deposits, with salt-saturated deposits that are in direct contact with salt-saturated marine sands (RER - Regione Emilia Romagna, 2018; Giambastiani, 2007; Giambastiani et al., 2021).
The development of the Po Plain coastal zone was influenced by alternating erosive and depositional stages. During the Quaternary, subsidence and alluvial continental deposits overlapped with marine sediments. The area's Holocene geomorphic history was driven by continental (Würmian) and marine depositions (post-Würmian transgression) in a coastal setting (Amorosi et al., 1999). The principal sedimentary packages are made up of a wedge of fine-grained (fine sand to silty clays, known as prodelta) sediments deposited in shallow marine water, as well as littoral sands from the foreshore, deep-shore, and nearby beach sand dune habitats (Fig. 1.10). The westernmost section also contains clay backshore lagoon deposits, with silty clay with peat and silty sands (Campo et al., 2017; Giambastiani et al., 2021). Westward, some continental alluvial deposits mainly represented by clay and silt, are deposited on the coastal sands and lagoon sediments, resulting in a semiconfined aquifer. The coastal phreatic aquifer is largely found in the littoral sands and shallow marine wedge deposits.

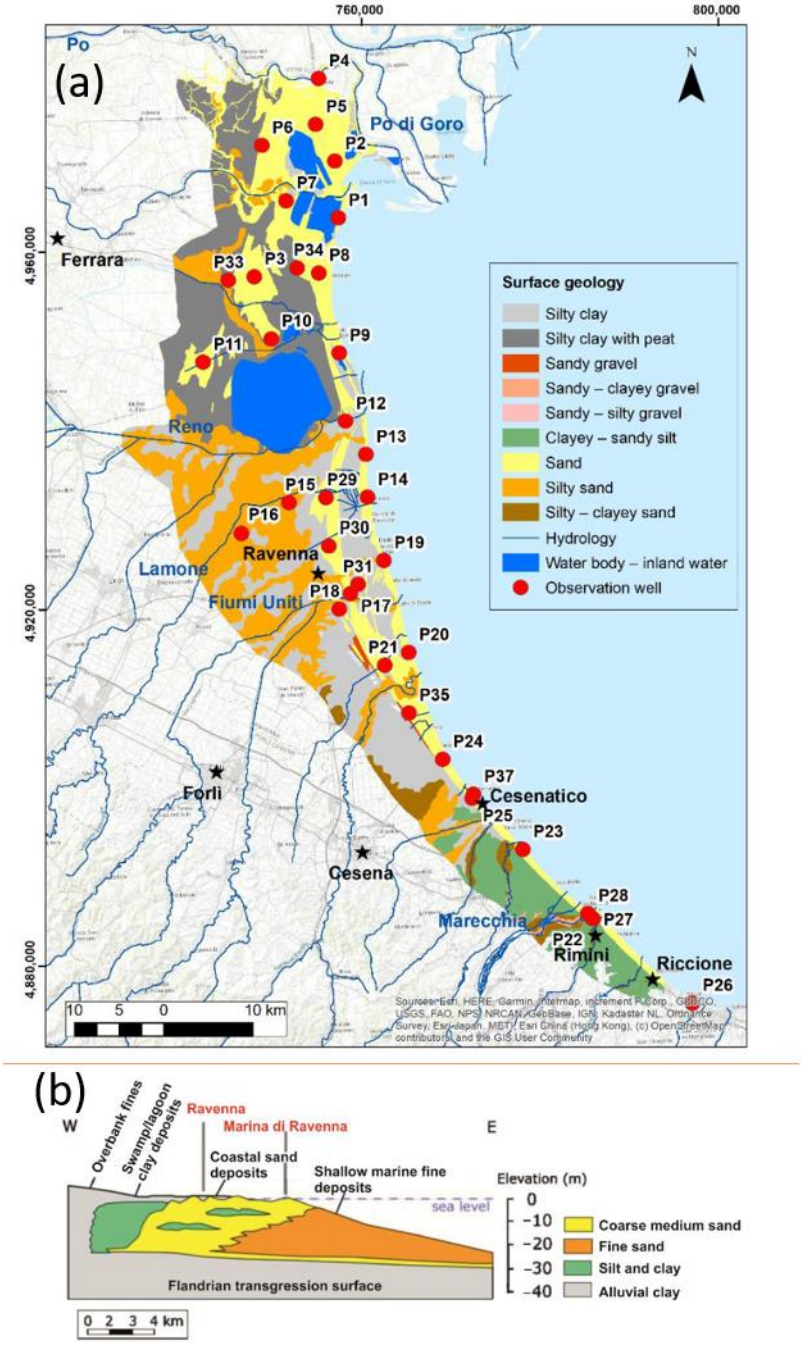

Fig. 1.10 - Surface geology of the coastal phreatic aquifer (a) and schematic stratigraphic section of the phreatic coastal aquifer (b) (from (Giambastiani et al., 2021)

In this area freshwater supply to the groundwater aquifer is through meteoric precipitation, water inputs from rivers and the system of canals and drainage ditches. However, it has been shown that the recharge is frequently insufficient to offset the discharges (drainage, water pumping, and evapotranspiration processes), but it is adequate to maintain a piezometric gradient toward the sea (Antonellini et al., 2008). The area's hydrological system is complicated since it includes natural and artificial water bodies, as well as watercourses with a variety of usage (Giambastiani et al., 2021). This

area's most important features include the brackish lagoon, wetlands, corrected rivers and dikes, a sophisticated land reclamation drainage network, pumping stations, irrigation input facilities, and the Adriatic Sea. Many watercourses pass this territory and interact with the aquifer, including as the Po, Reno, Lamone, Fiumi Uniti, and Savio rivers (Giambastiani et al., 2021)(Fig. 1.11).

The catchment areas of the Reno and Lamone rivers, as well as the reclamation district's drainage network, provide fresh water to SVP; these sources have recently been joined by the use of water derived from the Po River basin via the Canale Emiliano Romagnolo (CER).

In a natural setting, the river forms its own wetlands, replenishes them with fresh floodwaters, drains them during drought period, controls levels, and regenerates vegetation. Artificial river water control has severed connection of wetlands to the streams making their management completely artificial and leading to several conservation issues (Powers et al., 2012). The hydraulic system regulating water flows in this area consists of 35 artifacts (i.e. sluice gates, weirs, etc.). Each passage of water from the Lamone River to the Adriatic Sea is the result of management choices and hydraulic operations (RER - Regione Emilia Romagna, 2018).

The surface water network is comprehensive of numerous water bodies and their management operated by different agencies. It includes both natural water bodies, like Lamone River that receives water from the Canale Emiliano Romagnolo (created to provide water for irrigation), and artificial water bodies. These include the Canale Destra Reno (northern border) and Scolo Rivalone and its network, which together constitute a complex with a primary drainage role, the hydrometric levels of which are dominated by Basin II waterworks (Giambastiani, 2007; RER - Regione Emilia Romagna, 2018). The Fossatone Reclamation Consortium Canal, whose hydrometric levels are controlled and managed by HERA; Scolo Via Cerba, Scoli Tomba, and Palazzolo, whose hydrometric levels are dominated by the Via Cerba waterworks; and Scolo Canala, which represents the former Lamone reservoir's southern encircling canal and is delivered into the Chiaro del Pontazzo. There are also areas of brackish ponds such as Bassa del Pirottolo and Buca del Cavedone (Fig.9)(Giambastiani, 2007; RER - Regione Emilia Romagna, 2018).

The SVP is adjacent to Piallassa della Baiona, which is directly connected to the sea by the Canale Candiano and its tributaries (Giambastiani, 2007; RER - Regione Emilia Romagna, 2018). Only the Chiaro della Risega, which is near to the pine forest and hence directly connected to the sea, has remained open and convey tidal inputs to the lagoon. Chiaro del Pontazzo, Chiaro del Comune, and Chiaro di Mezzo have been embanked (Giambastiani, 2007; RER - Regione Emilia Romagna, 2018).

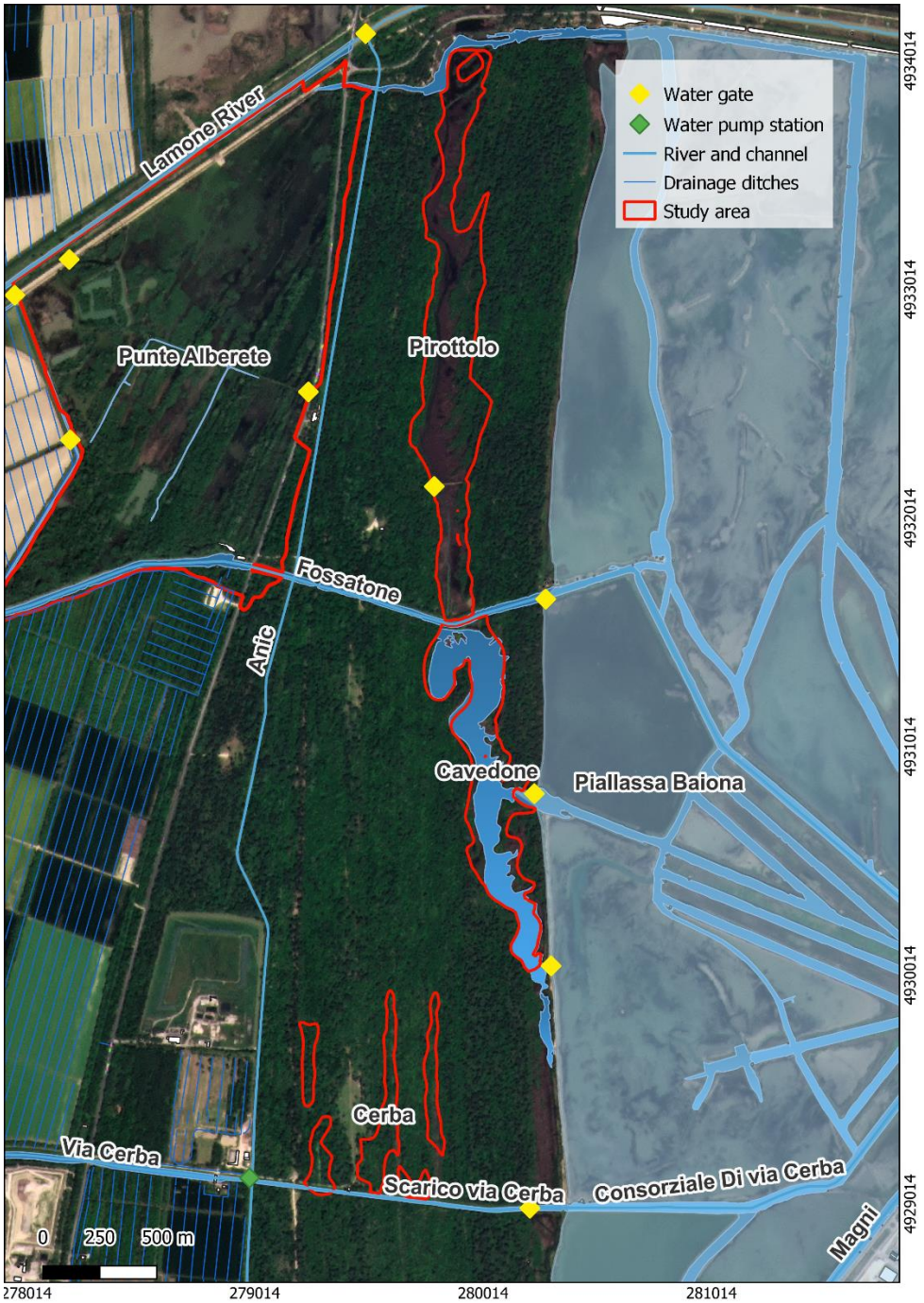

Fig. 1.11 – Network of superficial waterbodies, artificial canals and channels of the area. (Data extracted from Geoportal - Emilia Romagna Region (https://geoportale.regione.emilia-romagna.it/, last access Jan 2024. Elaborated in QGIS 3.26.0, EPSG: 32632)

1.5.5 Salinity

Ravenna's phreatic coastal aquifer is mostly brackish or salty, with a few isolated freshwater lenses (Mollema et al., 2013). The coastal aquifer is a closed system that can only be recharged by rainfall or irrigation infiltration in dune regions with exposed sandy deposits. The aquifer has seen restricted freshwater infiltration due to factors such as insufficient rainfall, high evaporation rates, sea-level rise, and subsidence (Mollema et al., 2012).

Furthermore, the infiltration of saltwater along rivers and canals contributes to the salinization process since there are no barriers to the sea, there is a low gradient (save for the Po River), and low flow river estuaries in microtidal conditions (Mollema et al., 2012). In certain circumstances, inverse riverbed slopes and large holes at the bottom of riverbeds make it easy for saltwater to enter the river and remain trapped for an extended period (Mollema et al., 2012). The salt pools on the river's bottom may be a major source of salinization for the surrounding aquifer, which connects surface and groundwater (Mollema et al., 2012).

The Lamone River is found to be fully compromised, with high salinities throughout the water column, affecting the water quality of the SVP wetlands (RER - Regione Emilia Romagna, 2018).

The main causes of saltwater intrusion in this area depends on (i) the destruction of coastal dunes allowing marine ingression; (ii) mechanical drainage, to avoid land flooding that mobilize saline groundwater previously preserved in the deepest portion of the aquifer; (iii) natural and anthropogenic subsidence (which strongly characterized the Ravenna area especially in the 1970s-1980s); (iv) insufficient aquifer recharge exacerbated by the strong urbanization of the coastline; (v) up-coning and seepage of saltwater from the bottom of the aquifer; (vi) water table close to or below sea level with a general inland-directed hydraulic gradient that is mainly forced by the drainage; (vii) encroachment of marine water along the rivers (Antonellini et al., 2008; Cozzolino et al., 2017; RER, 2018; Giambastiani et al., 2021). (Fig. 1.12)

The groundwater salinity already affects much of the Piallassa Baiona, the most critical area appears to be the south of the SVP; piezometers closer to the saltwater lagoon of Piallassa Baiona generally show shallow saltwater-freshwater interface, than those located in the inner lands (Giambastiani, 2007).

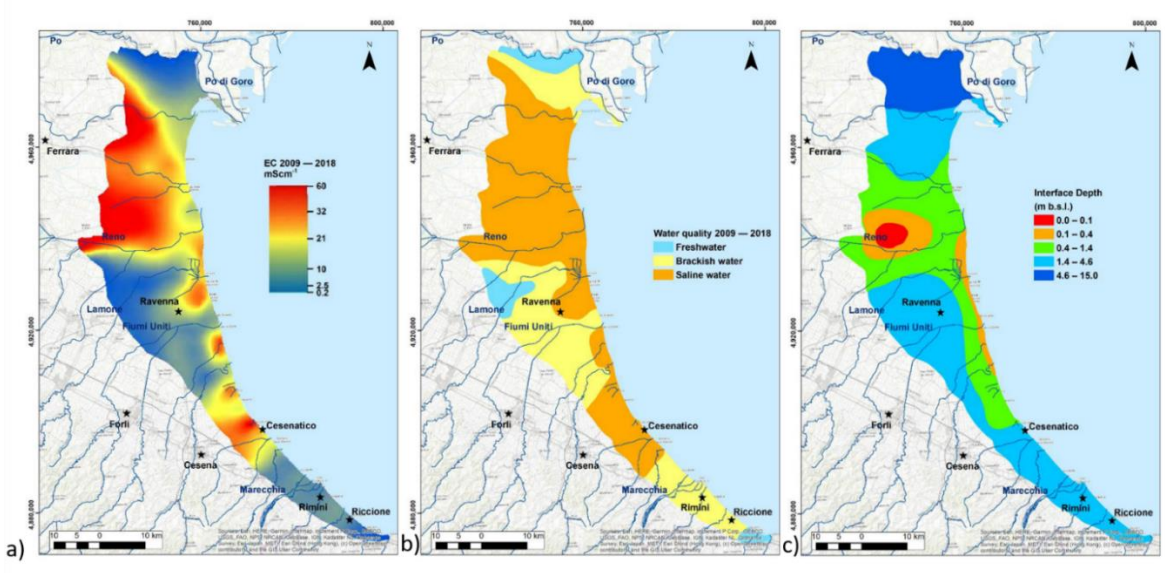

Fig. 1.12 – Data from 2009-2018 period showing (a) average EC distribution map ; (b) average water quality map of the aquifer showing the areal extent of freshwater, brackish and saline water, and (c) freshwater–saltwater interface in the studied area (from Giambastiani et al., 2021)

1.5.6 Environmental management and future challenges

The municipality of Ravenna recognizes the value of these environments and has analyzed in the " PAESC - Piano di Azione per l'Energia Sostenibile e il Clima - Resilienza e adattamento agli effetti del

cambiamento climatico" (Sustainable Energy and Climate Action Plan - Resilience and Adaptation to the Effects of Climate Change), the challenges and threats that these environments will face in the future due to climate change, proposing several adaptation measures (Comune di Ravenna, 2019).
The topography of the studied area will further change due to the combined action of subsidence and rising of the sea. In Ravenna alone, in the scenario that assumes a relative sea level rise of 55 cm, as much as 224 km^2 of territory will be "below mean sea level", enhancing the risk conditions for much of the land of the coastal plain. Although much of this is not directly connected to the sea and therefore not necessarily affected by marine ingression, the combined effect of low topography and sea-level rise, will make operations for draining water to the sea more complex and facilitating saltwater intrusion in the backshore areas (Perini et al., 2017)
Moreover, the areas that will potentially experience medium-frequency flooding with a 100-year return period, will be more extended than those at the present. In the next 100 years, along with the 2100 projections, it is expected that the combined effects of subsidence and sea level rise - assuming the absence of anthropogenic intervention - will increase the instability of the coastline, causing a further retreat of the coastline estimated, depending on local conditions, in an interval between 500 m and 1 km. (Perini et al., 2017)

In the PAESC, the Ravenna municipality recognizes the value of the wetlands and they defined strategies that can ensure, over the medium term (2050), the maintenance of biodiversity and environmental conditions favorable to sustain the peculiar fauna-vegetation structure of the wetlands. Currently, the environmental management of these habitats is oriented more to conserve the naturalistic elements in accordance with the European directives (Comune di Ravenna, 2019). Some limitation of the PAESC consists in providing only management and conservation strategies on a short-term scenario of climate change, and only for a restricted portion of territory, considering just those environments more exposed on the coast and not for a very different climate. Also, in the PAESC, there is no consideration on the carbon sequestration provided by these environments, but they focus mostly on the ecosystem services provided for biodiversity and coast protection. Therefore, there is a gap concerning the coastal wetlands laying in the transition zone, and the future of the carbon sink function of these environments.

1.6 Thesis aims and structure

This study aims at investigating the role of abiotic and biotic factors influencing the CH_4 and CO_2 emissions in temperate coastal wetlands, by resolving the following research question:

- How much CH_4 and CO_2 temperate coastal wetlands emit?
- How climate-change related variables will be involved in future GHGs emissions rates from these environments?

The specific aims of this research are to: 1) quantify CH_4 and CO_2 fluxes from the selected study sites; 2) quantify environmental drivers of GHGs production and their effects on the emission rates; 3) analyze biogeochemical pathways and microbial community involved in GHGs production in a progressive salinized environment; 4) study the possible effects of different hydrology pattern on CH_4 and CO_2 emissions.

This thesis consists of five parts, including an introduction (Part I), three data chapters, and a final synthesis of the findings and conclusions (Part V). Each chapter provides a concise literature review and methodology sections; therefore, no separate methodology section is included in this thesis.

- **Part I**: Provides a review of the state of the art of the topic. This part also contains a detailed overview of the study site, the environmental settings, its environmental management and how it is affected by climate change;
- **Part II**: Shows results on the environmental drivers involved in GHGs production in temperate coastal wetlands;
- **Part III**: Investigates the role of salinity in shaping the microbial community and biogeochemical cycle involved in CH_4 and CO_2 production in temperate coastal wetlands;
- **Part IV**: Analyses how different levels of water column depth promote CH_4 production rates in different temperate wetlands ecosystems;
- **Part V**: This section integrates the thesis's primary results and conclusions to address the specific thesis objectives.

References

Amorosi, A., Colalongo, M. L., Pasini, G., and Preti, D.: Sedimentary response to Late Quaternary sea-level changes in the Romagna coastal plain, Sedimentology, 99–121, https://doi.org/10.1046/j.1365-3091.1999.00205.x, 1999.

An, L., Yan, Y.-C., Tian, H.-L., Chi, C.-Q., Nie, Y., and Wu, X.-L.: Roles of sulfate-reducing bacteria in sustaining the diversity and stability of marine bacterial community, Front. Microbiol., 14, 1218828, https://doi.org/10.3389/fmicb.2023.1218828, 2023.

Antonellini, M., Mollema, P., Giambastiani, B., Bishop, K., Caruso, L., Minchio, A., Pellegrini, L., Sabia, M., Ulazzi, E., and Gabbianelli, G.: Salt water intrusion in the coastal aquifer of the southern Po Plain, Italy, Hydrogeol J, 16, 1541–1556, https://doi.org/10.1007/s10040-008-0319-9, 2008.

Balbo, A. L., Martinez-Fernández, J., and Esteve-Selma, M.: Mediterranean wetlands: archaeology, ecology, and sustainability, WIREs Water, 4, e1238, https://doi.org/10.1002/wat2.1238, 2017.

Barbier, E. B.: The Value of Coastal Wetland Ecosystem Services, in: Coastal Wetlands, Elsevier, 947–964, https://doi.org/10.1016/B978-0-444-63893-9.00027-7, 2019.

Bar-On, Y. M., Phillips, R., and Milo, R.: The biomass distribution on Earth, Proc. Natl. Acad. Sci. U.S.A., 115, 6506–6511, https://doi.org/10.1073/pnas.1711842115, 2018.

Bartlett, K. B., Bartlett, D. S., Harriss, R. C., and Sebacher, D. I.: Methane emissions along a salt marsh salinity gradient, Biogeochemistry, 4, 183–202, https://doi.org/10.1007/BF02187365, 1987.

Bhullar, G. S., Iravani, M., Edwards, P. J., and Olde Venterink, H.: Methane transport and emissions from soil as affected by water table and vascular plants, BMC Ecol, 13, 32, https://doi.org/10.1186/1472-6785-13-32, 2013.

Bridgham, S. D., Cadillo-Quiroz, H., Keller, J. K., and Zhuang, Q.: Methane emissions from wetlands: biogeochemical, microbial, and modeling perspectives from local to global scales, Glob Change Biol, 19, 1325–1346, https://doi.org/10.1111/gcb.12131, 2013.

Campo, B., Amorosi, A., and Vaiani, S. C.: Sequence stratigraphy and late Quaternary paleoenvironmental evolution of the Northern Adriatic coastal plain (Italy), Palaeogeography, Palaeoclimatology, Palaeoecology, 466, 265–278, https://doi.org/10.1016/j.palaeo.2016.11.016, 2017.

Comune di Ravenna: PAESC - Piano di Azione per l'Energia Sostenibile e il Clima, Resilienza e adattamento agli effetti del cambiamento climatico, 2019.

Cozzolino, D., Greggio, N., Antonellini, M., and Giambastiani, B. M. S.: Natural and anthropogenic factors affecting freshwater lenses in coastal dunes of the Adriatic coast, Journal of Hydrology, 551, 804–818, https://doi.org/10.1016/j.jhydrol.2017.04.039, 2017.

Erwin, K. L.: Wetlands and global climate change: the role of wetland restoration in a changing world, Wetlands Ecol Manage, 17, 71–84, https://doi.org/10.1007/s11273-008-9119-1, 2009.

Finlayson, C. M., Davidson, N. C., Spiers, A. G., and Stevenson, N. J.: Global wetland inventory - current status and future priorities, Mar. Freshwater Res., https://doi.org/10.1071/MF99098, 1999.

Forster, P., Storelvmo, T., Armour, P., Collins, W., Dufresne, J.-L., Frame, D., Lunt, D. J., Mauritsen, T., Palmer, M. D., Watanabe, M., Wild, M., and

Zhang, H.: 2021: The Earth's Energy Budget, Climate Feedbacks, and Climate Sensitivity. In Climate Change 2021: The Physical Science Basis. Contribution of Working Group I to the Sixth Assessment Report of the Intergovernmental Panel on Climate Change, in: 2021: The Earth's Energy Budget, Climate Feedbacks, and Climate Sensitivity. In Climate Change 2021: The Physical Science Basis. Contribution of Working Group I to the Sixth Assessment Report of the Intergovernmental Panel on Climate Change, Cambridge University Press, 923–1054, https://doi.org/10.1017/9781009157896, 2023.

Giambastiani, B. M. S., Kidanemariam, A., Dagnew, A., and Antonellini, M.: Evolution of Salinity and Water Table Level of the Phreatic Coastal Aquifer of the Emilia Romagna Region (Italy), Water, 13, 372, https://doi.org/10.3390/w13030372, 2021.

Giambastiani M.S. Beatrice: Evoluzione Idrologica ed idrogeologica della Pineta di San Vitale (Ravenna), Tesi di Dottorato, Università di Bologna, 2007.

Hamdan, L. J. and Wickland, K. P.: Methane emissions from oceans, coasts, and freshwater habitats: New perspectives and feedbacks on climate, Limnology & Oceanography, 61, https://doi.org/10.1002/lno.10449, 2016.

Holmquist, J. R., Eagle, M., Molinari, R. L., Nick, S. K., Stachowicz, L. C., and Kroeger, K. D.: Mapping methane reduction potential of tidal wetland restoration in the United States, Commun Earth Environ, 4, 353, https://doi.org/10.1038/s43247-023-00988-y, 2023.

Hu, M., Sardans, J., Yang, X., Peñuelas, J., and Tong, C.: Patterns and environmental drivers of greenhouse gas fluxes in the coastal wetlands of China: A systematic review and synthesis, Environmental Research, 186, 109576, https://doi.org/10.1016/j.envres.2020.109576, 2020.

IPCC: IPCC, 2023: Climate Change 2023: Synthesis Report. Contribution of Working Groups I, II and III to the Sixth Assessment Report of the Intergovernmental Panel on Climate Change [Core Writing Team, H. Lee and J. Romero (eds.)]. IPCC, Geneva, Switzerland., Intergovernmental Panel on Climate Change (IPCC), https://doi.org/10.59327/IPCC/AR6-9789291691647, 2023.

IUSS Working Group and WRB: World Reference Base for Soil Resources. International soil classification system for naming soils and creating legends for soil maps, International Union of Soil Sciences (IUSS), Vienna, Austria, 2022.

Jackson, R. B., Saunois, M., Bousquet, P., Canadell, J. G., Poulter, B., Stavert, A. R., Bergamaschi, P., Niwa, Y., Segers, A., and Tsuruta, A.: Increasing anthropogenic methane emissions arise equally from agricultural and fossil fuel sources, Environ. Res. Lett., 15, 071002, https://doi.org/10.1088/1748-9326/ab9ed2, 2020.

Kotsyurbenko, O. R., Glagolev, M. V., Merkel, A. Y., Sabrekov, A. F., and Terentieva, I. E.: Methanogenesis in Soils, Wetlands, and Peat, in: Biogenesis of Hydrocarbons, edited by: Stams, A. J. M. and Sousa, D., Springer International Publishing, Cham, 1–18, https://doi.org/10.1007/978-3-319-53114-4_9-1, 2019.

Kristensen, E., Quintana, C. O., and Petersen, S. G. G.: The role of biogenic structures for greenhouse gas balance in vegetated intertidal wetlands, in: Carbon Mineralization in Coastal Wetlands, Elsevier, 233–267, https://doi.org/10.1016/B978-0-12-819220-7.00001-7, 2022.

La, W., Han, X., Liu, C.-Q., Ding, H., Liu, M., Sun, F., Li, S., and Lang, Y.: Sulfate concentrations affect sulfate reduction pathways and methane consumption in coastal wetlands, Water Research, 217, 118441,

https://doi.org/10.1016/j.watres.2022.118441, 2022.

Lynas, M., Houlton, B. Z., and Perry, S.: Greater than 99% consensus on human caused climate change in the peer-reviewed scientific literature, Environ. Res. Lett., 16, 114005, https://doi.org/10.1088/1748-9326/ac2966, 2021.

Mariotti, A., Zeng, N., Yoon, J.-H., Artale, V., Navarra, A., Alpert, P., and Li, L. Z. X.: Mediterranean water cycle changes: transition to drier 21st century conditions in observations and CMIP3 simulations, Environ. Res. Lett., 3, 044001, https://doi.org/10.1088/1748-9326/3/4/044001, 2008.

Mcleod, E., Chmura, G. L., Bouillon, S., Salm, R., Björk, M., Duarte, C. M., Lovelock, C. E., Schlesinger, W. H., and Silliman, B. R.: A blueprint for blue carbon: toward an improved understanding of the role of vegetated coastal habitats in sequestering CO_2, Frontiers in Ecol & Environ, 9, 552–560, https://doi.org/10.1890/110004, 2011.

Melillo, J. M., Naiman, R. J., Aber, J. D., and Linkins, A. E.: Factors Controlling Mass Loss and Nitrogen Dynamics of Plant Litter Decaying in Northern Streams, 1984.

Mitsch, W. J. and Gosselink, J. G.: Wetlands, Fifth edition., John Wiley and Sons, Inc, Hoboken, NJ, 736 pp., 2015.

Mollema, P., Antonellini, M., Gabbianelli, G., Laghi, M., Marconi, V., and Minchio, A.: Climate and water budget change of a Mediterranean coastal watershed, Ravenna, Italy, Environ Earth Sci, 65, 257–276, https://doi.org/10.1007/s12665-011-1088-7, 2012.

Mollema, P. N., Antonellini, M., Dinelli, E., Gabbianelli, G., Greggio, N., and Stuyfzand, P. J.: Hydrochemical and physical processes influencing salinization and freshening in Mediterranean low-lying coastal environments, Applied Geochemistry, 34, 207–221, https://doi.org/10.1016/j.apgeochem.2013.03.017, 2013.

ONU (Ed.): The Mediterranean region under climate change: a scientific update, IRD éditions, Marseille, 2016.

Perini, L., Calabrese, L., Luciani, P., Olivieri, M., Galassi, G., and Spada, G.: Sea-level rise along the Emilia-Romagna coast (Northern Italy) in 2100: scenarios and impacts, Nat. Hazards Earth Syst. Sci., 17, 2271–2287, https://doi.org/10.5194/nhess-17-2271-2017, 2017.

Peterson, B. J., Howarth, R. W., and Garritt, R. H.: Sulfur and Carbon Isotopes as Tracers of Salt-Marsh Organic Matter Flow, Ecology, 67, 865–874, https://doi.org/10.2307/1939809, 1986.

Poffenbarger, H. J., Needelman, B. A., and Megonigal, J. P.: Salinity Influence on Methane Emissions from Tidal Marshes, Wetlands, 31, 831–842, https://doi.org/10.1007/s13157-011-0197-0, 2011.

Powers, S. M., Johnson, R. A., and Stanley, E. H.: Nutrient Retention and the Problem of Hydrologic Disconnection in Streams and Wetlands, Ecosystems, 15, 435–449, https://doi.org/10.1007/s10021-012-9520-8, 2012.

Ramsar Convention Secretariat: The Ramsar Convention Manual: a guide to the Convention on Wetlands (Ramsar, Iran, 1971), 2013.

Reddy, K. R. and DeLaune, R. D.: Biogeochemistry of wetlands: science and applications, CRC Press, Boca Raton, 774 pp., 2008.

RER - Regione Emilia Romagna: MISURE SPECIFICHE DI CONSERVAZIONE DEL SIC-ZPS IT4070003 “PINETA DI SAN VITALE, BASSA DEL PIROTTOLO,” 2018.

Rosentreter, J. A., Borges, A. V., Deemer, B. R., Holgerson, M. A., Liu, S., Song, C., Melack, J., Raymond, P. A., Duarte, C. M., Allen, G. H.,

Olefeldt, D., Poulter, B., Battin, T. I., and Eyre, B. D.: Half of global methane emissions come from highly variable aquatic ecosystem sources, Nat. Geosci., 14, 225–230, https://doi.org/10.1038/s41561-021-00715-2, 2021.

Salimi, S., Almuktar, S. A. A. A. N., and Scholz, M.: Impact of climate change on wetland ecosystems: A critical review of experimental wetlands, Journal of Environmental Management, 286, 112160, https://doi.org/10.1016/j.jenvman.2021.112160, 2021.

Saunois, M., Bousquet, P., Poulter, B., Peregon, A., Ciais, P., Canadell, J. G., Dlugokencky, E. J., Etiope, G., Bastviken, D., Houweling, S., Janssens-Maenhout, G., Tubiello, F. N., Castaldi, S., Jackson, R. B., Alexe, M., Arora, V. K., Beerling, D. J., Bergamaschi, P., Blake, D. R., Brailsford, G., Brovkin, V., Bruhwiler, L., Crevoisier, C., Crill, P., Covey, K., Curry, C., Frankenberg, C., Gedney, N., Höglund-Isaksson, L., Ishizawa, M., Ito, A., Joos, F., Kim, H.-S., Kleinen, T., Krummel, P., Lamarque, J.-F., Langenfelds, R., Locatelli, R., Machida, T., Maksyutov, S., McDonald, K. C., Marshall, J., Melton, J. R., Morino, I., Naik, V., O'Doherty, S., Parmentier, F.-J. W., Patra, P. K., Peng, C., Peng, S., Peters, G. P., Pison, I., Prigent, C., Prinn, R., Ramonet, M., Riley, W. J., Saito, M., Santini, M., Schroeder, R., Simpson, I. J., Spahni, R., Steele, P., Takizawa, A., Thornton, B. F., Tian, H., Tohjima, Y., Viovy, N., Voulgarakis, A., van Weele, M., van der Werf, G. R., Weiss, R., Wiedinmyer, C., Wilton, D. J., Wiltshire, A., Worthy, D., Wunch, D., Xu, X., Yoshida, Y., Zhang, B., Zhang, Z., and Zhu, Q.: The global methane budget 2000–2012, Earth Syst. Sci. Data, 8, 697–751, https://doi.org/10.5194/essd-8-697-2016, 2016.

Soil Survey Staff and United States Department of Agriculture Natural Resources Conservation Service: Keys to Soil Taxonomy, 13th Edition, 2022.

Stagg, C. L., Baustian, M. M., Perry, C. L., Carruthers, T. J. B., and Hall, C. T.: Direct and indirect controls on organic matter decomposition in four coastal wetland communities along a landscape salinity gradient, Journal of Ecology, 106, 655–670, https://doi.org/10.1111/1365-2745.12901, 2018.

Temmink, R. J. M., Lamers, L. P. M., Angelini, C., Bouma, T. J., Fritz, C., Van De Koppel, J., Lexmond, R., Rietkerk, M., Silliman, B. R., Joosten, H., and Van Der Heide, T.: Recovering wetland biogeomorphic feedbacks to restore the world's biotic carbon hotspots, Science, 376, eabn1479, https://doi.org/10.1126/science.abn1479, 2022.

Torres-Alvarado, R., Ramírez-Vives, F., and Fernández, F. J.: Methanogenesis and methane oxidation in wetlands. Implications in the global carbon cycle Metanogénesis y metano-oxidación en humedales. Implicaciones en el ciclo del carbono global, 15, 23, 2005.

Vile, M. A., Bridgham, S. D., and Wieder, R. K.: Response of anaerobic carbon mineralization rates to sulfate amendments in a boreal peatland, Ecological Applications, 13, 720–734, https://doi.org/10.1890/1051-0761(2003)013[0720:ROACMR]2.0.CO;2, 2003.

Weston, N. B., Dixon, R. E., and Joye, S. B.: Ramifications of increased salinity in tidal freshwater sediments: Geochemistry and microbial pathways of organic matter mineralization, J. Geophys. Res., 111, 2005JG000071, https://doi.org/10.1029/2005JG000071, 2006.

Zannoni, D.: Uso sostenibile dei suoli forestali di ambiente costiero in relazione ai fattori di pressione esistenti, Dottorato di Ricerca in Scienze Ambientali: Tutela e Gestione delle Risorse Naturali, University of Bologna, 2008.

Part II – Environmental drivers of GHGs fluxes in temperate coastal wetlands

The chapter has been submitted and published as a scientific paper in EGU - Biogeosciences under the title "Driving and limiting factors of CH_4 and CO_2 emissions from coastal brackish-water wetlands in temperate regions" Chiapponi, E., Silvestri, S., Zannoni, D., Antonellini, M., and Giambastiani, B. M. S. EC, BMSG and SS conceptualized the research and carried out the field sampling campaign for data collection. All authors (EC, BMSG, DZ, SS, MA) participated in the methodology development and supplied the necessary resources for the research. BMSG, SS, and MA supervised the research. EC performed the formal analysis. EC, BMSG and SS interpreted and validated the results. EC prepared the original draft and the visualization content, while all authors (EC, BMSG, DZ, SS, MA) participated in the revision and editing process.

Chiapponi, E., Silvestri, S., Zannoni, D., Antonellini, M., and Giambastiani, B. M. S.: Driving and limiting factors of CH_4 and CO_2 emissions from coastal brackish-water wetlands in temperate regions, Biogeosciences, 21, 73–91, https://doi.org/10.5194/bg-21-73-2024, 2024.

Abstract

Coastal wetlands play a fundamental role in mitigating climate change thanks to their ability to store large amounts of organic carbon in the soil. However, degraded freshwater wetlands are also known to be the first natural emitter of methane (CH_4). Salinity is known to inhibit CH_4 production, but its effect in brackish ecosystems is still poorly understood. This study provides a contribution to understanding how environmental variables may affect greenhouse gas emissions (GHG) in coastal temperate wetlands. We present the results of over one year of measurements performed in four wetlands located along a salinity gradient on the northeast Adriatic coast near Ravenna, Italy. Soil properties were determined by coring soil samples, while carbon dioxide (CO_2) and CH_4 fluxes from soils and standing waters were monthly monitored by a portable gas flux-meter. Additionally, water levels and surface and groundwater physical-chemical parameters (temperature, pH, electrical conductivity, and sulfate concentrations of water) were monthly monitored by multiparametric probes. We observed a substantial reduction in CH_4 emissions when water height exceeded the critical threshold of 50 cm. Regardless of the water salinity value, the mean CH_4 flux was 5.04 g/m^2/day in freshwater systems and 12.27 g/m^2/day in brackish ones. In contrast, when water height was shallower than 50 cm, CH_4 fluxes reached an average of 196.98 g/m^2/day in freshwater systems, while non-significant results are available for brackish/saline waters. Results obtained for CO_2 fluxes showed the same behaviour described for CH_4 fluxes, even though they were statistically non-significant. Temperature and irradiance strongly influenced CH_4 emissions from water and soil, resulting in higher rates during summer and spring.

2.1 Introduction

Wetlands store large amounts of carbon (C) in sediments and soils for long periods and in a more effective way than other environments (Whalen, 2005; Saunois et al., 2016b), and this capability puts them among the largest C pools of the world. Even though the majority of C tends to remain in wetland soils, some of it is recombined producing carbon dioxide (CO_2) and methane (CH_4), two greenhouse

gases (GHGs) released into the atmosphere. CH_4 is the second most important GHG after CO_2, responsible for 20% of the direct radiative forcing since 1750 (Mar et al., 2022). Increased CH_4 emissions in wetlands could trigger a positive feedback loop that further increases temperatures, potentially making wetlands the first natural emitters of CH_4 in nature and worsening climate change effects (Gedney et al., 2019; Saunois et al., 2016b).

Over the last three decades, variations in wetland emissions have dominated the year-to-year variability in surface emissions, and it is estimated that just in the 2000s natural wetlands have accounted globally for the production of 175-217 Tg CH_4 yr^{-1} (Kirschke et al., 2013); among them, if only temperate wetlands are considered, they have been reported to emit an average of 0.109 g $m^{-2}day^{-1}$ of methane (Turetsky et al., 2014). In a recent study by Peng et al. (2022), it is estimated that between 2019-2020 the emissions from wetlands have increased by 6.0 ± 2.3 Tg CH_4 yr^{-1}. Nevertheless, large uncertainties still affect estimates of the total contribution of wetlands at different scales (Abdul-Aziz et al., 2018). Therefore, understanding the C cycle in wetlands is a key factor in fighting climate change and achieving climate targets by compensating for anthropogenic carbon emissions (Erwin, 2009b; Howard et al., 2017).

Water table level, temperature, and salinity are only some of the environmental factors that have an impact on air-water CH_4 fluxes, especially in wetlands (Huertas et al., 2019). Salinity has an inhibitory effect on organic carbon mineralization and CH_4 production especially in coastal systems due to the presence of sulfate (SO_4^{2-}) (Poffenbarger et al. 2011). This ion, at certain concentrations, allows sulfate-reducing bacteria to outcompete methanogens for energy sources, consequently inhibiting CH_4 production. No consensus has been reached for salinity threshold under which the system becomes a CH_4 source. This process can be complicated by site-specific conditions that can allow CH_4 production to continue in coastal environments despite the inhibitory effect of SO_4^{2-} (Megonigal et al., 2004; Poffenbarger et al., 2011).

The water table level has a direct effect on CH_4 production by affecting vegetation productivity, redox potential, and oxidation process in the rhizosphere (Bhullar et al., 2013), but its overall function is still unclear, posing a significant source of uncertainty for estimating its contribution to the global budget of CH_4 (Whalen, 2005; Calabrese et al., 2021).

Site-specific conditions highly affect CH_4 production, resulting in a high spatial-temporal heterogeneity in these ecosystems (Poffenbarger, et al. 2011). Each type of coastal wetland ecosystem must be taken into account separately because of the differences in CH_4 release and regulatory mechanisms to properly estimate global wetland methane emissions and to evaluate possible changes as a result of environmental stressors (Turetsky et al., 2014).

To our knowledge, no previous studies have been conducted on GHG emissions in coastal wetlands in the Po River Delta, and just an exiguous number of studies have been carried out in the overall Mediterranean Basin (Huertas et al., 2019; Venturi et al., 2021). Temperate Mediterranean coastal wetlands are unique ecosystems that are subject to Mediterranean climate forcing and therefore subjected to a strong seasonality (Alvarez Cobelas et al., 2005). Although some earlier studies have been conducted from both a global perspective and within the regional context of coastal wetlands, few are known on temperate wetlands and specifically on temperate coastal systems (de Vicente, 2021).

In this work, we explore the relationships between CH_4 and CO_2 emissions fluxes and environmental variables from a group of four different coastal wetlands located in the province of Ravenna, an area in the Northern Adriatic coastal zone (Italy). The selected four different ecosystems are located along a salinity gradient, ranging from fresh- to strong-brackish water and, being near to each other, belonging to the same climate zone. This set-up offers the opportunity to closely investigate physical-chemical environmental drivers and their relationships with CH_4 and CO_2 production. Our findings can be useful for modelling the C cycle accounting in temperate coastal wetlands improving environmental management strategies and evaluating climate change future trends (increase in temperature, sea level rise, change in precipitation patterns).

In this chapter, after the characterization of the study area (Section 2.2), we examine the physical and chemical variables that affect CH_4 and CO_2 production (Section 2.3) and provide a detailed analysis of the relationships between the environmental variables and the measured gases (Section 2.4). We close by discussing the meaning of the findings for future environmental management.

2.2 Materials and methods

2.2.1 Study Area

The study area is located along the Northern Adriatic Coast, in the province of Ravenna (Italy) (Fig. 2.1) and includes four natural wetlands in pristine conditions named *Punte Alberete*, *Pirottolo*, *Cavedone* and *Cerba*, delimited to the North by the Lamone River and to the South by the Cerba channel. The entire area is part of the Po River Delta Natural Park, protected by the European Union legislation (Punte Alberete SCI/SPA IT4070001 and San Vitale pine forest IT4070003; EEC 1979; 1992). The site is characterized by a temperate climate with an annual rainfall of about 643 mm (data from Dext3r website (https://simc.arpae.it/dext3r/), mainly concentrated in autumn and spring. Temperatures range from 24 °C in summer to 3 °C in winter (Zannoni, 2008b), with a mean annual temperature of 13.3°C (Zannoni, 2008b) . Precipitations, temperature and evapotranspiration greatly influence the water table, saltwater intrusion (Laghi et al., 2010; Giambastiani et al. 2021) and soil salinity (Buscaroli and Zannoni, 2017a)

The topography of this area lies below mean sea level and the coastal area is prone to saltwater intrusion for both natural (subsidence and high hydraulic conductivity) and anthropogenic stressors (Antonellini et al. 2010; Giambastiani et al. 2021); riverbanks, palaeodunes in the forest and current coastal dunes constitute the highest areas with an elevation of 1-3 m a.s.l. The alternation of highs and lows in the topography, which correspond to different past coastlines and the different stages in the Po Delta evolution (Amorosi et al., 1999) affects vegetation distribution.

The water table is around 0 m a.s.l. or below sea level, and the coastal phreatic aquifer is salinized with the occasional presence of shallow freshwater lenses floating on brackish-salty water and shallow freshwater–saltwater interface (Antonellini et al. 2008a; Giambastiani et al. 2021). During the dry and warm season, the water table decreases (Giambastiani et al., 2021) and groundwater salinity increases in most of the area, as shown in Fig. 2.1b. Salinization of surface and ground waters is especially significant in, and along, canals and rivers, and close to the Piallassa Baiona lagoon, which is directly connected to the Adriatic sea (Fig. 2.1; Antonellini et al. 2008a).

The entire study area is subjected to mechanical drainage that is necessary to manage floodwater and allow nearby farmland activities by maintaining constant water table depth in the range of 1.5-2 m

below ground level during the year (Soboyejo et al., 2021). The complex system of drain canals and water pumping stations avoids flooding but creates a general inland-directed hydraulic gradient with consequent saltwater intrusion from the lagoon and sea (Giambastiani et al., 2021). The water level is also controlled in large areas of the wetlands, some of which are kept constantly flooded thanks to a system of ditches and sluices. Given the naturalistic and ecological importance of these wetlands, water quality and water table management are crucial for preserving these environments against the ongoing salinization process.

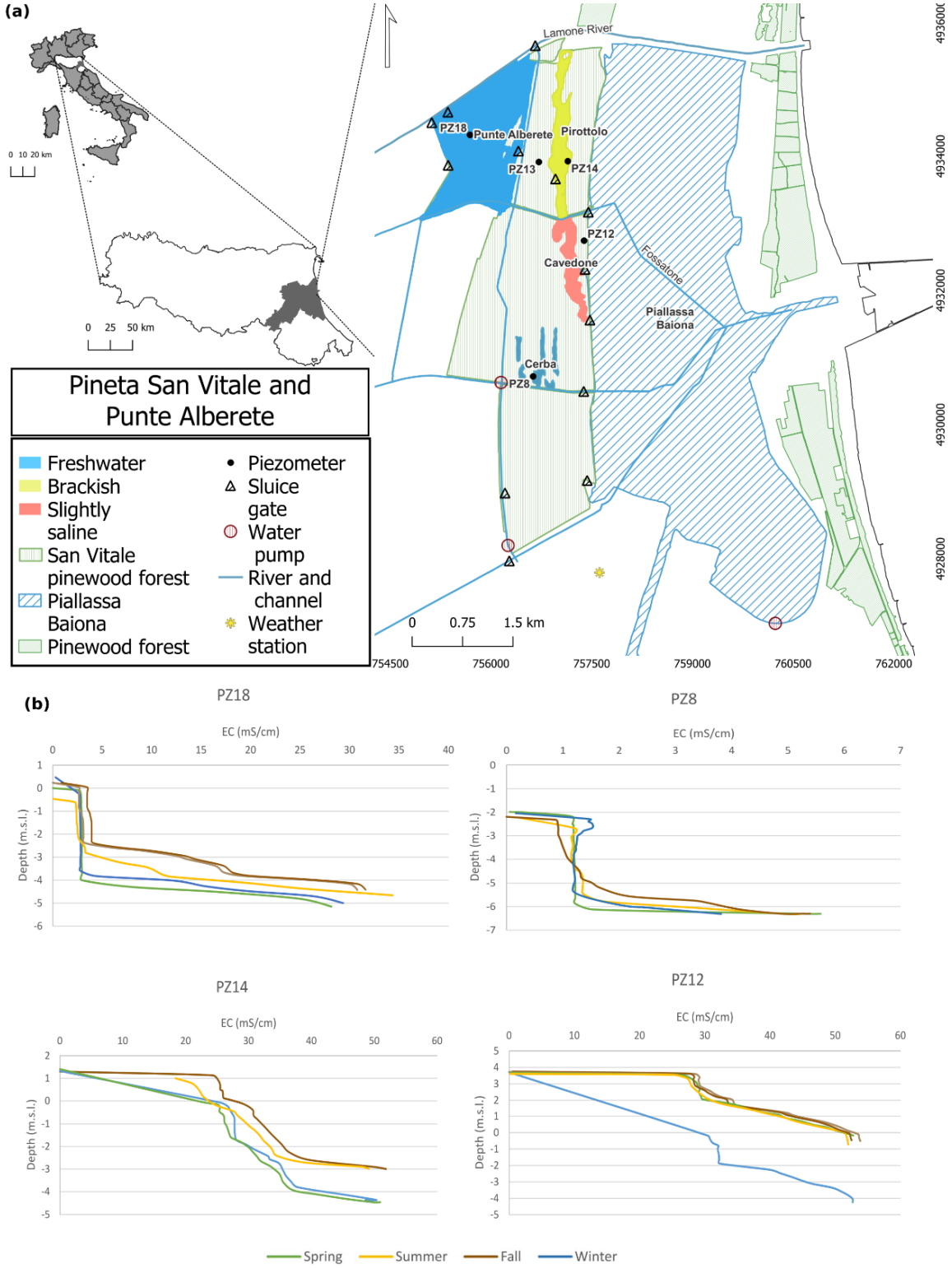

Fig. 2.1 – (a) Study area (EPSG: 32632 – WGS 84 UTM zone 32N) and (b) vertical distribution of groundwater electrical conductivity (EC in mS/cm) measured in four piezometers located in the four selected wetlands during the sampling period.

2.2.1.1 Punte Alberete

The site of *Punte Alberete* (PA) (Fig.2.1), about 190 ha, is a predominantly hygrophilous forest dominated by *Fraxinus oxycarpa, Ulmus minor, Populus alba*, and *Salix alba* (Merloni and Piccoli, 2001). The area is almost permanently flooded, and sediment grain size is typically fine (<64 μm). The sediments are calcareous and moderately alkaline. It alternates microenvironments and plant formations depending on the depth and seasonal variation in water levels. A predominance of common reed patches of hygrophilous and flooded forests is observed (RER, 2018b). The sedimentary substrate is calcareous and characterized by fine-grain size (<64 μm) in the western part and coarser in the eastern part. Soils have different textures depending on the substrate, are calcareous, moderately alkaline and with superficial organic horizons (RER, 2021). *Punte Alberete* is classified as "wetlands of international importance" under the Ramsar Convention and falls entirely within a protected oasis (EEC, 1979; 1992; RER, 2018b). The local municipality is in charge of the management of the area, and specifically of vegetation, and water levels. The water inflow is through a sluice located on the right bank of the Lamone River. This area is characterized by the presence of superficial inflow: water flows westward along the west perimetral canal till the *Fossatone Canal*, and from here it feeds the entire forest through sub-lagoonal canals. This area is characterized by the presence of surface freshwater, and a slightly saline deep groundwater (Fig. 1b) (Giambastiani, 2007). Part of the Lamone water comes from the *Canale Emiliano Romagnolo* (CER), which is the channel that brings the Po River water to the Romagna region for drinking, agricultural, and industrial uses. The water recharge of the area is often stopped in summer (June-August) when the mowing of the halophytic vegetation is often performed.

2.2.1.2 Cerba

The monitored site belonging to the *Cerba* area (CER) is an elongated wetland located between palaeodunes deposited between the 10th and 15th century at the mouth of the Po River delta (Lazzari et al., 2010; Regione Emilia Romagna 2018a). On a larger scale, the site is part of the *San Vitale* pine forest, the northernmost of the coastal forests that historically separated the city of Ravenna from the sea. The forest is characterized by a succession of ancient dune belts and interdunal wetlands, with sandy and calcareous soils forming on sandbar deposits consolidated by old forestations (Zannoni, 2008; Vittori Antisari et al., 2013; Ferronato et al., 2016; RER 2018a). Here, soils with thinner vadose zones may accumulate salts in the surface horizons during the summer season (Buscaroli and Zannoni, 2017). In this area surface water is fresh, whereas groundwater becomes increasingly saline with depth (Fig. 2.1b) (Giambastiani, 2007).

2.2.1.3 Bassa del Pirottolo

The northern part of the *San Vitale* pine forest is crossed from north to south by the *Bassa del Pirottolo* (PIR), a reed swamp of fresh and brackish water located in an interdunal zone. The swamp originates from the southern bank of the *Lamone* River and is crossed in the east-west direction by numerous feeder canals ((Vittori Antisari et al. 2013; RER 2016; 2018a). The water here is superficially slightly saline till becoming brackish along the depth (Fig. 2.1b) (Giambastiani, 2007) The soils have a medium-grain sandy, sandy-loam texture and hydromorphic or subaqueous features (Vittori Antisari et al., 2013; Ferronato et al., 2016).

2.2.1.4 Buca del Cavedone

The *Buca del Cavedone* (CAV) wetland is located south of the *Bassa del Pirottolo* and has slightly brackish water. This strip of interdunal lowlands extends until the adjacent *Pialassa Baiona* (Vittori

Antisari et al. 2013; RER 2018a) and has sandy, calcareous soils with subaqueous features (Ferronato et al., 2016). Shallow water is medium saline, with salinity increasing along the depth, till reaching very saline concentrations (Fig. 2.1b) (Giambastiani, 2007). The area is permanently flooded. The progressive water freshening due to freshwater inflow from the *Fossatone* canal and isolation from the *Pialassa Baiona* basin is causing the disappearance of the halophilic vegetation. This habitat is of considerable naturalistic and ecological value, with rushes and large open-water pools harbouring submerged hydrophyte communities, typical of still water (RER 2018a).

2.2.2 Data collection

2.2.2.1 Gas fluxes

Field observations were collected once a month from April 2021 to June 2022 for a total of 748-point fluxes observations (Tab.2.1A – Appendix). Direct measurements of gas fluxes from soils and standing water were performed by a portable CH_4-CO_2 flux-meter (West Systems srl, Pontedera, Italy) equipped with two infrared spectrophotometer detectors: (i) Licor 8002 for CO_2 and (ii) tunable laser diode with multipass cell for CH_4. All measurements were retrieved using a dark chamber, equipped with a floating device for measurements on standing water (Fig. 2.2), recording a measurement approximately every 15-20 m along a transect or the wet border of the wetland. Spacing depended on environmental conditions and settings. (Fig.2.3). Every point was georeferenced by GPS included in the portable fluxmeter.

Gas flux measurements were based on the accumulation chamber "time 0" method (Cardellini et al., 2003; Capaccioni et al., 2015). Based on the linear regression of increased CH_4 and CO_2 concentration values over time inside the dark chamber, fluxes from single-point sources were estimated, using the Flux Revision Software produced by West System s.r.l. (Giovenali et al., 2013). Based on the lowest sensitivity limit of the instrument indicated by the manufacturer, a value of 0.05 mol/m2/day was assigned to all fluxes larger than zero and lower than the sensitivity limit to avoid errors (0.2 mol/m^2). The 21 negative measurements and the 55 zero measurements were considered incorrect and thus removed from the dataset, resulting in 671 single observations used for data analysis.

Soil samples were collected using a soil corer and extracting a 40 cm long core. The samples were weigheded and later dried in the oven for 24 hours at 105°. The dry weight was used to obtain bulk density (Al-Shammary et al., 2018). Later the sample was homogenized in a mortar to perform loss-on-ignition analysis: 2-3 gr of the sample were then dried in crucibles in a furnace for 8 hours, gradually increasing the temperature from 100°C to 450°C (Roner et al., 2016). After cooling, all samples were reweighted and organic carbon contents were calculated (Roner et al., 2016).

Fig. 2.2 - Measuring GHGs fluxes with accumulation chamber on (a) deep and (b) shallow water with floating device, and on (c) flooded soils.

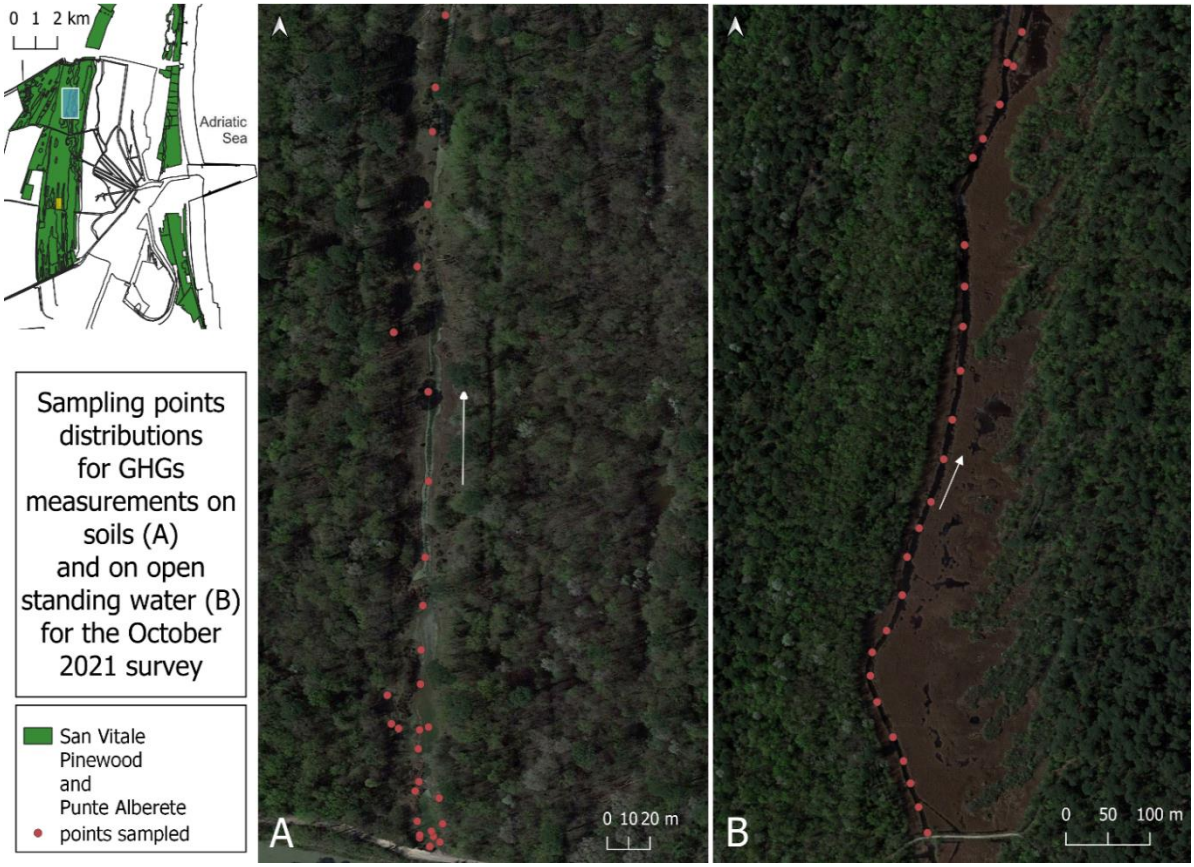

Fig. 2.3– Example of distribution of points measurements in both type of sampling: soil (a) and open standing water (b).

2.2.2.2 Environmental variables

Monthly physical-chemical parameters such as EC, pH, Eh and T of surface water were retrieved using Eutech probes connected to a data logger in all four sites. All measurements were repeatedly performed in the same spot for every location. Moreover, four piezometers at 6 m depth were monitored to retrieve monthly physical-chemical parameters for groundwater in every location. A

phreatimeter and level logger were used to measure water table level, EC, T and pressure, respectively (Fig. 2.1a).

Irradiance was retrieved monthly from both in-situ measurements and the nearby ARPAe (Regional Agency for Prevention, Environment and Energy of Emilia-Romagna) weather station of Ravenna (Fig. 2.1a), whose data are available from the Dext3r website (https://simc.arpae.it/dext3r/). The local weather station also provided atmospheric pressure measurements to calibrate the calculation of the gas fluxes.

Finally, water samples were collected monthly at each station and in the same spot to measure SO_4^{2-} concentrations by using a HACH DR/2010 spectrophotometer.

2.2.2.3 Statistical Analysis

All data were tested for normality distribution using the Shapiro-Wilk Normality Test (Package *stats* version 4.2.1) and for homoscedasticity with the Fligner-Killeen Test (Package *stats* version 3.6.2) in R (version 4.2.2).

Principal Component Analysis (PCA) is a multivariate statistical technique used to analyse the linear components of the considered variables. PCA was used to summarize and visualize the relationships between CH_4 and CO_2 fluxes with environmental variables by using the "FactoMineR" (Lê et al., 2008) and "factoextra" (Komlan Mawuli Afiademanyo et al., 2020) R packages. Variables have been previously standardized using the function "scale.unit" in the "FactoMineR" package. The first principal component PC1 captures the maximum variance in the dataset, whereas the second principal component captures the remaining variance in data and is uncorrelated with PC1. In a Cartesian plane with the first and the second PCs as principal axes, the point measurements of the several variables considered in this study were plotted and a vector was calculated for each variable. Variable vectors which are close to each other are positively related while opposing variables are negatively related.

We also investigated the sample structure through the score plot. The position of observations along the components indicates similarities between the samples that are positioned close to each other. Observations particularly influenced by a specific variable will be positioned along its vector.

Autocorrelations between CH_4 emissions and environmental variables were calculated using the Pearson's and Spearman's correlation matrix in the R "ggplot2" package (Wickham, 2016). Initially only Pearson's correlation was considered for this study while Spearman's correlation being indicated for non-normal distributed data. The two types of correlation gave similar results, with Spearman better highlighting correlations between environmental variables. Data have been tested for normality and homoscedasticity using the function "shapiro.test" and "fligner.test " of the R package "stats" ver. 4.3.3 (R Core Team, 2023), respectively. The same package was used to compute the probability density function (PDF) of CH_4 and CO_2 fluxes. The effect of different environmental variables was statistically proven by the Mann Whitney test function performed with the "ggstatsplot" package in R (version 0.10.0).

2.3. Results

2.3.1 GHG fluxes and environmental variables

2.3.1.1 Environmental variables

For a general overview, data are divided into two groups, i.e. those collected in the Fall/Winter (FW) period and those collected in the Summer/Spring (SS) period (Tab.2.1).

PA is always the site with the coldest water temperature (9.4 °C in FW and 18.7 in SS), and the lowest water EC value (0.67 mS/cm in both FW and SS) of the whole study area for both seasons. This site also always has the second-highest water column levels (51 cm in FW and 58 cm for SS) of the overall study area, and the lowest irradiance values (139.7 W/m^2 in FW and 532.2 W/m^2 in SS).

CER, while still being a freshwater site, has a higher salinity than PA during both seasons (1.49 mS/cm in FW and 2.24 mS/cm in SS) and records the highest mean water temperature in SS (22.3 °C). In the same period, also air temperature had one of the highest values recorded during the field campaign (25.1°C). CER is also the site where the mean water column is the lowest (14 cm in FW and 19 cm in SS), and the mean irradiance is the highest (486.4 W/m^2 in FW and 650.5 W/m^2 in SS) during both SS and FW. CER has the lowest mean soil content of organic matter (1.4%) of the four sites.

PIR has the second-highest value of EC (7.06 mS/cm in FW and 6.79 mS/cm in SS) of all four sites during both seasons and it has the second-highest concentration of SO_4^{2-} during SS (640.8 mg/l). PIR is also the site with the highest water column level during both seasons (80 cm in FW and 72 cm in SS), and the highest mean content of organic matter in the sediments (2.2%) but the lowest bulk density (1 g/cm^3).

CAV is the site with the highest EC of all studied areas during both seasons (38.85 mS/cm in FW and 21.97 mS/cm in SS), and the highest concentration of SO_4^{2-} during SS (875.1 mg/l). Here, the mean air temperature is the lowest of all sites during FW (13°C). For this site, no record of the water column level is collected, due to fluxes being always under the detection limit of the instrument.

Tab. 2.2 (A) Mean seasonal values ± standard deviation for recorded environmental parameters. No values for the water column in CAV were collected; (B) Mean values of bulk density and organic matter content were measured on soil cores.

(A)	Parameters	n. total samples per site	Punte Alberete (PA)	Cerba (CER)	Bassa del Pirottolo (PIR)	Buca del Cavedone (CAV)
Fall-Winter (FW) (Oct-Feb)	T air (°C)	14	15.4 ± 3.91	16.2 ± 4.9	14.6 ± 2.11	13.0 ± 4.54
	T water (°C)	14	9.4 ± 3.14	10.9 ± 3.85	11.7 ± 1.6	14.6 ± 3.82
	EC (mS/cm)	14	0.67 ± 0.12	1.5 ± 0.35	7.06 ± 5.15	38.85 ± 6.03
	Irradiance (W/m^2)	14	139.7 ± 201.06	486.4 ± 185.13	294.2 ± 259.86	224.3 ± 133.31
	Water column (cm)	14	51 ± 14.89	14 ± 10.96	80 ± 18.99	-
	SO_4^{2-} (mg/l)	CAV=10, CER=10, PIR=14, PA= 12	342.86 ± 593.11	136.50 ± 104.22	911.88 ± 780.10	905± 654.2935
Spring-Summer (SS) (March-Sept)	T air (°C)	14	23.0 ± 4.59	25.1 ± 6.3	22.6 ± 5.25	22.8 ± 4.97
	T water (°C)	14	18.7 ± 3.35	22.3 ± 4.94	21.1 ± 5.25	22.9 ± 5.07
	EC (mS/cm)	14	0.67 ± 0.20	2.2 ± 0.85	6.79 ± 4.54	21.97 ± 11.47
	Irradiance (W/m^2)	14	532.2 ± 198.99	650.5 ± 221.15	604.4 ± 217.90	619.7 ± 287.31

	Water column (cm)	14	58 ± 26.05	19 ± 10.33	72 ± 23.01	-
	SO_4^{2-}(mg/l)	CAV=10, CER=10, PIR=14, PA= 12	292.6 ± 343.17	89.69 ± 154.2	686.09± 933.37	875.1± 550.95
(B)	**Parameters**	**n. total samples per site**	**Punte Alberete (PA)**	**Cerba (CER)**	**Bassa del Pirottolo (PIR)**	**Buca del Cavedone (CAV)**
Mean value (April '21-June'22)	**Bulk Density (g/cm^3)**	CAV=5, CER =5, PA=4, PIR=4	1.1 ± 0.36	1.2 ± 0.11	1.0 ± 0.30	1.3 ± 0.33
Mean value (April '21-June'22)	**SOM (%)**	CAV=5, CER =5, PA=4, PIR=4	1.5 ± 1.37	1.4 ± 0.16	2.2 ± 0.61	1.5 ± 0.78

2.3.1.2 GHGs fluxes

Fig. 2.4 shows the seasonal pattern in the CH_4 emissions recorded through the sampling campaign. Higher fluxes are recorded throughout the spring and summer months, declining in winter and fall. Also, fluxes in freshwater environments (PA and CER) are often higher than those recorded in brackish environments (PIR and CAV).

CH_4 and CO_2 fluxes in PA are always lower than those recorded in CER while being both sites characterized by the presence of freshwater. During SS in particular, PA has the lowest mean flux of CH_4 of the whole study area (6.04 g/m^2/day), while CER is the highest (254.09 g/m^2/day) (Tab.2.2).

The highest mean values of CH_4 and CO_2 for both seasons are recorded in CER (Tab.2). Mean CH_4 fluxes account for 61.83 g/m2/day during the FW and 254.09 g/m^2/day during the SS, and CO_2 fluxes for 20.34 g/m^2/day during the FW and 100.62 g/m^2/day during the SS (Tab. 2.2).

In PIR, CH_4 are 1.99 g/m^2/day in FW and 15.80 g/m^2/day in SS, among the lowest during SS, except for PA. CO_2 fluxes are 16.02 g/m^2/day in FW, the lowest record for the season, and 19.37 g/m^2/day in SS (Tab. 2.2).

CAV is the site with both the highest salinity and the lowest emissions. CH_4 and CO_2 fluxes are the lowest during the FW with a recorded mean value of 1.10 g/m^2/day and 2.16 g/m^2/day, respectively.

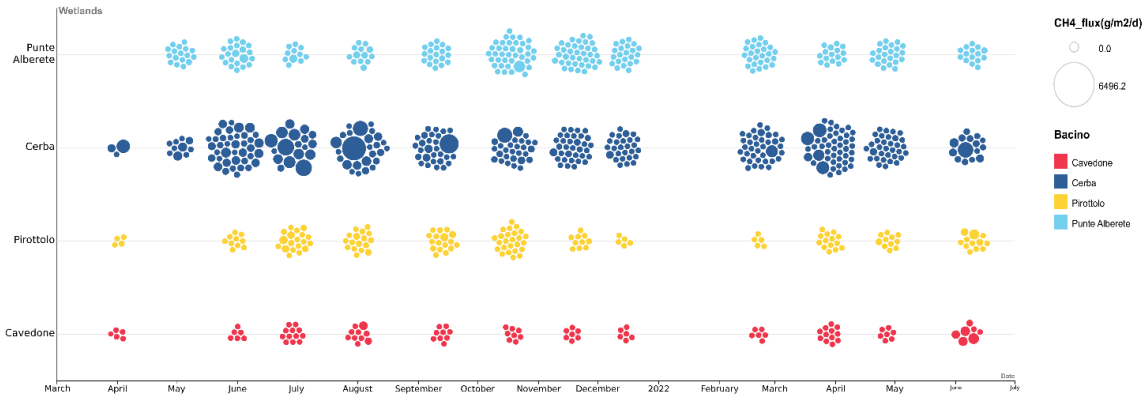

Fig. 2.4 -Bubble graph representing CH_4 fluxes from June 2021 to July 2022 in the four studied wetlands. During January 2022 it was not possible to perform measurements due to frosting.

Tab. 2.3 Seasonal values for CO_2 and CH_4 fluxes. SD= Standard Deviation; CV (%) = Coefficient of Variation.

Season	GHGs fluxes ($g/m^2/day$)	Punte Alberete (PA)		Cerba (CER)		Bassa del Pirottolo (PIR)		Buca del Cavedone (CAV)	
Fall-Winter (Oct-Feb)		CO_2	CH_4	CO_2	CH_4	CO_2	CH_4	CO_2	CH_4
	n. points	80	80	121	121	37	37	20	20
	mean	8.62	7.56	20.34	61.83	16.02	1.99	2.16	1.10
	max	69.74	184.15	270.62	1269.68	29.81	6.55	6.67	1.21
	min	0.22	2.17	0.27	2.17	9.43	2.17	0.24	2.17
	SD	13.87	33.67	54.26	250.44	7.83	1.90	0	0.00
	CV(%)	160.92	445.58	266.77	405.02	48.88	95.70	0	0.00
Spring-Summer (March-Sept)	GHGs fluxes ($g/m^2/day$)	Punte Alberete (PA)		Cerba (CER)		Bassa del Pirottolo (PIR)		Buca del Cavedone (CAV)	
		CO_2	CH_4	CO_2	CH_4	CO_2	CH_4	CO_2	CH_4
	n. points	122	122	177	177	84	84	51	51
	mean	12.38	6.04	100.62	254.09	19.37	15.80	21.83	33.63
	max	66.37	52.33	626.39	2214.42	66.53	119.41	89.33	110.18
	min	2.80	2.17	8.34	2.17	7.22	2.17	3.10	2.17
	SD	17.20	12.65	157.87	549.93	18.11	33.89	30.18	39.10
	CV(%)	138.97	209.55	156.90	216.43	93.52	214.52	138.25	116.27

2.3.2 Principal Component Analysis

2.3.2.1 PCA results

PCAs analysis is performed considering separately CO_2 and CH_4 fluxes to better investigate their correlation with the environmental variables and the two Principal Components that better explain the most variance percentages.

In this section, PCA analysis on fluxes from soils and water is presented jointly. Fig. 2.5 shows the plots of PC1 and PC2 for CH_4 (Fig. 2.5a) and CO_2 (Fig. 2.5b) and all measured environmental variables. For CH_4 in particular the two components explain 63.9% of the total variance, and specifically PC1 explains 38.5% and PC2 25.4% of variance (Fig. 2.6). Water temperature, air temperature and irradiance are clustered in one group to the right, indicating close relation among each other. They all increase as the PC1 increases, while they are barely affected by PC2. CH_4 emissions also increase as the PC1 increases, but they increase as PC2 decreases. On the contrary, both salinity and SO_4^{2-} increase as PC2 increases, showing a limited contribution of PC1 (Fig. 2.5a). This result shows a positive correlation between CH_4 production, water and air temperature, and irradiance, whereas CH_4 production is negatively correlated to salinity (Fig. 2.7).

Points in the biplot represent the field measurements. Plotted in Fig. .5a, points in red represent data collected at CAV and have in general higher PC2 values than those collected in the other three study sites. Their distribution goes accordingly with the strong positive correlation between PC2 and salinity, and CAV presenting higher salinity values than the other sites. Similarly, CAV appears to be the site with the lowest CH_4 emissions in the FW period (Tab.2.2), given that CH_4 emissions increase as salinity decreases. We conclude that measurements performed in brackish environments such as CAV are characterized by generally lower emissions if we compare them to those measured in freshwater sites.

When the PCA is performed on CO_2 and the observed environmental variables, PC1 explains 38.6 % and PC2 24% of the total variance, accounting together for 62.6% of the total variance (Fig. 2.8). The

results are shown in Fig. 2b. Similarly, to the results obtained for CH_4, water and air temperature and irradiance cluster together, highly contributing to PC1. These variables also show a positive correlation with CO_2 production and are highly correlated within themselves (Fig.2.9). On the contrary, salinity is displayed along PC2 and shows a negative correlation with CO_2 emissions.

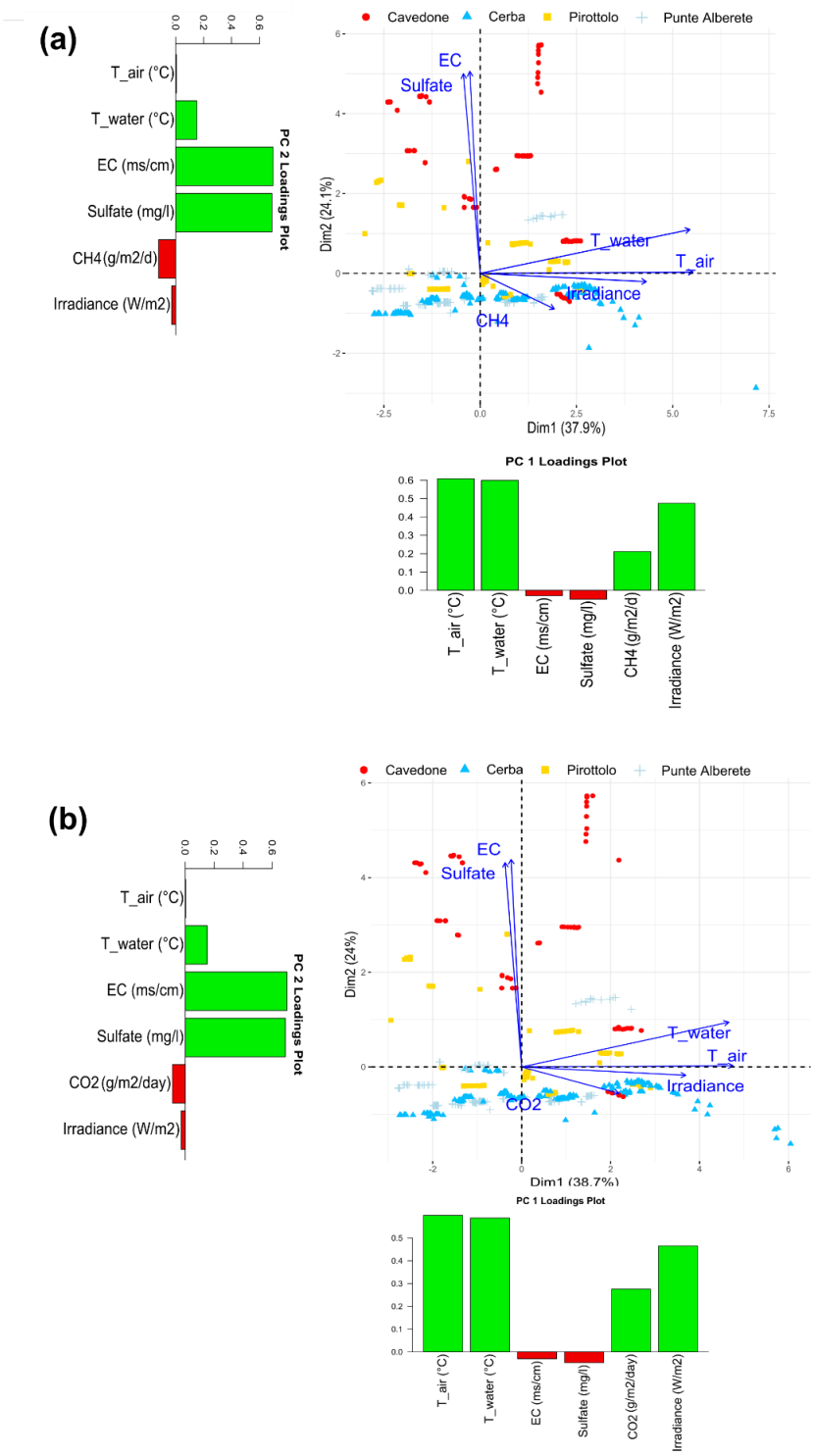

Fig. 2.5 – Biplot representing PC1 and PC2 for (a) CH_4 fluxes and the observed environmental variables, and (b) CO_2 fluxes and the observed environmental variables. Along the axis of the biplot, the histograms report the loadings values for the respective component.

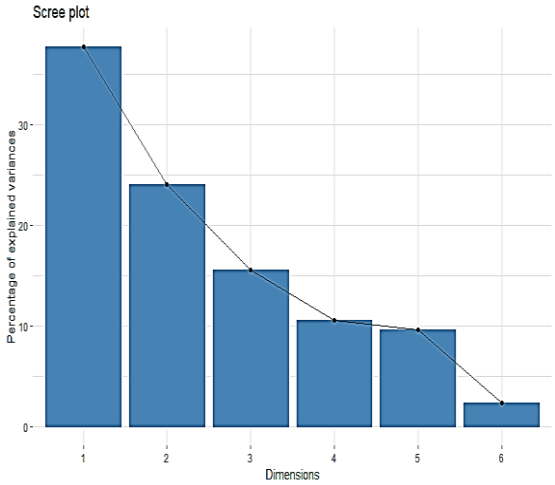

Fig. 2.6– Scree plot of PCA analysis for CH_4 fluxes and environmental variables

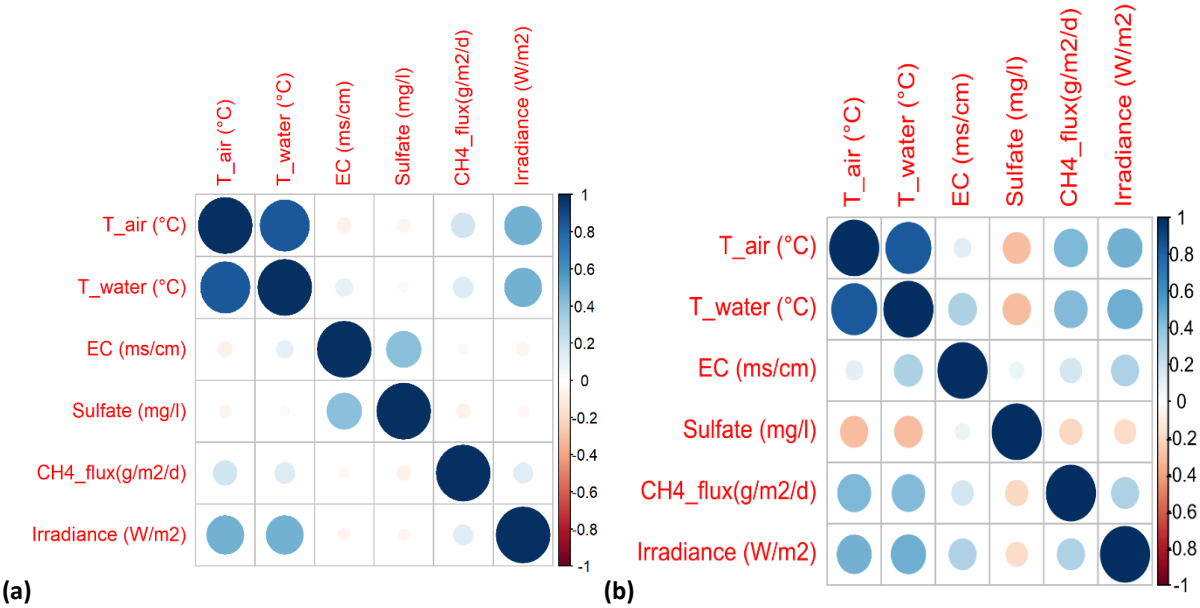

Fig. 2.7 – Correlation matrix with (a) Pearson's correlation and (b) Spearman's correlation for CH_4 fluxes and environmental variables

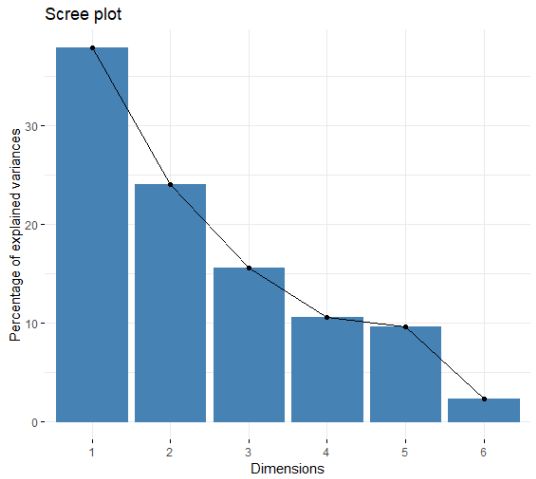

Fig.2.8 – Scree plot of PCA analysis for CO_2 fluxes and environmental variables

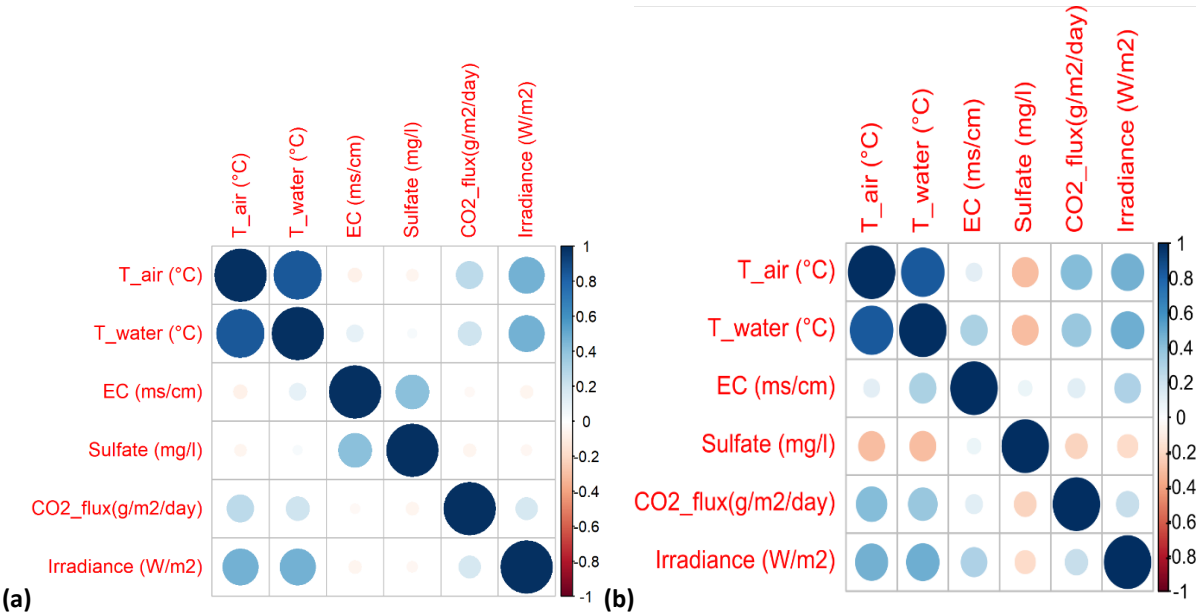

Fig. 2.9 - Correlation matrix with (a) Pearson's correlation and (b) Spearman's correlation for CO_2 fluxes and environmental variables

2.3.3 GHGs fluxes from flooded areas

Considering exclusively fluxes measured on flooded areas, i.e. areas permanently or seasonally characterized by the presence of water, Tab. 2.3 summarizes the results.

In PA, CH_4 fluxes are relatively low (5.04 g/m^2/day) with moderate variability, as indicated by the coefficient of variation (CV) of 422.23%. The maximum CH_4 flux (228.49 g/m^2/day) measured at this location suggests occasional spikes in emissions. CER exhibits high mean CH_4 flux (196.98 g/m^2/day) along with CV of 341.95%. PIR shows a mean CH_4 flux of 12.27 g/m^2/day, which is comparable to PA and lower than CER. Tab. 3 includes the values recorded at CAV even though their number is smaller

than the ones obtained at other sites and most values are very low, often close to the limits of the instrument detection, therefore influencing the statistical significance of the data set. Therefore, we excluded this dataset from the analyses described in the next chapters.

The CH_4 flux dynamics underscore the significant variations in methane emissions across the different wetland locations. CER stands out with the highest mean and maximum values of CH_4 fluxes and presenting high variability. PA and PIR also exhibit variability in CH_4 emissions but with lower mean and maximum values.

In PA, the mean CO_2 flux is relatively low (5.67 $g/m^2/day$), and the CV is 86.25%, indicating moderate variability. The maximum CO_2 flux recorded at PA is 47.39 g/m2/day, suggesting occasional picks. CER exhibits a much higher mean CO_2 flux, equal to 71.42 $g/m^2/day$. The maximum CO_2 flux recorded in CER is exceptionally high at 1355.04 $g/m^2/day$, indicating the presence of significant emission spikes. PIR has a mean CO_2 flux of 15.47 $g/m^2/day$ The maximum CO2 flux recorded is 142.62 $g/m^2/day$, indicating intermittent peaks in CO_2 emissions.

Tab. 2.3 Values for CO_2 and CH_4 fluxes measured from standing waters. SD= Standard Deviation; CV (%) = Coefficient of Variation., N. points= points fluxes measured.

	Punte Alberete (PA)		**Cerba (CER)**		**Bassa del Pirottolo (PIR)**		**Buca del Cavedone (CAV)**	
GHGs fluxes ($g/m^2/day$)	CO_2	CH_4	CO_2	CH_4	CO_2	CH_4	CO_2	CH_4
n. points	175	175	129	129	140	140	2	2
mean	5.67	5.04	71.42	196.98	15.47	12.27	1.39	2.17
max	47.39	228.49	1355.04	6496.20	142.62	425.44	2.08	2.17
min	0.22	2.17	0.01	2.17	1.17	2.17	0.69	2.17
SD	4.89	21.26	194.99	673.57	19.89	42.51	0.98	0.00
CV (%)	86.25	422.23	273.04	341.95	128.60	346.58	70.97	0.00

2.3.3.1 PCA results

For the dataset presented in Tab. 2.3, PCA is performed considering CH_4 fluxes and all environmental variables, alternately excluding sulfate and EC (Fig. 2.10a). The analyses are repeated for CO_2 fluxes (2.10b).

PCA performed on CH_4 fluxes is influenced by water column height and SO_4^{2-} concentrations: PC1 and PC2 explain 38.3% and 24% of the variance respectively for a total of 62.3% of the total variance (Fig. 2.11). Similarly, considering EC and water column height in performing the PCA analysis, it is found that PC1 account for 36.1% of the variance and PC2 for 20.1%, for a total of 56.2% of cumulative variance.

Fig. 4 (a and b) shows that air, water temperature, and irradiance vectors cluster together on the right of the graph, suggesting a strong correlation among them. On the opposite side, along PC2, salinity, sulfate and water column increase as PC2 increases, while they are negatively correlated to PC1. CH_4 emissions increase as PC1 increases while decreasing as PC2 increases, therefore showing a negative correlation with both EC and water height. Looking at the distribution of the scores, representing field

observations, their variability is controlled by EC and SO_4^{2-} concentrations, water column height, and CH_4 emissions. All measurements collected in PIR (characterized by brackish waters) fall in the higher part of the graph, where PC2 values are positive whereas those collected in CER (shallow and slightly fresh waters) cluster in the lower section of the graph, and finally observations collected in PA (deep and fresh waters) are in the midsection of the graph.

When CO_2 fluxes are considered together with sulfate and water column height (Fig. 2.12a+b), PC1 and PC2 explain respectively 39.5% and 24% of dataset variance, for a total of 63.5% of the cumulative variance (Fig. 2.13). When performing the same analysis on the dataset considering EC and water height the first two components explain a total of 57.5% of the variance. PC1 account for 37.5% of the variance and PC2 for 20% (Fig. 2.13). In both analyses on CH_4 and CO_2 fluxes, the presence of sulfate can better describe the dataset. The results from the biplot (Fig. 2.12) are similar to those obtained for CH_4 (Fig. 2.10). The vectors of air, water temperature, and irradiance are correlated positively with CO_2 production and distribute along PC1 (Fig. 2.12). EC, sulfate, and water height column follow the PC2 axis and have a negative correlation with CO_2 emissions.

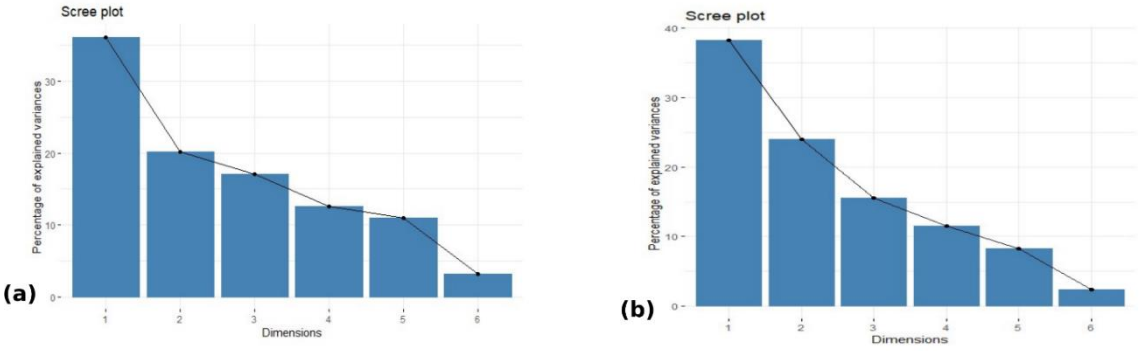

2.11 – Scree plot of PCA analysis for CH_4 fluxes from standing waters and EC (a), sulfate (b), water column depth and environmental variables

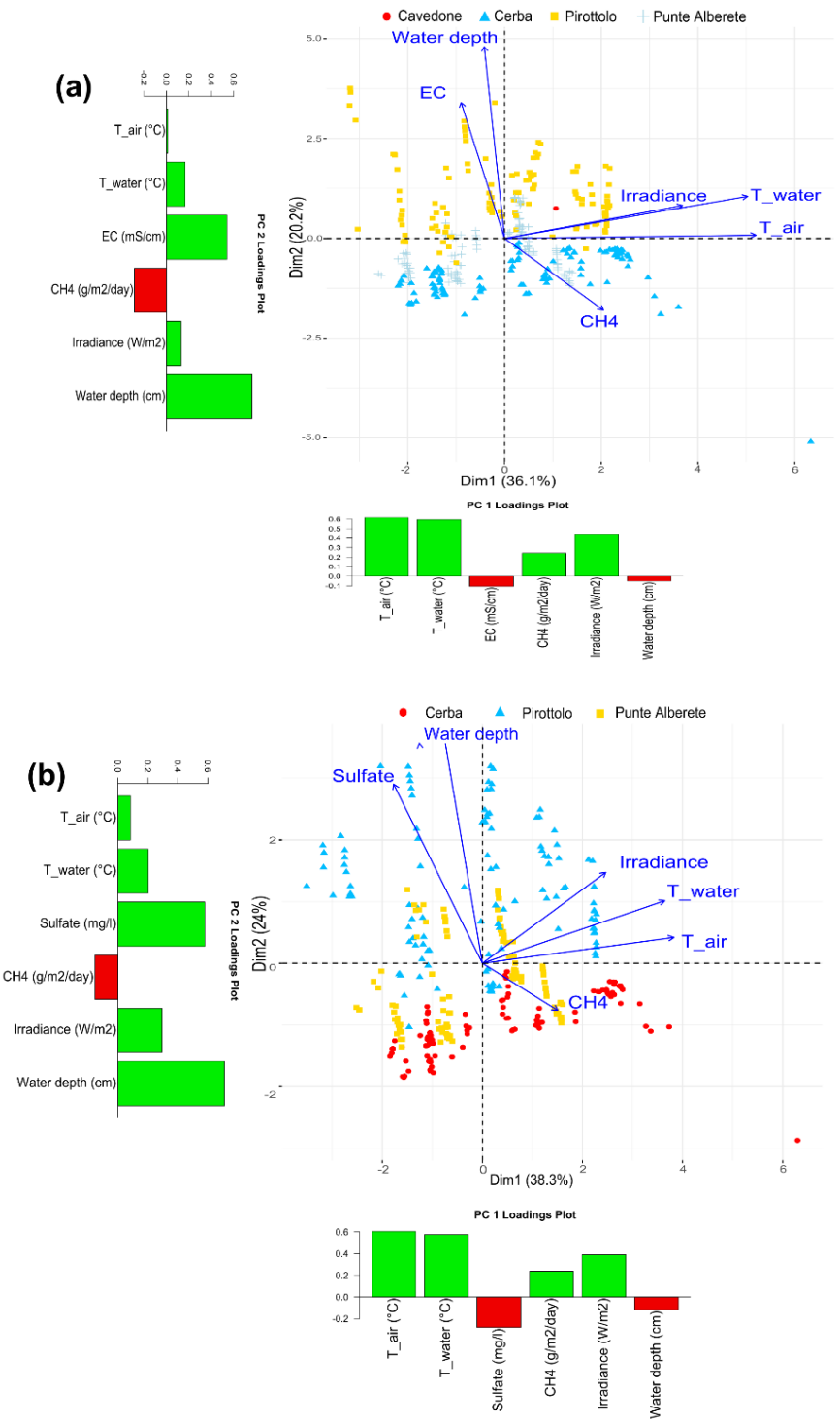

Fig.2.10 PCA analysis of CH_4 fluxes from open waters in flooded areas. The biplot represents the relationships between CH_4 fluxes and salinity (a), sulfate (b) and water column depth.

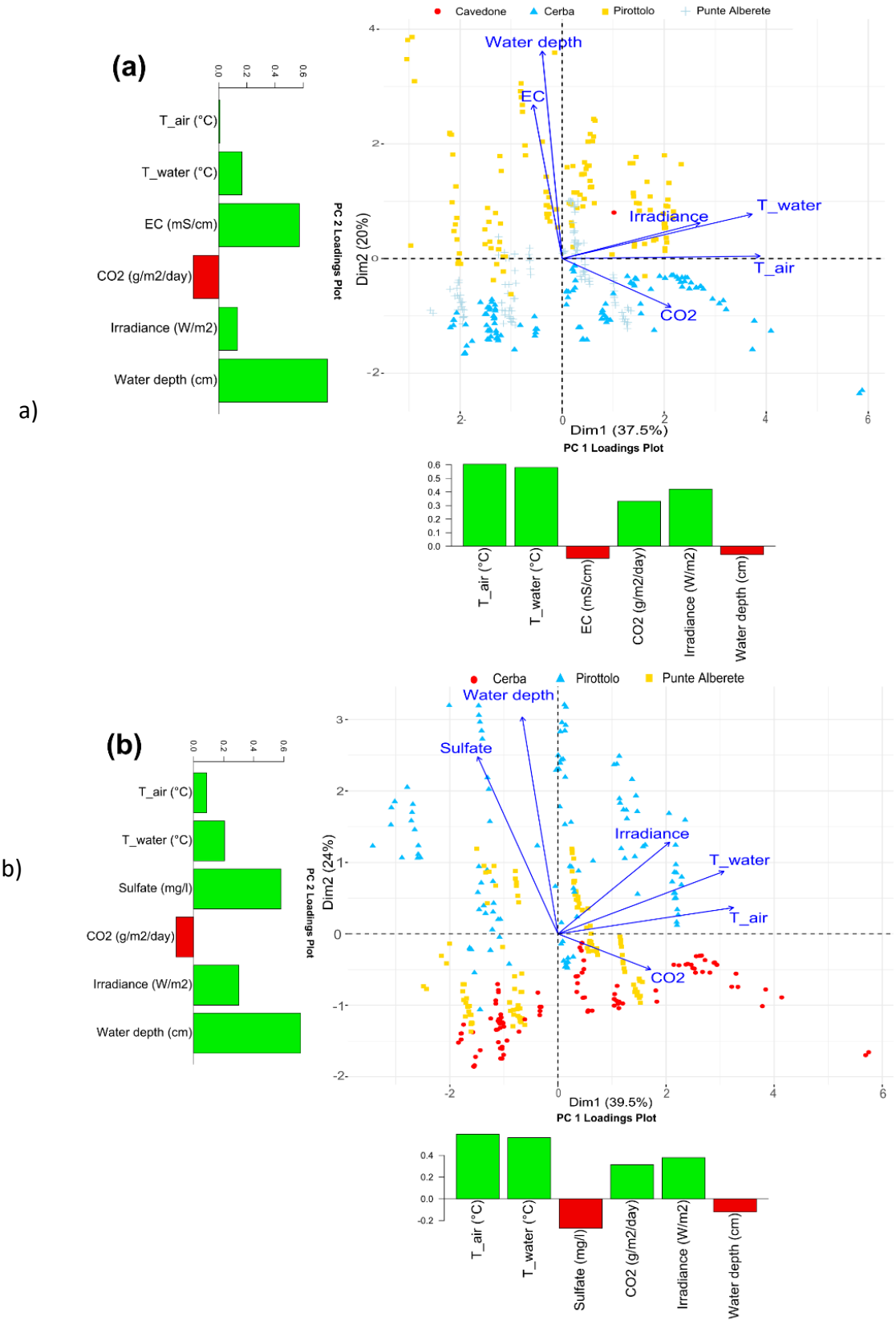

Fig. 2.12 – PCA analysis of CO_2 fluxes from open waters in flooded areas. The biplot represents the relationships between CH_4 fluxes and salinity (a), sulfate (b) and water column depth.

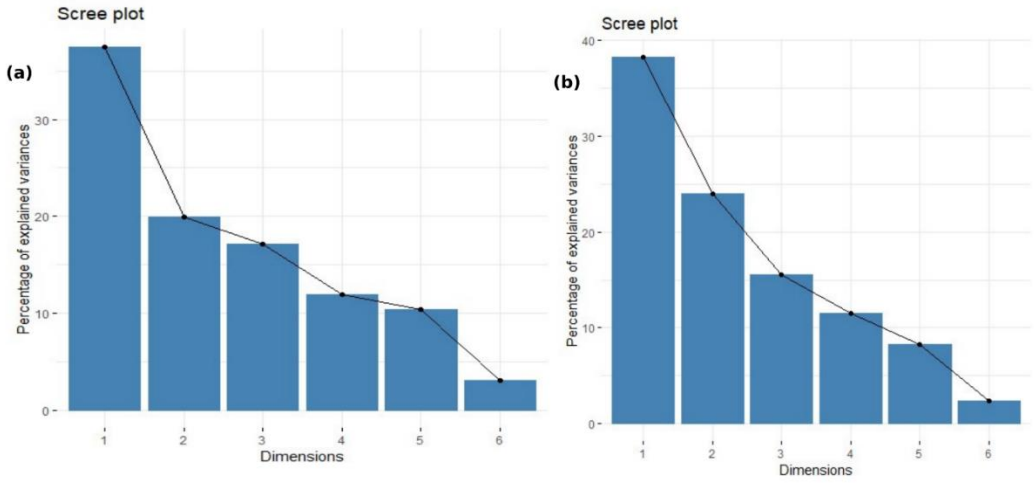

Fig. 2.13 – Scree plot of PCA analysis for CO_2 fluxes from standing waters and EC (a), sulfate (b), water column depth and environmental variables

2.3.3.2 Water column effect

The effect of water temperature and water column height on CH_4 and CO_2 fluxes distribution is examined and shown in Fig.2.14 a-b and 2.14 c-d respectively. High fluxes occur when the water height is lower than 50 cm, tendentially with high temperatures. For larger water heights, the emissions are small despite the presence of high temperatures.

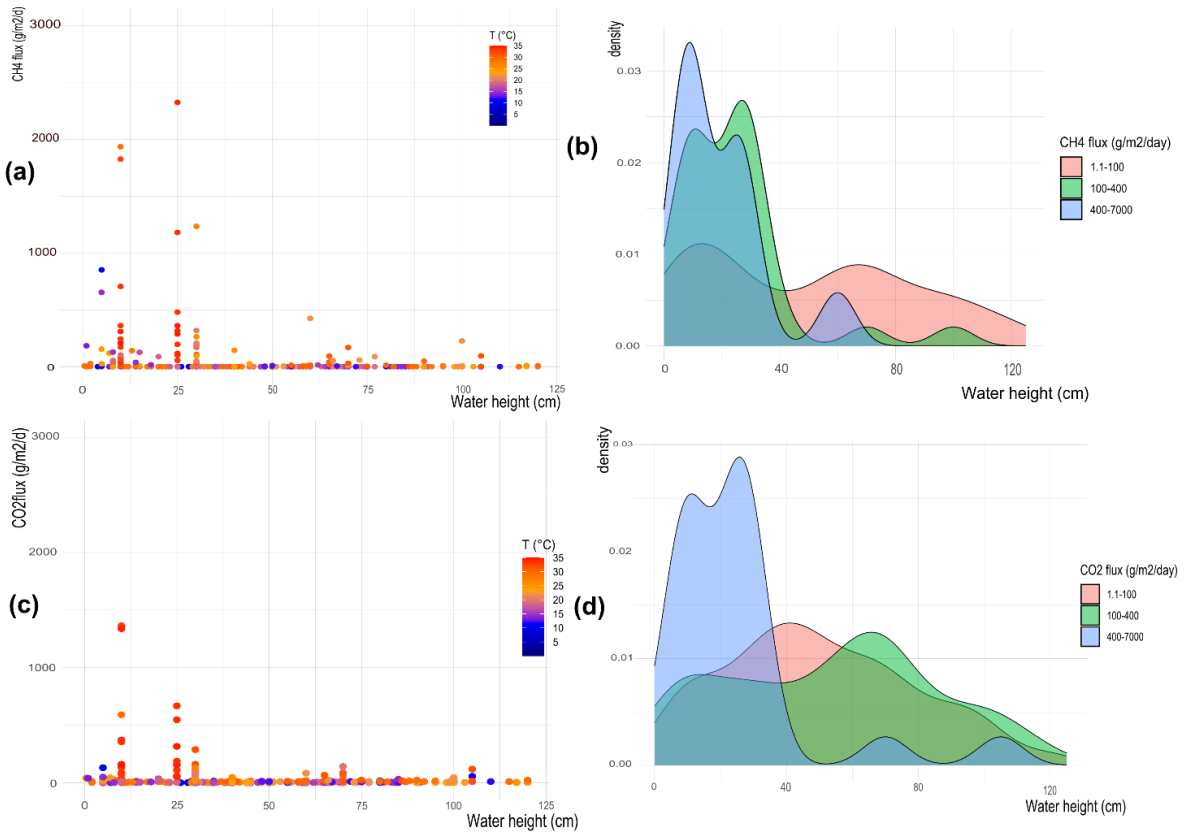

Fig. 2.14- a) and c) Heat maps showing fluxes distribution depending on water column height; the colours indicate the water temperature; b) and d) represent the Probability Density Function (PDF) showing at which water columns height is more probable to observe high (blue), medium (green), and low (pink) fluxes. The top panels are for CH_4 fluxes, while the bottom panels are for CO_2 fluxes.

The Probability Density Function (PDF) in Fig. 2.14b shows the probability of observing certain ranges of CH_4 fluxes for different water column heights. Results show that low fluxes of CH_4 (i.e. 1-100 g/m^2/day) are observed in both shallow and deep waters but medium and high fluxes (i.e. 100-7000 g/m^2/day) are observed only when the water column height is less than 50 cm deep. To further confirm these results, data are grouped into two classes deep (> 50 cm) and shallow (<50 cm) waters. A Mann-Whitney test is run on the two data classes, returning a *p*-value of 4.66 e-06 for CH_4 (Fig. 2.15) confirming that the two classes are statistically different and that there is a threshold depth below which the wetland becomes an important source of CH_4.

The same analysis is applied to CO_2 fluxes (Fig. 2.14c). The heatmap shows a behavior similar to CH_4, with higher fluxes recorded only for low waters, (Fig. 2.14c), independently of the water temperature. The PDF in Fig. 6d confirms that low fluxes of CO_2 (i.e. 1-100 g/m^2/day) are observed in both shallow and deep waters while higher fluxes (i.e. 100-1300 g/m^2/day) are observed only when the water column height is less than 50 cm deep. However, differently from the analysis performed on CH_4 measurements, the Mann-Whitney test shows a non-significant difference for the two water height classes > 50 cm and < 50 cm of water height for CO_2 emissions (p=0.82 for CO_2) (Fig. 2.16).

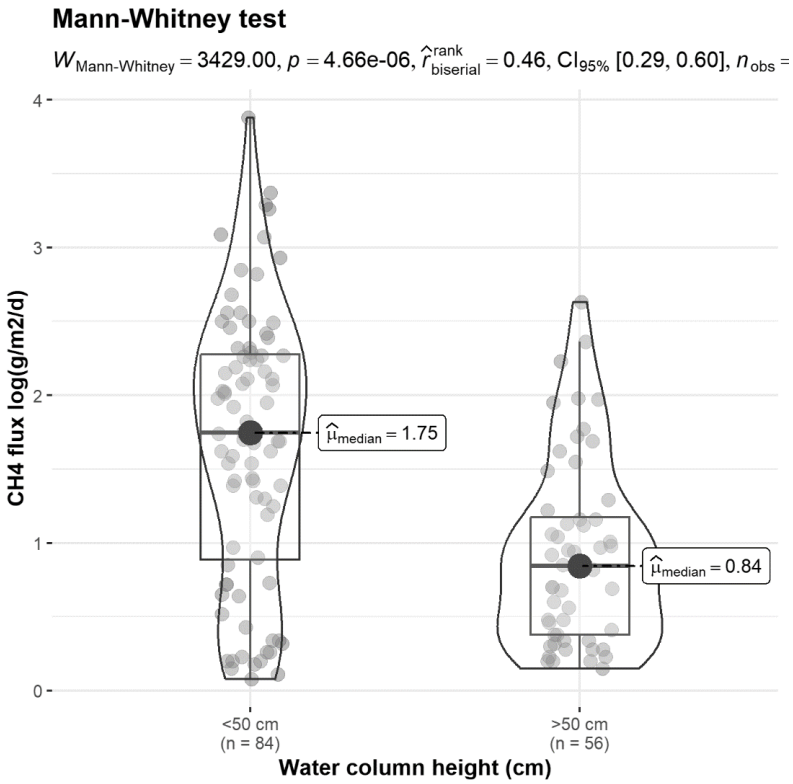

Fig. 2.15 - Mann Whitney test performed between CH_4 measurements from open waters with inundation levels <50 cm and >50cm. The two group are statistically different (***) with p= 4.66 e^{-06}

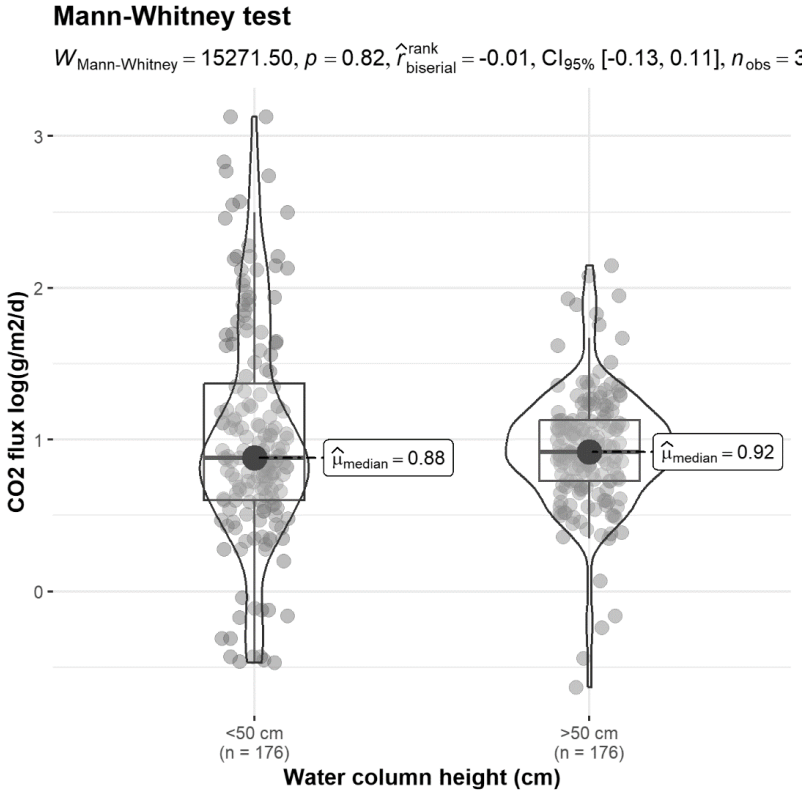

Fig. 2.16 - Mann Whitney test performed between CO2 measurements from open waters with inundation levels <50 cm and >50cm. The two group are not statistically different with p= 0.82.

When the influence of salinity and sulfates is considered, both heatmaps in Fig. 2.17a and Fig. 2.17b show that higher CH_4 emissions are concentrated in the low-left portion of the graphs, i.e. at water heights smaller than 50 cm and low EC and sulfate concentrations, and this happens for both EC and sulfates even though it is more pronounced for sulfate than for EC. When the water level is higher than 50 cm, CH_4 emissions are small, whatever EC and SO_4^{2-} concentrations were measured. We notice that there are no data available for the case of low water-high EC or for low water-high sulfates, we speculate because our study sites do not include shallow salted wetlands.

If we compare Fig. 6a, 6b, 7a and 7b we notice that independently of T, EC and SO_4^{2-}, emissions of CH_4 are low for water heights larger than 50 cm.

Similar results are obtained for CO_2 fluxes. Fig. 2.17c, d show that high CO_2 emissions are only recorded when the water height is lower than 50 cm, while in deeper waters the CO_2 emissions are always small, independently from EC and sulfate concentrations. In line with the results shown for CH_4 fluxes, also in the case of CO_2, we confirm that high values of T, EC and SO_4^{2-} do not influence CO_2 emissions (Fig. 2.14c, 2.14d, 2.17c and 2.17d), that remain small when the water height exceeds 50 cm. As already stated, no data were available for low-salted waters.

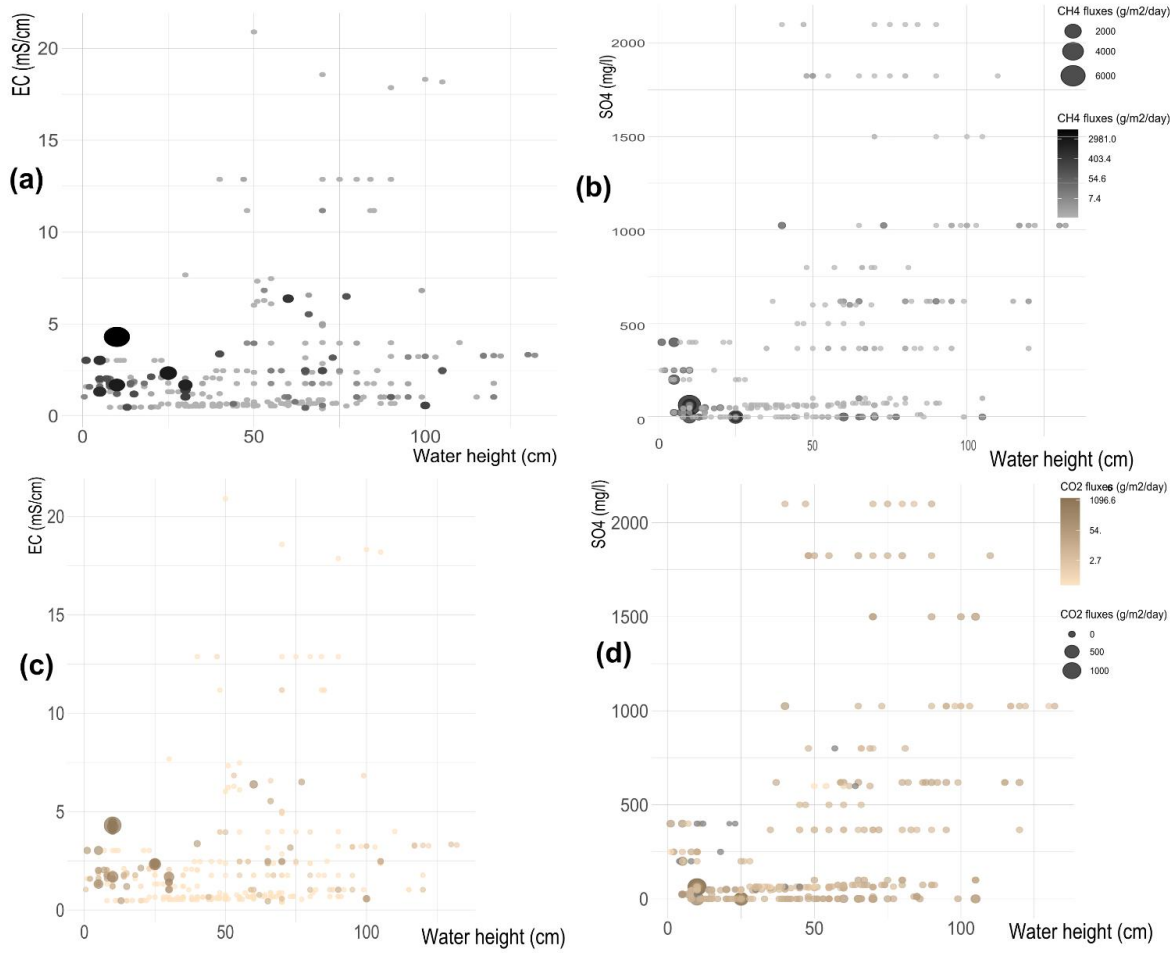

Fig. 2.17- Heat maps comparing the CH_4 fluxes distribution depending on water column height and EC values (a) and SO_4^{2-} concentrations (b). Heat maps comparing the CO_2 fluxes distribution depending on water column height and EC values (c) and SO_4^{2-} concentrations (d).

2.4. Discussion

This study explores how the spatial and temporal variability of environmental drivers such as water and air T, salinity, irradiance and inundation levels, influence CH_4 and CO_2 emissions in four adjacent coastal wetlands.

In general, when all data collected on flooded areas as well as on wet soils were considered, lower fluxes of CH_4 were observed in meso/polyhaline environments (PIR and CAV), compared to what was observed in freshwater sites (PA and CER) (Tab.2.1). PIR and CAV are the richest in SO_4^{2-} (Fig. 2.1), an ion that can be used by sulfate-reducing bacteria as a terminal electron acceptor during anaerobic decomposition (Hackney and Avery, 2015; Zhou et al., 2022). In contrast to methanogenesis, the sulfate reduction process is naturally favored since sulfate reducer bacteria compete more efficiently for available substrates, like acetate and hydrogen than methanogenic bacteria (Lovley and Klug, 1986).

Our results confirm the strong inhibiting function of EC and sulfates. CH_4 emissions are found to be negatively correlated to EC and SO_4^{2-} (Fig.2.7), which is consistent with the existing literature on coastal wetlands (Hines, 1996; Poffenbarger et al., 2011b; Chen et al., 2018).

b)

On average from PCA results, it is possible to observe two groups of environmental controls: i) one aggregated component related to seasonality, grouping air and water T and irradiance, with a strong positive control on GHG emissions; ii) one related to the hydrological aspect of the wetlands represented by EC, SO_4^{2-} and water column height with a significative negative impact on GHG production.

CH_4 emissions show a seasonal pattern and generally are higher in the warmer season (Emery and Fulweiler, 2014; Al-Haj and Fulweiler, 2020), as shown in Fig. 2.2 with the highest values recorded in summer (Tab.2). In general, CH_4 and CO_2 emissions are positively correlated with air and water temperature, and irradiance. Temperature affects directly CH_4 production stimulating methanogenic kinetics (Zinder and Koch, 1984) (Fig 2.5). In fact, methanogen bacteria are reported to be generally mesophilic, with a growth temperature between 30° and 40° (Zinder, 1993).

CO_2 fluxes are also correlated to temperature and irradiance (Fig.S8 Supplement), highlighting a seasonal pattern with higher fluxes in the Spring-Summer season. It is known that CO_2 fluxes mainly come from soil respiration, including roots and microbial activity (Rustad et al., 2000). Additionally, methanotrophs in the soil surface layer may be able to oxidize part of the CH_4 and aerobic microbes can use more O_2 to oxidize organic matter. This condition is observed in CER (Tab. 2.2), which accounts for the overall highest mean fluxes of CO_2 during spring and summer.

CO_2 and CH_4 emissions are also linked to vegetation composition and organic matter presence. In our case, the second highest mean fluxes of CO_2 are measured at PIR (Tab. 2.2). This can be mainly related to the high presence in this area of *Praghmites australis,* which is reported to be particularly effective in transporting gas through its structures, from the submerged soil to the atmosphere (Martin and Moseman-Valtierra, 2015). Moreover, the high presence of *Phragmites* has the potential of increasing C turnover rates providing higher rates of primary production that may be offset by enhanced rates of plant litter decomposition (Duke et al., 2015). Anyway, this could also explain the high percentage of %SOM measured at the PIR site (Tab. 2.1).

When we concentrate on flooded areas examining only fluxes collected over standing waters, we observe some important differences. Even though the principal components are pretty much in line with those determined for the entire dataset (Fig. 2.1. and Fig. 2.12), we find a strong influence of water height on CH_4 and CO_2 emissions. Fig. 2.14 and 2.17 show that there is a water column height threshold that separates low from high emissions. It is known that CH_4 emission from wetlands depends, in part, on the balance between methanogenesis and CH_4 oxidation. Methanogenesis occurs in the submerged, anoxic soil layers, and so it depends on the vertical extension of the saturated zone determined by the water table level. When the level of the water table increases reaching the soil surface, creating anaerobic conditions favoring methanogenesis, which is a strictly anaerobic process (Mander et al., 2011; Calabrese et al., 2021). After being produced, CH_4 can be transported vertically or horizontally. The nature of the transport pathway (length, direction, presence of methanotrophs) determines the potential for CH_4 to be oxidized or, on the contrary, released as it is in the atmosphere (Dean et al., 2018). The constant presence of a deep water column on top of sediments creates the temporal and spatial condition for methanotroph bacteria to consume CH_4 in the water column (Henneberger et al., 2015; Sawakuchi et al., 2016), resulting in decreasing rate of CH_4 fluxes, as shown in Fig. 6. This agrees with the case of PA (Tab. 2.2) where the lower CH_4 fluxes compared to those in CER could be linked to a deep and permanent water column that may act as a physical barrier to CH_4 diffusion (Cheng et al.,

2007). The ensemble of these processes creates a critical zone where the availability of methanogenic substrates, anoxic portions of soil, and gas transport compete in creating either a favorable or unfavorable environment for CH_4 emissions (Calabrese et al., 2021). A further increase in the water column level, however, is more likely to decrease CH_4 production limiting plant growth and available substrate for decomposition (Calabrese et al., 2021)

Even though these processes are well known, in the literature it is not clear if the CH_4 emissions steadily increase with decreasing the water height or if, on the contrary, there is a threshold in water column height that separates emitting condition from no-emission condition. For the first time regarding temperate coastal wetlands, our results suggest that there is a critical threshold of water height, which, in our case, corresponds to about 50 cm below which wetlands release large quantities of CH_4 to the atmosphere. Fig. 6a and 6b show that high CH_4 emissions are recorded only where the water height is lower than this threshold as further confirmed by the Mann-Whitney test performed on shallow and deep waters (Fig. 2.15). This process explains, for instance, the differences in observed emissions between CA and PA where in CA, CH_4 emissions are 8 times higher than those measured in PA (Tab.2.2). These two sites have comparable salinity and temperature but differ greatly in their inundation levels (54 cm in PA and 18 cm in CER).

As for the case of CO_2 emissions, the behavior is similar for CH_4, however, the Mann-Whitney Test suggests that there is no significant difference between CO_2 emissions coming from waters higher and lower than 50 cm (Fig. 2.16). Bacteria responsible for CH_4 oxidation are less limited by exposure to anoxic conditions than methanogenic bacteria to oxic (Roslev and King, 1996), so CO_2 fluxes can be expected at low as well as at high water levels. Moreover, CO_2 emissions in seawater are higher than in freshwater because of the increased availability of SO_4^{2-} to serve as a terminal electron acceptor in anaerobic microbial respiration (Zhao et al., 2020). Finally, there is a relation between oxidation mechanisms and CH_4 fluxes depending on the efficiency of the gas transport within the ecosystem (Torres-Alvarado et al., 2005). (Torres-Alvarado et al., 2005). In shallow waters In shallow waters, CH4 diffusion is favored by low pressure and oxidation performed by oxidizing bacteria is limited (Weber et al., 2019). On the contrary, CH4 oxidation is favored in deeper water which slows down the diffusion of CH_4 and allows it to accumulate and providing more substrate for CH4-oxidizing bacteria to grow and consume CH_4 (Weber et al., 2019). The combination of these processes may explain why no significant differences of CO_2 emissions were observed in waters deeper or shallower than 50 cm, while significant differences are observed for CH_4 emissions.

Concluding, our results suggest that above a certain threshold, the water height is the main limiting factor of GHG emissions and at our study sites such threshold is 50 cm. When water is deeper than the threshold, the emission of CH_4 and CO_2 is very limited, regardless of the temperature being high or low (Fig. 2.14), but also independently of EC and sulfate concentrations (Fig. 2.17). High CH_4 emissions are observed only in shallow waters with small EC and sulfate concentrations (Fig. 2.17).

The results presented in this study are of relevance for the water management of this and other wetland areas that are controlled and managed by authorities. Knowing that the water height should never be lower than 50 cm to minimize GHG emissions is crucial information for proper management of the area.

Methanogenesis is a complex interplay of environmental factors and site-specific conditions (Kotsyurbenko et al., 2019), , and the inclusion of more variables in the analyses may improve the results allowing a more comprehensive understanding of the processes investigated in this research. In particular, vegetation, primary productivity and Chlorophyll-α can influence the organic matter supplied to sediments, influencing methanogenesis rates in wetland sediments both in freshwater and saltwater ecosystems (Grasset et al., 2018; Huertas et al., 2019). Another aspect that should be further considered is that the methanogenesis process depends on soil characteristics found in wetlands. There is a strong association between the quantity of methanogenic archaea and the concentration of organic C in wetland soils, and the amount of it influences the population of methanogens in wetland ecosystems (Liu et al., 2019). Because it has an impact on the soil capacity to oxidize CH_4, bulk density is a crucial variable in the management of GHG emissions in wetlands. The capacity of aerobic soil to oxidize CH_4 is reduced when the soil is submerged, leading to high CH_4 concentrations in these wetlands (Zhao et al., 2020).

Research that focuses on microbial community structure, the interaction between microbial communities and carbon-functional composition, and the ecological factors influencing both microbial communities and carbon-functional composition are essential to better understand the complex methanogenesis process in coastal environments.

Future research will be conducted to accomplish these goals, primarily concentrating on biogeochemistry and the organization of microbial communities, and promoting a comprehensive knowledge of the complex processes that underlie methanogenesis in coastal environments.

2.5 Conclusions

This study aims to identify the driving and limiting environmental factors for CH_4 and CO_2 production in temperate coastal wetlands with varying water salinity. It shows, for the first time, that CH_4 and CO_2 emissions in the Po River Delta Natural Park exhibit strong variations within a few kilometers and during different periods of the year, indicating a strong dependence on seasonality. Temperature and irradiance strongly influence CH_4 emissions from water and soil, resulting in higher rates during summer and spring.

We observe a significant decrease in CH_4 emissions when the water height exceeds the critical threshold of 50 cm. Regardless of the water salinity, the average CH_4 flux is 5.04 g/m^2/day in freshwater environments and 12.27 g/m^2/day in brackish settings. In contrast, when the water height is less than 50 cm, CH_4 emissions strongly increases to average value of 196.98 g/m^2/day in freshwater areas (Fig. 2.18). Same behaviors are observed for CO_2 fluxes, although they are statistically non-significant. Additionally, temperature and irradiance exert a strong influence on CH_4 emissions from both water and soil, resulting in higher emissions in summer and spring seasons than cold season.

Our results suggest that CH_4 oxidation by oxidizing bacteria is limited in shallow waters due to enhanced CH_4 diffusion, while CH_4 oxidation is more pronounced in deep waters, resulting in larger CO_2 emissions. The combination of these processes may explain why water height is a key limiting factor of CH_4 emissions, while CO_2 emissions remain constant regardless of the water height.

For water column depths less than 50 cm, we identify additional constraining factors, particularly the inhibitory roles of salinity and sulfate concentrations on CH_4 emissions, although specific threshold values for these variables could not be established, highlighting the complexity of the processes at play.

Considering the impacts of climate change, carefully studying temperate coastal wetlands and understanding the dynamic of CH_4 and CO_2 production are critically important to develop targeted management measures to reduce emissions from wetlands. These strategies are essential in the collective effort to meet climate targets, such as the 2030 Agenda for Sustainable Development and the objectives of the Paris Agreement on Climate Change (European Commission, 2020).

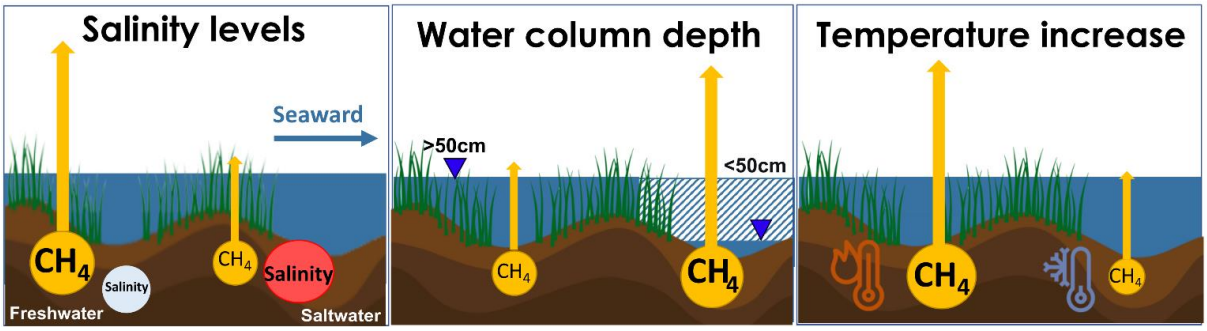

Fig. 2.18 – Keyfinding on environmental drivers ruling CH4 production in temperate coastal wetlands in the Ravenna Province.

References

Al-Haj, A. N. and Fulweiler, R. W.: A synthesis of methane emissions from shallow vegetated coastal ecosystems, Glob. Change Biol., 26, 2988–3005, https://doi.org/10.1111/gcb.15046, 2020.

Al-Shammary, A. A. G., Kouzani, A. Z., Kaynak, A., Khoo, S. Y., Norton, M., and Gates, W.: Soil Bulk Density Estimation Methods: A Review, Pedosphere, 28, 581–596, https://doi.org/10.1016/S1002-0160(18)60034-7, 2018.

Alvarez Cobelas, M., Rojo, C., and Angeler, D. G.: Mediterranean limnology: current status, gaps and the future, J. Limnol., 64, 13, https://doi.org/10.4081/jlimnol.2005.13, 2005.

Amorosi, Colalongo, Pasini, and Preti: SSedimentary response to Late Quaternary sea-level changes in the Romagna coastal plain .pdf, Sedimentology, 99–121, https://doi.org/10.1046/j.1365-3091.1999.00205.x, 1999.

Antonellini, M., Mollema, P., Giambastiani, B., Bishop, K., Caruso, L., Minchio, A., Pellegrini, L., Sabia, M., Ulazzi, E., and Gabbianelli, G.: Salt water intrusion in the coastal aquifer of the southern Po Plain, Italy, Hydrogeol. J., 16, 1541–1556, https://doi.org/10.1007/s10040-008-0319-9, 2008.

Antonellini, M., Balugani, E., Gabbianelli, G., Laghi, M., Marconi, V., and Mollema, P.: Lenti d'acqua dolce nelle dune della costa Adriatico-Romagnola, 23, 2010.

ARPAE: Rapporto IdroMeteoClima Emilia-Romagna, 2020.

Bhullar, G. S., Iravani, M., Edwards, P. J., and Olde Venterink, H.: Methane transport and emissions from soil as affected by water table and vascular plants, BMC Ecol., 13, 32, https://doi.org/10.1186/1472-6785-13-32, 2013.

Bubier, J. L., Moore, T. R., and Juggins, S.: Predicting Methane Emission from Bryophyte Distribution in Northern Canadian Peatlands, Ecology, 76, 677–693, https://doi.org/10.2307/1939336, 1995.

Buscaroli, A. and Zannoni, D.: Soluble ions dynamics in Mediterranean coastal pinewood forest soils interested by saline groundwater, CATENA, 157, 112–129, https://doi.org/10.1016/j.catena.2017.05.014, 2017.

Calabrese, S., Garcia, A., Wilmoth, J. L., Zhang, X., and Porporato, A.: Critical inundation level for methane emissions from wetlands, Environ. Res. Lett., 16, 044038, https://doi.org/10.1088/1748-9326/abedea, 2021.

Capaccioni, B., Tassi, F., Cremonini, S., Sciarra, A., and Vaselli, O.: Ground heating and methane oxidation processes at shallow depth in Terre Calde di Medolla (Italy): Observations and conceptual model: SOIL HEATING DUE TO METHANE OXIDATION, J. Geophys. Res. Solid Earth, 120, 3048–3064, https://doi.org/10.1002/2014JB011635, 2015.

Cardellini, C., Chiodini, G., Frondini, F., Granieri, D., Lewicki, J., and Peruzzi, L.: Accumulation chamber measurements of methane fluxes: application to volcanic-geothermal areas and landfills, Appl. Geochem., 18, 45–54, https://doi.org/10.1016/S0883-2927(02)00091-4, 2003.

Chen, Q., Guo, B., Zhao, C., and Xing, B.: Characteristics of CH4 and CO2 emissions and influence of water and salinity in the Yellow River delta wetland, China, Environ. Pollut., 239, 289–299, https://doi.org/10.1016/j.envpol.2018.04.043, 2018.

Cheng, X., Peng, R., Chen, J., Luo, Y., Zhang, Q., An, S., Chen, J., and Li, B.: CH4 and N2O emissions from Spartina alterniflora and Phragmites australis in experimental mesocosms, Chemosphere, 68, 420–427, https://doi.org/10.1016/j.chemosphere.2007.01.004, 2007.

Dean, J. F., Middelburg, J. J., Röckmann, T., Aerts, R., Blauw, L. G., Egger, M., Jetten, M. S. M., de Jong, A. E. E., Meisel, O. H., Rasigraf, O., Slomp, C. P., in't Zandt, M. H., and Dolman, A. J.: Methane Feedbacks to the Global Climate System in a Warmer World, Rev. Geophys., 56, 207–250, https://doi.org/10.1002/2017RG000559, 2018.

Duke, S. T., Francoeur, S. N., and Judd, K. E.: Effects of Phragmites australis Invasion on Carbon Dynamics in a Freshwater Marsh, Wetlands, 35, 311–321, https://doi.org/10.1007/s13157-014-0619-x, 2015.

EEC - Council of the European Union: Council Directive 79/409/EEC of 2 April 1979 on the conservation of wild birds.pdf, OJ 103, 1–18, 1979.

EEC - Council of the European Union: Council Directive 92/43/EEC of 21 May 1992 on the conservation of natural habitats and of wild fauna and flora, Off. J. 206, 92/43/EEC, P. 7-50, 1992.

Emery, H. E. and Fulweiler, R. W.: Spartina alterniflora and invasive Phragmites australis stands have similar greenhouse gas emissions in a New England marsh, Aquat. Bot., 116, 83–92, https://doi.org/10.1016/j.aquabot.2014.01.010, 2014.

Erwin, K. L.: Wetlands and global climate change: the role of wetland restoration in a changing world, Wetl. Ecol. Manag., 17, 71–84, https://doi.org/10.1007/s11273-008-9119-1, 2009.

European Commission: COMMUNICATION FROM THE COMMISSION TO THE EUROPEAN PARLIAMENT, THE COUNCIL, THE EUROPEAN ECONOMIC AND SOCIAL COMMITTEE AND THE COMMITTEE OF THE REGIONS, , COM(2020) 380, 2020.

Ferronato, C., Falsone, G., Natale, M., Zannoni, D., Buscaroli, A., Vianello, G., and Vittori Antisari, L.: Chemical and pedological features of subaqueous and hydromorphic soils along a hydrosequence within a coastal system (San Vitale Park, Northern Italy), Geoderma, 265, 141–151, https://doi.org/10.1016/j.geoderma.2015.11.018, 2016.

Gedney, N., Huntingford, C., Comyn-Platt, E., and Wiltshire, A.: Significant feedbacks of wetland methane release on climate change and the causes of their uncertainty, Environ. Res. Lett., 14, 084027, https://doi.org/10.1088/1748-9326/ab2726, 2019.

Giambastiani, B. M. S., Kidanemariam, A., Dagnew, A., and Antonellini, M.: Evolution of Salinity and Water Table Level of the Phreatic Coastal Aquifer of the Emilia Romagna Region (Italy), Water, 13, 372, https://doi.org/10.3390/w13030372, 2021.

Giambastiani M.S. Beatrice: The Piallassa Baiona lagoon is located at the eastern boundary of the pine forest. This brackish coastal lagoon was formed three to four centuries agoDottorato_Giambastiani_XIXCICLO.pdf, Tesi di Dottorato, Università di Bologna, 2007.

Giovenali, E., Coppo, L., Virgili, G., Continanza, D., and Raco, B.: THE FLUX-METER: IMPLEMENTATION OF A PORTABLE INTEGRATED INSTRUMENTATION FOR THE MEASUREMENT OF CO2 AND CH4 DIFFUSE FLUX FROM LANDFILL SOIL COVER., 11, 2013.

Grasset, C., Mendonça, R., Villamor Saucedo, G., Bastviken, D., Roland, F., and Sobek, S.: Large but variable methane production in

anoxic freshwater sediment upon addition of allochthonous and autochthonous organic matter, Limnol. Oceanogr., 63, 1488–1501, https://doi.org/10.1002/lno.10786, 2018.

Hackney, C. T. and Avery, G. B.: Tidal Wetland Community Response to Varying Levels of Flooding by Saline Water, Wetlands, 35, 227–236, https://doi.org/10.1007/s13157-014-0597-z, 2015.

Henneberger, R., Cheema, S., Franchini, A. G., Zumsteg, A., and Zeyer, J.: Methane and Carbon Dioxide Fluxes from a European Alpine Fen Over the Snow-Free Period, Wetlands, 35, 1149–1163, https://doi.org/10.1007/s13157-015-0702-y, 2015.

Hines, M. E.: Emissions of sulfur gases from wetlands, SIL Commun. 1953-1996, 25, 153–161, https://doi.org/10.1080/05384680.1996.11904076, 1996.

Howard, J., Sutton-Grier, A., Herr, D., Kleypas, J., Landis, E., Mcleod, E., Pidgeon, E., and Simpson, S.: Clarifying the role of coastal and marine systems in climate mitigation, Front. Ecol. Environ., 15, 42–50, https://doi.org/10.1002/fee.1451, 2017.

Huertas, I. E., de la Paz, M., Perez, F. F., Navarro, G., and Flecha, S.: Methane Emissions From the Salt Marshes of Doñana Wetlands: Spatio-Temporal Variability and Controlling Factors, Front. Ecol. Evol., 7, 32, https://doi.org/10.3389/fevo.2019.00032, 2019.

J. P. Megonigal, M. E. Mines, and P. T. Visscher: in: Anaerobic Metabolism: Linkages to Trace Gases and Aerobic Processes, vol. Biogeochemistry, Elsevier-Pergamon, Oxford, 317–424, 2004.

Kirschke, S., Bousquet, P., Ciais, P., Saunois, M., Canadell, J. G., Dlugokencky, E. J., Bergamaschi, P., Bergmann, D., Blake, D. R., Bruhwiler, L., Cameron-Smith, P., Castaldi, S., Chevallier, F., Feng, L., Fraser, A., Heimann, M., Hodson, E. L., Houweling, S., Josse, B., Fraser, P. J., Krummel, P. B., Lamarque, J.-F., Langenfelds, R. L., Le Quéré, C., Naik, V., O'Doherty, S., Palmer, P. I., Pison, I., Plummer, D., Poulter, B., Prinn, R. G., Rigby, M., Ringeval, B., Santini, M., Schmidt, M., Shindell, D. T., Simpson, I. J., Spahni, R., Steele, L. P., Strode, S. A., Sudo, K., Szopa, S., van der Werf, G. R., Voulgarakis, A., van Weele, M., Weiss, R. F., Williams, J. E., and Zeng, G.: Three decades of global methane sources and sinks, Nat. Geosci., 6, 813–823, https://doi.org/10.1038/ngeo1955, 2013.

Komlan Mawuli Afiademanyo, Kwami Lumo Awaga, Kamilou Ouro-Sama, and Hodabalo Dheoulaba Solitoke: Factoextra: Extract and Visualize the Results of Multivariate Data Analyses. R Package Version 1.0.7., 2020.

Kotsyurbenko, O. R., Glagolev, M. V., Merkel, A. Y., Sabrekov, A. F., and Terentieva, I. E.: Methanogenesis in Soils, Wetlands, and Peat, in: Biogenesis of Hydrocarbons, edited by: Stams, A. J. M. and Sousa, D., Springer International Publishing, Cham, 1–18, https://doi.org/10.1007/978-3-319-53114-4_9-1, 2019.

Laghi, M., Mollema, P., and Antonellini, M.: The Influence of River Bottom Topography on Salt Water Encroachment Along the Lamone River (Ravenna, Italy), and Implications for the Salinization of the Adjacent Coastal Aquifer, in: World Environmental and Water Resources Congress 2010, World Environmental and Water Resources Congress 2010, Providence, Rhode Island, United States, 1124–1135, https://doi.org/10.1061/41114(371)123, 2010.

Lazzari, G., Merloni, N., and Saiani, D.: Flora delle Pinete storiche di Ravenna San Vitale, Classe, Cervia, Parco del Delta del Po-Emilia Romagna, L'Arca, Ravenna, 2010.

Lê, S., Josse, J., and Husson, F.: **FactoMineR** : An *R* Package for Multivariate Analysis, J. Stat. Softw., 25, https://doi.org/10.18637/jss.v025.i01, 2008.

Liu, L., Wang, D., Chen, S., Yu, Z., Xu, Y., Li, Y., Ge, Z., and Chen, Z.: Methane Emissions from Estuarine Coastal Wetlands: Implications for Global Change Effect, Soil Sci. Soc. Am. J., 83, 1368–1377, https://doi.org/10.2136/sssaj2018.12.0472, 2019.

Lovley, D. R. and Klug, M. J.: Model for the distribution of sulfate reduction and methanogenesis in freshwater sediments, Geochim. Cosmochim. Acta, 50, 11–18, https://doi.org/10.1016/0016-7037(86)90043-8, 1986.

Mander, Ü., Maddison, M., Soosaar, K., and Karabelnik, K.: The Impact of Pulsing Hydrology and Fluctuating Water Table on Greenhouse Gas Emissions from Constructed Wetlands, Wetlands, 31, 1023–1032, https://doi.org/10.1007/s13157-011-0218-z, 2011.

Mar, K. A., Unger, C., Walderdorff, L., and Butler, T.: Beyond CO2 equivalence: The impacts of methane on climate, ecosystems, and health, Environ. Sci. Policy, 134, 127–136, https://doi.org/10.1016/j.envsci.2022.03.027, 2022.

Martin, R. M. and Moseman-Valtierra, S.: Greenhouse Gas Fluxes Vary Between Phragmites Australis and Native Vegetation Zones in Coastal Wetlands Along a Salinity Gradient, Wetlands, 35, 1021–1031, https://doi.org/10.1007/s13157-015-0690-y, 2015.

Merloni, N. and Piccoli, F.: LA VEGETAZIONE DEL COMPLESSO PUNTE ALBERETE E VALLE MANDRIOLE (PARCO REGIONALE DEL DELTA DEL PO - ITALIA), Dipartimento di Botanica ed Ecologia dell'Università - Camerino et Station de Phytosociologie - Bailleul, 2001.

Peng, S., Lin, X., Thompson, R. L., Xi, Y., Liu, G., Hauglustaine, D., Lan, X., Poulter, B., Ramonet, M., Saunois, M., Yin, Y., Zhang, Z., Zheng, B., and Ciais, P.: Wetland emission and atmospheric sink changes explain methane growth in 2020, Nature, 612, 477–482, https://doi.org/10.1038/s41586-022-05447-w, 2022.

Poffenbarger, H. J., Needelman, B. A., and Megonigal, J. P.: Salinity Influence on Methane Emissions from Tidal Marshes, Wetlands, 31, 831–842, https://doi.org/10.1007/s13157-011-0197-0, 2011.

RER - Regione Emilia Romagna: RETE NATURA 2000 – SIC/ZPS IT4070001 PUNTE ALBERETE, VALLE MANDRIOLE – QUADRO CONOSCITIVO, 2018.

RER - Regione Emilia Romagna: Piano Stralcio di Bacino per il Rischio Idrogeologico, 2016.

RER - Regione Emilia Romagna: MISURE SPECIFICHE DI CONSERVAZIONE DEL SIC-ZPS IT4070003 "PINETA DI SAN VITALE, BASSA DEL PIROTTOLO," 2018.

RER - Regione Emilia Romagna: Carta dei suoli dell'Emilia Romagna, 2021.

Roner, M., D'Alpaos, A., Ghinassi, M., Marani, M., Silvestri, S., Franceschinis, E., and Realdon, N.: Spatial variation of salt-marsh organic and inorganic deposition and organic carbon accumulation: Inferences from the Venice lagoon, Italy, Adv. Water Resour., 93, 276–287, https://doi.org/10.1016/j.advwatres.2015.11.011, 2016.

Roslev, P. and King, G. M.: Regulation of methane oxidation in a freshwater wetland by water table changes and anoxia, FEMS Microbiol. Ecol., 19, 105–115, https://doi.org/10.1111/j.1574-6941.1996.tb00203.x, 1996.

Rustad, L. E., Huntington, T. G., and Boone, D.: Controls on soil respiration: Implications for climate change, 6, 2000.

Salimi, S., Almuktar, S. A. A. A. N., and Scholz, M.: Impact of climate change on wetland ecosystems: A critical review of experimental wetlands, J. Environ. Manage., 286, 112160,

https://doi.org/10.1016/j.jenvman.2021.112160, 2021.

Saunois, M., Bousquet, P., Poulter, B., Peregon, A., Ciais, P., Canadell, J. G., Dlugokencky, E. J., Etiope, G., Bastviken, D., Houweling, S., Janssens-Maenhout, G., Tubiello, F. N., Castaldi, S., Jackson, R. B., Alexe, M., Arora, V. K., Beerling, D. J., Bergamaschi, P., Blake, D. R., Brailsford, G., Brovkin, V., Bruhwiler, L., Crevoisier, C., Crill, P., Covey, K., Curry, C., Frankenberg, C., Gedney, N., Höglund-Isaksson, L., Ishizawa, M., Ito, A., Joos, F., Kim, H.-S., Kleinen, T., Krummel, P., Lamarque, J.-F., Langenfelds, R., Locatelli, R., Machida, T., Maksyutov, S., McDonald, K. C., Marshall, J., Melton, J. R., Morino, I., Naik, V., O'Doherty, S., Parmentier, F.-J. W., Patra, P. K., Peng, C., Peng, S., Peters, G. P., Pison, I., Prigent, C., Prinn, R., Ramonet, M., Riley, W. J., Saito, M., Santini, M., Schroeder, R., Simpson, I. J., Spahni, R., Steele, P., Takizawa, A., Thornton, B. F., Tian, H., Tohjima, Y., Viovy, N., Voulgarakis, A., van Weele, M., van der Werf, G. R., Weiss, R., Wiedinmyer, C., Wilton, D. J., Wiltshire, A., Worthy, D., Wunch, D., Xu, X., Yoshida, Y., Zhang, B., Zhang, Z., and Zhu, Q.: The global methane budget 2000–2012, Earth Syst. Sci. Data, 8, 697–751, https://doi.org/10.5194/essd-8-697-2016, 2016.

Sawakuchi, H. O., Bastviken, D., Sawakuchi, A. O., Ward, N. D., Borges, C. D., Tsai, S. M., Richey, J. E., Ballester, M. V. R., and Krusche, A. V.: Oxidative mitigation of aquatic methane emissions in large Amazonian rivers, Glob. Change Biol., 22, 1075–1085, https://doi.org/10.1111/gcb.13169, 2016.

Soboyejo, L. A., Giambastiani, B. M. S., Molducci, M., and Antonellini, M.: Different processes affecting long-term Ravenna coastal drainage basins (Italy): implications for water management, Environ. Earth Sci., 80, 493, https://doi.org/10.1007/s12665-021-09774-5, 2021.

Torres-Alvarado, R., Ramírez-Vives, F., and Fernández, F. J.: Methanogenesis and methane oxidation in wetlands. Implications in the global carbon cycle Metanogénesis y metano-oxidación en humedales. Implicaciones en el ciclo del carbono global, 15, 23, 2005.

Turetsky, M. R., Kotowska, A., Bubier, J., Dise, N. B., Crill, P., Hornibrook, E. R. C., Minkkinen, K., Moore, T. R., Myers-Smith, I. H., Nykänen, H., Olefeldt, D., Rinne, J., Saarnio, S., Shurpali, N., Tuittila, E.-S., Waddington, J. M., White, J. R., Wickland, K. P., and Wilmking, M.: A synthesis of methane emissions from 71 northern, temperate, and subtropical wetlands, Glob. Change Biol., 20, 2183–2197, https://doi.org/10.1111/gcb.12580, 2014.

Venturi, S., Tassi, F., Cabassi, J., Randazzo, A., Lazzaroni, M., Capecchiacci, F., Vietina, B., and Vaselli, O.: Exploring Methane Emission Drivers in Wetlands: The Cases of Massaciuccoli and Porta Lakes (Northern Tuscany, Italy), Appl. Sci., 11, 12156, https://doi.org/10.3390/app112412156, 2021.

de Vicente, I.: Biogeochemistry of Mediterranean Wetlands: A Review about the Effects of Water-Level Fluctuations on Phosphorus Cycling and Greenhouse Gas Emissions, Water, 13, 1510, https://doi.org/10.3390/w13111510, 2021.

Vittori Antisari, L., Dinelli, E., Buscaroli, A., Covelli, S., Pontalti, F., and Vianello, G.: Potentially toxic elements along soil profiles in an urban park, an agricultural farm, and the san vitale pinewood (Ravenna, Italy), EQA-International Journal of Environmental Quality, 1–14, https://doi.org/10.6092/ISSN.2281-4485/3822, 2013.

Weber, T., Wiseman, N. A., and Kock, A.: Global ocean methane emissions dominated by shallow coastal waters, Nat. Commun., 10, 4584, https://doi.org/10.1038/s41467-019-12541-7, 2019.

Whalen, S. C.: Biogeochemistry of Methane Exchange between Natural Wetlands and the

Atmosphere, Environ. Eng. Sci., 22, 73–94, https://doi.org/10.1089/ees.2005.22.73, 2005.

Wickham, H.: ggplot2: Elegant Graphics for Data Analysis, Springer-Verlag, New York, 2016.

Zannoni, D.: Uso sostenibile dei suoli forestali di ambiente costiero in relazione ai fattori di pressione esistenti., 2008.

Zhao, M., Han, G., Li, J., Song, W., Qu, W., Eller, F., Wang, J., and Jiang, C.: Responses of soil CO2 and CH4 emissions to changing water table level in a coastal wetland, J. Clean. Prod., 269, 122316, https://doi.org/10.1016/j.jclepro.2020.122316, 2020.

Zhou, J., Theroux, S. M., Bueno de Mesquita, C. P., Hartman, W. H., Tian, Y., and Tringe, S. G.: Microbial drivers of methane emissions from unrestored industrial salt ponds, ISME J., 16, 284–295, https://doi.org/10.1038/s41396-021-01067-w, 2022.

Zinder, S. H.: Physiological Ecology of Methanogens, in: Methanogenesis, edited by: Ferry, J. G., Springer US, Boston, MA, 128–206, https://doi.org/10.1007/978-1-4615-2391-8_4, 1993.

Zinder, S. H. and Koch, M.: Non-aceticlastic methanogenesis from acetate: acetate oxidation by a thermophilic syntrophic coculture, Arch. Microbiol., 138, 263–272, https://doi.org/10.1007/BF00402133, 1984.

Part III – Salinity's Impact on Microbial Communities and Biogeochemical Cycling

This chapter has been submitted as a scientific paper in JGR Biogeosciences, with the title: "Investigating Salinity Effect on Temperate Coastal Wetland Soil Microbes and Greenhouse Gas Emissions." Chiapponi E., Zannoni D., Giambastiani B.M.S., Silvestri S., Buscaroli A., Costantini F.

Abstract

Coastal wetlands capture carbon dioxide from the atmosphere at high rates and store large amounts of "blue carbon" in soils. These habitats are home to a variety of microbial communities that break down organic matter and cycle nutrients, playing a substantial role in coastal biogeochemical balance. Rising sea levels make coastal wetlands more susceptible to saltwater intrusion, which might disrupt biogeochemical processes, such as the sulfur cycle and methane generation/consumption by bacteria thus disrupting existing equilibria. A change in biogeochemical equilibria may produce important climate-related feedback because these systems, while involved in carbon sequestration, also have the potential to emit greenhouse gases, with reported higher emissions in freshwater ecosystems compared to brackish ones. In this study, we characterize the microbial community and geochemical properties in soils of three temperate coastal wetlands along a salinity gradient to assess the effect of salinity on organic matter decomposition and related greenhouse gas emissions. The full-length Oxford Nanopore MinION 16S rRNA amplicon sequencing is used to characterize bacterial communities from soil samples. Results indicate a prevalence of sulfur-reducing bacteria in salinized sites compared to freshwater sites. In brackish environments, there is an emergence of obligate anaerobic taxa associated with sulfate reduction, fatty acid degradation, and denitrifying bacteria. These microbial communities play a significant role in reducing CH_4 emissions while simultaneously increasing CO_2 emissions within these habitats. This study reveals the structure of microbial communities in wetland soils, crucial for ecosystem understanding and implications in wetland conservation, management, and climate change mitigation

3.1 Introduction

Coastal vegetated wetlands are transitional ecosystems found at the edge of terrestrial and marine habitats (Mitsch et al., 2013). The amount of carbon, also defined as "blue carbon", stored in coastal wetland soils is estimated to equal 25 Pg at the global scale (Duarte et al., 2013) and comes from a constant sink of organic matter associated with slow rates of decomposition. Coastal wetlands are among the most efficient ecosystems in terms of carbon sequestration rate, storing 67–215 Tg C yr^{-1} (Hopkinson et al., 2012), thus playing a crucial role in global biogeochemical cycles (IPCC, 2022). Wetland soils are home to diverse microbial communities that are responsible for driving the processes of organic matter breakdown, nutrient cycling, and greenhouse gas emissions (Bridgham et al., 2013). The elements that drive microbial metabolism, such as temperature and precipitation, local environmental characteristics like vegetation, hydrology and soil type, and land use (undisturbed vs. disturbed), influence the rates at which organic carbon mineralizes (Bonetti et al., 2021).

Coastal wetlands are increasingly vulnerable to saltwater intrusion due to sea level rises (White and Kaplan, 2017) and this might reduce the amount of carbon that they can sequester through vegetation

and microbial communities disrupting biogeochemical cycles (Morrissey et al., 2014; Dang et al., 2019). Methanogenic, fermentative, and respiratory pathways are only a few of the many bacterial metabolic activities that drive the complex processes of organic matter breakdown in these environments (Liang et al., 2023). Due to the restricted availability of terminal electron acceptors, methanogenesis is more prevalent in freshwater settings whereas sulfate reduction is prevalent in coastal saltwater systems (Poffenbarger et al., 2011).

The sulfur cycle is one of the most important biogeochemical cycles in these environments, as it is closely linked to the production and consumption of methane (U.S. DOE, 2008). Sulfate reduction, being energetically favored in comparison to fermentative processes and methanogenesis, plays a pivotal role in diminishing gross methane production, consequently curtailing methane emissions into the environment (Capone and Kiene, 1988). The significance of sulfate reduction within coastal wetland soils is well acknowledged, yet the intricacies governing its rates and pathways in these specific environments remain a subject of uncertainty (McCuen et al., 2021). Methanogens are known to be outcompeted by sulfate-reducing bacteria (SRB) for electron donors, which can disrupt microbial activity and lower methane production (An et al., 2023). Saltwater may promote the growth of bacteria that reduce sulfate, which further complicates the biogeochemical processes that take place in wetlands (Jørgensen et al., 2019).

The balance between rates of sea level rise, sulfate intrusion, and wetland accretion will have strong impacts on the capacity to store and sequestering carbon (Yousefi Lalimi et al., 2018; Candry et al., 2023). By the end of the 21st century, ecosystems like eutrophic, shallow, and microtidal estuaries in temperate and high latitudes will be at moderate to high risk of submergence and erosion under future emission scenarios (IPCC , 2022; Yang et al., 2023). There may be conflicting effects among different rates of sea level rise (SLR), with possible increases in net carbon absorption for steadily rising sea levels and net carbon release for faster SLR (IPCC, 2022). The overall response of vegetated coastal ecosystems to rising sea levels is shaped by the diverse interactions among plant growth, sedimentation processes, and inundation(Marani et al., 2006, 2010; Yang et al., 2023). These complex dynamics give rise to contrasting feedback between different scenarios (Gonneea et al., 2019). Biogeochemical studies in wetlands are important for understanding the impact of climate change on the ecosystem services provided by these environments, improving water quality, and mitigating climate change through carbon sequestration (Trettin et al., 2019; Salimi et al., 2021).

In a previous study by Chiapponi et al. (2024), the environmental variables driving CH_4 and CO_2 emissions from temperate coastal wetlands on the Adriatic coast were analyzed and it was shown that salinity and water column level are the major limiting factors of CH_4 emissions in these environments. The present study uses a pioneering multidisciplinary approach to understand the influence of salinity on gas emissions through biogeochemical analysis. Our primary objective is to examine the interplay between microbial communities and sulfur concentrations in hydromorphic soils of three distinct sites, strategically located along a salinity gradient. Specifically, we aim to characterize microbial community composition and structure and to characterize the geochemical composition of the soils harboring the present bacterial communities to investigate the influence of salinity on methanogenic, fermentative, and respiratory pathways that drive the complex processes of organic matter breakdown in temperate coastal wetlands. The biogeochemical results are then discussed with regard to GHG emissions measured in the same areas and reported in Chiapponi et al. (2024). The semiquantitative paper analysis method is applied to assess acid volatile sulfides (AVS) in soils. X-ray fluorescence spectrometry (XRF) was implied to measure elemental composition including total sulfur, while concentrations of

total carbon (TC), total hydrogen (TH), total nitrogen (TN), and total organic carbon (TOC) were detected with an elemental analyzer as described in the following section.

3.2. Materials and methods

3.2.1 Study area

The research was conducted in three sites in the province of Ravenna (Italy) (Fig.3.1), along the Adriatic coast. The San Vitale pine forest and the Punte Alberete marsh are located 3 to 5 km inland of the Northern Adriatic Sea on a dune belt system. The area is characterized by the presence of the Piallassa Baiona, the only brackish intertidal lagoon on the Emilia-Romagna coast. The entire study area is part of the Po River Delta Natural Park and under the European environmental special protection directive (Punte Alberete SCI/SPA IT4070001 and San Vitale pine forest IT4070003 legislation (CEE, 1979, 1992; RER, 2018)).

The area is characterized by a subcontinental temperate climate with about 600 mm of annual rainfall and a monthly mean temperature ranging from 3.6 to 24.3 °C in January and July respectively (ARPAE - Regional Agency for Prevention, Environment and Energy of Emilia-Romagna, weather station of Marina di Ravenna https://simc.arpae.it/dext3r/).

The whole coastal area is highly affected by saltwater intrusion due to both natural and anthropogenic stressors (Antonellini et al., 2019). The unconfined coastal aquifer is primarily based upon beach and dune sandy deposits reaching a depth of 30 m with a central layer of finer sediment (silt) at a depth of 15-16 m (Giambastiani et al., 2007). The only topographical assets above mean sea level are river banks, palaeodunes, and current coastal dunes with elevations of 1-3 m a.s.l. Vegetation distribution is impacted by the topographic highs and lows that correlate to various previous coastlines and stages in the evolution of the Po Delta (Amorosi et al., 1999). This low-lying topography causes the coastal phreatic aquifer to be salinized with a sporadic presence of shallow freshwater lenses floating on brackish-salty water and shallow freshwater-saltwater interfaces (Antonellini et al., 2008; Giambastiani et al., 2021). Weather variables, such as temperature, rainfall, and evapotranspiration have a significant impact on the extent of saltwater intrusion in the deep aquifer. Most of the region experiences an increase in groundwater salinity and a drop in water throughout the dry and warm seasons (Giambastiani et al., 2021).

Mechanical drainage is used across the area to regulate floodwater and allow agricultural activities by keeping a steady water table depth of 1.5-2 m below ground level throughout the year (Soboyejo et al., 2021). The intricate network of drain canals and water pumping stations prevents floods but provides a general inland-directed hydraulic gradient, resulting in saltwater intrusion from the salty lagoon and sea (Giambastiani et al., 2021). Salinization of surface and ground waters is particularly substantial around the Piallassa Baiona lagoon, which is directly connected to the Adriatic Sea, along canals and rivers, and in and around those areas (Antonellini et al., 2008). The water level is also managed in extensive portions of the wetlands, some of which are maintained permanently inundated by a network of ditches and sluices. Compared to natural systems, managed areas where drainage systems regulate water table and flow direction and maintain constant inland hydraulic heads, are more susceptible to climate-change related threats (Giambastiani et al., 2020, 2021). Climate change, SLR and changes in recharge and evapotranspiration patterns will exacerbate the pressure on coastal systems, making the studied areas of Pineta S. Vitale and Punte Alberete particularly vulnerable (Colombani et al., 2016; Giambastiani et al., 2021). The seasonal imbalance in the groundwater budget is exacerbated by the local climate and weather unpredictability (Greggio et al., 2012), with consequences on the biogeochemical cycles of the studied wetlands.

The three selected sites are characterized by a water salinity gradient, ranging from freshwater to slightly brackish to saline waters moving toward the lagoon. Punte Alberete (PA) is the most freshwater site of the area with a mean annual salinity of 0.67 dS m-1; Cerba (CER) is an area characterized by slightly higher salinity, values between 1.4 and 2.2 dS m-1; while Pirottolo (PIR) is characterized by brackish EC values of 6-7.06 dS m-1 (Chiapponi et al., 2024).

Based on regional pedological data from the Emilia-Romagna geoportal (https://ambiente.regione.emilia-romagna.it/) and previous research in the area (Buscaroli et al., 2009; Buscaroli and Zannoni, 2010; Ferronato et al., 2016), a succession of soils was observed where topography is the main factor of pedogenesis. The alternation of dunes and lowlands determines a different depth of the water table with respect to the ground level, strongly conditioning the soil moisture regime and the salinity degree. Climatic condition, together with the carbonate sandy substrate and spontaneous vegetation land use generate poorly evolved soil profiles with O/A/C horizon sequence, according to Soil Survey Staff (2022) classification. From the dune crests, where the water table is deepest, to the perennially flooded interdune lowlands, the soil morphosequence is classified as Psamments, Aquents, and Wassents sub-orders according to the Soil Taxonomy (Soil Survey Staff, 2022). In this area, Aquents and Wassents represent hydromorphic and subaqueous soils respectively in a typical coastal transition system (Ferronato et al., 2016). Seasonal variability also affects the soils of this area: spring and autumn rainfall causes salt leaching from soil horizons, a decrease in the water table depth and its salt content dilution; summer weather conditions cause an increase in water table depth and an increase in soil salinity in surface horizons (Buscaroli and Zannoni, 2010, 2017). Changes in the water table level and the total period of saturation have a significant impact on specific soil-forming processes related to the S cycle, $CaCO_3$ accumulation and depletion, and P and salt concentration (Ferronato et al., 2016).

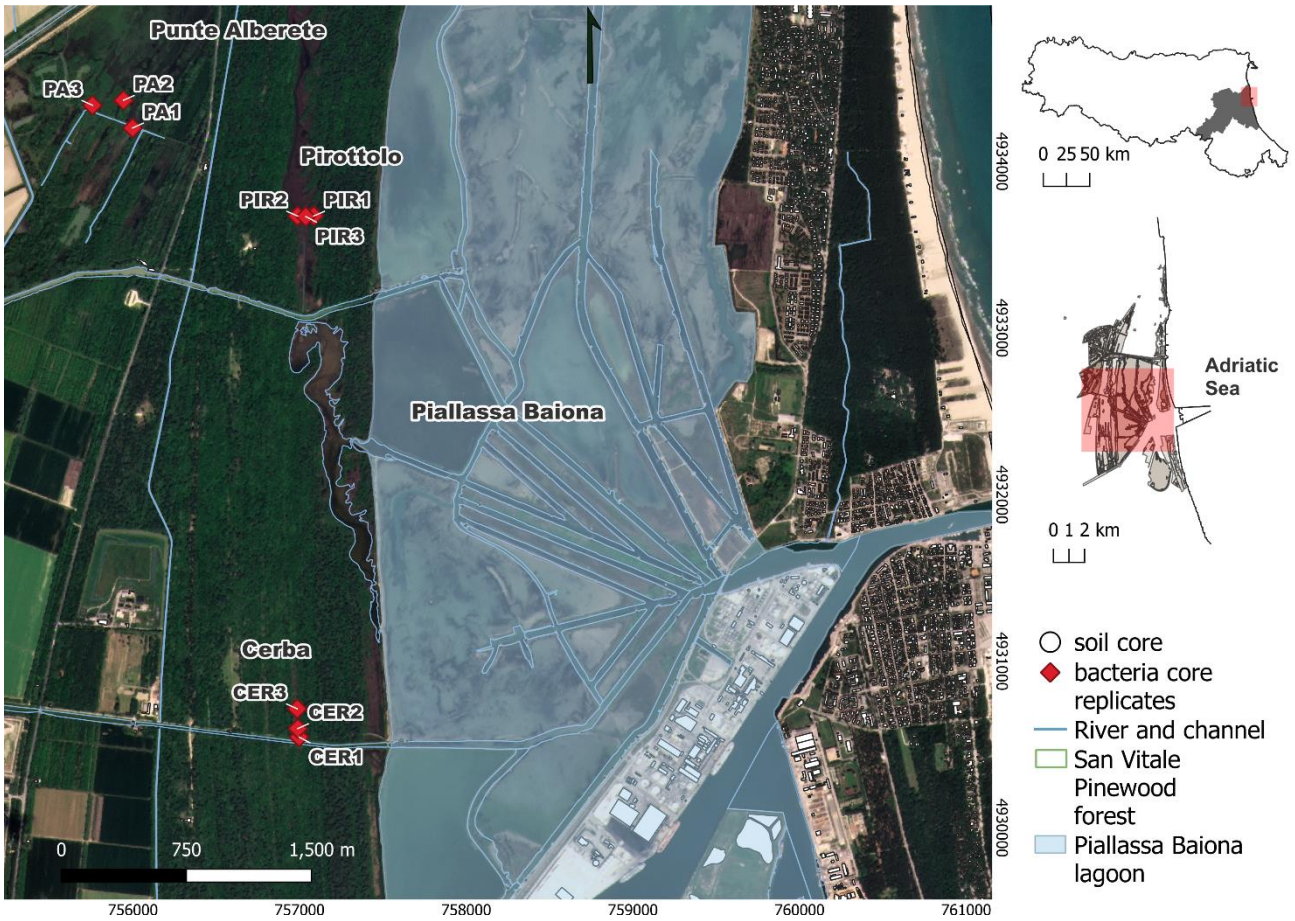

Fig. 3. 1 - Study Area representing the three selected temperate coastal wetlands along with the location of sampled cores for molecular and geochemical analysis (original data elaborated in QGIS 3.26.0; coordinate 756856, 4930514; EPSG 32632).

3.2.2 Sampling (coring)

Cores were taken in four replicates at each location using transparent plexiglass liners. Three cores were used for the molecular analysis, while the fourth core was used to perform the geochemical analysis (Fig.3.2a). Each core-liner was inserted in soil ensuring that at least 50 cm of soil was retrieved (Fig. 3.2b). To avoid oxidation, the headspace was filled with water sampled in the same location and immediately sealed with parafilm and tight stopper. To avoid layer mixing, all the tubes have been ensured in vertical position during transport. Corers used for bacterial analysis were previously disinfected with a solution of 20% of NaClO to avoid sample contamination. In the laboratory, a section of sediment sample was extruded at 0-20 cm for bacteria analysis (Fig. 3.2c) from each core and later preserved at -25 °C in sterilized Falcon tubes for DNA extraction. Cores for geochemical analysis were used as a whole and were stored in vertical position at -25 °C until performing any morphological and analytical manipulation.

Fig. 3. 2 – Sediment core sampling design using plexiglass tubes (a) and (b), and core sections at different depths extracted in the laboratory for microbial analysis (B).

3.2.3 Environmental parameters

Water temperature (°C), pH, Eh (mV), and EC (dS m^{-1}) were taken at each location using probes logged to an EUTECH datalogger. Moreover, to assess the influence of salinity on shaping the bacterial communities, samples of water were collected to analyze sulfate (SO_4^{2-}) and sulfide (S^{2-}) concentrations. At each location, a bottle of water of 500 mL was retrieved, being careful to leave no headspace, put in a cooler and transported to the lab for geochemical analysis, performed on the same day. Sulfate (SO_4^{2-}) concentrations have been measured by using HAACH spectrophotometer: 25 mL of sample (pure or diluted) was added into the sample cell while a blank sample cell was used as reference; Sulfate Ver 4 reagent powder pillow was also added, stirred, and then left for 5 minutes for reaction to take place, and then read to retrieve sulfate concentration (Hach Company, 2019). Similarly, S^{2-} concentration was retrieved adding 1 mL of Sulfide Reagents 1 and 2 to 25 mL of sample and to deionized water for reference, stirred and measured after 5 minutes accordingly to the manual instructions (Hach Company, 2014).

3.2.4 GHG emissions measurements

In the same study area, emissions of CH_4 and CO_2 from open standing waters and soils were measured (Chiapponi et al., 2024). Details about methodology and results are reported in the cited study, which investigated the relationship of abiotic environmental variables with CH_4 and CO_2 emissions in the same temperate coastal wetlands. A summary of the emission rates is provided in Table 3.2

3.2.5 Soil characterization

3.2.5.1 Pedological characterization

Cores were carefully extruded on a suitable support. Then soil horizons boundaries were identified and marked. For each horizon, thickness, depth, boundaries, matrix Munsell color (moist), texture, structure, fluidity, coats/film, redoximorphic features, peroxide color change and presence of organic fragments or roots, were described. After the core extrusion, in water saturated soil samples, pH, electrical conductivity (EC sp), oxidation reduction potential (ORP) and AVS were measured in each horizon. All other analyses were performed on air-dried soil samples. After drying, electrical conductivity (EC) and pH were measured again for all samples in a 1:2.5 (w:v) soil: distilled water suspension. For TOC determination, a carbonates dissolution with 1.5 M HCl was performed before analysis with the elemental analyzer (Thermo Fisher CHNS-O Flash EA 2000) by Dumas flash

combustion at 1800 °C, while for TN and TH determination, this pretreatment was not necessary (ISO, 1995). To determine the presence of sulfidic material, an aliquot of each soil horizon was incubated for 16 weeks after which its pH was measured again according to the Soil Survey Staff (2022) methodology.

3.2.5.2 Sulfides from soils

Acid Volatile Sulfides (AVS) were determined in sampled cores of soils using a semiquantitative method proposed by Pellegrini et al. (2018). The blackening of a paper strip, produced by the precipitation of PbS, was compared with a reference table, previously calibrated. The paper sensor method for S^{2-} is very suitable for field screening and has sensitivity levels comparable to laboratory methods (Pellegrini et al., 2018).

The reference chart was prepared by adding standard S^{2-} solutions ranging from 0.1 to 10 mmoles/L following the method suggested by Pellegrini et al. (2018). Paper strips (3x6 cm) were cut from Whatman ® N.1 filter paper and impregnated with 6 drops (approximately 0.3 mL) with 1.5 M Pb $(NO_3)_2$ shortly before use. The impregnated area was roughly 3x4 cm, with the remaining 3 cm dry for pinching the paper strip to a 250 mL polyethylene jar. An aliquot of 10 mL standard solution or fresh soil was placed in the disruptor tube, provided by the extraction kit. The cap was promptly closed after 50 mL of 6M HCl was gently added. The jar was then swirled for about 15 seconds to ensure thorough contact between the soil and the acid and to speed up H_2S volatilization.
The volatilized H_2S combined with the Pb_2 on the paper strips to generate PbS, which darkened the paper in a hue proportional to the amount of H_2S developed. The jar was opened after 5 minutes, and the paper strip was removed and immediately compared to the reference colorimetric chart and scanned.

3.2.5.3 Sulfur characterization

Total sulfur and elemental composition were measured from each soil horizon with X-ray fluorescence (XRF). Each aliquot of dried and milled material was pressed in a thin pallet in a boric acid binder and used to analyze the elemental chemistry with an Axios-Panalytical sequential wavelength dispersive XRF spectrometer with a 4 kW Rh tube and SuperQ 3.0 software. Thermogravimetric analysis was carried out using an Eltra Thermostep thermogravimetric analyzer (Eltra GmbH, Haan, Germany) in an oxidant atmosphere (air, 90 mL min-1) at 10 °C min-1 to 600 °C for organic matter determination and then at 25 °C min-1 to 950 °C for carbonate determination (Kasozi et al., 2009).

3.2.6 DNA extraction, 16S rRNA gene amplification and sequencing

From each location and replicate (3 locations, 3 replicates per location), a representative sample of the 0-20 cm core was collected and used for DNA extraction. Total DNA was extracted using the E.Z.N.A.® SOIL DNA KiT (Omega Bio-Tek) inserting 250 mg of the homogenized sample inside the Distruptor Tube provided by the manufacturer. DNA extraction for each sample was performed on the same day together with two negative controls: a tube with only nucleotide-free water and a tube with laboratory aerosol. The latter was prepared by leaving a 2 mL Eppendorf vial open on the laboratory workbench for several hours and later proceeding with the extraction procedure as the biological sample. DNA concentrations were quantified by using the Qubit dsDNA HS As say Kit with a Qubit 2.0 fluorometer (Invitrogen).

The portable DNA sequencer (MinION) from Oxford Nanopore Technologies (ONT) was utilized to characterize the microbial communities (Kerkhof et al., 2017). The MinION is a third-generation platform for direct sequencing of individual strands of DNA translocating nanoscale pores in a

semiconductor membrane (Schneider and Dekker, 2012; Wang et al., 2015). Library preparation for the MinION relies on the ligation of adaptor and hairpin to rRNA amplicons. Following the manufacturer's instructions, sequencing libraries were prepared using the 16S Barcoding Kit (SQK-16S024) from Oxford Nanopore Technologies (ONT), Oxford, UK. For each sample, 10 ng of DNA was used for PCR amplification. The PCR procedure consisted of 30 cycles of initial denaturation at 95 °C for 1 minute, denaturation at 95 °C, annealing at 55 °C, and extension at 65 °C, followed by a final extension at 65 °C for 1 minute. Negative PCR controls (PCR reagents without DNA) were amplified at the same time.

Barcoded samples were pooled in equimolar proportions, and about 82 fmol of the pooled sample was loaded into a MinION flow cell (R10.3, FLOMIN111). The flow cell was inserted in the MinION for sequencing and the run, operated by ONT's MinKNOW 4.3.12 software (Oxford Nanopore Technologies, Oxford, UK) lasted for 20 hours and the raw fast5 reads were basecalled and demultiplexed using Guppy v2.3.

Passed reads were analyzed using the EPI2ME pipeline (V5.0.2) using the workflow wf_metagenomics (v2.4.1). The parameter settings of the workflow were: minimum length filter 1350, maximum length filter 1650, minimum read quality 7, batch size 32000, bracken length 10000, and default values in the remaining parameters. The pipeline of this workflow does not process by default reads in the unclassified directory.

Ecological functions of different genus have been assessed using literature references (Tab. 3.1), and SILVA (Pruesse et al., 2012) and NCBI (Sayers et al., 2022) databases.

Tab. 3.1 - References used to identify ecological functions of most abundant genus

Genus	Function	Reference	DOI
Thiobacillus	Sulfur oxidation	Haaijer et al., 2007	10.1080/01490450701436489
Sulfovorum	Sulfur oxidation	Sharma et al., 2020	10.1186/s12866-020-01923-3
Sulfuricurvum	Sulfur oxidation	Cron B et al., 2019	10.3389/fmicb.2019.02710
Desulfatiglans	Sulfate reduction	Galushko et al., 2019	https://doi.org/10.1002/9781118960608.gbm01679
Desulfosarcina	Sulfate reduction	Watanabe et al., 2020	https://doi.org/10.1002/9781118960608.gbm01020.pub2
Desulforomonas	Sulfate reduction	Widdel et al. 1992	https://doi.org/10.1007/978-1-4757-2191-1_22
Syntrophus	Syntrophic relationships	Galushko et al., 2019	https://doi.org/10.1002/9781118960608.gbm01064.pub2

3.2.7 Statistical Analysis

For all the samples, stacked histograms representing microbial taxa and their relative abundance were drawn using R (version 4.2.2) and “ggplot2” package v.3.4.2 (Wickham, 2016). Only bacteria with more than >0.5% of total relative abundance were considered. Also, all genus presenting a relative abundance <5% have been collapsed into a macro group labelled “Other”.

Alpha diversity was calculated for each location (PA, CER, and PIR) on normalized abundance data at genus level as (1) total taxa richness (S), (2) Pielou's Evenness index (J) (Pielou, 1966), and (3) Shannon's index (H’). Pielou's Evenness index estimates the degree of uniformity in the distribution of individuals

among different species. The index is maximum when all species are present with the same abundance, instead is low when there is only one abundant, while the Shannon index considers both richness and evenness.

To test the spatial differences in the diversity indexes and on microbial community structure among locations, univariate and multivariate permutational analyses of variance (PERMANOVA) were performed with PERMANOVA+ (Anderson, 2008) using Primer 7 (Clarke and Gorley, 2015). PERMANOVA was based on Euclidean distance matrices for univariate analysis and on Bray-Curtis similarity matrices of square-root transformed data for multivariate. Unconstrained permutation of the raw data with 9999 permutations due to the uneven experimental design (Clarke et al., 2006) were used.

Pattern in the distribution of samples was displayed using a Non-Linear Multi Dimensional Scaling (nMDS) Analysis performed using R software (version 4.2.2)(Oksanen et al., 2022) with the "vegan" package (version 2.6-4). The environmental variables used in the nMDS, have been collected once per location considered the heterogeneity of the environments. Hence, the data regarding geochemical characteristics of soils, such as total lime, AVS, EC, TOC, TN, Fe, S, and ORP have been superimposed.

3.3. Results

3.3.1 Geochemical characterization

In Tab. 3.2, a summary of key geochemical parameters of soil horizons identified in each core are displayed. The morphological features of the soils are reported in Tab. 3.3

Tab. 3.2 - Properties of water-saturated soils and air-dried soils for different horizons. Each row in the table corresponds to a specific horizon within a soil profile (codes according to Soil Survey Staff, 2022), and the columns present parameters retrieved for both water-saturated and air-dried samples. AVS = Acid Volatile Sulfides; TOC = Total Organic Carbon; TN = Total Nitrogen; TOC/TN = Total Organic Carbon to Total Nitrogen ratio; PIR = Pirottolo site; CER = Cerba site; PA = Punte Alberete site. Water reaction on air dry soil is reported before and after the 16 weeks incubation (In pH and Fin pH respectively).

			Analysis on water-saturated soils				Analysis on air dry soils						
Profile	**Horizon**	**Depth**	**H_2O reaction**	**EC sp 25 °C**	**Mean ORP**	**S - AVS (1)**	**H_2O reaction**		**EC 1:2.5 25 °C**	**Total lime**	**TOC**	**TN**	**TOC/TN**
		cm	**pH**	**dS m^{-1}**	**mV**	**mg kg^{-1}**	**In pH**	**Fin pH**	**dS m^{-1}**	**g kg^{-1}**	**g kg^{-1}**	**g kg^{-1}**	
PA	Ase	0 - 4	7.16	0.85	-86	412	7.3	7.75	1.77	191	100.5	6.30	16.0
	Ag	4 - 10	7	0.97	-95	10	7.51	7.71	0.74	144	101.2	5.16	19.6
	Cg1	10 - 17	6.78	1.18	-47	8	7.88	8.01	0.68	231	26.6	2.40	11.1
	Cg2	17 - 32+	7.02	0.96	-68	53	8.11	8.26	0.88	307	13.8	1.46	9.4
CER	Ase	0 - 5	7.37	1.14	-159	1562	7.58	7.74	2.39	283	36.7	3.67	10.0
	Ag	5 - 10	7.27	1.91	-130	174	7.81	7.82	1.52	260	23.5	2.38	9.9
	Cse	10 - 23	7.31	1.44	-223	673	7.96	7.85	1.31	205	11.0	1.21	9.1
	2Cse	23 -35	8.25	1.29	-224	1854	8.56	7.94	0.74	118	2.4	0.24	10.0
PIR	Oi/Ase	0 - 6/7	7.04	5.01	-233	4568	7.26	7.66	7.46	0	119.6	7.14	16.7
	Ase	6/7 - 15	7.43	11.6	-113	1508	7.52	6.96	7.80	0	69.8	4.57	15.3
	A/Cse	15 - 20	7.51	13.8	-77	2461	7.6	7.07	6.03	17	19.5	1.23	15.9
	Cse	20 - 31	7.33	11.8	-198	2168	7.96	6.99	4.27	19	6.5	0.55	11.8
	Cg	31 - 50+	7.34	12.9	-80	658	7.88	7.56	4.79	62	3.4	0.29	11.8

Horizon master: O = organic horizon; A = surface mineral horizon; C = parent material; I = slightly decomposed material; se = presence of sulfides; g = strong gleying.

PA soil profile shows a A/C horizons sequence and consists of 4 horizons, identified as Ase (0 – 4 cm), Ag (4 – 10 cm), Cg1 (10 – 17 cm) and Cg2 (17 - 32+ cm). Texture ranges from silty loam in upper horizons to silty clay loam in the deeper ones. The color is black (5Y 2.5/1) in 0-4 cm horizon and grey (5Y 5/1) in the deepest horizon at 17-32+ cm.

The total lime content is the largest at 17-32+ cm with 305 gkg^{-1}. The pH is highest in the superficial layer with 7.16 in the 0-4 cm horizon and decreases at 10-17 cm with 6.78. This horizon also shows the highest EC value with 1.18 dSm^{-1}, while the lowest is recorded at 0-4 cm with 0.85 dSm^{-1}. ORP is also the lowest in 10-17 cm with -47 mV, while is the lowest in 0-4 cm and 4-10 cm with -86 mV and -95 mV, respectively. The pH after incubation shows a slight increase in all the horizons. TOC and TN decrease with depth form 100.5 gkg^{-1} and 6.30 gkg^{-1} at the top horizon, to 13.8 gkg^{-1} and 1.46 gkg^{-1} at the bottom horizon, respectively. S is more concentrated in the 0-4 cm horizon, with a value of 9700 $mgkg^{-1}$, and gradually decreasing to 2700 $mgkg^{-1}$ in the 17-32+ cm horizon. AVS concentrations are the highest in the 0-4 cm horizon with 412 $mgkg^{-1}$ and observed the lowest values in the middle horizons with 10 $mgkg^{-1}$ and 8 $mgkg^{-1}$ in 4-10 cm and 10-17 cm, respectively. Overall, PA has the highest ORP values and the lowest AVS values compared to the other profiles, suggesting a less reduced and poorer

sulfide environment. On the basis of collected information, this soil profile can be classified as Fluic Frasiwassent, fine-loamy, mixed, calcareous, mesic (Soil Survey Staff, 2022).

CER soil profile shows a A/C horizon sequence and consists of 4 horizons identified as Ase (0 – 5 cm), Ag (5 – 10 cm), Cse (10 – 23 cm), and 2Cse (23 -35 cm). The soil has a silty loam-silty clay loam texture with sandy loam texture in the 23-35+ cm. The color is greenish black (Gley1 2.5/5GY) in Ase (0 – 5 cm) turning to very dark grey (Gley1 3/N) in 2Cse (23-35+ cm) horizon.
The total lime content is 283 gkg^{-1} in the superficial horizon and decreases with depth to 118 gkg^{-1}. The pH is 7.37 in the 0-5 cm horizon and increases with depth at 23-35+ cm reaching a value of 8.25. EC shows almost constant values along the profile, with the highest value of 1.91 dSm^{-1} at 5-10 cm. ORP decreases along the depth with a starting value of -159 mV in the 0-5 cm horizon, reaching -224 mV at 23-35+ cm of depth. AVS concentration are higher at the most superficial and deepest horizon with 1562 and 1854 $mgkg^{-1}$ respectively, while it is lower in between. S concentration reflects the same trend with the highest concentrations in the 0-5 cm and 23-35+cm horizon, with values 2440 $mgkg^{-1}$ and 8910 $mgkg^{-1}$ respectively. The two deeper horizons show a slight decrease of pH after the incubation. TOC content is larger in the upper horizons with a starting value of 36.7 gkg^{-1}, gradually diminishing to 2.4 gkg^{-1} at the bottom of the profile. TN shows the same behaviour starting with 3.67 gkg^{-1} in the 0-5 cm horizon and decreasing to 0.24 gkg^{-1} in the 23-35+ cm horizon. On the basis of collected information, this soil profile can be classified as Haplic Sulfiwassent, coarse-loamy, mixed, calcareous, mesic (Soil Survey Staff, 2022).

PIR soil profile shows a O/A/C horizon sequence and consists of 5 horizons identified as Oi/Ase, Ase, A/Cse, Cse, and Cg. The depth of each horizon is as follows: Oi/Ase (0 - 6/7 cm), Ase (6/7 – 15 cm), A/Cse (15 – 20 cm), Cse (20 – 31 cm), and Cg (31 - 50+ cm). The soil has a sandy loam texture in the upper most horizon becoming sandy with depth (Tab. 3.2). The color is black – yellowish (2.5Y 2.5/1) in the 0 – 6/7 cm horizon (Oi/Ase), becoming very dark greenish gray (Gley1 3/10Y) in the 31 - 50+ cm (Cg) horizon.
The lime content is null in the top horizons and increases till 62 gkg^{-1} in the 31-+50 cm horizon. The soil has pH of 7.04 which increases to 7.34 in the deeper horizons. EC increases as well, ranging from 5.01 dSm^{-1} in the top to 12.9 dSm^{-1} in the deepest horizon. Similarly, oxidation-reduction potential (ORP) increases from -233 mV in the upper horizon to -80 mV in the bottom horizon. The pH after incubation shows a decrease of 0.5 - 1 unit in the three middle horizons. Total organic carbon (TOC) is more abundant in the organic-rich layer at the surface with 119.6 gkg^{-1}, decreasing to 3.4 gkg^{-1} in the bottom horizon. Similar behavior can be observed for total nitrogen (TN), with a concentration of 7.14 gkg^{-1} in the superficial horizon, decreasing to 0.29 gkg^{-1} in the deeper horizon. AVS concentrations are higher in the superficial horizon with 4568 $mgkg^{-1}$ in the 0-6/7 cm horizon, decreasing to 658 $mgkg^{-1}$ in the 31-50+ cm horizon. Sulphur (S) content is 2840 $mgkg^{-1}$ at surface and its concentration remains constant with depth except for the horizon Cse (20-31 cm) where it decreases to 690 $mgkg^{-1}$.. On the basis of collected information, this soil profile can be classified as Sulfic Psammowassent, mixed, mesic (Soil Survey Staff, 2022).

Tab. 3.3- Morphological features of soil profiles

Profile	Horizon		Boundary (D/T)	Matrix Munsell Color (Wet)	Field texture class	Structure (T/G/S)	Fluidity class	Mottles/RMFs (K/Q/S/Sh)	Mottles/RMFs Munsell Color (WET)	Peroxide Color Change (Y/N)	Organic frag/Roots (Q/S)	Odor (K/I)
	Depth (cm)	Master										
PIR	0 - 6/7	Oi/Ase	AS	2.5Y 2.5/1	nd	gr/1/f	VF			N	3/f	S/ST
	6/7 - 15	Ase	CS	10YR 2/2	SaL	gr/1/f	MF			N	2/f	S/ST
	15 - 20	A/Cse	CS	5Y 52.5/2	Sa	sg/0	VF			N	1/m	S/ST
	20 - 31	Cse	CS	5Y 3/1	Sa	sg/0	VF	F3M/c/3/P	5Y 2.5/2	N	1/vf	S/ST
	31 - 50+	Cg	-	Gley1 3/10Y	Sa	sg/0	VF	OSF/c/3/D	Gley1 2.5/10Y	N	1/f	S/SM
CER	0 - 5	Ase	CW	Gley1 2.5/5GY	SiL	pl/1/f	VF			Y		S/ST
	5 - 10	Ag	CW	Gley1 4/10Y	SiL	pl/1/m	SF	F2M/c/2/P	Gley1 3/5GY	Y	1/vf	S/SM
	10 - 23	Cse	AW	Gley1 3/5GY	SiCL	pl/1/m	SF	F2M/m/3/P	Gley2 2.5/5PB	Y	1/vf	S/SM
	23 -35	2Cse	-	Gley1 3/N	LSa	sg/0	MF	F2M/m/4/P	Gley1 2.5/N	Y		S/ST
PA	0 - 4	Ase	CW	5Y 2.5/1	SiL	gr/1/m	VF	OSF/m/1/D	5Y 3/1	Y	2/f	S/SM
	4 - 10	Ag	AW	5Y 3/1	SiL	gr/1/m	MF	OSF/m/1/D	5Y 2.5/1	Y	1/f	S/SL
	10 - 17	Cg1	AW	5Y 4/1	SiCL	sbk/2/f	SF	F3M/c/3/P	5Y 4/2	Y	1/f	S/SL
	17 - 32+	Cg2	-	5Y 5/1	SiCL	sbk/2/f	SF	F3M/m/3/P	5Y 5/3; 2.5Y 5/4	Y		S/SL

Horizon master: se = presence of sulfide; g = gleying. **Horizon boundary:** (D) Distinctness: A = abrupt, C = clear, G = gradual, D = diffuse / (T) Topography: S = smooth, W = wavy, I = irregular, U = unknown; **Field texture class:** Sa = sand, SaL = Sandy Loam, L = Loam, LSa = Loamy Sand, SiL = Silty Loam; SiCL = Silty Clay Loam; **Structure:** (T) Type: gr = granular, abk = angular blocky, sbk = subangular blocky, pl = platy, sg = single grain / (G) Grade: 0 = structureless, 1 = weak, 2 = moderate / (S) Size: vf = very fine, f = fine, m = medium; **Fluidity classes:** SF = Slightly Fluid, MF = Moderately Fluid, VF = Very Fluid; **Mottles/redoximorphic features (RMFs):** (K) Kind: F2M = reduced iron, F3M = oxidated iron, OSF = organic stains / (Q) Quantity: f = few, c = common, m = many / (S) size: 1 = fine, 2 = medium, 3 = coarse, 4 = very coarse, 5 = extremely coarse / (Sh) Shape: D = dendritic, P = platy; **Roots:** (Q) Quantity: 1 = few, 2 = common, 3 = many / (S) Size: vf= very fine, f = fine, m = medium, co = coarse; **Odor:** (K) Kind: N = none, S = sulfurous / (I) Intensity: SL= slight, MD= moderate, ST= strong.

3.3.2 GHGs emissions

The GHGs fluxes measured in grams per square meter per day across different seasons at the three study sites are presented in Tab. 3.4 in the supplementary material (Chiapponi et al., 2024).

During the Fall-Winter season, the mean CO_2 fluxes varied among the sites: PA showed an average flux of 8.62 ± 13.87 g/m²/day, CER had 20.34 ± 54.26 g/m²/day, and PIR exhibited 16.02 ± 7.83 g/m²/day. For CH_4, PA and PIR recorded mean fluxes of 7.56 ± 33.67 g/m²/day and 1.99 ± 1.90 g/m²/day, respectively, while CER presented a substantially higher mean flux of 61.83 ± 250.44 g/m²/day. In contrast, during the Spring-Summer period, there was a noticeable increase in CO_2 and CH_4 fluxes across all sites. PA, CER, and PIR displayed higher mean CO_2 fluxes of 12.38 ± 17.20 g/m²/day, 100.62 ± 157.87 g/m²/day, and 19.37 ± 18.11 g/m²/day, respectively. Similarly, for CH_4, the mean fluxes rose to 6.04 ± 12.65 g/m²/day, 254.09 ± 549.93 g/m²/day, and 15.80 ± 33.89 g/m²/day for PA, CER, and PIR, respectively. The coefficient of variation percentage indicates higher variability in methane fluxes across both seasons and all sites.

Tab. 3.4 - CO_2 and CH_4 fluxes measured in the three studied temperate coastal wetlands in (Chiapponi et al., 2024) (Note: n. points = n. point source measured; SD = Standard Deviation; CV(%) = Coefficient of Variation).

Season	**GHGs fluxes (g/m²/day)**	**Punte Alberete (PA)**		**Cerba (CER)**		**Bassa del Pirottolo (PIR)**	
Fall-Winter (Oct-Feb)		CO_2	CH_4	CO_2	CH_4	CO_2	CH_4
	n. points	80	80	121	121	37	37
	mean	8.62	7.56	20.34	61.83	16.02	1.99
	SD	13.87	33.67	54.26	250.44	7.83	1.90
	CV(%)	160.92	445.58	266.77	405.02	48.88	95.70
Spring-Summer (March-Sept)	**GHGs fluxes (g/m²/day)**	**Punte Alberete (PA)**		**Cerba (CER)**		**Bassa del Pirottolo (PIR)**	
		CO_2	CH_4	CO_2	CH_4	CO_2	CH_4
	n. points	122	122	177	177	84	84
	mean	12.38	6.04	100.62	254.09	19.37	15.80
	SD	17.20	12.65	157.87	549.93	18.11	33.89
	CV(%)	138.97	209.55	156.90	216.43	93.52	214.52

3.3.3 Characterization of bacterial communities

MinION sequencing of the 8 core sediment samples yielded 2,639,917 high-quality reads (replicate PA3 was excluded from the analysis due to its low number of reads). On average, 310,254 ± 119,265 reads were obtained for Punte Alberete samples, 365,632 ± 73,054 for Cerba samples, and 264,371 ± 104,047 reads for Pirottolo. Two negative controls have been used in the analysis. Detected contamination was negligible in both negative controls.

3.3.3.1 Taxonomic composition

The 16S metabarcoding analysis identified 565 families and 3545 genera**.** Sample PA is dominated by genus *Syntrophus* (23.25±0.34%) and *Thiobacillus* (16.68±9.16%), followed by *Haliangium* (8.36±.7.78%), *Clostridium* (7.70±4.91%) as indicated by the prevalence of red/pink colors in Fig. 3.3.
In the CER location, on the contrary, we observed a prevalence of *Thiobacillus* (19,18±9.77%) and *Sulfuricurvum* (13.76±7.16%)*,* followed by similar mean abundances of *Lysobacter* (9.29±13.66%) and *Desulfuromonas* (9.18±4.66).
In the PIR brackish-water location we observed a different prevalence of taxa compared to the other locations. The most abundant taxa were *Desulfatiglans* (20.04±8.05%), and *Desulfosarcina* (10.69±5.08%),

represented by the yellow/green colors. Also, *Algorimarina* (10.17±6.59%), *Thiobacillus* (9.93±10.27%), and *Anaerohalosphaera* (7.73±3.79%) reported moderate high relative abundances.

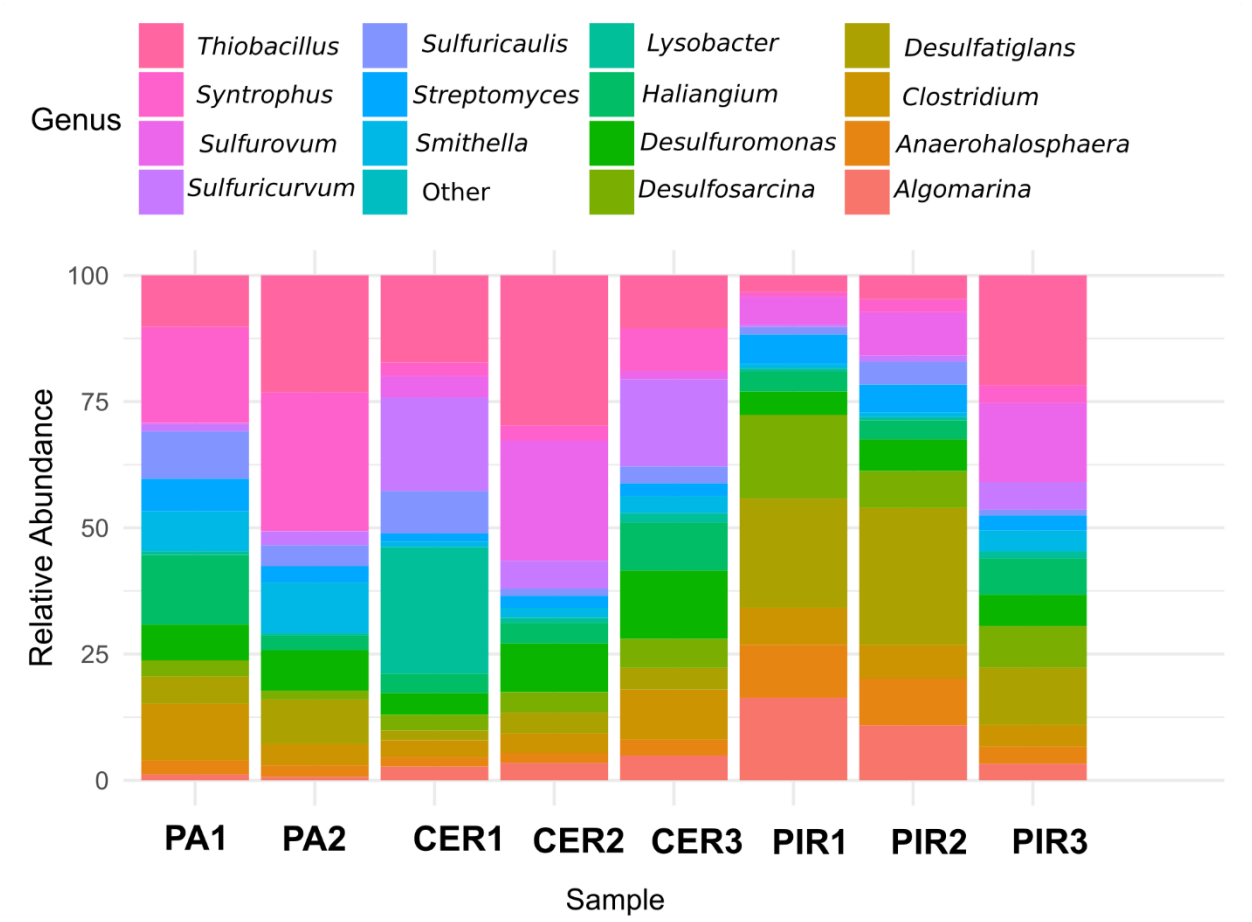

Fig. 3. 3 - Bacterial taxonomic profile (at the family level) and relative abundance found in each sample. Only taxa representing more than >0.5% of total relative abundance have been considered. The class "Other" includes all genus with abundance <5%. Note: Punte Alberete site (PA); Cerba site (CER); Pirottolo (PIR).

3.3.3.2 Alpha diversity indices

The bacterial communities at the three locations host a comparable Taxa Richness (S) with PA showing an average of 2,690.50±140.50 genus, CER with 2,920.67±56.41 taxa, and PIR with 2,742.67±193.77 taxa (Tab.3.5) (p>0.05, Tab. 3.6). Pielou's Evenness Index (J) ranged from 0.95±0.01 to 0.96± 0.0007 in PIR and CER, suggesting a high level of evenness in the number and abundance of each genus within these sites) (p>0.05, Tab. 3.7. Shannon's Index (H') values are also very similar among locations) (p>0.05, Tab. 3.8).

Tab. 3.5 – Table reporting different diversity indices for the three sites. S=total taxa richness; J= Pielou's index; H= Shannon's index.

		PA	CER	PIR
S	Mean	2690.5	2920.67	2742.67
	St.Dev	140.5	56.41	193.77
	Min	2550	2841	2481
	Max	2831	2964	2944
J'	Mean	0.96	0.96	0.95
	St.Dev	0	0	0.01
	Min	0.95	0.96	0.94
	Max	0.96	0.96	0.96
H	Mean	7.57	7.66	7.52
	St.Dev	0.09	0.02	0.12
	Min	7.48	7.63	7.36
	Max	7.65	7.68	7.65

Tab. 3.6 - Results of ANOVA analysis testing difference in: total taxa richness (S between sites). Df = Degrees of Freedom; Sum.Sq = Sum of Squares; Mean Sq.= Mean Square; Pseudo F = pseudo-F statistic; P (perm)= Permutation test.

S	**df**	**SS**	**MS**	**Pseudo-F**	**P(perm)**
Site	2	77418	38709	1.1972	0.3341
Res	5	1.6167E+05	32334		
Total	7	2.3909E+05			

Tab. 3.7 - Results of ANOVA analysis testing difference in Pielou's index (J).between sites. Df = Degrees of Freedom; Sum.Sq = Sum of Squares; Mean Sq.= Mean Square; Pseudo F = pseudo-F statistic; P (perm)= Permutation test .

J	**df**	**SS**	**MS**	**Pseudo-F**	**P(perm)**
Site	2	0.00013921	6.9604E-05	1.8722	0.1853
Res	5	0.00018589	3.7177E-05		
Total	7	0.0003251			

Tab.3.8 - Results of ANOVA analysis testing difference in Shannon's index (H.between sites. Df = Degrees of Freedom; Sum.Sq = Sum of Squares; Mean Sq.= Mean Square; Pseudo F = pseudo-F statistic; P (perm)= Permutation test.

H	**df**	**SS**	**MS**	**Pseudo-F**	**P(perm)**
Site	2	0.028593	0.014297	1.1586	0.3506
Res	5	0.061699	0.01234		
Total	7	0.090292			

3.3.3.3 Community structural analysis

The bacterial community structures were statistically significant among different locations (P(perm) = 0.004, Tab. 3.9) as also evidenced by the nMDS (Fig. 3.4). In the reduced space of nMDS, PA1 is located in the lower-left quadrant at coordinates MDS1 = -0.24 and MDS2 = -0.27, while PA2 is close at MDS1 = -0.23 and MDS2 = -0.21, demonstrating a resemblance in their lower-left quadrant position. CER1 is in the top portion of the reduced area, with MDS1 = -0.22 and MDS2 = 0.38, indicating dissimilarity to PA1 and PA2. CER2 is in the upper-left quadrant, with MDS1 = -0.04 and MDS2 = 0.09, indicating possible similarities with CER1. CER3, which has MDS1 = -0.15 and MDS2 = 0.07, is also in the upper-left quadrant, showing some dissimilarity to PA1 and PA2. PIR1 is located in the upper-right quadrant, with MDS1 = 0.36 and MDS2 = 0.06, indicating dissimilarity with PA1 and PA2, but probable similarity with CER2 and CER3. PIR2, with MDS1 = 0.42 and

MDS2 = -0.09, is in the down half of the reduced area, somewhat to the right of PIR1, showing considerable dissimilarity. PIR3, located in the lower-right quadrant with MDS1 = 0.08 and MDS2 = -0.03, indicates dissimilarity to CER1, CER2, and CER3. The points distribution on the nMDS plot, are displayed along a salinity range, with freshwater locations on the left quadrant, and brackish locations on the right.

In this nMDS analysis, environmental variables such as Total lime, Fe, S, AVS, EC, TN, TOC, and ORP, have been fitted as vectors (Fig. 3.4). The length and direction of the vectors indicate the direction and strength of the relationship between the variable and the replicates. Upon examination of the plot, we observe that AVS, EC sp 25 °C and EC 1:2.5 25 °C, are aligned along MDS1 influencing replicates from PIR location. On the opposite direction on axis MDS1 is aligned the vector representing Total lime which influences replicates from CER location. S, ORP are aligned on axis MDS2, and their directions indicate an influence on replicates from PA location.

Tab3.9– Results of Permanova results testing differences among the three study sites

	Df	SumOfSqs	R2	F	Pr(>F)
permanova_var$Group	2	0.354333	0.54102	2.946866	0.0043
Residual	5	0.300602	0.45898	NA	NA
Total	7	0.654934	1	NA	NA

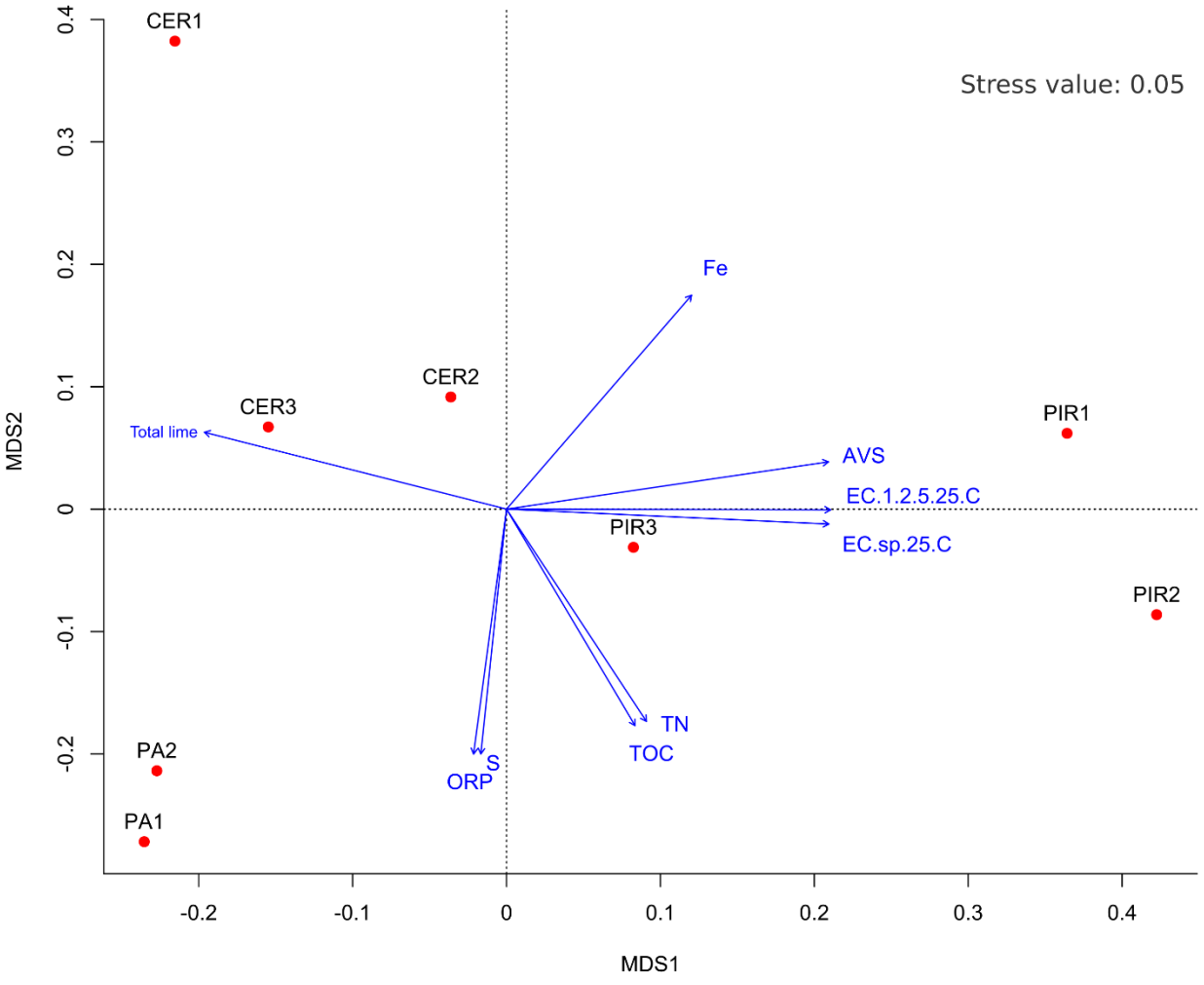

Fig. 3. 4 – Non-Metric Multidimensional Scaling (NMDS) used to analyze the microbial community structure of samples. Square Root is used for transformation and the Bray-Curtis distance metric to calculate the similarity matrix.

3.4. Discussion

Due to their ability to function as carbon sources or sinks, wetlands have a significant impact on the global carbon cycle. Microbially mediated biogeochemical processes, which are further regulated by environmental factors, control the source-sink capacity of wetlands. In this study we investigate the microbial communities at three distinct locations, representing three different temperate coastal wetlands along a salinity gradient: Punte Alberete (PA) is characterized by freshwater ecosystems, Cerba (CER) is another freshwater ecosystem characterized by waters slightly saltier than PA, and Pirottolo (PIR), presenting brackish waters. The significance of salinity as an ecological process driver in tidal fresh-/brackish-water wetlands is particularly important in the study area given the increase of saltwater intrusion, and its exacerbation in the future scenario due to climate change (Giambastiani et al., 2021). The results of this study suggest that salinity and sulfur content lead the major changes in the bacterial community structure along the gradient. The NMDS analysis (Fig. 3.4) shows that the samples are organized along a salinity gradient from the most freshwater environment, PA, to the most brackish site PIR. PIR exhibits the highest EC compared to CER and PA, explaining the nMDS pattern observed. In PIR location the EC increases from 5.01 dSm^{-1} of the top horizon to 12.9 dSm^{-1} of the bottom horizon. Additionally, Fe concentration is the highest in the PIR site, decreasing from 34.5 gkg^{-1} in the upper horizon to 28.1 gkg^{-1} in the 31-50 cm horizon.

Moreover, at the PIR site, the upper horizon contains the highest TOC and TN content, while AVS and S concentrations vary among horizons. The previous study by Chiapponi et al. (2024) performed in the same study site proved that salinity and water column height play a major role in limiting CH_4 and CO_2 emissions in these coastal wetlands. As summarized in Tab. 3.4, the present study gives a complementary look at how seawater presence allows SRB (Sulfate Reducing Bacteria) to outcompete methanogenic bacteria for carbon substrates (Lovley and Klug, 1986). The presence of sulfate ions favors sulfur-cycling processes in wetland soils to a greater extent at the expense of other redox zone activities, hence decreasing CH_4 emissions (Poffenbarger et al., 2011). Sulphates are abundant in brackish/saline ecosystems, as found in PIR, and act as oxidizing agents in the decomposition of organic matter, reducing methanogenesis and lowering overall emissions (Bridgham et al., 2013; Chiapponi et al., 2024). Because sulfate reduction is more energy-efficient than methanogenesis and fermentative processes, it is critical for lowering gross methane production and, as a result, lowering methane emissions into the environment (Capone and Kiene, 1988).

The freshwater location of PA shows a distinct preponderance of *Synthrophus* (23.25±5.99%) (Fig. 3.3). Its presence is linked to CH_4 production, as syntrophic bacteria engage with methanogenic archaea in cooperative interspecies metabolic interactions, breaking down organic matter into smaller molecules for secondary fermentation, which is the final step in the processes that produce CH_4 (Berrier et al., 2022). Also, *Haliangium* (8.37±7.69%), and *Thiobacillus* (16.68±9.16%) were present (Fig. 3.3). *Haliangium* is a salt-tolerant myxobacteria found in saline and riparian soils (Fudou et al., 2002) and has a selective predation for methanotrophs and this can explain the almost absence of such taxa in these samples (Kaupper et al., 2022). The presence of *Thiobacillus* suggests the higher potential for sulfur reduction (Bonetti et al., 2021). According to these results, PA has a specialized community, with some genera being essential to the breakdown of organic waste or the cycling of nutrients.

In contrast, the structure of the microbial population at the CER site is noticeably different, with the presence of *Lysobacter* (9.29±13.66%%), *Sulfuricurvum* (13.76±7.16%), *Thiobacillus* (19.18± 9.77%), and *Sulfuricaulis* (4.39±3.61%). The existence of these genera—particularly *Thiobacillus*—indicates that the CER ecosystem may be involved in sulfur cycling or other biogeochemical processes. CER stands out with the highest species richness, while the PA site shows the lowest.

Lysobacter is linked to the presence of Fe(III) in soils (Ko et al., 2009; Luo et al., 2019). Moreover, *Lysobacter* can replace other microorganisms in the system to reduce the competition with sulfate reducing bacteria as electron acceptors (Wang et al., 2021), and can fix and supply nitrogen for other biota and is positive for the reduction of nitrate to nitrite (Iwata et al., 2010). *Sulfuricurvum* and *Thiobacillus* are sulfur oxidizing bacteria

(SOBs) that are involved in the oxidation of sulfur compounds and the production of sulfuric acid (Haaijer et al., 2008). These bacteria may be present in soils with high sulfur concentrations (She et al., 2016), like the ones we find both in the topmost (0-5 cm) and the deepest (23-35+ cm) horizons. *Thiobacillus species* may be key players in nitrate-dependent iron sulfide dissolution in freshwater wetlands (Haaijer et al., 2008). This could explain the inverse Pearson correlation between soluble nitrate and AVS in PA and CER soil profiles (-0.99 and -0.45 respectively).

A distinct shift in the microbial community structure is observable at the brackish-water site PIR. Within PIR, the most prevalent genus is *Desulfatiglans* (20.04±8.05%), along with *Desulfosarcina* (10.69±5.08%), *Algorimarina* (10.17±6.59%), and *Thiobacillus* (9.93±10.27%). The differences in microbial community, compared to PA and CER, imply that the brackish-water location PIR has a distinct microbial community structure, with distinct taxa dominating each sample. In this specific context, *Desulfatiglans* may have a role in sulfur metabolism (Fortin et al., 2000). *Desulfosarcina* is a SRB that can utilize acetate and other fatty acids, oxidizing them completely (Jackson et al., 2014). *Algomarina* spp have a syntrophic butyrate metabolism and are phylogenetically related to SRB from the genera *Desulfonema* and *Desulfosarcina* (McInerney et al., 2008). *Anaerohalosphaera* (7.73±3.79%) is an obligately anaerobic bacteria, moderately halophilic and mesophilic, and can assimilate sulfate (Pradel et al., 2020). Sulfur-cycling process seems also to enhance C mineralization, potentially both reducing CH_4 emissions and enhancing C storage (Candry et al., 2023). *Desulfatiglans* is, ad an example, the most prevalent genus in all samples from PIR, and this is probably linked to its role in sulfur metabolism (Kevorkian et al., 2020). Chiapponi et al. (2024) have in fact clearly shown the low CH_4 fluxes coming from PIR areas but has also enhanced large CO_2 fluxes, comparable to those from freshwater environments, despite the presence of salinity. Similar results were observed in other studies that show how high salinity and CO_2 enhance the presence of SRB (Kim et al., 2020), while decreasing CH_4 emissions (Poffenbarger et al., 2011). However, exceptions are present, as oxidation of reduced sulfur compounds by *Thiobacillus* may release CO_2 as a byproduct (Kleindienst et al., 2014; Jackson et al., 2014). The reduction of sulfate to sulfide and the consequent breakdown of organic materials, which can also lead to the release of CO_2, are also caused by SRB, such as *Desulfatiglans* and *Desulfosarcina* (Kleindienst et al., 2014; Jackson et al., 2014). While SRB competition may prevent the production of CH_4, it may also cause a rise in CO_2 emissions as a consequence, which might counteract the decrease in CH_4 emissions, and the carbon sink capacity of wetlands (Pester, 2012; La et al., 2022). Also, it is known that regular changes in soil redox conditions caused by dry-wet transitions can reduce CH_4 output while increasing N_2O emissions at the same time, offsetting the advantages of CH_4 mitigation (Peyron et al., 2016). The variations in microbial populations responsible for the carbon cycle across sites primarily stem from differences in salinity and sulfate levels. (Fig. 3.5).

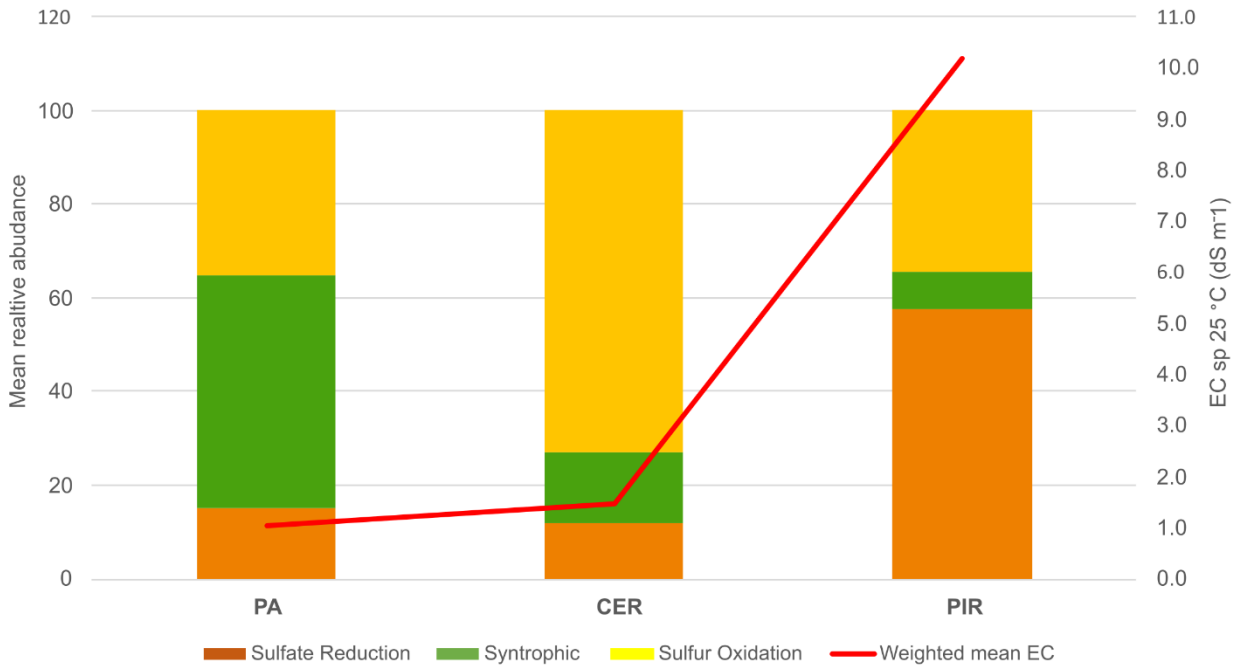

Fig. 3.5 – Mean abundances of functional group per site. Functional group for each genus has been extracted from the cited literature.

Despite having measured CH_4 fluxes in all three sites, no methanogens are found in the sampled soil cores. The absence of methanogens in the soil cores may be due to a variety of factors, including the specific environmental conditions of the studied coastal wetlands (Angel et al., 2012), the limited depth of soil cores, the limited number of replicates for each core because of budget limitations, and the limitations of the experimental design itself. Exposure to oxygen in the soils, among other environmental factors, can decrease methanogen activity (Angel et al., 2012). They are also sensitive to temperature, pH and salt (Angel et al., 2012). Extrusion of soil samples may result in the loss of anoxic conditions existing in the soil. This is because the soil is exposed to oxygen during the extrusion process, which might modify the redox conditions (Fiedler et al., 2007) and lead to the loss of anaerobic microsites where methanogens grow. The depth of the soil cores can affect methanogen identification since deeper soil layers are more likely to retain anoxic conditions than shallow levels. When taking samples from a shallow depth of 20 cm (Angle et al., 2017), the little exchange of oxygen with the water column may not guarantee anoxic conditions, resulting in the lack of methanogens in the samples (Angle et al., 2017).
Further studies at a more detailed level, as an example at each pedological-horizon level and involving more control replicates can be done to investigate the presence and role of methanogens in these complex environments.

3.5. Conclusion

In this study, we investigated the microbial communities at three distinct temperate coastal wetlands of the Northern Adriatic coast (Italy) along a salinity gradient to assess the interplay between biogeochemical characteristics in submerged soils and GHG emissions. For the first time to our knowledge, a characterization of the microbial community involved in GHGs production has been conducted in these areas, shedding a light on the C mineralization process occurring in these habitats.

The results suggest that EC and S content lead the major changes in bacterial community structure in different habitats. The clustering analysis reveals three clearly defined clusters of communities that exhibit significant differences from one another: taxa inhabiting freshwater ecosystems, taxa specific to shallow-freshwater

habitats, and communities thriving in brackish ecosystems. In freshwater ecosystems like PA and CER, SOB dominate, while in brackish environments like PIR, SRBs are prevalent. The high EC and elevated Fe levels at the brackish-water PIR site drive a shift in bacterial communities towards an abundance of SRB. These findings underscore the role of salinity and sulfur in inhibiting methane CH_4 emissions: the sulfur-rich brackish environment, with its SRB prevalence, shows lower CH_4 emissions compared to freshwater settings.

The study underscores the critical role of characterizing microbial communities in coastal wetlands to unravel their significance in the intricate biogeochemical processes driving carbon cycling. While acknowledging the study's limited scope and the complex nature of wetland systems, it emphasizes a potential trade-off between reduced CH_4 emissions and increased CO_2 emissions with rising salinity levels, as supported by current research (Candry et al., 2023). Although CO_2 is a less potent greenhouse gas than CH_4, higher CO_2 emissions could counterbalance wetlands' carbon sequestration capacity, potentially shifting them from carbon sinks to carbon sources. To craft effective environmental management strategies aimed at mitigating wetlands' global warming potential, it is imperative to consider the diverse greenhouse gas emissions comprehensively (Peyron et al., 2016).

Biogeochemical studies in wetlands play a pivotal role in detecting the intricate interplay between living organisms and environmental factors (Trettin et al., 2019). By delving into the impacts of climate-induced changes like sea level rise and saltwater intrusion on these processes, these studies offer invaluable insights to shape wetland management strategies. This approach not only highlights the long-term health and sustainability of these ecosystems but also contributes to climate change mitigation efforts.

„,

Acknowledgment

This study was performed with the support of the Ravenna municipality (Italy) that granted access to the reserve and the support of the Office for Biodiversity Protection of Punta Marina (Carabinieri Forestali). The authors would like to thank Dr. Francesco Mugnai and Miss. Martina La Torre for the support during the metagenomics analysis and Prof. Enrico Dinelli for performing XRF analysis on samples. This study was carried out within the 490 RETURN Extended Partnership and received funding from the European Union Next-GenerationEU (National Recovery and Resilience Plan – NRRP, Mission 4, Component 2, Investment 1.3 – D.D. 1243 2/8/2022, PE0000005).

References

Amorosi, A., Colalongo, M. L., Pasini, G., and Preti, D.: Sedimentary response to Late Quaternary sea-level changes in the Romagna coastal plain, Sedimentology, 99–121, https://doi.org/10.1046/j.1365-3091.1999.00205.x, 1999.

An, L., Yan, Y.-C., Tian, H.-L., Chi, C.-Q., Nie, Y., and Wu, X.-L.: Roles of sulfate-reducing bacteria in sustaining the diversity and stability of marine bacterial community, Front. Microbiol., 14, 1218828, https://doi.org/10.3389/fmicb.2023.1218828, 2023.

Anderson, M. J.: PERMANOVA+ for PRIMER: guide to software and statistical methods., Primer-E Limited, 2008.

Angel, R., Claus, P., and Conrad, R.: Methanogenic archaea are globally ubiquitous in aerated soils and become active under wet anoxic conditions, ISME J, 6, 847–862, https://doi.org/10.1038/ismej.2011.141, 2012.

Angle, J. C., Morin, T. H., Solden, L. M., Narrowe, A. B., Smith, G. J., Borton, M. A., Rey-Sanchez, C., Daly, R. A., Mirfenderesgi, G., Hoyt, D. W., Riley, W. J., Miller, C. S., Bohrer, G., and Wrighton, K. C.: Methanogenesis in oxygenated soils is a substantial fraction of wetland methane emissions, Nat Commun, 8, 1567, https://doi.org/10.1038/s41467-017-01753-4, 2017.

Antonellini, M., Mollema, P., Giambastiani, B., Bishop, K., Caruso, L., Minchio, A., Pellegrini, L., Sabia, M., Ulazzi, E., and Gabbianelli, G.: Salt water intrusion in the coastal aquifer of the southern Po Plain, Italy, Hydrogeol J, 16, 1541–1556, https://doi.org/10.1007/s10040-008-0319-9, 2008.

Antonellini, M., Giambastiani, B. M. S., Greggio, N., Bonzi, L., Calabrese, L., Luciani, P., Perini, L., and Severi, P.: Processes governing natural land subsidence in the shallow coastal aquifer of the Ravenna coast, Italy, CATENA, 172, 76–86, https://doi.org/10.1016/j.catena.2018.08.019, 2019.

Berrier, D. J., Neubauer, S. C., and Franklin, R. B.: Cooperative microbial interactions mediate community biogeochemical responses to saltwater intrusion in wetland soils, FEMS Microbiology Ecology, 98, fiac019, https://doi.org/10.1093/femsec/fiac019, 2022.

Bonetti, G., Trevathan-Tackett, S. M., Carnell, P. E., Treby, S., and Macreadie, P. I.: Local vegetation and hydroperiod influence spatial and temporal patterns of carbon and microbe response to wetland rehabilitation, Applied Soil Ecology, 163, 103917, https://doi.org/10.1016/j.apsoil.2021.103917, 2021.

Bridgham, S. D., Cadillo-Quiroz, H., Keller, J. K., and Zhuang, Q.: Methane emissions from wetlands: biogeochemical, microbial, and modeling perspectives from local to global scales, Glob Change Biol, 19, 1325–1346, https://doi.org/10.1111/gcb.12131, 2013.

Buscaroli, A. and Zannoni, D.: Influence of ground water on soil salinity in the San Vitale Pinewood (Ravenna – Italy), Vol. LIV-N. 5, 2010.

Buscaroli, A. and Zannoni, D.: Soluble ions dynamics in Mediterranean coastal pinewood forest soils interested by saline groundwater, CATENA, 157, 112–129, https://doi.org/10.1016/j.catena.2017.05.014, 2017.

Buscaroli, A., Gherardi, M., Vianello, G., Vittori Antisari, L., and Zannoni, D.: Soil survey and classification in a complex territorial system: Ravenna (85taly), EQA – International Journal of Environmental Quality, Vol. 2, 15–28, https://doi.org/10.6092/ISSN.2281-4485/3815, 2009.

Candry, P., Abrahamson, B., Stahl, D. A., and Winkler, M. H.: Microbially mediated climate feedbacks from wetland ecosystems, Global Change Biology, 29, 5169–5183, https://doi.org/10.1111/gcb.16850, 2023.

Capaccioni, B., Tassi, F., Cremonini, S., Sciarra, A., and Vaselli, O.: Ground heating and methane

oxidation processes at shallow depth in Terre Calde di Medolla (Italy): Observations and conceptual model: SOIL HEATING DUE TO METHANE OXIDATION, J. Geophys. Res. Solid Earth, 120, 3048–3064, https://doi.org/10.1002/2014JB011635, 2015.

Capone, D. G. and Kiene, R. P.: Comparison of microbial dynamics in marine and freshwater sediments: Contrasts in anaerobic carbon catabolism1: Microbial dynamics in sediments, Limnol. Oceanogr., 33, 725–749, https://doi.org/10.4319/lo.1988.33.4part2.0725, 1988.

Cardellini, C., Chiodini, G., Frondini, F., Granieri, D., Lewicki, J., and Peruzzi, L.: Accumulation chamber measurements of methane fluxes: application to volcanic-geothermal areas and landfills, Applied Geochemistry, 18, 45–54, https://doi.org/10.1016/S0883-2927(02)00091-4, 2003.

Chiapponi, E., Silvestri, S., Zannoni, D., Antonellini, M., and Giambastiani, B. M. S.: Driving and limiting factors of CH 4 and CO 2 emissions from coastal brackish-water wetlands in temperate regions, Biogeosciences, 21, 73–91, https://doi.org/10.5194/bg-21-73-2024, 2024.

Clarke, K. R. and Gorley, R. N.: Getting started with PRIMER v7, vol. PRIMER-E, lymouth: Plymouth Marine Laboratory, 2015.

Clarke, K. R., Somerfield, P. J., and Chapman, M. G.: On resemblance measures for ecological studies, including taxonomic dissimilarities and a zero-adjusted Bray–Curtis coefficient for denuded assemblages, Journal of Experimental Marine Biology and Ecology, 330, 55–80, https://doi.org/10.1016/j.jembe.2005.12.017, 2006.

D. Fortin, R. Goulet, M. Roy: Seasonal Cycling of Fe and S in a Constructed Wetland: The Role of Sulfate-Reducing Bacteria, Geomicrobiology Journal, 17, 221–235, https://doi.org/10.1080/01490450050121189, 2000.

Dang, C., Morrissey, E. M., Neubauer, S. C., and Franklin, R. B.: Novel microbial community composition and carbon biogeochemistry emerge over time following saltwater intrusion in wetlands, Global Change Biology, 25, 549–561, https://doi.org/10.1111/gcb.14486, 2019.

Duarte, C. M., Losada, I. J., Hendriks, I. E., Mazarrasa, I., and Marbà, N.: The role of coastal plant communities for climate change mitigation and adaptation, Nature Clim Change, 3, 961–968, https://doi.org/10.1038/nclimate1970, 2013.

EEC – Council of the European Union: Council Directive 79/409/EEC of 2 April 1979 on the conservation of wild birds.pdf, OJ L 103, 1–18, 1979.

EEC – Council of the European Union: Council Directive 92/43/EEC of 21 May 1992 on the conservation of natural habitats and of wild fauna and flora, Official Journal L 206, 92/43/EEC, P. 7-50, 1992.

Ferronato, C., Falsone, G., Natale, M., Zannoni, D., Buscaroli, A., Vianello, G., and Vittori Antisari, L.: Chemical and pedological features of subaqueous and hydromorphic soils along a hydrosequence within a coastal system (San Vitale Park, Northern Italy), Geoderma, 265, 141–151, https://doi.org/10.1016/j.geoderma.2015.11.018, 2016.

Fiedler, S., Vepraskas, M. J., and Richardson, J. L.: Soil Redox Potential: Importance, Field Measurements, and Observations, in: Advances in Agronomy, vol. 94, Elsevier, 1–54, https://doi.org/10.1016/S0065-2113(06)94001-2, 2007.

Fudou, R., Jojima, Y., Iizuka, T., and Yamanaka, S.: Haliangium ochraceum gen. nov., sp. Nov. and Haliangium tepidum sp. Nov.: Novel moderately halophilic myxobacteria isolated from coastal saline environments., J. Gen. Appl. Microbiol., 48, 109–115, https://doi.org/10.2323/jgam.48.109, 2002.

Giambastiani, B. M. S., Antonellini, M., Oude Essink, G. H. P., and Stuurman, R. J.: Saltwater intrusion in the unconfined coastal aquifer of Ravenna (Italy): A numerical model, Journal of Hydrology, 340, 91–104,

https://doi.org/10.1016/j.jhydrol.2007.04.001, 2007.

Giambastiani, B. M. S., Kidanemariam, A., Dagnew, A., and Antonellini, M.: Evolution of Salinity and Water Table Level of the Phreatic Coastal Aquifer of the Emilia Romagna Region (Italy), Water, 13, 372, https://doi.org/10.3390/w13030372, 2021.

Gonneea, M. E., Maio, C. V., Kroeger, K. D., Hawkes, A. D., Mora, J., Sullivan, R., Madsen, S., Buzard, R. M., Cahill, N., and Donnelly, J. P.: Salt marsh ecosystem restructuring enhances elevation resilience and carbon storage during accelerating relative sea-level rise, Estuarine, Coastal and Shelf Science, 217, 56–68, https://doi.org/10.1016/j.ecss.2018.11.003, 2019.

Haaijer, S. C. M., Harhangi, H. R., Meijerink, B. B., Strous, M., Pol, A., Smolders, A. J. P., Verwegen, K., Jetten, M. S. M., and Op Den Camp, H. J. M.: Bacteria associated with iron seeps in a sulfur-rich, neutral pH, freshwater ecosystem, ISME J, 2, 1231–1242, https://doi.org/10.1038/ismej.2008.75, 2008.

Hach Company: Sulfide, Methylene Blue Method, Method 10254, 2014.

Hach Company: Sulfate, SulfaVer 4 Method (70 mg/L), 2019.

Hopkinson, C. S., Cai, W.-J., and Hu, X.: Carbon sequestration in wetland dominated coastal systems—a global sink of rapidly diminishing magnitude, Current Opinion in Environmental Sustainability, 4, 186–194, https://doi.org/10.1016/j.cosust.2012.03.005, 2012.

ISO – International Standard Organization, S.: ISO 10694:1995, Soil quality – Determination of organic and total carbon after dry combustion (elementary analysis), Technical Committee ISO/TC 190, 1995.

IPCC – Intergovernmental Panel On Climate Change (Ipcc): The Ocean and Cryosphere in a Changing Climate: Special Report of the Intergovernmental Panel on Climate Change, 1st ed., Cambridge University Press, https://doi.org/10.1017/9781009157964, 2022.

Iwata, K., Azlan, A., Yamakawa, H., and Omori, T.: Ammonia accumulation in culture broth by the novel nitrogen-fixing bacterium, Lysobacter sp. E4, Journal of Bioscience and Bioengineering, 110, 415–418, https://doi.org/10.1016/j.jbiosc.2010.05.006, 2010.

Jackson, K. L., Whitcraft, C. R., and Dillon, J. G.: Diversity of Desulfobacteriaceae and Overall Activity of Sulfate-Reducing Microorganisms in and Around a Salt pan in a Southern California Coastal Wetland, Wetlands, 34, 969–977, https://doi.org/10.1007/s13157-014-0560-z, 2014.

Jørgensen, B. B., Findlay, A. J., and Pellerin, A.: The Biogeochemical Sulfur Cycle of Marine Sediments, Front. Microbiol., 10, 849, https://doi.org/10.3389/fmicb.2019.00849, 2019.

Kasozi, G. N., Nkedi-Kizza, P., and Harris, W. G.: Varied Carbon Content of Organic Matter in Histosols, Spodosols, and Carbonatic Soils, Soil Sci. Soc. Am. J., 73, 1313–1318, https://doi.org/10.2136/sssaj2008.0070, 2009.

Kaupper, T., Mendes, L. W., Poehlein, A., Frohloff, D., Rohrbach, S., Horn, M. A., and Ho, A.: The methane-driven interaction network in terrestrial methane hotspots, Environmental Microbiome, 17, 15, https://doi.org/10.1186/s40793-022-00409-1, 2022.

Kerkhof, L. J., Dillon, K. P., Häggblom, M. M., and McGuinness, L. R.: Profiling bacterial communities by MinION sequencing of ribosomal operons, Microbiome, 5, 116, https://doi.org/10.1186/s40168-017-0336-9, 2017.

Kevorkian, R., Callahan, S., Winstead, R., and Lloyd, K. G.: ANME-1 archaea drive methane accumulation and removal in estuarine sediments, Microbiology, https://doi.org/10.1101/2020.02.24.963215, 2020.

Kim, S.-Y., Freeman, C., Lukac, M., Lee, S.-H., Kim, S. D., and Kang, H.: Elevated CO2 and high salinity enhance the abundance of sulfate reducers in a salt marsh ecosystem, Applied Soil Ecology, 147,

103386, https://doi.org/10.1016/j.apsoil.2019.103386, 2020.

Kleindienst, S., Herbst, F.-A., Stagars, M., Von Netzer, F., Von Bergen, M., Seifert, J., Peplies, J., Amann, R., Musat, F., Lueders, T., and Knittel, K.: Diverse sulfate-reducing bacteria of the Desulfosarcina/Desulfococcus clade are the key alkane degraders at marine seeps, ISME J, 8, 2029–2044, https://doi.org/10.1038/ismej.2014.51, 2014.

Ko, H.-S., Jin, R.-D., Krishnan, H. B., Lee, S.-B., and Kim, K.-Y.: Biocontrol Ability of Lysobacter antibioticus HS124 Against Phytophthora Blight Is Mediated by the Production of 4-Hydroxyphenylacetic Acid and Several Lytic Enzymes, Curr Microbiol, 59, 608–615, https://doi.org/10.1007/s00284-009-9481-0, 2009.

La, W., Han, X., Liu, C.-Q., Ding, H., Liu, M., Sun, F., Li, S., and Lang, Y.: Sulfate concentrations affect sulfate reduction pathways and methane consumption in coastal wetlands, Water Research, 217, 118441, https://doi.org/10.1016/j.watres.2022.118441, 2022.

Liang, S., Li, H., Wu, H., Yan, B., and Song, A.: Microorganisms in coastal wetland sediments: a review on microbial community structure, functional gene, and environmental potential, Front. Microbiol., 14, 1163896, https://doi.org/10.3389/fmicb.2023.1163896, 2023.

Luo, M., Huang, J.-F., Zhu, W.-F., and Tong, C.: Impacts of increasing salinity and inundation on rates and pathways of organic carbon mineralization in tidal wetlands: a review, Hydrobiologia, 827, 31–49, https://doi.org/10.1007/s10750-017-3416-8, 2019.

Marani, M., Zillio, T., Belluco, E., Silvestri, S., and Maritan, A.: Non-Neutral Vegetation Dynamics, PloS ONE, 1, e78, https://doi.org/10.1371/journal.pone.0000078, 2006.

Marani, M., D'Alpaos, A., Lanzoni, S., Carniello, L., and Rinaldo, A.: The importance of being coupled: Stable states and catastrophic shifts in tidal biomorphodynamics, J. Geophys. Res., 115, 2009JF001600, https://doi.org/10.1029/2009JF001600, 2010.

McCuen, M. M., Pitesky, M. E., Buler, J. J., Acosta, S., Wilcox, A. H., Bond, R. F., and Díaz-Muñoz, S. L.: A comparison of amplification methods to detect Avian Influenza viruses in California wetlands targeted via remote sensing of waterfowl, Transbound Emerg Dis, 68, 98–109, https://doi.org/10.1111/tbed.13612, 2021.

McInerney, M. J., Struchtemeyer, C. G., Sieber, J., Mouttaki, H., Stams, A. J. M., Schink, B., Rohlin, L., and Gunsalus, R. P.: Physiology, Ecology, Phylogeny, and Genomics of Microorganisms Capable of Syntrophic Metabolism, Annals of the New York Academy of Sciences, 1125, 58–72, https://doi.org/10.1196/annals.1419.005, 2008.

Mitsch, W. J., Bernal, B., Nahlik, A. M., Mander, Ü., Zhang, L., Anderson, C. J., Jørgensen, S. E., and Brix, H.: Wetlands, carbon, and climate change, Landscape Ecol, 28, 583–597, https://doi.org/10.1007/s10980-012-9758-8, 2013.

Morrissey, E. M., Gillespie, J. L., Morina, J. C., and Franklin, R. B.: Salinity affects microbial activity and soil organic matter content in tidal wetlands, Global Change Biology, 20, 1351–1362, https://doi.org/10.1111/gcb.12431, 2014.

Oksanen, J., Simpson, G., Blanchet, F. G., Kindt, R., Legendre, P., R. Minchin, P., O'Hara, R. B., Solymos, P., Stevens, M. H. H., Szoecs, E., Wagner, H., Barbour, M., Bedward, M., Bolker, B., Borcard, D., Carvalho, G., Chirico, M., DE Caceres, M., Durand, S., Antoniazi Evangelista, H. B., FitzJohn, R., Friendly, M., Furneaux, B., Hannigan, G., Hill, M. O., Lahti, L., McGlinn, D., Ouellette, M.-H., Ribeiro Cunha, E., Smith, T., Adrian, S., Ter Braak, C. J. F., and Weedon, J.: Community Ecology Package, 2022.

Pellegrini, E., Contin, M., Vittori Antisari, L., Vianello, G., Ferronato, C., and De Nobili, M.: A new paper sensor method for field analysis of acid

volatile sulfides in soils: Paper sensor method for field analysis of acid volatile sulfides, Environ Toxicol Chem, 37, 3025–3031, https://doi.org/10.1002/etc.4279, 2018.

Pester, M.: Sulfate-reducing microorganisms in wetlands – fameless actors in carbon cycling and climate change, Front. Microbio., 3, https://doi.org/10.3389/fmicb.2012.00072, 2012.

Peyron, M., Bertora, C., Pelissetti, S., Said-Pullicino, D., Celi, L., Miniotti, E., Romani, M., and Sacco, D.: Greenhouse gas emissions as affected by different water management practices in temperate rice paddies, Agriculture, Ecosystems & Environment, 232, 17–28, https://doi.org/10.1016/j.agee.2016.07.021, 2016.

Poffenbarger, H. J., Needelman, B. A., and Megonigal, J. P.: Salinity Influence on Methane Emissions from Tidal Marshes, Wetlands, 31, 831–842, https://doi.org/10.1007/s13157-011-0197-0, 2011.

Pradel, N., Fardeau, M.-L., Tindall, B. J., and Spring, S.: Anaerohalosphaera lusitana gen. nov., sp. Nov., and Limihaloglobus sulfuriphilus gen. nov., sp. Nov., isolated from solar saltern sediments, and proposal of Anaerohalosphaeraceae fam. Nov. within the order Sedimentisphaerales, International Journal of Systematic and Evolutionary Microbiology, 70, 1321–1330, https://doi.org/10.1099/ijsem.0.003919, 2020.

Pruesse, E., Peplies, J., and Glöckner, F. O.: SINA: Accurate high-throughput multiple sequence alignment of ribosomal RNA genes, Bioinformatics, 28, 1823–1829, https://doi.org/10.1093/bioinformatics/bts252, 2012.

RER – Regione Emilia Romagna: MISURE SPECIFICHE DI CONSERVAZIONE DEL SIC-ZPS IT4070003 “PINETA DI SAN VITALE, BASSA DEL PIROTTOLO,” 2018.

Salimi, S., Almuktar, S. A. A. A. N., and Scholz, M.: Impact of climate change on wetland ecosystems: A critical review of experimental wetlands, Journal of Environmental Management, 286, 112160, https://doi.org/10.1016/j.jenvman.2021.112160, 2021.

Sayers, E. W., Bolton, E. E., Brister, J. R., Canese, K., Chan, J., Comeau, D. C., Connor, R., Funk, K., Kelly, C., Kim, S., Madej, T., Marchler-Bauer, A., Lanczycki, C., Lathrop, S., Lu, Z., Thibaud-Nissen, F., Murphy, T., Phan, L., Skripchenko, Y., Tse, T., Wang, J., Williams, R., Trawick, B. W., Pruitt, K. D., and Sherry, S. T.: Database resources of the national center for biotechnology information, Nucleic Acids Research, 50, D20–D26, https://doi.org/10.1093/nar/gkab1112, 2022.

Schneider, G. F. and Dekker, C.: DNA sequencing with nanopores, Nat Biotechnol, 30, 326–328, https://doi.org/10.1038/nbt.2181, 2012.

Schoeneberger, P. J., Wysocki, D. A., Benham, E. C., and Soil. Survey Staff: Field Book for Describing and Sampling Soils; Version 3.0, , National Soil Survey Center, Lincoln, NE, 2012.

She, C. X., Zhang, Z. C., Cadillo-Quiroz, H., and Tong, C.: Factors regulating community composition of methanogens and sulfate-reducing bacteria in brackish marsh sediments in the Min River estuary, southeastern China, Estuarine, Coastal and Shelf Science, 181, 27–38, https://doi.org/10.1016/j.ecss.2016.08.003, 2016.

SSS – Soil Survey Staff and United States Department of Agriculture Natural Resources Conservation Service: Keys to Soil Taxonomy, 13th Edition, 2022.

Trettin, C. C., Jurgensen, M. F., and Dai, Z.: Effects of climate change on forested wetland soils, in: Developments in Soil Science, vol. 36, Elsevier, 171–188, https://doi.org/10.1016/B978-0-444-63998-1.00009-4, 2019.

U.S. DOE: Carbon Cycling and Biosequestration Integrating Biology and Climate Through Systems Science, U.S. Department of Energy Office of Science Office of Biological and Environmental Research, 2008.

Wang, Q., Zhou, G., Qin, Y., Wang, R., Li, H., Xu, F., Du, Y., Zhao, C., Zhang, H., and Kong, Q.: Sulfate removal performance and co-occurrence patterns of microbial community in constructed wetlands

treating saline wastewater, Journal of Water Process Engineering, 43, 102266, https://doi.org/10.1016/j.jwpe.2021.102266, 2021.

Wang, Y., Yang, Q., and Wang, Z.: The evolution of nanopore sequencing, Front. Genet., 5, https://doi.org/10.3389/fgene.2014.00449, 2015.

White, E. and Kaplan, D.: Restore or retreat? Saltwater intrusion and water management in coastal wetlands, Ecosyst Health Sustain, 3, e01258, https://doi.org/10.1002/ehs2.1258, 2017.

Yang, Z., Tognin, D., Finotello, A., Belluco, E., Puppin, A., Silvestri, S., Marani, M., and D'Alpaos, A.: Long-Term Monitoring of Coupled Vegetation and Elevation Changes in Response to Sea Level Rise in a Microtidal Salt Marsh, JGR Biogeosciences, 128, e2023JG007405, https://doi.org/10.1029/2023JG007405, 2023.

Yousefi Lalimi, F., Silvestri, S., D'Alpaos, A., Roner, M., and Marani, M.: The Spatial Variability of Organic Matter and Decomposition Processes at the Marsh Scale, JGR Biogeosciences, 123, 3713–3727, https://doi.org/10.1029/2017JG004211, 2018

.

Part IV – Hydrological Control on CH_4 Emissions from Standing Waters in Temperate Wetlands

Abstract

Wetlands have multiple functions as carbon sink, storing carbon in organic soils, and CH_4 sources due to anoxic conditions. This literature review looks at the complex relationship between the hydrological cycle and CH_4 emissions in 59 temperate wetlands obtained by literature review effort. In general, wetland soils serve as a substantial carbon sink by storing complex organic matter. However, this process is greatly affected by water level oscillations that can be caused by both natural and anthropogenic factors, including climate change. The hydroperiod, or duration of flooding, is critical for wetland soils' biogeochemical function. Dynamic hydrologic processes, associated with seasonality and alternating inundation and drought periods, have an influence on redox conditions, impacting CH_4 production by methanogenic bacteria. In anoxic settings, such as submerged marsh soils, methanogenic bacteria produce CH_4 during the anaerobic decomposition of organic molecules. Moreover, environmental variables such as temperature, salinity, and water level play a crucial role, influencing CH_4 budgets and carbon balance in wetland soils. The study aims at correlating water depth in several temperate submerged wetlands with CH_4 emissions in order to investigate how varied hydrological patterns influence CH_4 production and examine similarity trends across habitats. This work, by examining the impacts of hydrological processes on water level changes, provides critical insights for interpreting biogeochemical and CH_4 cycles in wetlands, underlining the need of comprehensive information in guiding sustainable ecosystem management.

4.1 Introduction

Wetlands serve as C sinks by storing carbon in the soils organic matter but they also play an important role as sources of CH_4 due to soil anoxic conditions (Whalen, 2005). Environmental controls, such as temperature, salinity and water table depth, play a role in controlling CH_4 budget and carbon balance in wetland soils (Bridgham et al., 2013). The functioning of wetland soils highly depends on their hydroperiod to maintain their biogeochemical function (Mitsch et al., 2013).

Many reports have shown that temperate wetlands function as CH_4 source (Moore and Knowles, 1989; Fiedler and Sommer, 2000; Fortuniak et al., 2017). Wetlands are characterized by dynamic hydrologic conditions, with dynamic hydroperiods linked to seasonality and patterns of inundations alternated to drought periods (Bridgham et al., 2013). Variations in hydrology influence the redox condition in soils, which directly affects CH_4 generation because of methanogenic bacteria functions thrive in soils that are in anoxic and reducing condition (Mitsch et al., 2013).

Methanogenic bacteria produce CH_4 in anoxic conditions, such as submerged soils of wetlands and paddy fields, during the anaerobic breakdown of organic materials. However, CH_4 net emissions from aquatic environments are determined by factors regulating both methane production and methane oxidation (Bridgham et al., 2013). If there is enough oxygen, methanotrophic bacteria in the soil or water column can oxidize CH_4 to CO_2 and H_2O (Reddy and DeLaune, 2008). Oxygen availability is limited to the water column and top soil layers when there is constant flooding, and plant transfer of oxygen into the root zone (Reddy and DeLaune, 2008). Microbial oxidation in aerobic soils is considered the primary process that removes atmospheric CH_4, in addition to the oxidation of CH_4 by hydroxyl (OH-) radicals in the troposphere.

Wetlands are sensitive to water level variations and rely on hydrological patterns, highlighting the importance of water supply in determining the dynamics involved in the C cycle (de Vicente, 2021; IPCC, 2022). While recurrent flooding reduces decomposition, short-term inundation has been shown to increase decomposition (Itoh et al., 2007). Furthermore, flooding patterns have a significant influence on plant distribution, directly affecting carbon inputs to soil substrates (Owers et al., 2020). According to the literature, CH_4 fluxes production rates increase due to anaerobic conditions that promote the activity of methanogenic bacteria (Sha et al., 2011). When wetlands are flooded, the absence of oxygen accelerates the breakdown of organic waste by methanogenic bacteria, which increases methane emissions (Sha et al., 2011). But, CH_4 fluxes can be also impacted negatively, when periodic floods and extensively varying soil chemistry resulted in disequilibrium between the plant community and environmental circumstances, leading to nutrient shortage and poor primary production (Ahearn et al., 2006). Therefore, recognizing the environmental drivers of CH_4 production is essential to maximize carbon storage and offset anthropic carbon emissions (IPCC, 2022). More information on the effects of hydrological processes regulating water levels fluctuation, and detailed information on their effects is required to interpret biogeochemical and CH_4 cycles.

In Chiapponi et al. (2024), the environmental drivers of CH_4 fluxes have been identified in four temperate coastal wetlands located along the northeast Adriatic coast. The study shows that in flooded parts of these wetlands, the water column depth is a key limiting factor of CH_4 fluxes, along with salinity. In this study we analyze water table levels and CH_4 emissions of 51 different temperate wetlands, in coastal and continental areas, including those studied in (Chiapponi et al., 2024). Our objective is to explore how different hydrological pattern affects CH_4 production and assess similarity patterns in different ecosystem.

4.2. Materials and Methods

4.2.1 Data source and methodology

Data were derived from the SCOPUS database (https://www.scopus.com/home.uri?zone=header&origin=). The online databased was searched using the following keywords: (“temperate wetlands” OR “wetlands) AND (“CH4” OR “methane”) AND (“water table” OR “hydrology”) to compile a list of published researches studying water table effect on CH_4 emissions in temperate wetlands (Fig 4.1).
Further rules applied to select suitable studies were the following: 1) the experimental sites had to include only natural wetlands, excluding constructed wetlands and mesocosms; 2) the experimental sites had to be located preferably in a temperate climatic zone, or at least presenting a cold and a warm season; 3) the water table had to be higher than the ground level, thus including only ponded wetland areas; 4) the gas fluxes considered in this study had to come from in situ observation, therefore mesocosm incubations and batch experiments were excluded; 5) the gas fluxes had to be measured using eddy tower, or portable field gas analyzer, or chamber methods, or direct gas sampling. Therefore, simulated gas fluxes retrieved from models have been excluded from the list.
From all selected articles the following information have been listed and compared: Latitude and Longitude, method used for gas sampling, methods used for flux measurements, type of wetlands, water level, CH_4 flux. When GHG data were given in graphical form, PlotDigitalizer v.3 program was used to extract the data.

4.2.2. Statistical Analysis

The data processing procedure involved compiling an excel files reporting all comparative factors. R software (R-4.3.2) was used to perform the statistical analysis. The “ggplot2” package ver. 3.4.4 (Wickham, 2016) was used to compute the probability density function (PDF) of CH_4 fluxes versus water height. The same package

has been used to produce all statistical graphical content unless specified otherwise. Kernel Density Estimation was computed with EnvStats ver.2.8.1 package in R (Millard, 2013) to reveal the presence of basins of attraction in the data structure. . Kernel Density Estimation (KDE) is a statistical method used in data analysis to estimate the probability density function of a random variable (Scheffer et al., 2012). KDE can be used to identify tipping points by analyzing the probability density of a system's behavior over time. Tipping points are critical thresholds where a small change can lead to a significant and often irreversible shift in the system's state or behavior. In the context of KDE, tipping points can be identified by examining the peaks and valleys in the density plot, which represent areas of higher and lower probability density, respectively (Scheffer et al., 2012).

4.2.3 Gas sampling methods applied in the selected studies

4.2.3.1 Accumulation chamber

The "accumulation chamber" approach is widely used in different field of applications to quantify diffuse gas emissions of CH_4, CO_2 and VOC. This technique is commonly applied in volcanic and geothermal locations (Cardellini et al., 2003), as well as for GHGs emissions from biological activity in soil (Ueyama et al., 2014; Chiapponi et al., 2024) and landfills (Capaccioni et al., 2015). The three most often used chamber techniques for measuring soil gas fluxes are i) non-steady-state non-through-flow chamber (also known as closed static chamber), ii) non-steady-state through-flow chamber (closed dynamic chamber), and iii) steady-state through-flow chamber (open dynamic chamber) (Pumpanen et al., 2004).

The gas efflux in non-steady-state chambers, both through-flow and non-through-flow kinds, is calculated by the rate of concentration rise in an isolated chamber placed on the soil surface for a known amount of time (Janssens et al., 2000). In steady-state chambers, gas efflux is determined as the difference between gas concentrations at the chamber's entrance and outflow (Cardellini et al., 2003).

Each of the methods implying the use of accumulation chambers has an effect on the gas measured, and each chamber type has its own set of constraints (Davidson et al., 2002). For example, when a non-steady-state chamber is placed on the soil and the concentration in the chamber headspace begins to change, rising concentration within the chamber may affect gas efflux from the soil by altering the natural soil concentration gradient (Davidson et al., 2002). Furthermore, pressure anomalies generated by placing the chamber on the soil surface may potentially disrupt the gas concentration gradient in the soil (Davidson et al., 2002).

No single approach has been established as a standard since methods have seldom been compared and calibrated in absolute terms (Pumpanen et al., 2004). Previous studies, however, have revealed relative differences across chamber types (Janssens et al., 2000) or highlighted chamber-specific restrictions. As an example, non-steady-state chambers have been found to provide consistently lower fluxes than steady-state chambers (Rayment and Jarvis, 1997; Pumpanen et al., 2003).

4.2.3.2 Eddy Covariance

A wide range of approaches may be used to measure gas fluxes in and out of an ecosystem, estimate evaporative water losses from an agricultural field, or monitor gas emission rates at a carbon sequestration injection site (Burba, 2021). The eddy covariance method is one of the most direct, accurate, and defensible ways available for measuring emission and consumption rates of different gases and water vapor across regions ranging from a few hundred to millions of square meters (Burba, 2021).

The eddy covariance is a micrometeorological method that measures vertical turbulent fluxes in the atmospheric boundary layer. It is almost direct, theoretically sound, time-tested, very adaptable in applications, and verifiable using other approaches (Burba, 2021). H_2O, CO_2, CH_4, N_2O, and other gas fluxes are measured at a single point above soil and water surfaces, plant canopies, and urban or industrial regions

using fixed or mobile stations. The approach necessitates certain assumptions, and modifications. It necessitates rigorous experimental design, instrument selection, execution, processing, and analysis tailored to the unique objective of the experimental site (Burba, 2021). Measurements precision however is affected by assumptions, physical phenomena, instrument issues, and geography or setup characteristics (Billesbach, 2011). Measurements at a single location are supposed to represent an upwind area, and they are taken within the boundary layer and constant flux layer respectively. An accurate flux measurement assumes enough fetch and footprint (Aubinet et al., 2012). Other assumptions include a completely turbulent flux, level and homogeneous topography, minor flow divergences, and air density changes (Burba, 2021). Instruments are intended to detect minor changes at high frequencies, and installation structures should not distort mean airflow or turbulence levels (Burba, 2021). Moreover, eddy covariance systems tend to be expensive due to the necessity for specialized equipment and regular maintenance (Burba, 2021).

4.3 Results

4.3.1 GHGs fluxes dataset

The review work considered data obtained at a total of 51 study sites (Tab.4.1 and Fig. 4.1). The flux values range between 0.0002 and 196.98 g/m2/day of CH4 (Tab. 4.1). The highest CH4 emissions of all datasets come from the study by Chiapponi et al. (2024). Specifically, the mean CH4 flux measured in the Cerba study site is exceptionally high, with a value of 196.98 g/m2/day (n.25, Tab. 4.1) if compared to the Punte Alberete study site, where the mean value equals 5.04 g/m2/day (see values obtained from standing waters n. 23, Tab. 4.1), and to the Pirottolo site where the mean CH4 flux is 12.2704 g/m2/day (n. 24, Tab. 4.1) (Chiapponi et al., 2024). The value recorded in Cerba is extremely high if compared to the values measure by Venturi et al. (2021) in the Porta Lake (Italy), measured with a sampling flask. All this considered, the Cerba value has been excluded from further analyses, also considering that the measurements performed at this study site were likely affected by artifacts. This site is located right behind an ancient dune system, and the water level is very low, between 14 ± 10.96. cm and 19 ± 10.33 cm during the performed field surveys (Tab. 2.2A) (Chiapponi et al., 2024). To take measurements, the operator had to walk in the pond, causing a strong resuspension of the bottom and sinking with every step. The pressure exerted on the bottom of the pond certainly interfered with the measurements, probably resulting in an overestimation of the measured values.

Tab. 4.1– Database of CH_4 emissions and water column height from different temperate and continental wetlands around the world.

n.	Author	Year	Location	Region	Gas collection method	Water column height（cm）	Wetland type	CH4 $g/m^2/d$
1	Yongxin Lin	2021	Sanjiang Plain	China	Open Top Chamber	2.00	Freshwater Marsh	0.356
2	Yongxin Lin	2021	Sanjiang Plain	China	Open Top Chamber	2.00	Freshwater Marsh	0.618
3	Kang	Unpublished data	Abergwyngregyn	UK	free air CO2 enrichment	5.00	Freshwater Marsh	0.021
4	Yongxin Lin	2021	Sanjiang Plain	China	Open Top Chamber	8.00	Freshwater Marsh	0.808
5	Yongxin Lin	2021	Sanjiang Plain	China	Open Top Chamber	8.00	Freshwater Marsh	0.730
6	Huttunen et al	(2002b)	Reservoir Lokka	Finland	floating static chambers	5.00	Peatland	0.012
7	Huttunen et al	(2002b)	Reservoir Lokka	Finland	floating static chambers	5.00	Peatland	0.034
8	Huttunen et al	(2002b)	Reservoir Porttipahta	Finland	floating static chambers	6.30	Peatland	0.004
9	Huttunen et al	(2002a)	Jänkäläisenlampi Pond	Finland	floating static chambers	1.80	Peatland	0.008
10	Huttunen et al	(2002a)	Kotsamolampi Pond	Finland	floating static chambers	3.20	Peatland	0.004
11	Unpublished data, Huttunen et al	(2001b)	Lake Postilampi	Finland	floating static chambers	4.30	Peatland	0.058
12	Unpublished data		Lake Postilampi	Finland	floating static chambers	4.30	Peatland	0.059
13	Unpublished data, Huttunen et al	2000	Lake Postilampi	Finland	floating static chambers	4.30	Peatland	0.078
14	Unpublished data		Lake Heinälampi	Finland	floating static chambers	5.00	Peatland	0.006
15	Unpublished data		Lake Kevätön	Finland	floating static chambers	2.30	Peatland	0.082

16	Unpublished data, Huttunen et al	1999	Lake Kevätön	Finland	floating static chambers	2.30	Peatland	0.051
17	Unpublished data		Lake Valkjärvi	Finland	floating static chambers	3.90	Peatland	0.006
18	Unpublished data, Huttunen et al	1999	Lake Valkjärvi	Finland	floating static chambers	3.90	Peatland	0.002
19	Unpublished data		Lake Mäkijärvi	Finland	floating static chambers	3.40	Peatland	0.003
20	Unpublished data, Huttunen et al	1999	Lake Mäkijärvi	Finland	floating static chambers	3.40	Peatland	0.002
21	Manuel Acostaa	2019	Padul	Spain	eddy covariance	21.00	Fluvial and lacustrine wetlands	0.015
22	Manuel Acostaa	2019	Padul	Spain	non-stationary chamber	21.00	Fluvial and lacustrine wetlands	0.042
23	Chiapponi et al.	2024	Punte Alberete, Ravenna	Italy	static chamber	54.50	Fluvial and lacustrine wetland	5.040
24	Chiapponi et al.	2024	Pirottolo, Ravenna	Italy	static chamber	76.00	Coastal Swamp	12.270
25	Chiapponi et al.	2024	Cerba, Ravenna	Italy	static chamber	16.50	Fluvial and lacustrine wetland	196.980
26	Venturi et. al	2021	Lake Porta	Italy	sampling flask	45.00	Lake	1.66
27	Moore T. R. et al.	1994	Bog Leduc	USA	static chamber	3.00	Peatland	0.037
28	Moore T. R. et al.	1994	Bog Leduc	USA	static chamber	29.00	Peatland	0.057
29	Moore T. R. et al.	1994	James Bay Hudson Bay	USA	static chamber	100.00	Peatland	0.011
30	Moore T. R. et al.	1994	James Bay Hudson Bay	USA	static chamber	5.00	Peatland	0.105
31	Casper et al.	2000	Priest Pot	UK	Gas trap	2.55	Lake	0.012
32	Smith and Lewis	1992	Dillon Lake- Southern Rocky Mountains	USA	static chamber	239.00	Lake	0.021
33	Smith and Lewis	1992	Red Rock Lake - Southern Rocky Mountains	USA	static chamber	90.00	Lake	0.047
34	Smith and Lewis	1992	Red Rock Lake - Southern Rocky Mountains	USA	static chamber	83.00	Lake	0.047

35	Smith and Lewis	1992	Rainbow Lake- Southern Rocky Mountains	USA	static chamber	72.00	Lake	0.029
36	Smith and Lewis	1992	Long Lake - Southern Rocky Mountains	USA	static chamber	224.00	Lake	0.001
37	Smith and Lewis	1992	Pass Lake - Southern Rocky Mountains	USA	static chamber	224.00	Lake	0.028
38	Smith and Lewis	1992	Dillon Lake- Southern Rocky Mountains	USA	static chamber	0.70	Fluvial and lacustrine wetland	0.000
39	Smith and Lewis	1992	Red Rock Lake - Southern Rocky Mountains	USA	static chamber	1.20	Fluvial and lacustrine wetland	0.087
40	Smith and Lewis	1992	Rainbow Lake- Southern Rocky Mountains	USA	static chamber	0.30	Fluvial and lacustrine wetland	0.038
41	Smith and Lewis	1992	Long Lake - Southern Rocky Mountains	USA	static chamber	0.70	Fluvial and lacustrine wetland	0.014
42	Smith and Lewis	1992	Pass Lake - Southern Rocky Mountains	USA	static chamber	0.70	Fluvial and lacustrine wetland	0.002
43	Knox et al.	2019	Siikaneva-2 Bog	Finland	eddy covariance	9	Peatland	0.068
44	Knox et al.	2019	Siikaneva	Finland	eddy covariance	4	Peatland	0.050
45	Knox et al.	2019	Old Woman Creek, Ohio	USA	eddy covariance	70	Freshwater Marsh	0.796
46	Knox et al.	2019	Winous Point North Marsh, Ohio	USA	eddy covariance	38	Freshwater Marsh	0.197
47	Wilson O. J. et al.	1989	Newport News Swamp, Virginia	USA	closed chamber	20	Coastal Swamp	0.155
48	Wilson O. J. et al.	1989	Newport News Swamp, Virginia	USA	closed chamber	21	Coastal Swamp	0.152
49	Knox et al.	2014	Sacramento-San Joaquin Delta, CA	USA	eddy covariance	107	Freshwater Marsh	0.173
50	Knox et al.	2014	Sacramento-San Joaquin Delta, CA	USA	eddy covariance	29	Freshwater Marsh	0.127

4.3.2 Distribution of studies in different regions

The selected field studies on CH_4 fluxes in natural wetlands, spanning temperate and cold temperate regions globally, are primarily located in the USA (21 sites) and Northern Europe (17 sites). (Fig. 4.1, Tab 4.2). The studies include different types of habitats, which have been grouped together along with the classification given in the different studies. The dataset includes peatlands (including bogs and fens), freshwater wetlands (including flooded forests, fluvial and lacustrine wetlands), freshwater marshes, and coastal swamps. The studies have been grouped by type of wetlands, along the classification provided in each corresponding study, and their vegetation characteristics. 21 of the 49 sites are peatlands followed by freshwater river and lacustrine wetlands with 10 sites reported, and 8 study sites for freshwater marshes (Tab. 4.3). This review included also emissions from standing open waters from shallow mountain lakes, represented by 7 study sites (Tab.4.3).

Tab. 4.2 – Distribution per location of the study sites considered.

Location	**n. of studies**
China	4
North Europe	17
Italy	3
Spain	2
UK	2
USA	21

Tab. 4.3 - List of wetlands classes distribution among the 59 studies retrieved for this PhD research

Type of wetlands	**n. of studies**	**Description**
Coastal Swamp	3	Coastal swamps
Fluvial and lacustrine wetlands	10	Freshwater lacustrine wetlands, flooded forests, coastal freshwater lakes
Freshwater Marsh	8	Freshwater marshes, with *Tyhpa spp.*, *C. angustifolia, Carex meyeruana,* and *C. lasiocarpa*
Peatland	21	Peatlands, bogs, fens
Shallow mountain lakes	7	Standing waters from lakes

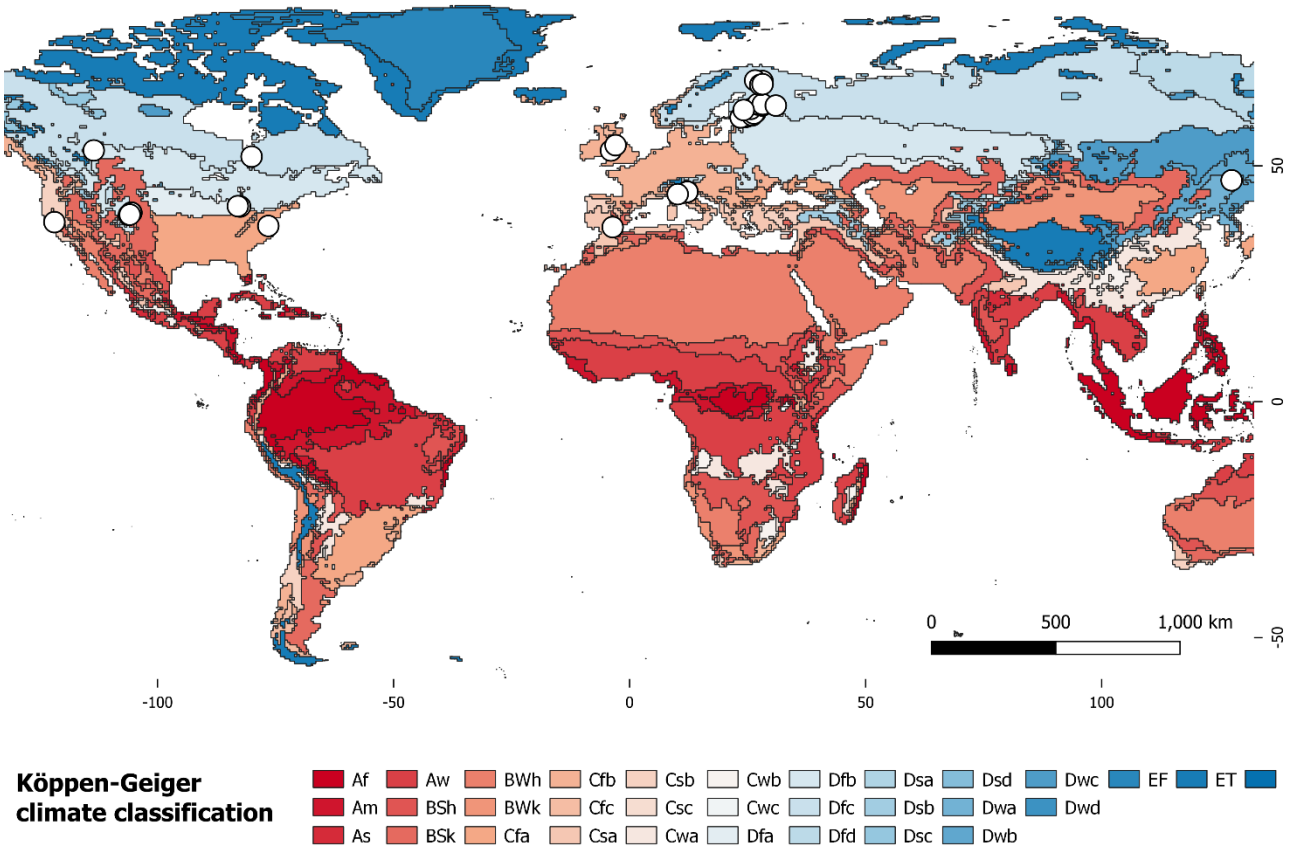

Fig. 4.1 -Distribution of the study sites along the climatic classification of Kopper-Geiger (elaborated in QGIS. 3.26.0., EPSG:4326; data from the World Bank Data Catalog - https://datacatalog.worldbank.org/search/dataset/0042325 Last access: Jan 2024) The first letter represents the 5 types of climates; A=Tropical, B= dry; C=Temperate; D=Continental; E= polar. The second letter the seasonal precipitation type: f= rainforest t; m=monsoon; w= savanna, dry winter; s= savanna or dry summer; W= arid desert; S= semi-arid or steppe. The third letter indicates the level of heat: h= hot; k=cold; a=hot summer; b= warm summer; c= cold summer; d= very cold winter; T= tundra; F= ice cap (Beck et al., 2018)

4.3.3 Gas sampling techniques

The studies considered in this review, have employed a diverse array of gas sampling methods (Tab. 4.4). Eddy covariance has been employed in 7 investigations. Floating static chambers have been used in 15 investigations, demonstrating their usefulness in measuring gas fluxes over water surfaces. The static chamber approach, which involves placing a sealed chamber over a specified location, has been used in investigating 17 sites. A gas trap approach was used in 1 investigation. One study also implied a non-stationary chamber. This approach includes catching and storing gases for later examination, allowing gas concentrations to be quantified over a given time. Open top chambers were employed in 4 investigations. These chambers have an open top, allowing for natural exchange with the environment while also allowing for controlled gas flow measurements. The sample flask approach was used in 1 investigation. This method generally includes collecting gas samples in a sealed container for later laboratory examination, providing a discrete picture of gas concentrations. Main differences between type of chambers used can be found in Tab. 4.5.

Tab. 4.4 – Table resuming the gas sampling techniques used for the different studies listed.

Gas sampling method	n. of study sites
Free air CO2 enrichment	1
Gas trap	1
Non-stationary chamber	1
Sampling flask	1
Closed chamber	2
Open top chamber	4
Eddy covariance	7
Floating static chambers	15
Static chamber	17

Tab. 4.5 Main differences between types of accumulation chambers

Type of chamber	**Criteria**
Stationary	the concentration of analytes present in the gas mixture inside the chamber remains constant over time at each point in the chamber.
Nonstationary	the concentration of analytes present in the gas mixture inside the chamber over time does not remain constant at each point in the chamber, but increases.
Dynamic	It is continuously traversed by an inert gas (e.g., nitrogen, helium, purified air, etc.) at a fixed flow rate. The recirculated inert gas can also be the gas taken into the chamber and fed back in after being purified
Static	No inert gas is passed through; sometimes gas tapped from the chamber is recirculated without any treatment for the purpose of in-line field analysis
Open	An opening (vent) is present that brings the inside pressure of the chamber into equilibrium with the external atmospheric pressure
Closed	There is no opening (vent) present that balances the internal pressure with the external pressure

4.3.4 GHGs emissions in different wetland regions

Averaging the water column depth obtained from 21 studies performed in peatlands we obtained a value equal to 10±21 cm, with a minimum value of 2 cm and a maximum value of 100 cm across the research locations (Tab. 4.6). Fluvial and lacustrine wetlands have a mean water column level of 15±20 cm at 10 study locations ranging between 0.3 to 55 cm. Shallow mountain lakes varied in depth, with a mean of 134±94 cm, a minimum value of 3 cm and a maximum of 239 cm. Among freshwater marshes, the average water column depth is 30±37 cm, with a maximum of 107 cm. Coastal swamps have an average water column level of 39±32 cm, ranging from 20 to 16 cm.

Tab. 4.6 – Table resuming the water table level found for each wetlands type; n= number of study sites

Type of wetland	Water column height (cm)				
	n.	**Mean**	**Max**	**Min**	**St. Deviation**
Coastal Swamp	3	39	76	20	32
Fluvial and lacustrine wetlands	10	15	55	0.3	20
Freshwater Marsh	8	33	107	2	38
Peatland	21	10	100	2	21
Shallow mountain lakes	7	134	239	3	94

21 investigations on peatlands reported an average CH_4 flow of 0.03± 0.03 g/m²/d (Tab.4.7, Fig. 4.2). The range of 0.002g/m²/d to 0.10 g/m²/d implies rather stable flow values. 10 investigations on fluvial and lacustrine wetlands found an average CH_4 flux of 0.73±1.60 g/m²/d, ranging from 0.0002 to 5.04 g/m²/d.
7 investigations on shallow mountain lakes found an average CH_4 flow of 0.03±0.02 g/m²/d, ranging from 0.001 to 0.05 g/m²/d. 8 investigations on freshwater marshes found an average CH_4 flow of 0.43±0.33 g/m²/d, ranging from 0.02 to 0.81 g/m²/d. 3 investigations on coastal swamp found an average CH_4 flow of 4.19±7 g/m²/d, with a range of 0.15 to 12.27 g/m²/d. The highest CH_4 flux of the whole study has been recorded in swamp with the max flux of CH_4 of 12.27 g/m²/d.

Tab. 4.7- Table resuming the CH_4 fluxes found for each wetland type; n= number of study sites.

Type of wetland	CH_4 flux (g/m^2/day)				
	n.	**Mean**	**Max**	**Min**	**St. Deviation**
Coastal Swamp	3	4.19	12.27	0.15	7.00
Fluvial and lacustrine wetlands	10	0.73	5.04	0.0002	1.60
Freshwater Marsh	8	0.43	0.81	0.02	0.33
Peatland	21	0.03	0.10	0.002	0.03
Shallow mountain lakes	7	0.03	0.05	0.001	0.02

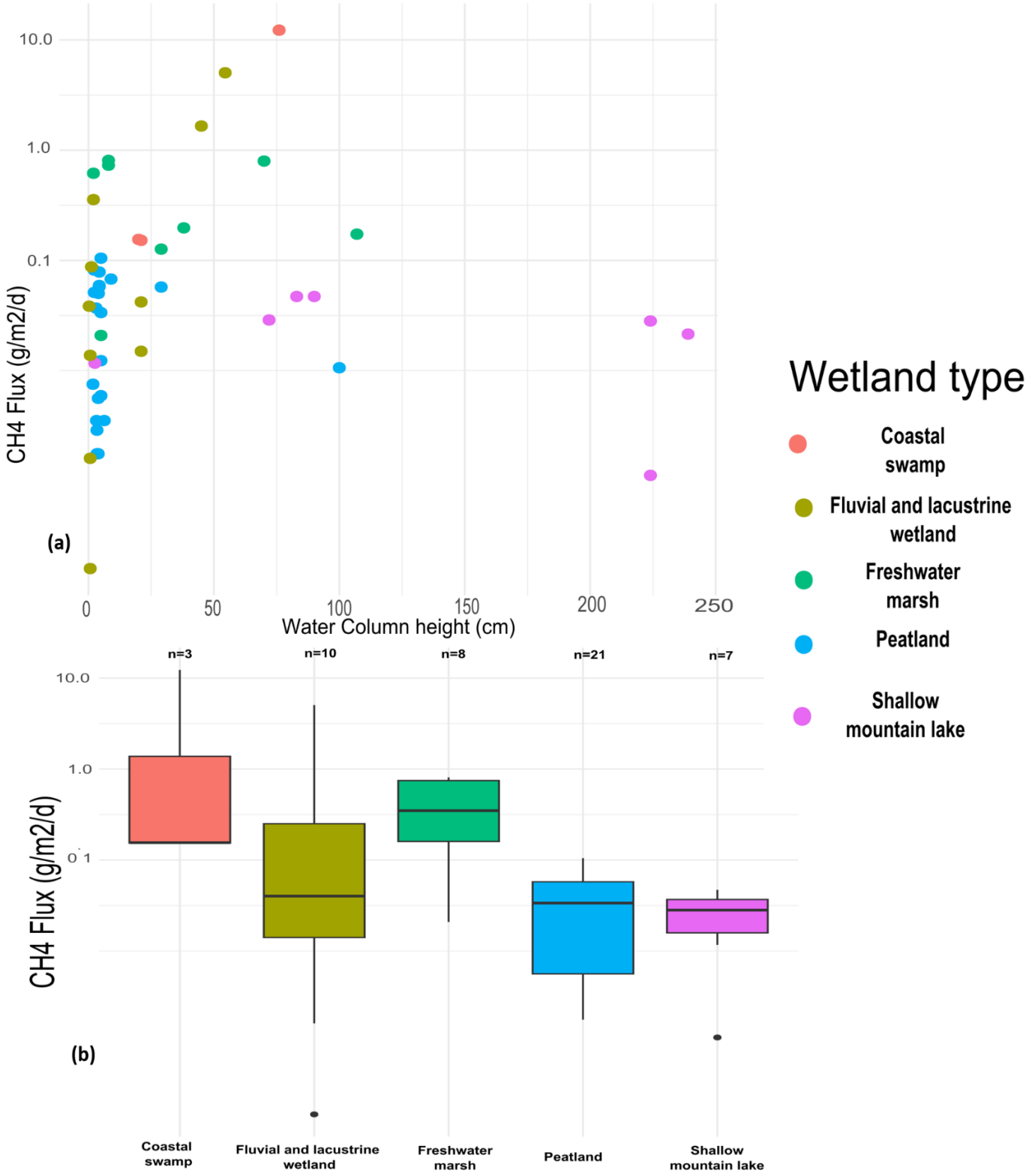

Fig. 4.2 - Scatter plot (a) and boxplot (b) showing log-linear distribution of CH_4 fluxes retrieved from literature for different wetlands type; n= number of study sites

4.3.5 Hydrology effect on CH_4 fluxes from different ecosystems

Fig. 4.3 shows the PDF and the reversed KDE of observing a specific CH_4 flux range at different water column heights. The KDE plot depicts the abundances of CH4 fluxes in dependence on the water column depth. Using a smoothed two-dimensional kernel density estimate the results show that at depths lower and higher than around 40 cm, there are peaks (red dots) in the density estimate, indicating low CH4 emissions (0.001 – 0.4 $g/m^2/day$) (Fig.4.3) in the density estimate, indicating low CH_4 emissions (0.001 – 0.4 $g/m^2/day$). Around the 40 cm depth, the density estimation shows a valley (blue dot), indicating high CH4 (0.6-12.27 g/m2/day) emissions. These valleys in the KDE plot can signify potential boundaries between different clusters in the data distribution, pointing out possible critical thresholds in the system (Scheffer et al., 2012).

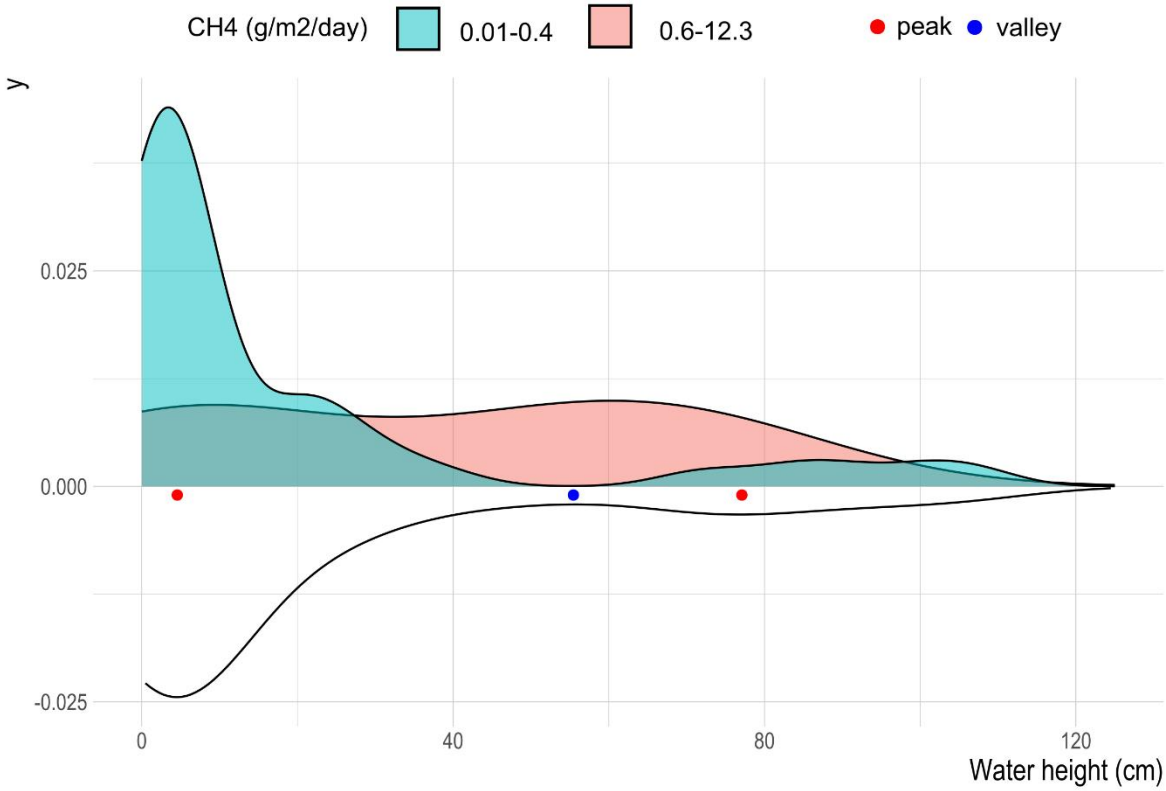

Fig. 4.3 – PDF and KDE showing probability of finding lower CH_4 emissions (in blue) and higher CH_4 emissions (in pink), at different water height, with peaks (red dot) and valley (blue dot) of data accumulation.

4.4 Discussion

This study reports results across different latitude and types of ecosystems, including those from Chiapponi et al. (2024), which showed how the water column height is a major limiting driver on CH_4 production, and specifically high emissions were recorded only when the water level was lower than 50 cm. The PDF and KDE analysis performed on the data selected with the literature review (Fig. 4.3) are in substantial agreement with Chiapponi et al. (2024) findings. The valley in the KDE graph highlights a distinct shift in CH_4 emissions, emphasizing the importance of water column depth as a key determinant of CH_4 release in wetland habitat (Fig. 4.3). Fig. 4.3 shows how the highest emissions are always recorded when and where the water column depth is <40 cm, while low emissions are recorded independently of the water height. It is known that the water table level regulates the diffusion of CH_4 into the atmosphere (Reddy and DeLaune, 2008). What is

evident from this review is that the CH_4 emission does not constantly increase as water height decreases, but there is a water height threshold (around 40 cm, Fig. 4.3) under which emissions can be very high, in agreement with Chiapponi et al. (2024) that, however, found a threshold at 50 cm. Calabrese et al. (2021) report a similar behavior, confirming that the water height acts as primary controlling factor. High water height influence specific gas production rates, where the interplay of substrate availability and temperature significantly impacts the rate of CH_4 emissions (Calabrese et al., 2021). These considerations, indicate an interaction between production, oxidation, and transport that causes maximal CH_4 emissions under a crucial level of water height. Because various factors may impact the precise location and variance of the critical threshold, thorough site-specific investigations are required.

Despite the clear agreement found for all the studies examined in this review, limitations must be highlighted. Different studies used different methodologies to determine the CH_4 fluxes, thus introducing important uncertainties in the comparison process. The fluxes reported in Chiapponi et al. (2024) are the highest of all examined studies, with a mean CH_4 flux of 5.04 g/m^2/day in Punte Alberete reporting from standing waters (n. 23, Tab. 4.1), but in the same order of magnitude of CH_4 fluxes registered by Venturi et al., 2021 in a similar environment. Pirottolo reported a mean CH_4 flux of 12.27 g/m^2/day (n. 24, Tab. 4.1), almost one order of magnitude higher than what found in Venturi et al. (2021). As already explained, we excluded data collected at Cerba, that due to artifacts introduced by the sampling methodology reported an exceptionally high flux (196.98 g/m^2/day, n.25 Tab. 4.1). Moreover, GHG Fluxes from Chiapponi et al. (2024) have been measured using a static accumulation chamber connected to a portable fluxmeter on a floating device. This method was used because is suited for local, high-resolution measurements and for studying specific microsite-scale processes (Simpson et al., 2019) and are preferable for monitoring the interaction between low-standing vegetation and the atmosphere. (Simpson et al., 2019). In fact, chamber measurements are a versatile and easy-to-use tool for research when the eddy covariance method is not applicable. Chamber methods are useful to identify spatial variation in GHG fluxes and separating C fluxes into respiration and gross primary output from an environment (Pavelka et al., 2018). Despite our best efforts, given the environmental setup and the instrumentation used, we hypothesize that compression-induced perturbation was not possible to be avoided. However, given the small-footprint of the area, and being under canopy, other techniques such as eddy covariance methods are not suitable for retrieving CH_4 fluxes in Cerba and can substantially increase experiments cost (Kormann and Mu, 2001).

Further uncertainties may have affected the results reported in Chiapponi et al. 2024. The technique used in Chiapponi et al, 2024 allows the user to choose the concentration range near ambient concentrations over which a flux is computed when the gas concentration increases (Giovenali et al., 2013). Using linear regression to estimate gas emissions rates is common (Winton and Richardson, 2016). The flux is estimated while the chamber is near true ambient levels of the measured gas, hence reducing the change in the natural diffusion gradient (Giovenali et al., 2013; Davidson et al., 2002). If the concentration of the emitted gas is higher than the atmospheric values, lowering the chamber gas concentration may result in a significant error in the opposite direction, by creating an unnaturally large diffusion gradient and thus overestimating the fluxes calculation (Davidson et al., 2002). As a result, the concentration range used to compute the flux must be carefully chosen. However, increased number of samples can help reduce artifact uncertainty (Forbrich et al., 2010). Also, it is difficult to accurately discern between process-related concentration variations and chamber artifacts, and patterns of errors are similar between different microsites (Forbrich et al., 2010).
Another issue encountered during field campaigns may be linked to soil compression and perturbation from paddling too near the wetlands bottom. CH_4 dissolved in saturated or inundated wetlands soil pores is very sensitive to pressure fluctuations, which can cause disturbance-induced resulting in non-linear CH_4 fluxes.

The positioning of the chamber on saturated soils and the proximity of the operator to it might cause brief disruptions that compromise the accuracy of soil gas flux estimation leading to an overestimation (Winton and Richardson, 2016). Repeated sampling from static chambers can cause soil disturbance and significant deviations from linearity (Forbrich et al., 2010). Results from Punte Alberete and Pirottolo, despite being high, are in the order of magnitude of fluxes reported from other studies, and consequently they were included in the dataset used for this review work. In Punte Alberete and Pirottolo site a less invasive method of sampling fluxes have been used, with the operator on a canoe. However, given the shallow ecosystem, perturbation on the submerged soils due to the rowing cannot be excluded, consequently causing an overestimation of CH_4 fluxes. However, given also the high number of point source measurements in Chiapponi et al. (2024), it can be concluded that the high fluxes measured from Cerba, Punte Alberete and Pirottolo ecosystems can be the combination of overestimation from both the instruments and naturally high environmental CH_4 fluxes.
The study covered various wetland ecosystems. Differences in emissions may not only be related to different water levels but are certainly related to other factors involved in biogeochemical processes, such as vegetation, microbial communities, and substrates for methanogenesis. Looking at the whole dataset (Tab. 4.1, Tab. 4.7) and the scatterplot (Fig. 4.2), shallow mountain lakes reported the highest mean water column depth with 134±94 cm and their mean emissions are 0.03±0.02 CH_4 g/m^2/day among the lowest analyzed in this study.
The highest CH_4 fluxes are reported for coastal swaps and fluvial and lacustrine wetlands, with 4.16±7 and 0.73±1.60 CH_4 g/m^2/day with a mean water column height of 39±32 cm and 15±320 cm respectively (Tab. 4.6 and Tab.4.7). Freshwater wetlands naturally harbor the condition to be a natural hotspot of CH_4 emissions (Bridgham et al., 2013). Waterlogged and anoxic soils create the perfect condition for methanogens bacteria to thrive and produce CH_4 (Li et al., 2021). The presence in swamps of macrophytes with aerenchyma such as reeds, can contribute to higher transport of CH_4, and thus explaining higher CH_4 fluxes from these ecosystem (Acosta et al., 2019).

4.5 Conclusions

This study examines CH_4 fluxes and water column heights in distinct wetland habitats in temperate and continental climates, extracting data from 50 studies. It emphasizes the dual role of wetlands as ecological service providers and carbon sinks, while also recognizing the issue of high CH_4 emissions. The analysis reveals that the water column height is a crucial factor limiting CH_4 generation, with a sudden decrease in emissions as the water column exceeds 40 cm. Thus, water column depth emerges as a critical factor, with ecosystems below 40 cm depth displaying the highest emissions.

The use of accumulation chambers and portable fluxmeters proves to be valuable for measuring GHG fluxes when the eddy covariance method is impractical. However, potential artifacts in the methodology, such as concentration range selection and linear regression, raise concerns about overestimations. Issues like soil compression and CH_4 sensitivity to atmospheric pressure fluctuations contribute to uncertainties.
Variability in CH_4 fluxes is observed across ecosystems, with lakes showing the lowest emissions and swamps and freshwater wetlands exhibiting the highest ones. The study focuses on the regulating function of water table levels in CH_4 emissions, stressing the complex relationship between production, oxidation, and transport. KDE and PDF could be used to visualize and analyze the patterns in CH_4 emissions data, helping to identify critical thresholds and tipping points in the system.

Site-specific research is essential due to the diverse influence of variables on these critical thresholds. In addition to advancing understanding, the study exposes methodological constraints in wetlands gas measurements, which will help guide future wetland research.

References

Acosta, M., Dušek, J., Chamizo, S., Serrano-Ortiz, P., and Pavelka, M.: Autumnal fluxes of CH4 and CO2 from Mediterranean reed wetland based on eddy covariance and chamber methods, CATENA, 183, 104191, https://doi.org/10.1016/j.catena.2019.104191, 2019.

Aubinet, M., Vesala, T., and Papale, D. (Eds.): Eddy covariance: a practical guide to measurement and data analysis, Springer, Dordrecht ; New York, 438 pp., 2012.

Beck, H. E., Zimmermann, N. E., McVicar, T. R., Vergopolan, N., Berg, A., and Wood, E. F.: Present and future Köppen-Geiger climate classification maps at 1-km resolution, Sci Data, 5, 180214, https://doi.org/10.1038/sdata.2018.214, 2018.

Billesbach, D. P.: Estimating uncertainties in individual eddy covariance flux measurements: A comparison of methods and a proposed new method, Agricultural and Forest Meteorology, 151, 394–405, https://doi.org/10.1016/j.agrformet.2010.12.001, 2011.

Bridgham, S. D., Cadillo-Quiroz, H., Keller, J. K., and Zhuang, Q.: Methane emissions from wetlands: biogeochemical, microbial, and modeling perspectives from local to global scales, Glob Change Biol, 19, 1325–1346, https://doi.org/10.1111/gcb.12131, 2013.

Burba, G.: Eddy covariance method: for scientific, regulatory, and commercial applications, LI-COR Biosciences, Lincoln, Nebraska, 2021.

Calabrese, S., Garcia, A., Wilmoth, J. L., Zhang, X., and Porporato, A.: Critical inundation level for methane emissions from wetlands, Environ. Res. Lett., 16, 044038, https://doi.org/10.1088/1748-9326/abedea, 2021.

Capaccioni, B., Tassi, F., Cremonini, S., Sciarra, A., and Vaselli, O.: Ground heating and methane oxidation processes at shallow depth in Terre Calde di Medolla (Italy): Observations and conceptual model: SOIL HEATING DUE TO METHANE OXIDATION, J. Geophys. Res. Solid Earth, 120, 3048–3064, https://doi.org/10.1002/2014JB011635, 2015.

Cardellini, C., Chiodini, G., Frondini, F., Granieri, D., Lewicki, J., and Peruzzi, L.: Accumulation chamber measurements of methane fluxes: application to volcanic-geothermal areas and landfills, Applied Geochemistry, 18, 45–54, https://doi.org/10.1016/S0883-2927(02)00091-4, 2003.

Chiapponi, E., Silvestri, S., Zannoni, D., Antonellini, M., and Giambastiani, B. M. S.: Driving and limiting factors of CH_4 and CO_2 emissions from coastal brackish-water wetlands in temperate regions, Biogeochemistry: Wetlands, https://doi.org/10.5194/egusphere-2023-605, 2024.

Davidson, E. A., Savage, K., Verchot, L. V., and Navarro, R.: Minimizing artifacts and biases in chamber-based measurements of soil respiration, Agricultural and Forest Meteorology, 113, 21–37, https://doi.org/10.1016/S0168-1923(02)00100-4, 2002.

Fiedler, S. and Sommer, M.: Methane emissions, groundwater levels and redox potentials of common wetland soils in a temperate-humid climate, Global Biogeochemical Cycles, 14, 1081–1093, https://doi.org/10.1029/1999GB001255, 2000.

Forbrich, I., Kutzbach, L., Hormann, A., and Wilmking, M.: A comparison of linear and exponential regression for estimating diffusive CH4 fluxes by closed-chambers in peatlands, Soil Biology and Biochemistry, 42, 507–515, https://doi.org/10.1016/j.soilbio.2009.12.004, 2010.

Fortuniak, K., Pawlak, W., Bednorz, L., Grygoruk, M., Siedlecki, M., and Zieliński, M.: Methane and carbon dioxide fluxes of a temperate mire in Central Europe, Agricultural and Forest Meteorology, 232, 306–318,

https://doi.org/10.1016/j.agrformet.2016.08.023, 2017.

Giovenali, E., Coppo, L., Virgili, G., Continanza, D., and Raco, B.: The flux-meter: implementation of a portable integrated instrumentation for the measurement of co2 and ch4 diffuse flux from landfill soil cover., in: Proceedings Sardinia 2013, Fourteenth International Waste Management and Landfill Symposium, 11, 2013.

IPCC: Climate Change 2022: Impacts, Adaptation and Vulnerability, Cambridge University Press, Cambridge University Press, 2022.

Janssens, I. A., Kowalski, A. S., Longdoz, B., and Ceulemans, R.: Assessing forest soil CO2 efflux: an in situ comparison of four techniques, Tree Physiology, 20, 23–32, https://doi.org/10.1093/treephys/20.1.23, 2000.

Li, D., Ni, H., Jiao, S., Lu, Y., Zhou, J., Sun, B., and Liang, Y.: Coexistence patterns of soil methanogens are closely tied to methane generation and community assembly in rice paddies, Microbiome, 9, 20, https://doi.org/10.1186/s40168-020-00978-8, 2021.

Millard, S. P.: EnvStats: An R Package for Environmental Statistics, Springer New York, New York, NY, https://doi.org/10.1007/978-1-4614-8456-1, 2013.

Mitsch, W. J., Bernal, B., Nahlik, A. M., Mander, Ü., Zhang, L., Anderson, C. J., Jørgensen, S. E., and Brix, H.: Wetlands, carbon, and climate change, Landscape Ecol, 28, 583–597, https://doi.org/10.1007/s10980-012-9758-8, 2013.

Moore, T. R. and Knowles, R.: THE INFLUENCE OF WATER TABLE LEVELS ON METHANE AND CARBON DIOXIDE EMISSIONS FROM PEATLAND SOILS, Can. J. Soil. Sci., 69, 33–38, https://doi.org/10.4141/cjss89-004, 1989.

Pavelka, M., Acosta, M., Kiese, R., Altimir, N., Brümmer, C., Crill, P., Darenova, E., Fuß, R., Gielen, B., Graf, A., Klemedtsson, L., Lohila, A., Longdoz, B., Lindroth, A., Nilsson, M., Jiménez, S. M., Merbold, L., Montagnani, L., Peichl, M., Pihlatie, M., Pumpanen, J., Ortiz, P. S., Silvennoinen, H., Skiba, U., Vestin, P., Weslien, P., Janous, D., and Kutsch, W.: Standardisation of chamber technique for CO2, N2O and CH4 fluxes measurements from terrestrial ecosystems, International Agrophysics, 32, 569–587, https://doi.org/10.1515/intag-2017-0045, 2018.

Pumpanen, J., Ilvesniemi, H., PERÄMÄKi, M., and Hari, P.: Seasonal patterns of soil CO_2 efflux and soil air CO_2 concentration in a Scots pine forest: comparison of two chamber techniques, Global Change Biology, 9, 371–382, https://doi.org/10.1046/j.1365-2486.2003.00588.x, 2003.

Pumpanen, J., Kolari, P., Ilvesniemi, H., Minkkinen, K., Vesala, T., Niinistö, S., Lohila, A., Larmola, T., Morero, M., Pihlatie, M., Janssens, I., Yuste, J. C., Grünzweig, J. M., Reth, S., Subke, J.-A., Savage, K., Kutsch, W., Østreng, G., Ziegler, W., Anthoni, P., Lindroth, A., and Hari, P.: Comparison of different chamber techniques for measuring soil CO2 efflux, Agricultural and Forest Meteorology, 123, 159–176, https://doi.org/10.1016/j.agrformet.2003.12.001, 2004.

Rayment, M. B. and Jarvis, P. G.: An improved open chamber system for measuring soil CO_2 effluxes in the field, J. Geophys. Res., 102, 28779–28784, https://doi.org/10.1029/97JD01103, 1997.

Reddy, K. R. and DeLaune, R. D.: Biogeochemistry of wetlands: science and applications, CRC Press, Boca Raton, 774 pp., 2008.

Scheffer, M., Carpenter, S. R., Lenton, T. M., Bascompte, J., Brock, W., Dakos, V., Van De Koppel, J., Van De Leemput, I. A., Levin, S. A., Van Nes, E. H., Pascual, M., and Vandermeer, J.: Anticipating Critical Transitions, Science, 338, 344–348, https://doi.org/10.1126/science.1225244, 2012.

Sha, C., Mitsch, W. J., Mander, Ü., Lu, J., Batson, J., Zhang, L., and He, W.: Methane emissions from freshwater riverine wetlands, Ecological Engineering, 37, 16–24, https://doi.org/10.1016/j.ecoleng.2010.07.022, 2011.

Simpson, G., Runkle, B. R. K., Eckhardt, T., and Kutzbach, L.: Evaluating closed chamber evapotranspiration estimates against eddy covariance measurements in an arctic wetland, Journal of Hydrology, 578, 124030, https://doi.org/10.1016/j.jhydrol.2019.124030, 2019.

Ueyama, M., Iwata, H., and Harazono, Y.: Autumn warming reduces the CO_2 sink of a black spruce forest in interior Alaska based on a nine-year eddy covariance measurement, Global Change Biology, 20, 1161–1173, https://doi.org/10.1111/gcb.12434, 2014.

Venturi, S., Tassi, F., Cabassi, J., Randazzo, A., Lazzaroni, M., Capecchiacci, F., Vietina, B., and Vaselli, O.: Exploring Methane Emission Drivers in Wetlands: The Cases of Massaciuccoli and Porta Lakes (Northern Tuscany, Italy), Applied Sciences, 11, 12156, https://doi.org/10.3390/app112412156, 2021.

Whalen, S. C.: Biogeochemistry of Methane Exchange between Natural Wetlands and the Atmosphere, Environmental Engineering Science, 22, 73–94, https://doi.org/10.1089/ees.2005.22.73, 2005.

Wickham, H.: ggplot2: Elegant Graphics for Data Analysis, Springer-Verlag, New York, 2016.

Winton, R. S. and Richardson, C. J.: A cost-effective method for reducing soil disturbance-induced errors in static chamber measurement of wetland methane emissions, Wetlands Ecol Manage, 24, 419–425, https://doi.org/10.1007/s11273-015-9468-5, 2016.

Part V – Conclusions

This study was conducted in four distinct types of wetlands located within the boundaries of the San Vitale Pinewood, in the Ravenna province (Italy). This study aims to investigate the complex interplay of abiotic and biotic factors influencing CH_4 and carbon dioxide CO_2 emissions in temperate coastal wetlands, with the dual goals of quantifying current emission rates and determining the impact of climate-change-related variables on future GHG emissions from these ecosystems.

In conclusion, the comprehensive investigation of CH_4 and CO_2 emissions in temperate coastal wetlands reveals a complex interplay of environmental factors influencing greenhouse gas dynamics. The study, spanning diverse ecosystems in the Po River Delta Natural Park and Adriatic coast wetlands, underscores the significance of water height, temperature, irradiance, salinity, and microbial community composition in regulating CH_4 and CO_2 production. The findings highlight a strong seasonality dependence, with higher CH_4 emissions during summer and spring, primarily driven by temperature and irradiance. Water height emerges as a critical limiting factor, with a notable decrease in CH_4 emissions when exceeding 50 cm, while water column depths below this threshold show a substantial increase. Salinity and sulfate concentrations further constrain CH_4 emissions in shallower waters, emphasizing the complexity of influencing variables.

Microbial community analysis in the selected wetlands have been identified for the first time. The analysis conducted identifies distinct clusters corresponding to freshwater, shallow-freshwater, and brackish environments. Salinity and sulfur content significantly influence bacterial community structure, linking the prevalence of sulfate-reducing bacteria to reduced CH_4 emissions in brackish settings. Moreover, the study acknowledges the potential trade-off between decreased CH_4 emissions and increased CO_2 emissions with rising salinity, posing challenges to wetlands' carbon sequestration capacity.

While drawing on data from 50 studies in temperate and continental climates, we remark dual role of wetlands as ecological service providers and carbon sinks, while acknowledging challenges related to CH_4 emissions. The research confirms the first hypothesis that a water column height represents a limiting factor for CH_4 generation. The research identifies variability in CH_4 fluxes across ecosystems, with freshwater wetlands exhibiting the highest emissions, particularly in depths below 40 cm. Emphasizing the regulating function of water table levels in CH_4 emissions, the study stresses the complex relationship between production, oxidation, and transport, necessitating site-specific research to account for diverse influences on critical thresholds. Also, from this study it emerges how the use of accumulation chambers and portable fluxmeters while being valuable, poses concerns about potential overestimations due to methodological artifacts emphasizing the need for careful interpretation and accurate experimental setup.

Given the effects of climate change on wetlands, this PhD study emphasizes the critical role of biogeochemical research. It gives new information on the environmental factors influencing carbon sequestration processes in Ravenna Province wetlands. This research provides fresh views for local stakeholders in charge of the area's environmental management. Understanding the biogeochemical processes in these habitats offers the opportunity to create novel management solutions. These methodologies can consider the interconnections of biotic and abiotic components, prospective changes in carbon sink dynamics, and the consequences of varied greenhouse gas emissions. This work adds important insights into wetland ecology and provides direction for future research on this essential topic.

Appendix

Tab. 2.1A - Dataset used for statistical analysis of the manuscript "Chiapponi, E., Silvestri, S., Zannoni, D., Antonellini, M., and Giambastiani, B. M. S.: Driving and limiting factors of CH4 and CO2 emissions from coastal brackish-water wetlands in temperate regions, EGUsphere, https://doi.org/10.5194/egusphere-2023-605, 2023."

Site	Sample	Date	T_air (°C)	T_water (°C)	EC (ms/cm)	Sulfate (mg/l)	CH4_flux(g/m2/d)	CO2_flux(g/m2/day)	Irradiance (W/m2)	Water height (cm)
Punte Alberete	Wet	10/09/2021	23.31	22.01	0.56	63	1.0827	4.432291	389	51
Punte Alberete	Wet	22/11/2021	11.89	10.66	0.65	57	1.0827	2.213351	118	45
Punte Alberete	Wet	22/11/2021	11.5	10.59	0.65	57	1.0827	2.951135	118	45
Cavedone	Wet	02/04/2021	25	23	7.67		1.0827	0.693069	747	30
Punte Alberete	Wet	22/11/2021	11.62	10.69	0.65	57	1.0827	0.368892	94	48
Punte Alberete	Wet	22/11/2021	11.75	10.69	0.65	57	1.0827	2.397797	94	59
Pirottolo	Wet	02/04/2021	25	13.2	20.89		1.0827	3.118813	794	50
Punte Alberete	Wet	22/11/2021	11.1	10.54	0.66	57	1.0827	18.81348	99	60
Punte Alberete	Wet	22/11/2021	11.49	10.58	0.65	57	1.0827	4.426702	118	50
Punte Alberete	Wet	22/11/2021	11.88	10.65	0.65	57	1.0827	2.028905	118	35
Punte Alberete	Wet	18/10/2021	20.81	13.7	0.52	65	1.0827	0	37.8	40
Punte Alberete	Wet	21/02/2022	16.13	8.6	0.8751	800	1.0827	3.320026	615	66
Punte Alberete	Wet	10/09/2021	22.39	22.14	0.57	63	1.0827	7.19339	389	70
Cerba	Wet	22/02/2022	10.5	10.8	1.317438	200	1.0827	2.280422	602	26
Punte Alberete	Wet	22/11/2021	11.44	10.6	0.65	57	1.0827	8.484512	118	45

Cerba	Wet	29/03/2022	13.5	16.7	3.022	400	1.0827	3.168781	102	11
Punte Alberete	Wet	18/10/2021	21.5	13.8	0.54	65	1.0827	3.622518	37.8	28
Pirottolo	Wet	31/05/2021	20.31	26.52	5.01		1.0827	15.12456	512	70
Punte Alberete	Wet	22/11/2021	11.51	10.62	0.65	57	1.0827	4.611148	118	30
Pirottolo	Wet	29/03/2022	15.6	16	12.87	2100	1.0827	5.376878	643	40
Punte Alberete	Wet	21/02/2022	14.04	8.6	0.8751	800	1.0827	5.902269	615	81
Punte Alberete	Wet	21/02/2022	14.8	8.6	0.8751	800	1.0827	5.902269	615	48
Punte Alberete	Wet	22/11/2021	11.21	10.56	0.66	57	1.0827	0.92223	99	40
Cerba	Wet	29/03/2022	13.5	16.7	3.022	400	1.0827	-6.16049	102	23
Cerba	Wet	18/11/2021	14.37	12.48	1.75	46	1.0827	4.119292	107	35
Punte Alberete	Wet	22/11/2021	11.22	10.55	0.66	57	1.0827	3.688918	99	50
Punte Alberete	Wet	10/09/2021	22.55	22.08	0.57	63	1.0827	3.048108	389	47
Pirottolo	Wet	13/09/2021	23.21	18.8	3.23	1025	1.0827	2.855558	722	98
Punte Alberete	Wet	22/11/2021	11.52	10.62	0.65	57	1.0827	10.69786	118	35
Cerba	Wet	19/10/2021	28.12	12.13	1.59	250	1.0827	7.26158	570	10
Punte Alberete	Wet	21/02/2022	15.37	8.6	0.8751	800	1.0827	3.688918	615	66
Punte Alberete	Wet	21/02/2022	15.21	8.6	0.8751	800	1.0827	2.213351	615	70
Cerba	Wet	18/11/2021	14.31	12.44	1.75	46	1.0827	8.484512	182	8
Punte Alberete	Wet	18/10/2021	19.42	13.89	0.54	65	1.0827	2.681844	0	39
Cerba	Wet	27/04/2022	18.7	17.9	2.02	50	1.0827	3.476973	789	40
Punte Alberete	Wet	03/05/2021	24	15.9	0.4		1.0827	3.912489	467.5	70
Cerba	Wet	14/12/2021	17.09	2.44	1.2	50	1.0827	0.357567	154	35

Punte Alberete	Wet	03/05/2021	25	15.9	0.4		1.0827	3.633026	382	70
Punte Alberete	Wet	21/02/2022	17.3	8.6	0.8751	800	1.0827	-0.73778	615	57
Cerba	Wet	14/12/2021	16.72	2.41	1.2	50	1.0827	13.50144	298	30
Punte Alberete	Wet	22/11/2021	11.45	10.6	0.65	57	1.0827	15.49346	118	35
Punte Alberete	Wet	22/11/2021	11.57	10.62	0.65	57	1.0827	4.426702	118	42
Cerba	Wet	27/04/2022	18.7	17.3	2.07	50	1.0827	3.970617	789	38
Punte Alberete	Wet	10/09/2021	23.17	22.06	0.56	63	1.0827	5.522199	389	50
Punte Alberete	Wet	15/12/2021	12.52	5.05	0.64	500	1.0827	3.819707	4	45
Cerba	Wet	27/04/2022	18.7	17.2	2.07	50	1.0827	-0.21677	789	23
Cerba	Wet	22/02/2022	10.36	10.8	1.317438	200	1.0827	5.701055	602	25
Cerba	Wet	19/10/2021	27.6	12.21	1.59	250	1.0827	9.627518	570	10
Pirottolo	Wet	28/04/2022	17.6	16.2	2.37	100	1.0827	12.44842	926	50
Punte Alberete	Wet	15/12/2021	17.17	5.34	0.63	500	1.0827	3.910253	75	66
Cerba	Wet	29/03/2022	13.5	16.7	3.022	400	1.0827	-8.96407	102	21
Pirottolo	Wet	29/03/2022	15.6	16	12.87	2100	1.0827	2.463191	643	84
Punte Alberete	Wet	15/12/2021	11.97	5.02	0.64	500	1.0827	4.905702	4	47
Punte Alberete	Wet	18/10/2021	20.53	13.67	0.53	65	1.0827	0.756228	37.8	38
Pirottolo	Wet	29/03/2022	15.6	16	12.87	2100	1.0827	5.413208	643	70
Punte Alberete	Wet	21/02/2022	17.3	8.6	0.8751	800	1.0827	5.902269	615	69
Punte Alberete	Wet	18/10/2021	19.42	13.84	0.54	65	1.0827	0.337167	37.8	35
Punte Alberete	Wet	22/11/2021	11.71	10.63	0.66	57	1.0827	3.873364	118	40
Pirottolo	Wet	18/10/2021	11.3	9.93	1.76	367	1.0827	7.5634	527	70

Punte Alberete	Wet	18/10/2021	20.49	13.64	0.53	65	1.0827	1.896104	37.8	34
Cerba	Wet	18/11/2021	14.66	12.39	1.78	46	1.0827	16.60013	182	29
Cerba	Wet	22/02/2022	9.64	10.8	1.317438	200	1.0827	-0.76014	647	8
Punte Alberete	Wet	18/10/2021	20.9	13.72	0.53	65	1.0827	2.943757	37.8	30
Punte Alberete	Wet	29/03/2022	15.6	13	0.7659	600	1.0827	0.235057	665	50
Punte Alberete	Wet	15/12/2021	15.27	5.16	0.63	500	1.0827	4.94315	75	60
Cerba	Wet	14/12/2021	17.7	2.47	1.21	50	1.0827	2.13035	154	40
Punte Alberete	Wet	29/03/2022	15.6	13	0.7659	600	1.0827	0.366936	665	54
Punte Alberete	Wet	18/10/2021	20.99	13.75	0.53	65	1.0827	2.194906	37.8	38
Punte Alberete	Wet	10/06/2022	26.9	19.06	0.65	0.013	1.0827	5.970307	715	40
Punte Alberete	Wet	10/09/2021	23.28	22.31	0.57	63	1.0827	2.590347	389	50
Cerba	Wet	29/03/2022	13.5	16.7	3.022	400	1.0827	1.589924	102	7
Cerba	Wet	29/03/2022	13.5	16.7	3.022	400	1.0827	-1.61575	102	12
Punte Alberete	Wet	18/10/2021	20.68	13.69	0.53	65	1.0827	2.770378	37.8	33
Punte Alberete	Wet	29/03/2022	15.6	13	0.7659	600	1.0827	0.577651	665	60
Cerba	Wet	22/02/2022	9.53	10.8	1.317438	200	1.0827	2.660493	647	10
Punte Alberete	Wet	10/09/2021	23.51	22.2	0.57	63	1.0827	7.411372	389	55
Punte Alberete	Wet	10/09/2021	22.45	22.1	0.57	63	1.0827	21.39852	389	60
Pirottolo	Wet	10/06/2022	22	20.94	6.02	0.55	1.0827	15.38206	176	50
Cerba	Wet	29/03/2022	13.5	16.7	3.022	400	1.0827	-1.5973	102	10
Punte Alberete	Wet	10/06/2022	23.6	19.02	0.65	0.013	1.0827	4.719067	599	42

Punte Alberete	Wet	10/06/2022	26.9	19.03	0.65	0.013	1.0827	6.918084	715	38
Cerba	Wet	27/04/2022	18.2	16.9	2.13	50	1.0827	-0.16991	753	23
Pirottolo	Wet	28/04/2022	17.6	16.2	2.37	100	1.0827	11.05334	926	105
Pirottolo	Wet	28/04/2022	17.6	16.2	2.37	100	1.0827	8.370491	926	80
Cerba	Wet	22/02/2022	10.74	10.8	1.317438	200	1.0827	-1.14021	602	4
Punte Alberete	Wet	01/06/2021	23.05	19.6	0.57		1.0827	6.902748	461	100
Punte Alberete	Wet	18/10/2021	19.42	13.83	0.54	65	1.0827	4.020921	37.8	38
Cerba	Wet	18/11/2021	15.02	12.45	1.75	46	1.0827	4.795594	182	30
Punte Alberete	Wet	18/10/2021	19.42	13.92	0.54	65	1.0827	0.770984	0	44
Cerba	Wet	18/11/2021	14.1	12.41	1.78	46	1.0827	0.374481	182	25
Punte Alberete	Wet	18/10/2021	19.42	13.93	0.54	65	1.0827	3.334782	0	77
Pirottolo	Wet	21/02/2022	14.32	11.5	11.17	12.3	1.0827	7.746728	6	84
Punte Alberete	Wet	18/10/2021	19.42	13.87	0.54	65	1.0827	6.271161	0	30
Pirottolo	Wet	29/03/2022	15.6	16	12.87	2100	1.0827	9.95449	643	90
Cerba	Wet	19/10/2021	18.92	11.61	1.59	250	1.0827	0	570	18
Pirottolo	Wet	18/10/2021	14	10.14	1.76	367	1.0827	7.264933	575	83
Pirottolo	Wet	28/04/2022	17.6	16.2	2.37	100	1.0827	14.02236	926	67
Pirottolo	Wet	31/05/2021	20.31	26.3	4.96		1.0827	11.98898	512	70
Cerba	Wet	18/11/2021	14.83	12.47	1.75	46	1.0827	5.902269	182	30
Punte Alberete	Wet	15/12/2021	16.14	5.18	0.63	500	1.0827	4.684926	75	55
Pirottolo	Wet	30/06/2021	30.89	28.69	2.45	0.142	1.0827	11.08911	670	48
Pirottolo	Wet	28/04/2022	17.6	17.9	2.37	100	1.0827	8.298948	926	75
Punte Alberete	Wet	10/09/2021	23.38	22.05	0.56	63	1.0827	7.302381	389	45
Cerba	Wet	14/12/2021	16.21	2.42	1.2	50	1.0827	0	154	30

Punte Alberete	Wet	10/06/2022	26.9	19.05	0.65	0.013	1.0827	7.028774	715	44
Punte Alberete	Wet	18/10/2021	20.56	13.62	0.53	65	1.0827	0.486937	108.9	45
Pirottolo	Wet	29/03/2022	15.6	16	12.87	2100	1.0827	3.589429	643	80
Pirottolo	Wet	30/06/2021	30.9	28.66	2.47	0.142	1.0827	13.23539	670	55
Punte Alberete	Wet	18/10/2021	20.6	13.62	0.53	65	1.0827	0.686139	37.8	50
Punte Alberete	Wet	10/06/2022	26.9	19.04	0.65	0.013	1.0827	6.617148	715	33
Cerba	Wet	27/04/2022	18.7	17.5	2.07	50	1.0827	5.508785	789	36
Cerba	Wet	27/04/2022	18.7	17.8	2.04	50	1.0827	4.721815	789	40
Pirottolo	Wet	18/10/2021	14.51	10.18	1.76	367	1.0827	7.002796	575	60
Pirottolo	Wet	18/10/2021	12.47	10.05	1.76	367	1.0827	7.677421	527	45
Cerba	Wet	27/04/2022	18.2	17.2	2.07	50	1.0827	2.868861	753	23
Punte Alberete	Wet	10/09/2021	23.65	22.05	0.56	63	1.0827	10.31779	389	60
Cerba	Wet	14/12/2021	16.81	2.3	1.19	50	1.0827	7.23028	154	32
Cerba	Wet	19/10/2021	28.65	12.05	1.59	250	1.0827	0.346266	570	1
Punte Alberete	Wet	18/10/2021	21.12	13.58	0.54	65	1.0827	6.787609	108.9	56
Punte Alberete	Wet	10/06/2022	26.9	19.03	0.65	0.013	1.0827	8.495408	715	42
Punte Alberete	Wet	10/06/2022	26.9	19.03	0.65	0.013	1.0827	3.521305	715	28
Punte Alberete	Wet	28/04/2022	18.3	16.3	0.68	74	1.0827	5.437242	930	91
Punte Alberete	Wet	29/03/2022	15.6	13	0.7659	600	1.0827	6.830088	665	69
Pirottolo	Wet	18/10/2021	14.18	10.14	1.76	367	1.0827	3.138152	575	60
Punte Alberete	Wet	28/04/2022	18.7	16.9	0.68	74	1.0827	6.116897	871	90
Punte Alberete	Wet	28/04/2022	18.7	16.4	0.68	74	1.0827	6.331525	871	73

Punte Alberete	Wet	10/06/2022	26.9	19.04	0.65	0.013	1.0827	6.074078	715	25
Punte Alberete	Wet	10/09/2021	22.27	22.1	0.57	63	1.0827	13.04256	389	70
Punte Alberete	Wet	18/10/2021	19.42	13.9	0.54	65	1.0827	2.257618	0	44
Punte Alberete	Wet	28/04/2022	18.7	16.6	0.68	74	1.0827	5.043757	871	58
Punte Alberete	Wet	28/04/2022	18.7	16.4	0.69	74	1.0827	7.79815	871	63
Punte Alberete	Wet	18/10/2021	21.2	13.77	0.53	65	1.0827	0.490626	37.8	32
Cerba	Wet	14/12/2021	16.46	2.38	1.2	50	1.0827	4.020921	298	10
Punte Alberete	Wet	28/04/2022	18.7	16.6	0.69	74	1.0827	8.048549	871	74
Punte Alberete	Wet	28/04/2022	18.7	16.5	0.68	74	1.0827	9.729801	871	68
Punte Alberete	Wet	10/09/2021	23.34	22.34	0.57	63	1.0827	3.705686	389	48
Punte Alberete	Wet	28/04/2022	18.7	16.3	0.68	74	1.0827	6.72501	871	66
Pirottolo	Wet	18/10/2021	13.24	10.08	1.76	367	1.0827	3.164365	575	90
Punte Alberete	Wet	28/04/2022	18.3	16.3	0.68	74	1.0827	2.310828	930	60
Punte Alberete	Wet	28/04/2022	18.3	16.3	0.68	74	1.0827	6.72501	930	90
Punte Alberete	Wet	28/04/2022	18.7	16.5	0.68	74	1.0827	4.721815	871	58
Pirottolo	Wet	28/04/2022	17.6	16.2	2.37	100	1.0827	19.10189	926	80
Pirottolo	Wet	14/12/2021	10.74	6.65	18.31	1500	1.0827	23.06804	68	100
Pirottolo	Wet	22/11/2021	12.73	11.73	3.96	1825	1.0827	11.06675	28	55
Pirottolo	Wet	22/11/2021	12.03	11.75	3.98	1825	1.0827	7.377836	28	90
Pirottolo	Wet	22/11/2021	11.97	11.75	3.99	1825	1.0827	7.746728	28	70

Punte Alberete	Wet	22/11/2021	11.83	10.66	0.65	57	1.0827	8.853404	118	40
Punte Alberete	Wet	22/11/2021	11.89	10.64	0.66	57	1.0827	7.377836	118	35
Punte Alberete	Wet	03/05/2021	24	16	0.4		1.0827	8.104442	441.5	70
Punte Alberete	Wet	03/05/2021	24	16	0.4		1.0827	5.309807	441.5	70
Pirottolo	Wet	30/06/2021	30.84	28.67	2.45	0.142	1.0827	11.80454	670	58
Pirottolo	Wet	30/06/2021	30.67	28.81	2.46	0.142	1.0827	16.45481	670	45
Punte Alberete	Wet	30/06/2021	28.62	24.07	0.47	0	1.0827	5.723412	474	8
Punte Alberete	Wet	30/06/2021	28.6	24.01	0.47	0	1.0827	5.723412	474	11
Punte Alberete	Wet	30/06/2021	28.44	23.87	0.47	0	1.0827	7.869692	474	15
Pirottolo	Wet	31/05/2021	20.31	26.46	5		1.0827	16.71192	512	70
Pirottolo	Wet	21/02/2022	14.73	11.5	11.17	12.3	1.0827	11.98898	6	48
Punte Alberete	Wet	01/06/2021	21.9	19.57	0.57		1.0827	8.719261	487.5	100
Punte Alberete	Wet	01/06/2021	22.47	19.5	0.57		1.0827	8.355959	461	100
Punte Alberete	Wet	01/06/2021	21.9	19.57	0.57		1.0827	9.082564	487.5	100
Punte Alberete	Wet	01/06/2021	22.47	19.5	0.57		1.0827	7.992656	461	100
Cerba	Wet	18/11/2021	14.82	12.39	1.78	46	1.0827	7.746728	182	10
Cerba	Wet	18/11/2021	14.34	12.41	1.78	46	1.0827	4.795594	182	14
Cerba	Wet	18/11/2021	14.38	12.43	1.78	46	1.0827	0.368892	182	25
Pirottolo	Wet	31/05/2021	19.67	27.14	4.93		1.0827	20.28905	316	70
Pirottolo	Wet	22/11/2021	11.93	11.75	3.99	1825	1.0827	11.80454	670	110
Pirottolo	Wet	21/02/2022	14.19	11.5	11.17	12.3	1.0827	12.17343	6	85
Cerba	Wet	22/02/2022	9.69	10.8	1.317438	200	1.0827	2.660493	647	28

Cerba	Wet	22/02/2022	9.77	10.8	1.317438	200	1.0827	1.900352	647	5
Pirottolo	Wet	18/10/2021	13.79	10.13	1.76	367	1.0827	10.78506	575	50
Punte Alberete	Wet	28/04/2022	18.7	16.4	0.69	74	1.0827	7.977006	871	74
Pirottolo	Wet	13/09/2021	22.09	18.45	3.16	1025	1.0827	6.394125	389	65
Cerba	Wet	27/04/2022	18.7	17.5	2.06	50	1.0827	6.331525	789	25
Pirottolo	Wet	10/06/2022	22	21.52	7.47	0.55	1.0827	9.201797	176	55
Pirottolo	Wet	13/09/2021	22.98	18.74	3.2	1025	1.0827	5.013575	722	103
Punte Alberete	Wet	28/04/2022	18.7	16.9	0.68	74	1.0827	9.872887	871	87
Pirottolo	Wet	28/04/2022	17.6	17.4	2.37	100	1.0827	17.02715	926	105
Punte Alberete	Wet	28/04/2022	18.7	16.5	0.68	74	1.0827	10.15906	871	67
Punte Alberete	Wet	10/09/2021	22.68	22.06	0.57	63	1.0827	5.231557	389	45
Punte Alberete	Wet	10/06/2022	26.9	19.05	0.65	0.013	1.0827	3.404043	715	29
Punte Alberete	Wet	28/04/2022	18.7	16.3	0.68	74	1.0827	8.191634	871	80
Pirottolo	Wet	02/08/2021	30.26	27.6	1.028	619	1.0827	8.940596	478	59
Punte Alberete	Wet	18/10/2021	20.8	13.61	0.54	65	1.0827	0	108.9	45
Pirottolo	Wet	02/08/2021	29.59	27.6	1.028	619	1.0827	9.495052	478	82
Punte Alberete	Wet	28/04/2022	18.7	16.9	0.68	74	1.0827	8.298948	871	60
Punte Alberete	Wet	28/04/2022	18.7	16.9	0.68	74	1.0827	7.297351	871	64
Pirottolo	Wet	14/12/2021	2.47	4.5	2.85	1500	1.0827	19.78434	380	70
Pirottolo	Wet	14/12/2021	11.55	6.59	18.57	1500	1.0827	28.46056	68	70
Pirottolo	Wet	13/09/2021	23.88	18.85	3.25	1025	1.0827	2.346934	722	100
Pirottolo	Wet	14/12/2021	10.15	6.69	17.86	1500	1.0827	22.6902	68	90
Pirottolo	Wet	29/03/2022	15.6	16	12.87	2100	1.0827	8.065317	643	75
Pirottolo	Wet	10/06/2022	22	20.95	6.28	0.55	1.0827	12.34996	176	53

Pirottolo	Wet	22/11/2021	12.14	11.74	3.97	1825	1.0827	14.01789	28	48
Pirottolo	Wet	10/06/2022	21.7	20.96	6.1	0.55	1.0827	13.65995	161	55
Pirottolo	Wet	30/06/2021	30.5	28.59	2.46	0.142	1.0827	11.44682	670	39
Pirottolo	Wet	30/06/2021	31.2	28.88	2.47	0.142	1.0827	22.53594	670	70
Punte Alberete	Wet	30/06/2021	28.7	24.4	0.49	0	1.0827	10.7314	470.5	21
Pirottolo	Wet	31/05/2021	20.31	26.55	5		1.0827	12.17343	512	70
Pirottolo	Wet	22/11/2021	12.21	11.73	3.96	1825	1.0827	17.33792	28	65
Pirottolo	Wet	13/09/2021	24.11	18.86	3.24	1025	1.0827	3.996328	704	90
Punte Alberete	Wet	29/03/2022	15.6	13	0.7659	600	1.0827	-2.14712	665	64
Pirottolo	Wet	02/08/2021	28.26	27.6	1.028	619	1.0827	11.69052	478	115
Pirottolo	Wet	10/06/2022	21.7	21.14	6.23	0.55	1.0827	10.93923	161	51
Pirottolo	Wet	18/10/2021	12.5	10.03	1.76	367	1.0827	3.462441	527	85
Cerba	Wet	14/12/2021	16.94	2.44	1.2	50	1.0827	0.67249	154	35
Pirottolo	Wet	31/05/2021	19.67	27.17	4.9		1.0827	41.31588	316	70
Pirottolo	Wet	21/02/2022	13.96	11.5	11.17	12.3	1.0827	32.09359	6	85
Punte Alberete	Wet	18/10/2021	20.65	13.62	0.52	65	1.0827	6.935166	37.8	31
Punte Alberete	Wet	10/06/2022	26.9	19.06	0.65	0.013	1.0827	7.741336	715	23
Punte Alberete	Wet	30/06/2021	28.08	23.52	0.46	0	1.0827	10.37369	474	20
Pirottolo	Wet	13/09/2021	22.49	18.6	3.21	1025	1.0827	4.795594	722	95
Pirottolo	Wet	30/06/2021	30.47	28.56	2.46	0.142	1.0827	13.95082	670	41
Punte Alberete	Wet	18/10/2021	19.42	13.77	0.54	65	1.0827	5.312042	108.9	55
Pirottolo	Wet	02/08/2021	28.45	27.6	1.028	619	1.0827	12.7821	478	92
Pirottolo	Wet	10/06/2022	21.7	21.52	7.33	0.55	1.0827	11.9881	161	51
Punte Alberete	Wet	30/06/2021	28.49	24.36	0.48	0	1.0827	7.511979	474	12
Punte Alberete	Wet	30/06/2021	28.66	24.44	0.48	0	1.0827	5.723412	474	22

Punte Alberete	Wet	01/06/2021	24.37	19.41	0.57		1.0827	5.449538	461	100
Pirottolo	Wet	30/06/2021	31.85	28.94	2.47	0.142	1.0827	18.9588	670	86
Pirottolo	Wet	02/08/2021	29.74	27.6	1.028	619	1.0827	11.74753	478	37
Pirottolo	Wet	18/10/2021	12.18	10	1.76	367	1.0827	12.50431	527	72
Pirottolo	Wet	22/11/2021	12.31	11.72	3.96	1825	1.0827	10.88231	28	75
Punte Alberete	Wet	22/11/2021	11.26	10.55	0.66	57	1.0827	3.320026	99	55
Punte Alberete	Wet	01/06/2021	21.9	19.6	0.57		1.0827	13.07889	487.5	100
Pirottolo	Wet	02/08/2021	28.88	27.6	1.028	619	1.0827	11.71287	478	115
Pirottolo	Wet	14/12/2021	10.67	6.69	18.17	1500	1.0827	57.29561	68	105
Punte Alberete	Wet	10/06/2022	23.6	19.02	0.65	0.013	1.133552	7.559603	599	40
Cerba	Wet	18/11/2021	14.66	12.45	1.75	46	1.143331	2.213351	182	30
Pirottolo	Wet	02/08/2021	29.39	27.6	1.028	619	1.148684	5.648516	620	99
Punte Alberete	Wet	30/06/2021	28.11	23.78	0.48	0	1.24727	9.300545	474	17
Cerba	Wet	18/11/2021	14.65	12.38	1.78	46	1.286248	10.69786	182	15
Cerba	Wet	27/04/2022	18.2	16.7	2.1	50	1.372968	-1.49524	753	14
Pirottolo	Wet	18/10/2021	15.96	10.23	1.77	367	1.391334	4.94315	518	120
Cerba	Wet	19/10/2021	18.92	11.43	1.58	250	1.514914	7.340947	570	10
Pirottolo	Wet	02/08/2021	28.85	27.6	1.028	619	1.557356	18.05446	478	88
Pirottolo	Wet	31/05/2021	19.67	26.55	5		1.57208	19.55127	316	70
Cerba	Wet	10/09/2021	24.75	19.81	1.85	24	1.579876	28.939	692	5
Cerba	Wet	10/09/2021	24.35	19.53	1.89	24	1.604561	0	692	10
Pirottolo	Wet	18/10/2021	13.7	10.11	1.76	367	1.624916	2.816098	575	70
Cerba	Wet	14/12/2021	16	2.35	1.2	50	1.629247	12.80055	298	10
Pirottolo	Wet	18/10/2021	13.35	10.09	1.76	367	1.668441	3.070745	575	65
Pirottolo	Wet	29/03/2022	15.6	16	12.87	2100	1.689012	6.394125	643	47
Pirottolo	Wet	31/05/2021	19.67	26.55	5		1.714997	90.0096	316	70
Pirottolo	Wet	18/10/2021	16.12	10.24	1.77	367	1.784506	6.778108	518	35

Cerba	Wet	14/12/2021	17.24	2.35	1.2	50	1.82933	36.37273	298	20
Pirottolo	Wet	31/05/2021	19.67	27.14	4.93		1.857913	142.7611	316	70
Pirottolo	Wet	22/11/2021	12.54	11.71	3.96	1825	1.857913	17.15347	28	80
Pirottolo	Wet	18/10/2021	12.37	10	1.75	367	1.884764	7.335358	527	95
Pirottolo	Wet	02/08/2021	29.7	27.6	1.028	619	1.986971	9.287131	478	87
Punte Alberete	Wet	30/06/2021	28.02	23.81	0.47	0	2.078784	4.650273	474	15
Punte Alberete	Wet	01/06/2021	21.9	19.57	0.57		2.111265	12.71559	487.5	100
Pirottolo	Wet	10/06/2022	21.7	21.25	6.82	0.55	2.154496	12.90322	161	99
Pirottolo	Wet	13/09/2021	24.68	19.08	3.26	1025	2.175794	4.077931	704	122
Punte Alberete	Wet	30/06/2021	28.92	24.61	0.48	0	2.21737	12.51996	474	20
Cerba	Wet	19/10/2021	29.66	11.71	1.59	250	2.231228	11.98339	570	2
Pirottolo	Wet	13/09/2021	24.3	18.89	3.24	1025	2.392767	3.175264	704	117
Pirottolo	Wet	31/05/2021	20.31	26.52	5.01		2.429579	17.33792	512	70
Pirottolo	Wet	10/06/2022	21.7	21.33	6.57	0.55	2.588123	12.11129	161	66
Cerba	Wet	27/04/2022	18.2	16.9	2.1	50	2.743995	3.233728	753	23
Pirottolo	Wet	13/09/2021	22.24	18.54	3.19	1025	2.941696	8.50128	722	95
Punte Alberete	Wet	01/06/2021	22.32	19.45	0.57		2.955771	3.996328	461	100
Pirottolo	Wet	30/06/2021	31.46	28.88	2.47	0.142	3.048883	15.73938	670	105
Cerba	Wet	27/04/2022	18.7	17.7	2.05	50	3.284479	7.297351	789	30
Pirottolo	Wet	02/08/2021	28.04	27.6	1.028	619	3.574209	9.084799	478	59
Pirottolo	Wet	30/06/2021	31.37	28.79	2.46	0.142	4.018982	24.3245	670	75
Cerba	Wet	10/09/2021	24.87	19.73	1.87	24	4.434739	0	692	5
Cerba	Wet	10/09/2021	24.63	18.85	2.03	24	4.546257	6.212474	692	8
Pirottolo	Wet	13/09/2021	25.13	19.29	3.28	1025	4.767345	6.689238	704	120
Pirottolo	Wet	18/10/2021	11.53	9.95	1.76	367	4.947506	5.396999	527	80
Pirottolo	Wet	13/09/2021	25.29	19.41	3.3	1025	4.975223	7.368894	704	132
Pirottolo	Wet	18/10/2021	12.63	10.06	1.76	367	4.99168	6.461196	575	55
Cerba	Wet	22/02/2022	9.64	10.8	1.317438	200	5.153652	7.981478	647	5

Pirottolo	Wet	22/11/2021	12.73	11.72	3.96	1825	5.287907	15.12456	28	48
Cerba	Wet	10/09/2021	24.53	18.96	2.04	24	5.432989	6.612106	692	8
Pirottolo	Wet	13/09/2021	22.79	18.67	3.21	1025	6.558997	5.921832	722	95
Pirottolo	Wet	21/02/2022	14.56	11.5	11.17	12.3	6.717071	11.43565	6	70
Pirottolo	Wet	10/06/2022	22	21.36	6.83	0.55	6.902356	10.39423	176	53
Cerba	Wet	03/05/2021	29	30.7	1.04		6.98125	42.27724	367	0.5
Pirottolo	Wet	30/06/2021	30.62	28.62	2.46	0.142	7.067866	13.5931	670	58
Pirottolo	Wet	18/10/2021	12.46	10.04	1.76	367	7.465433	7.449379	527	67
Cerba	Wet	02/08/2021	31.31	23.24	4.14	64	7.907608	4.158417	855	10
Pirottolo	Wet	02/08/2021	29.69	27.6	1.028	619	8.323798	13.54951	620	59
Pirottolo	Wet	13/09/2021	23.37	18.83	3.24	1025	8.754712	6.430455	722	100
Punte Alberete	Wet	01/06/2021	22.32	19.45	0.57		9.008064	47.22933	461	100
Cerba	Wet	10/09/2021	24.71	19.64	1.87	24	9.374017	10.31779	692	15
Pirottolo	Wet	02/08/2021	28.27	27.6	1.028	619	9.399352	18.66257	478	95
Pirottolo	Wet	02/08/2021	29.26	27.6	1.028	619	9.464963	24.04951	478	120
Pirottolo	Wet	13/09/2021	25.6	19.53	3.33	1025	10.1999	1.166145	704	130
Pirottolo	Wet	22/11/2021	12.45	11.72	3.95	1825	10.9331	11.80454	28	50
Pirottolo	Wet	13/09/2021	24.87	19.2	3.28	1025	11.62733	7.54775	704	117
Pirottolo	Wet	30/06/2021	30.64	28.59	2.46	0.142	13.20721	14.66624	670	55
Punte Alberete	Wet	10/09/2021	23.57	22.23	0.57	63	13.61062	6.067153	389	70
Pirottolo	Wet	02/08/2021	29.46	27.6	1.028	619	14.28471	11.78218	620	80
Pirottolo	Wet	02/08/2021	30.1	27.6	1.028	619	14.37869	17.4307	620	60
Cerba	Wet	07/06/2022	29.2	28.4	1.69	0.006	15.51082	15.796	385	14
Punte Alberete	Wet	29/03/2022	15.6	13	0.7659	600	16.46787	3.669356	665	62
Cerba	Wet	18/11/2021	14.06	12.35	1.77	46	17.69998	8.613065	182	18
Pirottolo	Wet	30/06/2021	30.56	28.6	2.46	0.142	19.54057	15.02396	670	65
Cerba	Wet	31/05/2021	20.35	25.53	1.41		20.12739	77.38344	912	30
Cerba	Wet	22/02/2022	9.59	10.8	1.317438	200	20.46736	0.760141	647	5
Cerba	Wet	10/09/2021	24.61	18.74	2.02	24	24.29406	28.47398	692	8

Cerba	Wet	19/10/2021	18.92	11.34	1.6	250	24.4387	1.925615	570	5
Cerba	Wet	10/09/2021	24.48	18.53	2.02	24	26.20784	16.89357	692	5
Punte Alberete	Wet	10/06/2022	23.6	19.05	0.66	0.013	26.53627	7.633065	599	44
Cerba	Wet	19/10/2021	28.8	11.93	1.58	250	27.46767	4.292559	570	2
Pirottolo	Wet	30/06/2021	31.22	28.78	2.46	0.142	30.90459	11.44682	670	70
Cerba	Wet	31/05/2021	32	25.8	1.42		34.37789	86.97463	818	30
Cerba	Wet	02/08/2021	33.36	23.19	4.39	64	34.97338	26.47525	855	10
Pirottolo	Wet	28/04/2022	17.6	16.2	2.37	100	35.3809	17.49218	926	65
Cerba	Wet	18/11/2021	14.52	12.38	1.78	46	39.01618	12.91121	182	14
Pirottolo	Wet	02/08/2021	30.46	21.92	0.44	619	41.32363	20.86139	620	65
Cerba	Wet	18/11/2021	14.22	12.36	1.78	46	41.78356	3.37033	182	8
Cerba	Wet	07/06/2022	29.2	28.13	1.69	0.006	41.9969	22.63933	385	8
Cerba	Wet	02/08/2021	34.13	23.2	4.33	64	47.73711	39.03826	855	10
Cerba	Wet	31/05/2021	20.35	24.86	1.42		48.87741	32.46248	912	30
Pirottolo	Wet	02/08/2021	29.28	27.6	1.028	619	49.31179	24.15347	620	90
Cerba	Wet	31/05/2021	20.38	25.47	1.43		49.44907	94.8052	818	30
Cerba	Wet	14/12/2021	16	2.36	1.2	50	49.87782	15.89924	298	10
Pirottolo	Wet	10/06/2022	21.7	20.61	5.53	0.55	52.9897	23.68406	161	66
Cerba	Wet	19/10/2021	18.92	11.24	1.6	250	55.20861	11.95209	570	8
Cerba	Wet	29/06/2021	33.39	30.4	2.33	0.128	55.58149	53.01982	523	25
Cerba	Wet	02/08/2021	33.87	23.2	4.37	64	59.16284	22.5024	855	10
Pirottolo	Wet	13/09/2021	22.17	18.5	3.17	1025	59.38285	4.395961	722	73
Cerba	Wet	02/08/2021	31.96	23.24	4.1	64	65.77143	21.00001	855	10
Cerba	Wet	02/08/2021	32.23	23.23	4.19	64	82.48615	133.5545	855	10
Cerba	Wet	27/04/2022	18.2	16.6	2.13	50	88.97196	16.49058	753	20
Pirottolo	Wet	10/06/2022	21.7	21.53	6.5	0.55	89.12524	13.60364	161	77
Pirottolo	Wet	30/06/2021	30.99	28.64	2.47	0.142	93.96104	66.89238	670	65
Cerba	Wet	03/05/2021	24	30.7	1.04		95.60241	43.87577	168	30
Pirottolo	Wet	30/06/2021	31.8	28.94	2.47	0.142	96.03982	120.5494	670	105
Cerba	Wet	29/06/2021	33.79	30.58	2.34	0.128	102.8392	58.21784	523	25
Cerba	Wet	19/10/2021	18.92	11.61	1.59	250	103.8573	12.32099	570	10

Cerba	Wet	31/05/2021	32	25.97	1.42		107.6355	162.3292	818	30
Cerba	Wet	29/06/2021	34	30.62	2.34	0.128	117.8757	161.4852	523	25
Cerba	Wet	10/09/2021	24.49	18.63	2.03	24	120.0888	44.35924	692	7
Cerba	Wet	14/12/2021	16.96	2.29	1.19	50	127.6243	5.164485	298	15
Cerba	Wet	18/11/2021	14.38	12.36	1.77	46	129.2679	5.242735	182	8
Punte Alberete	Wet	30/06/2021	28.23	23.86	0.47	0	141.3573	7.511979	474	13
Pirottolo	Wet	13/09/2021	25.74	19.66	3.37	1025	144.8081	48.75632	704	40
Cerba	Wet	10/09/2021	24.69	18.32	2.01	24	155.4515	50.54489	692	5
Pirottolo	Wet	30/06/2021	30.8	28.82	2.46	0.142	169.6288	77.26607	670	70
Cerba	Wet	31/05/2021	31.82	25.8	1.42		171.8895	289.4459	818	30
Cerba	Wet	02/08/2021	33.56	23.25	4.07	64	172.9975	140.3332	855	10
Cerba	Wet	31/05/2021	20.38	25.63	1.41		180.0747	104.7653	818	30
Cerba	Wet	29/03/2022	13.5	16.7	3.022	400	184.3622	41.31588	102	1
Cerba	Wet	31/05/2021	20.35	25.62	1.42		188.3248	71.2073	912	30
Cerba	Wet	29/06/2021	33.64	30.32	2.33	0.128	196.9518	111.5842	523	25
Cerba	Wet	31/05/2021	20.35	25.53	1.41		207.467	66.48437	912	30
Cerba	Wet	02/08/2021	34.56	23.21	4.32	64	208.4767	162.1196	855	10
Punte Alberete	Wet	01/06/2021	21.9	19.6	0.57		227.1721	19.61834	487.5	100
Cerba	Wet	02/08/2021	33.37	23.22	4.25	64	244.2729	87.58889	855	10
Cerba	Wet	03/05/2021	26	30.7	1.04		263.0961	19.84191	367	30
Cerba	Wet	29/06/2021	34.48	30.13	2.35	0.128	288.7821	317.4258	523	25
Cerba	Wet	02/08/2021	34.36	23.26	4.01	64	309.4194	372.7216	855	10
Cerba	Wet	29/06/2021	34.12	30.65	2.34	0.128	315.4988	59.95051	523	25
Cerba	Wet	31/05/2021	20.42	25.63	1.41		318.7036	82.63177	818	30
Cerba	Wet	29/06/2021	34.36	30.21	2.35	0.128	361.5482	156.6337	523	25
Cerba	Wet	02/08/2021	33.33	23.18	4.44	64	362.4074	77.79705	855	10
Pirottolo	Wet	10/06/2022	21.7	21.17	6.38	0.55	425.4448	84.89516	161	60
Cerba	Wet	29/06/2021	33.75	30.51	2.34	0.128	480.0952	188.8614	523	25
Cerba	Wet	29/03/2022	14.3	16.7	3.022	400	654.5571	51.27596	293	5
Cerba	Wet	02/08/2021	33.54	23.18	4.45	64	706.1668	357.4852	855	10

Cerba	Wet	22/02/2022	9.42	10.8	1.317438	200	851.9723	132.2645	647	5
Cerba	Wet	29/06/2021	33.64	30.47	2.34	0.128	1180.771	669.1586	523	25
Cerba	Wet	02/04/2021	27	27.9	1.68		1234.202	132.1862	481	30
Cerba	Wet	02/08/2021	32.78	23.22	4.23	64	1825.556	1363.718	855	10
Cerba	Wet	07/06/2022	29.2	27.94	1.68	0.006	1934.189	591.4478	793	10
Cerba	Wet	29/06/2021	33.96	30.24	2.33	0.128	2323.414	548.5645	523	25
Cerba	Wet	02/08/2021	34.21	23.21	4.3	64	7552.7	1338.518	855	10
Cerba	Dry	02/08/2021	34.33	23.3	3.75	64	1.0827	7.017328	855	
Cavedone	Dry	01/06/2021	20.77	27.62	25.7		1.0827	2.582243	507	
Punte Alberete	Dry	21/02/2022	17.3	8.6	0.8751	800	1.0827	9.960079	0	
Cavedone	Dry	02/08/2021	26.3	26.39	23.41	3200	1.0827	2.165842	628	
Punte Alberete	Dry	03/08/2021	34.45	23.8	1.38	1600	1.0827	6.601487	559.91	
Cavedone	Dry	27/04/2022	18.7	17.4	37.88	350	1.0827	5.151071	763	
Cerba	Dry	14/12/2021	6.36	2.02	1.21	50	1.0827	0.902667	380	
Cavedone	Dry	18/11/2021	15.77	14.91	44.06	1400	1.0827	6.271161	107	
Cavedone	Dry	29/03/2022	12.5	18.6	37.88345	400	1.0827	2.582243	7	
Cavedone	Dry	19/10/2021	19.64	17.72	30.54	20	1.0827	0.250846	396	
Cerba	Dry	14/12/2021	7.81	1.99	1.18	50	1.0827	0	380	
Cerba	Dry	22/02/2022	8.98	10.8	1.317438	200	1.0827	2.280422	638	
Cerba	Dry	22/02/2022	8.65	10.8	1.317438	200	1.0827	0.570106	638	
Cerba	Dry	10/09/2021	24.39	16.94	1.86	24	1.0827	7.851806	692	
Cerba	Dry	10/09/2021	23.96	16.71	1.85	24	1.0827	5.508785	692	
Punte Alberete	Dry	01/04/2022	14.9	14	0.7659	600	1.0827	7.294556	166.5	
Cerba	Dry	27/04/2022	17.5	14.9	2.21	50	1.0827	8.603004	645	
Cerba	Dry	29/03/2022	15.6	16.7	3.022	400	1.0827	4.574259	381	
Cerba	Dry	29/03/2022	15.6	16.7	3.022	400	1.0827	-2.12113	381	
Punte Alberete	Dry	19/10/2021	20.56	12.6	0.58	65	1.0827	28.03578	18.45	
Cerba	Dry	02/08/2021	33.11	23.32	3.65	64	1.0827	3.967823	855	

Punte Alberete	Dry	21/02/2022	17.3	8.6	0.8751	800	1.0827	9.960079	0	
Punte Alberete	Dry	15/12/2021	7.77	3.61	0.59	500	1.0827	1.257083	220.8	
Cerba	Dry	19/10/2021	18.92	10.44	1.59	250	1.0827	2.526909	615	
Cerba	Dry	19/10/2021	18.92	10.07	1.59	250	1.0827	9.572743	615	
Cerba	Dry	19/10/2021	18.92	9.83	1.58	250	1.0827	3.984032	615	
Cerba	Dry	18/11/2021	12.35	12.26	1.78	46	1.0827	1.106675	285	
Cerba	Dry	29/03/2022	15.6	16.7	3.022	400	1.0827	1.726414	381	
Cerba	Dry	22/02/2022	8.64	10.8	1.317438	200	1.0827	5.13095	638	
Punte Alberete	Dry	19/10/2021	20.58	12.58	0.59	65	1.0827	10.3843	18.45	
Cavedone	Dry	29/03/2022	12.5	18.6	37.88345	400	1.0827	3.652029	7	
Cerba	Dry	22/02/2022	8.34	10.8	1.317438	200	1.0827	1.710317	638	
Punte Alberete	Dry	01/04/2022	14.9	14	0.7659	600	1.0827	7.519804	166.5	
Cerba	Dry	27/04/2022	17.5	15	2.22	50	1.0827	5.955926	645	
Cerba	Dry	27/04/2022	17.5	15.8	2.18	50	1.0827	3.344619	645	
Cavedone	Dry	02/08/2021	26.32	26.45	26.1	3200	1.0827	4.782179	628	
Cavedone	Dry	02/04/2021	25	23	7.67		1.0827	33.26734	747	
Cavedone	Dry	02/08/2021	26.3	26.49	27.25	3200	1.0827	4.799506	628	
Punte Alberete	Dry	01/04/2022	14.9	14	0.7659	600	1.0827	32.9208	166.5	
Cavedone	Dry	01/06/2021	20.72	28.01	25.88		1.0827	4.795594	507	
Cerba	Dry	10/09/2021	23.59	16.58	1.89	24	1.0827	16.00767	692	
Punte Alberete	Dry	18/11/2021	15.19	12.11	0.65	41	1.0827	7.008945	49.5	
Cavedone	Dry	19/10/2021	18.68	17.72	30.54	20	1.0827	3.596695	396	
Cavedone	Dry	29/06/2021	25.43	27.2	17.81	0.024	1.0827	3.934846	849	
Cerba	Dry	19/10/2021	18.92	9.49	1.59	250	1.0827	3.37536	615	
Cerba	Dry	18/11/2021	12.77	12.29	1.78	46	1.0827	4.242256	285	
Cerba	Dry	10/09/2021	24.56	16.94	1.86	24	1.0827	12.44842	692	
Cerba	Dry	10/09/2021	24.35	17.5	1.88	24	1.0827	44.39222	692	

Punte Alberete	Dry	01/04/2022	14.9	14	0.7659	600	1.0827	10.67327	166.5	
Cavedone	Dry	13/09/2021	24.78	23.9	24.86	1300	1.0827	3.255191	589	
Cerba	Dry	27/04/2022	17.5	14.9	2.22	50	1.0827	12.82402	645	
Punte Alberete	Dry	07/06/2022	24.7	21	0.5898	0.013	1.0827	30.73307	6.3	
Cerba	Dry	27/04/2022	17.5	14.7	2.2	50	1.0827	5.544556	645	
Cerba	Dry	02/08/2021	32.02	23.33	3.52	64	1.0827	28.12129	855	
Cerba	Dry	19/10/2021	18.92	9.99	1.59	250	1.0827	6.271161	615	
Cerba	Dry	22/02/2022	8.9	10.8	1.317438	200	1.0827	-1.71032	638	
Punte Alberete	Dry	03/08/2021	34.83	23.84	1.4	1600	1.0827	8.420794	559.91	
Cavedone	Dry	15/12/2021	9.08	8.6	42.1	1400	1.0827	0.950176	362	
Cerba	Dry	19/10/2021	18.92	11.79	0.44	250	1.0827	12.67143	615	
Cavedone	Dry	21/02/2022	17.14	10.9	37.63091	800	1.0827	4.242256	32	
Cavedone	Dry	21/02/2022	15.38	10.9	37.63091	800	1.0827	1.475567	32	
Cerba	Dry	10/09/2021	25.1	17.22	1.86	24	1.0827	3.541361	692	
Cavedone	Dry	19/10/2021	16.13	17.72	30.54	20	1.0827	0	396	
Cavedone	Dry	02/08/2021	25.92	26.29	16.82	3200	1.0827	5.52667	628	
Cerba	Dry	10/09/2021	24.54	17.35	1.87	24	1.0827	6.224211	692	
Cerba	Dry	18/11/2021	12.2	12.25	1.78	46	1.0827	10.51342	285	
Cerba	Dry	22/02/2022	8.39	10.8	1.317438	200	1.0827	3.230598	638	
Punte Alberete	Dry	21/02/2022	17.3	8.6	0.8751	800	1.0827	8.484512	0	
Cavedone	Dry	01/06/2021	22.74	27.05	25.95		1.0827	8.406262	677	
Cerba	Dry	14/12/2021	11.62	1.99	1.21	50	1.0827	118.5059	380	
Cerba	Dry	10/09/2021	25.05	17.28	1.87	24	1.0827	7.422551	692	
Cavedone	Dry	21/02/2022	15.88	10.9	37.63091	800	1.0827	2.582243	32	
Cerba	Dry	29/03/2022	15.6	16.7	3.022	400	1.0827	-2.47158	381	
Cerba	Dry	14/12/2021	6.49	1.97	1.18	50	1.0827	4.845897	380	
Cerba	Dry	22/02/2022	8.26	10.8	1.317438	200	1.0827	5.701055	638	
Cerba	Dry	18/11/2021	12.34	12.25	1.78	46	1.0827	1.106675	285	

Punte Alberete	Dry	15/12/2021	7.59	3.62	0.59	500	1.0827	8.399555	220.8	
Punte Alberete	Dry	03/08/2021	28.89	22.46	0.86	1600	1.0827	7.43317	559.91	
Cavedone	Dry	29/06/2021	26.42	27.18	17.8	0.024	1.0827	17.52795	849	
Cavedone	Dry	21/02/2022	17.14	10.9	37.63091	800	1.0827	6.640053	32	
Punte Alberete	Dry	21/02/2022	17.3	8.6	0.8751	800	1.0827	4.242256	0	
Punte Alberete	Dry	03/08/2021	32.72	23.67	1.34	1600	1.0827	44.85892	559.91	
Cavedone	Dry	02/08/2021	26.34	26.59	28.84	3200	1.0827	4.9901	628	
Cerba	Dry	29/03/2022	15.6	16.7	3.022	400	1.0827	-4.20537	381	
Punte Alberete	Dry	21/02/2022	17.3	8.6	0.8751	800	1.0827	6.640053	0	
Cerba	Dry	10/09/2021	24.44	17.04	1.87	24	1.0827	7.082723	692	
Cerba	Dry	18/11/2021	12.36	12.27	1.78	46	1.0827	4.611148	285	
Cavedone	Dry	21/02/2022	17.3	10.9	37.63091	800	1.0827	0	32	
Cavedone	Dry	13/09/2021	22.3	23.97	24.86	1300	1.0827	1.754081	589	
Punte Alberete	Dry	18/11/2021	16.47	12.09	0.66	41	1.0827	8.484512	49.5	
Punte Alberete	Dry	27/04/2022	18.6	16.6	0.65	74	1.0827	10.46311	926	
Cerba	Dry	22/02/2022	8.73	10.8	1.317438	200	1.0827	7.601407	638	
Cavedone	Dry	29/06/2021	28.42	27.29	17.93	0.024	1.0827	17.34909	849	
Cavedone	Dry	27/04/2022	18.7	17.6	37.88	350	1.0827	6.939638	763	
Cavedone	Dry	29/06/2021	24.65	27.33	17.78	0.024	1.0827	8.942832	849	
Punte Alberete	Dry	19/10/2021	21.32	12.78	0.61	65	1.0827	12.22876	66.15	
Cerba	Dry	29/03/2022	15.6	16.7	3.022	400	1.0827	6.012937	381	
Cavedone	Dry	13/09/2021	24.97	23.88	24.81	1300	1.0827	9.175346	589	
Cavedone	Dry	29/03/2022	12.5	18.6	37.88345	400	1.0827	12.43165	7	
Cerba	Dry	27/04/2022	17.5	15.2	2.19	50	1.0827	3.881189	645	

Punte Alberete	Dry	27/04/2022	18.6	16.6	0.65	74	1.0827	9.175346	278.55	
Cerba	Dry	27/04/2022	17.5	15.1	2.19	50	1.0827	6.939638	645	
Cerba	Dry	10/09/2021	25.07	17.16	1.86	24	1.0827	9.461516	692	
Cerba	Dry	27/04/2022	16.5	14.7	2.19	50	1.0827	7.26158	681	
Punte Alberete	Dry	01/04/2022	14.9	14	0.7659	600	1.0827	6.393566	166.5	
Cavedone	Dry	13/09/2021	23.19	23.97	24.81	1300	1.0827	1.806452	589	
Cavedone	Dry	18/11/2021	14.5	14.99	44.38	1400	1.0827	0.368892	107	
Cerba	Dry	19/10/2021	18.92	9.64	1.6	250	1.0827	5.828491	615	
Cerba	Dry	02/08/2021	31.13	23.33	3.4	64	1.0827	5.63119	733	
Cerba	Dry	29/03/2022	15.6	16.7	3.022	400	1.0827	-0.89272	381	
Punte Alberete	Dry	01/04/2022	14.7	14	0.7659	600	1.0827	5.527229	117.9	
Punte Alberete	Dry	19/10/2021	21.12	12.63	0.59	65	1.0827	14.94012	18.45	
Cerba	Dry	03/05/2021	24	30.7	1.04		1.0827	12.01693	168	
Cerba	Dry	03/05/2021	26	30.7	1.04		1.0827	13.13478	367	
Punte Alberete	Dry	03/05/2021	24	15.9	0.4		1.0827	9.641491	470.5	
Punte Alberete	Dry	03/05/2021	25	15.9	0.4		1.0827	6.707124	382	
Pirottolo	Dry	02/04/2021	20	13.2	20.89		1.0827	14.20792	794	
Cavedone	Dry	29/06/2021	28.92	27.29	17.92	0.024	1.0827	3.398276	849	
Cavedone	Dry	18/11/2021	16.92	14.61	42.48	1400	1.0827	2.951135	107	
Cavedone	Dry	18/11/2021	14.15	15.05	44.08	1400	1.0827	0	107	
Cavedone	Dry	18/11/2021	13.79	15.07	44.11	1400	1.0827	2.397797	107	
Cavedone	Dry	21/02/2022	15.2	10.9	37.63091	800	1.0827	0	32	
Cerba	Dry	31/05/2021	22.42	20.85	1.4		1.0827	55.70266	902	
Cerba	Dry	31/05/2021	20.05	22.24	1.41		1.0827	10.32897	902	
Cerba	Dry	18/11/2021	12.72	12.28	1.78	46	1.0827	2.213351	285	
Cerba	Dry	18/11/2021	12.22	12.26	1.78	46	1.0827	5.164485	285	
Cerba	Dry	18/11/2021	12.3	12.26	1.78	46	1.0827	4.242256	285	

Punte Alberete	Dry	01/06/2021	22.45	20.49	0.57		1.0827	8.11562	482	
Punte Alberete	Dry	01/06/2021	22.45	20.01	0.57		1.0827	7.008945	482	
Punte Alberete	Dry	18/11/2021	13.68	13.24	0.64	41	1.0827	20.84239	49.5	
Punte Alberete	Dry	19/10/2021	20.4	12.61	0.58	65	1.0827	8.060286	18.45	
Cerba	Dry	02/08/2021	30.51	23.33	3.34	64	1.0827	23.40842	733	
Punte Alberete	Dry	15/12/2021	7.85	3.57	0.58	500	1.0827	8.207593	220.8	
Cerba	Dry	29/03/2022	14.3	16.7	3.022	400	1.0827	14.94012	293	
Cavedone	Dry	19/10/2021	17.55	17.81	33.25	20	1.0827	0	396	
Punte Alberete	Dry	03/08/2021	29.37	23.38	1.26	1600	1.0827	5.804457	559.91	
Cavedone	Dry	29/06/2021	27.27	27.19	17.77	0.024	1.0827	5.544556	849	
Cerba	Dry	14/12/2021	7.29	2.25	1.23	50	1.0827	7.677421	380	
Cavedone	Dry	02/08/2021	26.11	26.34	20.31	3200	1.0827	9.926544	628	
Punte Alberete	Dry	15/12/2021	7.43	3.62	0.59	500	1.0827	18.52843	220.8	
Punte Alberete	Dry	27/04/2022	18.6	16.6	0.65	74	1.0827	10.64197	278.55	
Cerba	Dry	29/03/2022	15.6	16.7	3.022	400	1.0827	5.994492	381	
Cavedone	Dry	13/09/2021	25.75	23.84	24.92	1300	1.0827	11.75088	589	
Cerba	Dry	10/09/2021	24.24	16.65	1.91	24	1.0827	23.8237	692	
Cavedone	Dry	13/09/2021	25.24	23.87	24.75	1300	1.0827	13.62888	589	
Cerba	Dry	02/08/2021	28.54	23.33	3.12	64	1.0827	30.51238	733	
Cavedone	Dry	27/04/2022	18.7	17.6	37.88	350	1.0827	7.833921	763	
Punte Alberete	Dry	03/05/2021	21	16	0.4		1.0827	5.170075	362.5	
Punte Alberete	Dry	03/05/2021	21	16	0.4		1.0827	7.824978	362.5	

Punte Alberete	Dry	03/05/2021	24	16	0.4		1.0827	12.85532	362.5	
Cerba	Dry	29/06/2021	30.63	24.77	2.37	0.128	1.0827	36.73268	926	
Cavedone	Dry	29/06/2021	28.61	27.29	17.92	0.024	1.0827	6.617696	849	
Cavedone	Dry	18/11/2021	13.73	15.09	44.19	1400	1.0827	0	107	
Punte Alberete	Dry	18/11/2021	16.8	12.08	0.66	41	1.0827	7.931174	49.5	
Punte Alberete	Dry	18/11/2021	16.67	12.1	0.66	41	1.0827	9.03785	49.5	
Cerba	Dry	22/02/2022	8.57	10.8	1.317438	200	1.0827	6.461196	638	
Cavedone	Dry	02/08/2021	26	26.31	18.79	3200	1.0827	6.939638	628	
Cerba	Dry	10/09/2021	24.28	16.68	1.91	24	1.0827	10.71351	692	
Cavedone	Dry	27/04/2022	18.7	17.5	37.88	350	1.0827	9.229003	763	
Cerba	Dry	10/09/2021	24.8	17.1	1.88	24	1.0827	2.575536	692	
Cavedone	Dry	29/03/2022	12.5	18.6	37.88345	400	1.0827	2.988024	7	
Cavedone	Dry	27/04/2022	18.7	17.7	37.88	350	1.0827	7.368894	763	
Cerba	Dry	14/12/2021	7.24	2.25	1.23	50	1.0827	0.285433	380	
Punte Alberete	Dry	03/05/2021	24	16.9	0.41		1.0827	6.287929	467.5	
Cerba	Dry	19/10/2021	18.92	11.96	0.31	250	1.0827	10.29208	615	
Cerba	Dry	10/09/2021	24.33	17.57	1.88	24	1.0827	24.27085	692	
Cerba	Dry	14/12/2021	14.97	2.15	1.19	50	1.0827	0	298	
Cavedone	Dry	29/06/2021	24.27	28.66	17.81	0.024	1.0827	5.902269	849	
Punte Alberete	Dry	19/10/2021	20.09	12.63	0.58	65	1.0827	13.90722	18.45	
Cerba	Dry	27/04/2022	16.5	14.6	2.16	50	1.0827	6.170554	681	
Punte Alberete	Dry	27/04/2022	18.6	16.5	0.65	74	1.0827	8.799747	278.55	
Cavedone	Dry	07/06/2022	27.9	22.7	2.43	0.45	1.0827	6.739293	810	
Punte Alberete	Dry	01/06/2021	22.45	20.47	0.57		1.0827	10.88231	482	
Punte Alberete	Dry	03/05/2021	24	15.9	0.4		1.0827	11.03881	467.5	

Punte Alberete	Dry	03/05/2021	24	16.9	0.41		1.0827	8.244173	470.5	
Cerba	Dry	29/06/2021	31.02	24.66	2.37	0.128	1.0827	49.20793	926	
Cavedone	Dry	27/04/2022	18.7	17.3	37.88	350	1.0827	6.492496	763	
Punte Alberete	Dry	07/06/2022	24.7	21	0.5898	0.013	1.0827	7.832087	6.3	
Cavedone	Dry	19/10/2021	16.16	17.78	33.96	20	1.0827	4.275792	396	
Cavedone	Dry	13/09/2021	24.59	23.95	24.76	1300	1.0827	8.08432	589	
Cerba	Dry	31/05/2021	23.78	20.02	1.4		1.0827	33.08848	971	
Cerba	Dry	19/10/2021	18.94	12.06	0.31	250	1.0827	13.40922	570	
Cerba	Dry	18/11/2021	12.32	12.26	1.78	46	1.0827	5.533377	285	
Cavedone	Dry	13/09/2021	23.83	23.96	24.83	1300	1.0827	5.598213	589	
Cavedone	Dry	19/10/2021	17.96	17.86	33.05	20	1.0827	12.83744	396	
Cerba	Dry	03/05/2021	29	30.7	1.04		1.0827	7.27723	617	
Punte Alberete	Dry	18/11/2021	16.8	12.07	0.66	41	1.0827	33.20026	49.5	
Punte Alberete	Dry	21/02/2022	17.3	8.6	0.8751	800	1.0827	10.69786	0	
Punte Alberete	Dry	03/05/2021	25	16	0.51		1.0827	4.471416	382	
Punte Alberete	Dry	21/02/2022	17.3	8.6	0.8751	800	1.0827	6.455607	0	
Punte Alberete	Dry	03/08/2021	29.88	23.17	1.18	1600	1.0827	15.43812	559.91	
Punte Alberete	Dry	01/06/2021	22.45	20.31	0.57		1.143331	4.611148	482	
Punte Alberete	Dry	03/05/2021	25	16.9	0.41		1.19097	9.082564	382	
Cerba	Dry	07/06/2022	28.3	24.64	1.62	0.006	1.281779	15.86055	832	
Punte Alberete	Dry	27/04/2022	18.6	16.6	0.65	74	1.408723	10.40946	278.55	
Cavedone	Dry	13/09/2021	21.62	24.04	24.91	1300	1.429164	6.031381	589	

Punte Alberete	Dry	01/06/2021	22.45	20.49	0.57		1.429164	28.40467	482	
Cerba	Dry	22/02/2022	9.03	10.8	1.317438	200	1.472472	7.791442	638	
Cerba	Dry	03/05/2021	29	30.7	1.04		1.54393	28.93565	617	
Punte Alberete	Dry	03/05/2021	24	16	0.51		1.569915	4.75088	467.5	
Cavedone	Dry	18/11/2021	16.98	14.61	42.48	1400	1.57208	0	107	
Cavedone	Dry	29/06/2021	24.61	27.89	17.84	0.024	1.663027	29.51135	849	
Cerba	Dry	27/04/2022	17.5	15.4	2.21	50	1.842496	3.738104	645	
Cerba	Dry	18/11/2021	12.25	12.25	1.79	46	2.072288	5.902269	285	
Cerba	Dry	02/04/2021	27	27.9	1.68		2.163235	24.59838	481	
Punte Alberete	Dry	01/06/2021	22.7	20.47	0.57		2.358121	10.14453	455	
Cerba	Dry	14/12/2021	6.98	2.25	1.23	50	2.407492	8.627597	380	
Cerba	Dry	31/05/2021	19.94	17.72	1.39		2.501037	58.10046	906	
Cerba	Dry	31/05/2021	19.75	19.14	1.4		3.215619	14.94012	971	
Cerba	Dry	31/05/2021	20.26	17.72	1.39		3.358535	26.9291	906	
Punte Alberete	Dry	03/08/2021	28.8	22.33	0.79	1600	3.457061	20.98268	559.91	
Punte Alberete	Dry	03/08/2021	29.03	23.26	1.21	1600	3.812836	20.46288	559.91	
Cerba	Dry	10/09/2021	24.07	16.77	1.85	24	4.261507	2.343022	692	
Cerba	Dry	03/05/2021	29	30.7	1.04		4.564663	14.72773	617	
Cerba	Dry	31/05/2021	19.75	19.14	1.4		4.642618	40.06389	971	
Cerba	Dry	02/08/2021	34.23	23.3	3.77	64	5.276214	42.53714	855	
Cerba	Dry	29/03/2022	15.6	16.7	3.022	400	5.609469	22.87129	381	
Punte Alberete	Dry	18/11/2021	15.89	12.06	0.65	41	5.716656	9.03785	49.5	
Cavedone	Dry	07/06/2022	28.3	22.66	2.43	0.45	5.848658	8.948866	832	
Punte Alberete	Dry	01/06/2021	21.9	19.91	0.57		6.145405	9.406741	482	
Cerba	Dry	03/05/2021	24	30.7	1.04		6.27966	24.59279	367	

Punte Alberete	Dry	03/05/2021	24	16	0.51		6.60447	5.309807	470.5	
Cerba	Dry	31/05/2021	21.96	21.33	1.41		6.788529	36.52029	902	
Punte Alberete	Dry	27/04/2022	18.6	16.5	0.65	74	8.294348	19.85309	278.55	
Cerba	Dry	07/06/2022	29.2	24.97	1.63	0.006	8.314897	29.33335	793	
Pirottolo	Dry	02/04/2021	20	13.2	20.89		8.860817	25.4703	794	
Cerba	Dry	22/02/2022	8.46	10.8	1.317438	200	10.24104	1.140211	638	
Cerba	Dry	02/08/2021	29.23	23.33	3.2	64	10.53229	93.07923	733	
Cavedone	Dry	02/08/2021	26.25	26.56	28.54	3200	11.19014	8.940596	628	
Cerba	Dry	31/05/2021	20.26	17.28	1.39		11.21894	66.95387	906	
Punte Alberete	Dry	19/10/2021	20.65	12.59	0.58	65	11.26896	18.35237	18.45	
Cerba	Dry	18/11/2021	12.21	12.25	1.79	46	12.36227	28.40467	285	
Cavedone	Dry	29/06/2021	29.54	27.31	17.93	0.024	12.81917	72.25808	849	
Cerba	Dry	07/06/2022	29.2	25.3	1.65	0.006	13.0313	14.72644	793	
Punte Alberete	Dry	18/11/2021	16.64	12.08	0.66	41	14.00581	10.88231	49.5	
Punte Alberete	Dry	19/10/2021	20.2	12.62	0.58	65	14.35595	12.41321	18.45	
Cerba	Dry	18/11/2021	12.44	12.27	1.8	46	14.64893	8.853404	285	
Cerba	Dry	31/05/2021	20.39	16.89	1.38		15.14914	26.56021	906	
Punte Alberete	Dry	03/05/2021	21	16	0.51		15.21194	8.104442	362.5	
Punte Alberete	Dry	18/11/2021	16.5	12.09	0.66	41	15.2206	38.73364	49.5	
Punte Alberete	Dry	03/08/2021	28.01	22.21	0.72	1600	18.44661	10.4307	559.91	
Cerba	Dry	31/05/2021	19.75	18.19	1.4		19.29371	50.53818	971	
Cerba	Dry	31/05/2021	19.93	19.59	1.4		19.36517	55.70266	971	
Cerba	Dry	27/04/2022	16.5	14.6	2.16	50	19.90089	10.30214	681	
Cerba	Dry	22/02/2022	8.56	10.8	1.317438	200	19.952	14.25264	638	
Cerba	Dry	31/05/2021	21.28	16.84	1.38		20.36559	35.96695	906	

Cerba	Dry	02/08/2021	28.13	23.26	2.62	64	22.41384	77.97032	733	
Cerba	Dry	31/05/2021	19.74	19.14	1.4		22.86662	46.29592	971	
Cerba	Dry	02/08/2021	28.5	23.32	2.89	64	28.07939	59.15348	733	
Cerba	Dry	19/10/2021	18.92	12.05	0.31	250	28.95486	68.83521	570	
Cerba	Dry	07/06/2022	29.2	25.54	1.64	0.006	28.97315	18.50835	793	
Punte Alberete	Dry	03/08/2021	26.8	21.92	0.44	1600	29.44944	16.79464	559.91	
Cerba	Dry	31/05/2021	26.81	21.83	1.41		30.21166	13.5931	902	
Cerba	Dry	07/06/2022	29.2	25.19	1.64	0.006	30.67979	47.19289	793	
Cerba	Dry	19/10/2021	18.92	9.5	1.59	250	31.16292	10.80853	615	
Cerba	Dry	07/06/2022	29.2	24.87	1.63	0.006	31.63233	25.45752	793	
Punte Alberete	Dry	03/08/2021	31.94	23.04	1.13	1600	33.00654	18.52228	559.91	
Cerba	Dry	31/05/2021	19.74	18.67	1.4		35.15743	33.93805	971	
Cerba	Dry	10/09/2021	23.2	16.55	1.87	24	35.26311	36.11116	692	
Cavedone	Dry	07/06/2022	28.3	22.53	2.44	0.45	37.04615	16.27861	832	
Cerba	Dry	19/10/2021	18.92	9.66	1.6	250	37.55128	13.44611	615	
Cerba	Dry	10/09/2021	22.78	16.66	1.83	24	38.15262	25.61227	692	
Punte Alberete	Dry	01/06/2021	22.7	20.62	0.57		38.23014	51.64485	455	
Cerba	Dry	31/05/2021	22.42	20.85	1.4		38.44451	48.14038	902	
Cerba	Dry	29/06/2021	31.28	24.55	2.37	0.128	43.69994	32.05446	926	
Cerba	Dry	31/05/2021	20.15	16.96	1.39		52.23594	334.4004	906	
Cerba	Dry	07/06/2022	29.2	25.97	1.66	0.006	53.67309	9.278081	793	
Punte Alberete	Dry	03/08/2021	31.4	23.51	1.29	1600	59.03855	308.208	559.91	
Cavedone	Dry	02/08/2021	26.37	26.61	29.29	3200	68.88614	48.58417	642	
Cerba	Dry	07/06/2022	29.2	26.31	1.66	0.006	69.25773	32.67988	793	
Cerba	Dry	22/02/2022	9.3	10.8	1.317438	200	76.49492	8.171513	638	
Punte Alberete	Dry	01/06/2021	22.7	20.55	0.57		78.31819	42.05367	455	
Cerba	Dry	31/05/2021	20.39	16.96	1.39		78.53256	156.5946	906	

Cerba	Dry	31/05/2021	26.81	21.83	1.41		86.54671	12.34111	902	
Cerba	Dry	31/05/2021	21.28	16.84	1.38		108.1163	86.87402	168	
Cerba	Dry	07/06/2022	28.3	24.52	1.62	0.006	131.6296	66.01566	832	
Cerba	Dry	07/06/2022	29.2	25.86	1.65	0.006	134.2158	10.29228	793	
Cerba	Dry	31/05/2021	20.26	17.72	1.39		141.3443	132.4322	906	
Cerba	Dry	02/04/2021	27	27.9	1.68		148.737	93.26256	481	
Cerba	Dry	31/05/2021	21.96	21.33	1.41		159.7091	35.78251	902	
Cerba	Dry	31/05/2021	20.2	17.13	1.4		182.5042	50.72263	906	
Cavedone	Dry	07/06/2022	27.9	22.81	2.35	0.45	183.8364	42.01118	810	
Cavedone	Dry	02/08/2021	25.5	26.28	15.05	3200	210.3106	335.8212	628	
Cerba	Dry	31/05/2021	19.93	19.59	1.4		216.8756	130.2188	971	
Cerba	Dry	03/05/2021	26	30.7	1.04		275.6013	185.1446	367	
Cerba	Dry	31/05/2021	19.75	18.19	1.4		278.7584	61.78938	971	
Cavedone	Dry	07/06/2022	27.9	22.79	2.42	0.45	284.6972	148.6866	810	
Cerba	Dry	07/06/2022	29.2	25.61	1.64	0.006	288.6069	54.50062	793	
Cavedone	Dry	07/06/2022	28.3	22.59	2.43	0.45	338.334	80.95614	832	
Cerba	Dry	31/05/2021	20.15	16.96	1.39		402.0238	970.5544	906	
Cerba	Dry	31/05/2021	20.2	17.13	1.4		402.0238	44.82036	906	
Cerba	Dry	31/05/2021	20.2	17.13	1.4		402.1667	150.5079	906	
Cerba	Dry	19/10/2021	16.56	12.06	0.31	250	424.5332	133.3728	570	
Cerba	Dry	29/06/2021	29.55	25.75	2.38	0.128	525.0315	60.99011	926	
Cavedone	Dry	07/06/2022	27.9	22.77	2.42	0.45	543.4644	108.3401	810	
Punte Alberete	Dry	19/10/2021	19.24	12.64	0.58	65	719.2268	211.0061	18.45	
Cerba	Dry	29/06/2021	31.75	24.28	2.39	0.128	737.5959	674.8764	905	
Cerba	Dry	29/06/2021	31.75	24.25	2.39	0.128	746.1211	1336.065	905	
Cerba	Dry	29/06/2021	31.76	24.22	2.39	0.128	812.1073	35.86635	905	
Cerba	Dry	19/10/2021	15.82	12.06	0.31	250	1754.325	679.7938	570	
Cerba	Dry	29/06/2021	31.19	24.32	2.39	0.128	2363.421	1491.312	905	
Cerba	Dry	10/09/2021	22.84	16.91	1.81	24	3485.185	394.1285	692	